US Army Corps
of Engineers
Waterways Experiment
Station

AD-A280 231

New York Bight Study

Report 2
Development and Application
of a Eutrophication/General
Water Quality Model

by   Ross W. Hall, Mark S. Dortch

DTIC
S ELECTE D
JUN 1 3 1994
F

WES

94-17983

DTIC QUALITY INSPECTED 1

94 6 10 091

The contents of this report are not to be used for advertising,
publication, or promotional purposes. Citation of trade names
does not constitute an official endorsement or approval of the use
of such commercial products.

New York Bight Study

Report 2
Development and Application
of a Eutrophication/General
Water Quality Model

by Ross W. Hall, Mark S. Dortch

U.S. Army Corps of Engineers
Waterways Experiment Station
3909 Halls Ferry Road
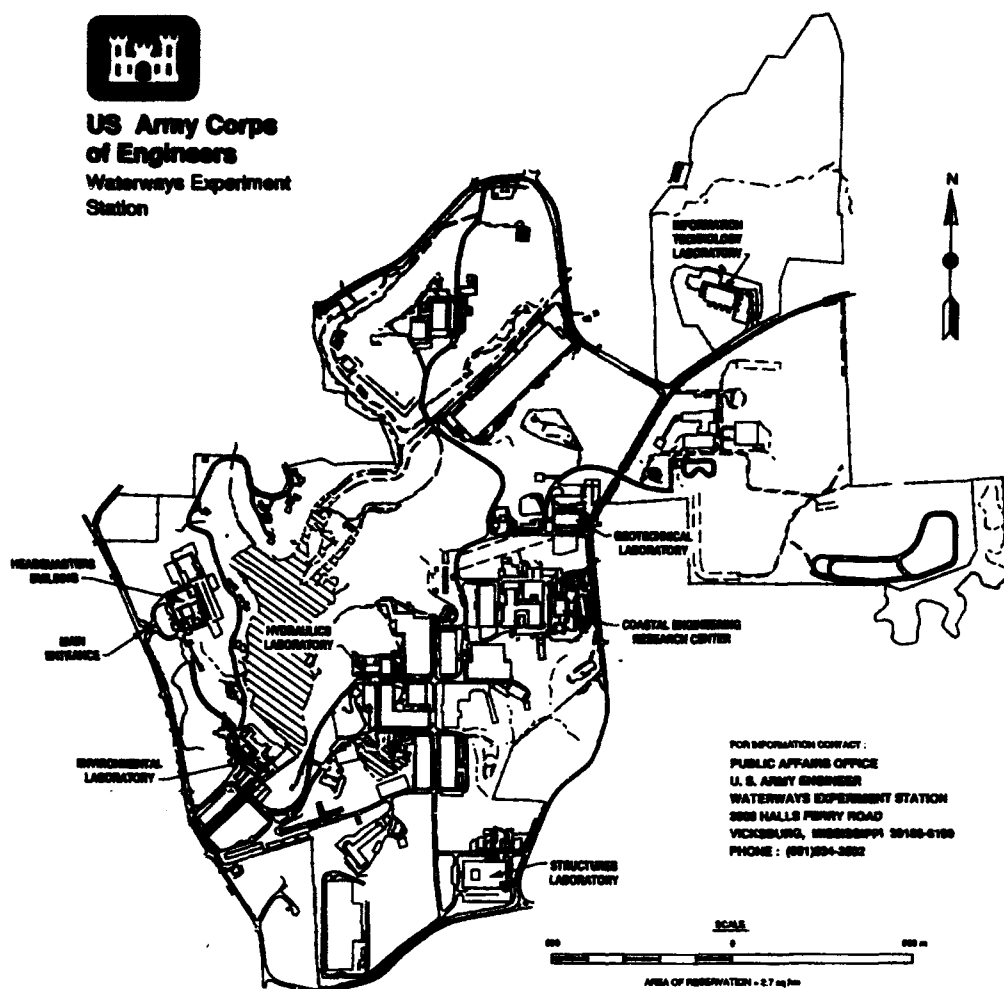Vicksburg, MS   39180-6199

Accesion For		
NTIS CRA&I	☑	
DTIC TAB	☐	
Unannounced	☐	
Justification		
By		
Distribution /		
Availability Codes		
Dist	Avail and / or Special	
A-1		

Report 2 of a series

Prepared for   U.S. Army Engineer District, New York
New York, New York   10278-0090

**US Army Corps
of Engineers**
Waterways Experiment
Station

Contents

SF 298

Preface

The eutrophication/general water quality aspect of the New York Bight
(NYB) Study was conducted at the U.S. Army Engineer Waterways
Experiment Station (WES) for the U.S. Army Engineer District, New York
(CENAN). The study was funded by CENAN under Section 728 of the Water
Resources Act of 1986. Mr. H. Lee Butler, Chief, Research Division, Coastal
Engineering Research Center, was the WES study manager. Ms. Lynn M.
Bocamazo and Mr. Bryce W. Wisemiller of CENAN were responsible for
overall project management of the NYB Study.

This study was conducted by Mr. Ross W. Hall of the Water Quality and
Contaminant Modeling Branch (WQCMB), Environmental Processes and
Effects Division (EPED), Environmental Laboratory (EL), WES. Dr. Mark S.
Dortch, Chief, WQCMB, assisted in the analysis and interpretation of results
and provided direct supervision. General supervision was provided by
Mr. Donald L. Robey, Chief, EPED, and Dr. John Harrison, Chief, EL. This
report was written by Mr. Hall and Dr. Dortch. Report review was provided
by Mr. Thomas M. Cole and Dr. Carl F. Cerco of the WQCMB.

At the time of publication of this report, Director of WES was
Dr. Robert W. Whalin. Commander was COL Bruce K. Howard, EN.

1   Introduction

Background

The New York Bight (NYB) Study, funded through Section 728 of the
Water Resources Act of 1986, is an investigation of the technical feasibility of
conducting hydro-environmental modeling and monitoring of the NYB system.
The modeling efforts of this study were focused on several aspects, including
hydrodynamics and circulation, eutrophication and general water quality, con-
taminants and toxic substances, and particle tracking for dissolved and sus-
pended matter, such as floatables. This report presents the results of the
eutrophication/general water quality model study.

In general, eutrophication refers to increased productivity and degraded
health of a water body as a result of excessive nutrient inputs. The health of a
system can be characterized in terms of the diversity and abundance of biolog-
ical communities. The term general water quality is used here to refer to the
more conventional water quality constituents that are used to measure the
health of a water body, such as dissolved oxygen (DO), nutrients, and algae.
The NYB is not considered globally eutrophic, but there are regions that
experience low dissolved oxygen in near-bottom waters, which is detrimental
to marine life. There is legitimate concern that human activities such as
municipal and industrial wastewater, combined sewer overflows, stormwater,
and various dumping operations may be increasing the eutrophication of the
Bight, as has happened in other coastal/estuarine systems around the United
States. The intent of the Section 728 legislation is to initiate activities that
could lead to improved awareness and protection of the New York Bight's
health. Numerical simulation models offer the most cost-effective and techni-
cally defensible means of assessing the impacts of natural events and human
activities.

Section 728 mandated studies to investigate the technical feasibility of
developing methods (e.g., modeling and monitoring) to assess environmental
conditions in the Bight and how the Bight environment will respond to human
influence. The term "technical feasibility" is used because the NYB system is
very large and complex. The system consists of tidally influenced estuaries,
harbors, and bays; Long Island Sound (LIS); the Apex region between the
open waters of the Bight and the harbors/estuaries; and the Bight, which

extends (for this study) from Cape May, NJ, northeasterly approximately
550 km along the coastline to Nantucket Island, MA, and extends approxi-
mately 160 km offshore to beyond the continental shelf. The depth of the
study site varies from 3 m to over 2,000 m seaward of the continental shelf.
The system is influenced by many physical processes, such as astronomical
tidal fluctuations, meteorological forcings, and large-scale oceanic circulation
patterns affecting the entire Middle Atlantic Bight. Significant local effects
include riverine inflows and bathymetric variations (Scheffner et al., in prepa-
ration). Water quality is affected by the above-mentioned physical processes
plus turbulent diffusion, material exchange with the atmosphere and bottom,
and chemical and biological processes. All of these factors and processes
present a substantial challenge for simulating the NYB system.

Objective

The objective of this study was to determine the technical feasibility of
developing a numerical eutrophication/general water quality simulation model
to assess the impacts of natural and human activities on the NYB. The best
way to investigate the feasibility of something is to create and develop it and
test it. This was the approach taken here.

Approach

The modeling technology recently developed for Chesapeake Bay (Cerco
and Cole 1989; 1992; in preparation) was applied to the Bight. This technol-
ogy consisted of three-dimensional (3-D), time-varying hydrodynamic and
water quality models. The hydrodynamic model (HM), which is described in a
separate report for the study (Scheffner et al., in preparation), provides the
circulation required by the transport terms of the water quality model (WQM).
The WQM is indirectly linked to the HM. Thus, the HM is applied, and the
output is stored and subsequently used as input for the WQM.

A workshop on Bight modeling was held in New York City (WMI 1989) at
the beginning of the Section 728 studies. One of the primary recommenda-
tions of this workshop was that the models should include the harbors and
estuaries, Long Island Sound, and the Bight out to the shelf-break. It is
important to capture the circulation among these three regions (e.g., Bight,
Sound, and harbors/estuaries). Therefore, this model does include all three
components.

Both the HM and WQM are mechanistic, deterministic, numerical models
based on conservation principles. The WQM is based on the conservation of
mass and includes sources and sinks of mass arising from kinetic reactions,
transfers, and transformations.

2

Application of the modeling technology to the Bight proceeded through the following steps:

a. Grid generation and WQM and HM linkage.

b. WQM and HM transport comparisons to test linkage.

c. Intratidal and intertidal transport tests.

d. WQM calibration for DO and nutrient simulation.

e. WQM sensitivity tests.

f. WQM demonstration of use for evaluating nutrient load reductions.

The DO hypoxia event of the summer of 1976 was selected for model application since this period had relatively abundant data and was a period of high environmental stress (i.e., low DO). The period April through September 1976 was used for steps *a* through *f* above.

Scope

The scope of the study reported herein was restricted to studying the feasibility of modeling this complex system. Although the models were calibrated and applied for various sensitivity conditions and nutrient loading scenarios, the results should not be used to judge the effects of altered nutrient loadings on eutrophication and water quality. This study did not include sufficient detail, accuracy, and degree of model calibration/verification required for a complete nutrient and eutrophication analysis.

This report documents the application steps *a* through *f* above. The steps were conducted concurrently with HM and WQM development. Steps *a* through *c* were conducted using a HM grid of 5 layers. Steps *d* through *f* were conducted using an enhanced HM grid of 10 layers with minor topographic changes.

Chapter 2 gives the model description, and Chapter 3 discusses WQM and HM linkage and transport comparisons. Chapter 4 summarizes input data and the use of water quality observations for model comparison. Chapter 5 presents the results of the model-prototype calibration, sensitivity tests, and demonstration scenarios. Conclusions and recommendations are discussed in Chapter 6.

2 Model Description

General

The NYB HM and WQM are based on the Chesapeake Bay modeling
system which consists of three interacting models: (1) the HM, (2) the WQM,
and (3) a bottom sediment diagenesis model (SM). The HM is an improved
version of CH3D (Curvilinear Hydrodynamics in Three Dimensions) developed
by Sheng (1986) for the U.S. Army Waterways Experiment Station (WES).
The HM was extensively modified in its application to Chesapeake Bay (John-
son et al. 1991a,b). The HM operates on an intratidal time scale (i.e., includes
tidal variations) and employs a curvilinear or boundary-fitted planform grid.
Two versions of CH3D are employed by WES: one version has stretched
(sigma) coordinates for the vertical dimension while the other has fixed verti-
cal, Cartesian coordinates, a modification for the Chesapeake Bay Study. The
sigma-stretched version was used for the NYB study. The HM was exten-
sively tested and verified during the Chesapeake Bay study (Johnson et al.
1991a).

The HM and WQM are operated as separate modules. Output from the
HM is written to a file that is subsequently used as input by the WQM. The
WQM can accept either intratidal or intertidal updates for hydrodynamics,
which are converted in a processor built into the HM (Dortch 1990). The
procedure is computationally efficient; numerous WQM runs can be executed
without recomputing the hydrodynamics.

The framework of the WQM (i.e., the Chesapeake Bay WQM and the
model used here) is based on the finite volume approach, similar to the
U.S. Environmental Protection Agency's (EPA) WASP (Water Quality Analy-
sis Simulation Program) model (Ambrose, Vandergrift, and Wool 1986).
Finite volume transport models, also referred to as integrated compartment and
multiple box models, have a desirable feature in that they can be linked to
finite difference and finite element hydrodynamic models.

Significant improvements were made to the solution schemes of the Chesa-
peake Bay model compared with WASP (Hall and Chapman 1982; Ray Chap-
man and Associates 1988; Hall 1990; Cerco and Cole, in preparation). The
solution recognizes terms in the horizontal plane and vertical direction. Thus,

4

explicit and implicit solution schemes are used in the horizontal and vertical dimensions, respectively. The implicit vertical solution can greatly reduce stability constraints on time-steps. A third-order accurate, upstream-weighted differencing scheme (QUICKEST, i.e., Quadradic Upstream Interpolation for Convective Kinematics with Estimated Streaming Terms, Leonard 1979) is used for the horizontal advective terms to greatly reduce unwanted numerical dampening. Additionally, the WQM time-step is variable and computed within the model based on stability requirements. The kinetic routines, which include the state variables and their interactions, were developed during the Chesapeake Bay Study (Cerco and Cole, in preparation).

The WQM and SM are run interactively rather than coupled indirectly as the HM and WQM. The SM, described by DiToro and Fitzpatrick (1992), simulates decay and mineralization (i.e., diagenesis) of organic matter deposited in the sediments and the exchange of nutrients, DO, and other substances between the sediments and overlying water column.

This study included the application of the HM and WQM, but the SM module was not used because little or no data required by the SM were available for this region when the study was initiated. Adaptation of the Chesapeake Bay WQM module essentially consisted of simulation of a subset of available state variables with minor coding changes to accommodate exclusion of the SM module and elimination of some state variables.

Model Adaptations

The Chesapeake Bay WQM simulated 22 state variables. A subset of 11 state variables were selected for the NYB application. Table 1 lists the state variables simulated in the NYB study and the naming conventions used in the NYB and Chesapeake Bay studies.

Although the SM module was not used, the WQM does have the option of specifying benthic fluxes as input data. Thus, benthic fluxes for sediment oxygen demand (SOD), NH_4-N, and NO_3-N were specified in this study.

Although most of the kinetic rate coefficients were specified in input files, some were hardwired in the computer code. Kinetic coefficients used in the NYB study are tabulated in Appendix A. The coefficients labeled "Hardwired" were coded, and the coefficients labeled "Input" were specified in input files.

Table 1 State Variables Simulated	
NYB	**Chesapeake Bay**
Temperature	Temperature
Salinity	Salinity
Net plankton	Diatoms
Nanoplankton	Green algae
Dissolved organic carbon (DOC)	DOC
Particulate organic carbon (POC)	Labile POC
NH_4-N	NH_4-N
NO_3-N	NO_3-N
Dissolved organic nitrogen (DON)	DON
Particulate organic nitrogen (PON)	Labile PON
DO	DO

3 Model Linkage and Transport Comparisons

The linkage and testing of the WQM and HM modules proceeded through three steps: (1) WQM grid generation and WQM and HM grid linkage, (2) WQM and HM transport comparison, and (3) intratidal and intertidal WQM transport tests. The linkage and testing were conducted using HM simulation conditions of tidal boundaries, wind, and freshwater flow.

WQM Grid Generation and Linkage

WQM grid generation is based on a HM grid file that includes node coordinates and cell depths. The HM grid file was used to construct a map file relating the HM and WQM grid cells. The WQM grid generation, WQM and HM grid linkage, and transport tests were conducted using a 76 × 44 HM grid consisting of 5 layers. Subsequent modifications of the HM grid consisted of (1) minor changes to the Connecticut shoreline and Upper Bay and (2) the use of 10 layers. Plate 1 displays the initial HM grid used for the transport tests while Plate 2 displays the final HM grid with changes to the Connecticut shoreline and Upper Bay. The HM grid depicted in Plate 2 was used for WQM calibration, sensitivity tests, and demonstration scenarios.

The WQM grid was a direct overlay (i.e., one-to-one cell correspondence) of the 76 × 44 cell HM grid. However, the row of HM cells along the ocean boundary were not included in the WQM grid to accomplish proper interfacing of the two models. Coding appended into the HM used the mapping information to initially write to an output file the initial cell volumes and time-invariant data that included cell surface areas and horizontal cell lengths. During the HM simulations, temporally averaged flows and vertical diffusivities were computed and written, along with cell volumes for mass continuity checks, to an output file. The details of these procedures are explained by Dortch (1990).

Proper linkage of the HM and WQM was ensured through mass conservation tests. Errors in the linkage are easily identified by observing cell mass deviations that cannot be accounted for through elementary mass balance

calculations. To conduct mass conservation tests, output data from the HM were used to simulate three conservative tracer scenarios: (1) initial conditions (IC) and boundary conditions (BC) of tracer concentration set to zero; (2) IC and BC of tracer concentration set to a constant; and (3) an instantaneous spot dump of tracer mass in the Apex with zero IC and BC for tracer concentration. In the first test, zero concentrations should be maintained throughout the grid if mass is conserved. In the second test, a constant concentration equal to the IC and BC should be maintained throughout the grid if mass is conserved. In the third test, no mass enters or leaves the grid, so the sum of the mass within the grid should equal the amount of mass dumped. Mass conservation was maintained (within the accuracy of the computer) in the three test scenarios indicating correct linkage.

HM Versus WQM Transport Comparison

Transport comparisons between the HM and WQM were required to verify that the WQM properly represented transport provided by the HM. It was assumed that the HM properly simulated transport in the prototype. The salinity state variable in the HM and WQM was used to simulate a conservative tracer. Two transport comparisons were conducted: (1) continuous tracer release in the Hudson River and (2) continuous tracer release in the Bight.

Hudson River continuous release

The Hudson River experiment consisted of maintaining a tracer concentration of 10 units in the column of cells corresponding to the junction of the Hudson River and Upper Bay. Plate 3 displays the location of the continuous release, cells sampled for time history plots, and cells sampled for transect plots. The grid displayed in Plate 3 is a window of the HM grid shown in Plate 1. Only a window of the grid is displayed in order to show detail. The solid shaded cell represents the location of the continuous release, the open circles represent the cells sampled for time series plots, and the solid lines represent the transects. Plate 4 is the time history concentration of corresponding HM and WQM cells. The cells displayed are surface cells located near the Brooklyn Bridge and near the Verrazano Narrows Bridge (WQM Cells 2422 and 2394, respectively). Plate 5 displays the two transects after 5 days. Transect 1 represents the surface cells extending north along the Hudson Canyon into Upper Bay. Transect 2 represents a transect extending from the Upper Bay, through East River, and into Long Island Sound. There was "exact" correspondence between HM and WQM transport using equivalent time-steps, flow updates at time-step intervals, UPWIND horizontal advection, and zero vertical advection. The HM and WQM were compared using UPWIND horizontal advection because the HM QUICKEST code required modification in order to handle the complex boundaries encountered in the Upper Bay. The HM QUICKEST code was being modified during the transport comparison.

8

Bight continuous release

The Bight continuous release experiment also demonstrated "exact" correspondence between HM and WQM transport using both the UPWIND and QUICKEST advection schemes. The HM and WQM were compared using the QUICKEST advection scheme because HM QUICKEST boundary formulations did not affect the simulations. The continuous release occurred in the Bight just seaward of the Rockaway Point-Sandy Hook Transect. Plate 6 shows the location of the release through solid shading and cells sampled for time series through open circles. Plates 7 and 8 are time series plots at corresponding WQM and HM cells using UPWIND and QUICKEST, respectively. The HM and WQM transport comparisons indicate that the WQM duplicates HM transport.

Intratidal and Intertidal Transport Comparison

The HM flows and vertical diffusivities can be averaged over intratidal periods (e.g., 1 to 2 hr) or intertidal periods (i.e. one or more tidal periods). The intertidal flows are averaged in a manner that preserves the residual currents associated with tidal forcing. The procedure involves approximating the Lagrangian residual velocities as the sum of the Eulerian and Stokes velocities (Dortch 1990). The use of intertidal hydrodynamics reduces time-step restrictions in the WQM and greatly reduces the amount of hydrodynamic information that must be stored and read in during WQM execution, thus reducing WQM execution time and disk storage needs.

During the sequence of mass conservation tests, stable time-step sizes for both intratidal and intertidal averaging were calculated. One hour intratidal averaging permitted a WQM time-step of 17 min and a 12.5 intertidal averaging permitted a 52-min time-step. The 52-min time-step represents a lower bound of the possible time-step because the calculated time-step in the WQM was limited to a maximum of 60 min. Intertidal averaging decreases required computer execution time. However, prior to the use of intertidal averaging, it is important to ensure that intertidal averaging duplicates intratidal transport.

A second HM and WQM Bight tracer comparison was conducted using intratidal (1-hr) and intertidal (12.5-hr) averaging. Instead of a continuous release, a spot dump was simulated. The tracer was uniformly injected over the depth. Plate 9 displays the location of the release and two perpendicular transects through the spot dump. Plate 10 represents the perpendicular transects through the spot dump area after 20 days using 1-hr intratidally averaged flows. Transect 1 represents the surface cells extending north along the Hudson Canyon into Upper Bay. Transect 2 represents a transect extending from the New Jersey Coastline to Long Island. There was good agreement between HM and WQM transport using 1-hr intratidal averaging.

Plate 11 demonstrates the same perpendicular transects using 12.5-hr intertidal averaging. Examination of Plate 11 reveals that a phase error is

detectable and a specification of 5 m² sec⁻¹ horizontal diffusion in the WQM was necessary to match the tracer magnitudes. The tracer tests used are extremely dynamic; the tracer front is being advected through a cell in a few hours. Any time averaging compromises the transient transport information. Information lost resulted in the appearance of phase error and required the addition of diffusion. However, even considering the difficulty of simulating a spot tracer dump in the Bight, the tracer experiment confirmed that with intertidal averaging the WQM could duplicate HM transport in the Bight. Except for accidental spills, water quality constituents in the Bight do not exhibit such strong gradients as were simulated in the spot dump. Therefore, intertidal averaging is appropriate for water quality simulation in the Bight. For simulating spills or other localized conditions with extremely sharp gradients, 1-hr hydrodynamic updates should be used in the WQM, or the particle tracking model that was developed as a part of the NYB study should be used.

In contrast with the Bight, the current dynamics of the Upper Bay and East River display greater magnitude and nonlinearity. A series of experiments were conducted in order to determine if intertidal averaging could be used for the Upper Bay/East River and select the optimum time-averaging interval. The experiments consisted of using 1-hr averaging as the base and comparing different averaging intervals. The comparisons were between WQM   and did not include HM tracer comparisons.

The experiments consisted of continuous release distributed uniformly from top to bottom in the water column at the junction of the Hudson River and Upper Bay. Plate 12 displays the location of the release through solid shading and cells sampled for time series through open circles. The sampled cells displayed are surface cells in the Upper Bay and near the Verrazano Narrow Bridge. The release cell is at the junction of the Hudson River and Upper Bay. Plates 13-17 represent the results of 1-hr intratidal, 4-hr intratidal, 8-hr intratidal, 12-hr intratidal, and 12-hr intertidal averaging for the continuous release experiment, respectively. Intratidal is used here to refer to Eulerian averages, and intertidal refers to Lagrangian averages. The HM was executed for 90 days with flow averaging recorded for a 30-day period extending from the 61st through 90th day of HM execution. The WQM simulated a 300-day period by repeating the 30-day HM record. Tracer concentrations were recorded at 1-hr intervals for plotting. To compare the different flow-averaging intervals, the plotting data were filtered with a running 12-hr average.

Examination of the plates reveals that 1- and 4-hr intratidal averaging results in nearly equivalent asymptotic results while 8- and 12-hr intratidal averaging results in a decrease in magnitude. The 12-hr intertidal averaging resulted in simulated concentrations that asymptotically approached an equilibrium value slightly exceeding the 1- and 4-hr values.

Intratidal transport with averaging intervals greater than 4 hr should not be used, especially in the bays and harbors of this system. Lagrangian residual processing should be used for intertidal transport. This procedure works well

10

for the Bight region and fairly well for the bays and harbors since the intertidal transport was roughly equivalent to the HM and the 1-hr transport. Although the intertidal transport through the transect is believed to be properly preserved, it was not actually tested. In retrospect, it should be verified that the first-order, Lagrangian residual, intertidal transport procedure does yield the proper net flux of material through the transect. Such tests should be conducted during the initial phases of any future Bight modeling.

11

4 Input Data

General

The eutrophication WQM required six types of input data:

a. Hydrodynamic transport information.

b. Boundary conditions and external loadings for modeled constituents.

c. Meteorological data.

d. Initial constituent concentrations.

e. Kinetic coefficients for transfers and transformations.

f. Observed water quality data for calibration.

Hydrodynamic transport information was stored during HM simulation as discussed in Chapter 3. Boundary conditions, external loadings, initial conditions, and water quality data for calibration were extracted from existing water quality observation data sets. Meteorological data were obtained from weather station observations. Kinetic coefficients were adjusted during model calibration, but were kept within expected bounds based upon previous modeling experience and values reported in the literature.

WQM calibration, sensitivity tests, and demonstration scenarios were conducted with the grid depicted in Plate 18, which included 10 vertical layers. Plate 19 is the transformed grid corresponding to the physical grid shown in Plate 2. The transformed grid, which is used in the HM solution, is included to more easily identify the location of a cell when given the HM grid coordinates. The WQM grid (Plate 18) was a direct overlay of the 76 × 44 cell HM grid. The row of HM cells along the ocean shelf boundary was not included in the WQM grid to accomplish proper interfacing of the two models. The WQM used 25,010 computational cells.

Hydrodynamic output required by the WQM includes initial cell volumes, surface areas, and horizontal cell dimensions; three-dimensional flows for all

12

cell faces; and vertical eddy diffusivities. Time of each hydrodynamic update and cell volumes for each update are also output for continuity checks.

Water quality observations were used by the WQM to specify initial and boundary conditions and external loadings, and were used for calibration comparisons. Readily available water quality data sets collected during 1975-1976 within the NYB were compiled, documented, and furnished in digital form by Creative Enterprises, Inc., and Han & Associates, Inc. (1990). The use of water quality data is described in more detail in the next section. Kinetic coefficients are discussed in Chapter 5.

Daily averaged solar radiation, water equilibrium temperatures, and coefficients of surface heat exchange were computed from meteorological data. Solar radiation values were used in the algal growth functions, and the equilibrium temperatures and the surface heat exchange coefficients were used as input for temperature simulation (Edinger, Brady, and Geyer 1974). The computations of these three variables from meteorological data were based on a Heat Exchange Program (Eiker 1977). The U.S. Air Force Environmental Technical Applications Center provided meteorological data in the form of Tape Deck 1440 WBAN Hourly Surface Observations for JFK Airport. Algal growth functions also required estimates of photoperiod. Photoperiod, the daylight fraction of a 24-hr day, was computed using a formula in Stoddard (1983).

Use of Water Quality Observations

The use of observed water quality data for initial conditions and boundary conditions is described in this section. The special treatment of observations for WQM calibration comparisons is described in Chapter 5 (Application Results).

Initial conditions

The WQM simulations extended from 15 Apr through 30 Sep 1976. Initial conditions were specified for each of the WQM state variables and for each cell at the initiation of the simulation. The water quality data collected during April 1976 were used to specify initial conditions. Because of the sparsity of data, initial conditions had to be specified on a regional basis. This was accomplished with an overlay grid.

A coarse overlay grid was superimposed on the transformed WQM grid (Plate 20). The 15 coarse grid cells roughly correspond to available data and the study area's bathymetry. Table 2 lists the number of surface cells included in the coarser grid cells and the average depth of the coarser grid cells.

Table 2 Attributes of Coarse Overlay Grid Used for Initial Conditions		
Overlay Cell No.	Number of Surface Cells	Average Depth, m
1	76	6
2	34	12
3	236	22
4	140	18
5	186	24
6	277	27
7	208	43
8	130	39
9	157	42
10	169	53
11	264	70
12	192	132
13	120	118
14	156	124
15	156	143

The coarse overlay grid also had 10 vertical layers. The observed data were assigned to each of the 150 cells (15 surface coarse grid cells × 10 layers) based on its horizontal location and depth of collection. The observed data for each coarse grid cell/layer were averaged to obtain a single value for that coarse cell/layer. Measured data were not available for assignment to each of the 150 cells; however, each coarse cell required an assignment for each state variable. The following procedure was used to assign missing values. Examination of observed data revealed two vertical patterns of distribution which were used for vertical assignments. One pattern, exemplified by all the state variables except plankton, varied with depth from a surface value to a value that remained constant through most of the water column. The depth at which values approached constancy corresponded to the depth of the pycnocline. The second pattern was characteristic of the phytoplankton. Maximum values occurred near pycnocline depth with minimum values at the bottom. Based on these observed vertical distributions, missing horizontal cells for the surface, middle, and bottom layers for the plankton and surface and bottom layers for the other state variables were assigned to the coarse grid. Assigned values were selected to maintain existing gradients. Values were interpolated for layers that did not have data as explained in the next paragraph. The initial condition values used for the 150 coarse overlay cells are tabulated in Appendix B. Observed values are underlined. The same overlay values were

14

then used for the initial conditions of each computational cell within the coarse overlay cell and layer.

The initial condition file listed in Appendix B specifies three values for net plankton and nanoplankton corresponding to surface, pycnocline, and bottom. All the other constituents specify two values, representing surface and bottom. For constituents with two values, the above pycnocline layers were assigned values varying linearly between the surface and bottom value. The below-pycnocline layers were assigned the bottom value. For plankton, the layer assignments were assigned through a parabolic function. For layers above the pycnocline, the pycnocline value was reflected through the surface; for layers below the pycnocline, the pycnocline value was reflected through the bottom.

Reflection needs some explanation. Three noncoincident points uniquely specify the coefficients of a parabola. The reflection of the pycnocline value through the bottom implies that an imaginary point of value equal to the pycnocline value is specified below the bottom. The distance below the bottom of the imaginary point is equal to the distance between the pycnocline and bottom. A parabola is then fitted using the pycnocline value, bottom value, and the imaginary value located below the bottom. Reflection through the surface is similar; the three points represent the pycnocline value, surface value, and an imaginary value located above the surface. The above-surface, imaginary point has a value equal to the pycnocline value and is located above the surface a distance equal to the distance between the pycnocline and surface. The reflection procedure was used to ensure maximum phytoplankton at pycnocline depth with rapid attenuation to surface and bottom values. The pycnocline depth was uniformly specified as 20 m for cell column.

Boundary conditions

Boundary condition files include the temporal and spatial specification of constituent concentrations for the seaward boundary and Hudson River, and specification of external mass loadings for all other sources of nutrients/water quality. Boundary condition files are also used to specify meteorological data and sediment-water fluxes. Monthly updates were used for the seaward boundary and the Hudson River, and the external mass loadings were held constant. These update frequencies were considered adequate for the purpose of this study, that is, a *feasibility* study. For a comprehensive eutrophication/nutrient analysis, more frequent updates should be used, such as daily or weekly updates for the Hudson River and monthly updates for external loadings.

Seaward boundary. Measured data collected seaward of the shelf break boundary, seaward of Atlantic City, and seaward of Montauk Point were used to prepare seaward boundary conditions. The seaward boundary was divided into seven segments, shown in Plate 21. Segment 8 refers to the Hudson River boundary segment, which is described below. The boundary condition values are tabulated in Appendix C. Observed values are underlined. The seaward boundary condition values were specified similarly to the initial condition files:

(1) assign observed data to each of the 840 space-time slots (7 surface segments × 10 layers × 12 months) and (2) assign layer values based on surface, pycnocline, and bottom values as described above. Then each computational cell is assigned the space-time slot value based on the simulation clock time and the cell location with respect to the segments and layers. Each entry in Appendix C corresponds to a surface, pycnocline, and bottom space-time slot. Examination of Appendix C reveals the sparsity of data available to fill the space-time slots. Empty space-time slots were filled. The criterion used for filling empty space-time slots was maintenance of spatial and temporal continuity.

Hudson River upstream concentrations and loadings. Water quality constituents can enter the Hudson River as "upstream" inputs (i.e., upper watershed runoff) and local point and nonpoint source loads (i.e., municipal and industrial discharges and tributaries that enter the Hudson downstream of the upstream model limits for the river). The Hudson River upstream inputs were specified in two ways, as concentrations and mass loadings. Temperature, salinity, and DO were specified as monthly varying boundary concentrations. Temperature values were calculated monthly averaged equilibrium temperatures. Dissolved oxygen values represented 80 percent saturation at the specified temperature and salinity. Salinity was specified constant at 20 parts per thousand (ppt). The Hudson River boundary segment is noted as Segment 8 on Plate 21, and the monthly temperature, salinity, and DO concentrations are tabulated in Appendix C.

Due to data limitations, it was necessary to use mass loadings for the other water quality constituents entering through the upstream model limits for the Hudson River. The USGS published daily measured flows at Green Island, downstream from the Troy and Mohawk River locks and dams. Mueller et al. (1976) published water quality data collected near Poughkeepsie, which is downstream from Green Island. Mueller used drainage basin areas and their ratio to compute a factor of 1.45 for scaling measured flows from Green Island to estimated flows at Poughkeepsie. Measured USGS flows at Green Island, Meuler's measured water quality values (Table 3), and the scale factor of 1.45 were used to compute daily Hudson River tributary mass loads.

Simulation period and annual averages of the computed daily loads for 1976 are compared in Table 4 to annual average daily loads estimated by Mueller et al. (1976). Table 4 reveals that the computed loads used in this study are nearly equivalent to those reported by Mueller et al. (1976). More accurate procedures for estimating Hudson River loads should be explored for a comprehensive eutrophication/nutrient analysis.

Constant external constituent loads. Constant external constituent loads (kilograms per day), arising from local runoff, point source discharges, and dump sites, were defined as follows:

16

Table 3 Upstream Hudson River Measured Concentrations	
Constituent	Concentration, g m⁻³
DOC	4.575
POC	1.525
NH₄-N	0.30
NO₃-N	1.03
DON	0.372
PON	0.248

New York-New Jersey Harbor and estuaries
  (referred to as Transect region)
New Jersey (NJ) Coast
Long Island (LI) Coast
Sewage sludge dump site
Dredged material dump site

The constant external constituent loads used in this study are listed in Table 5 and were extracted from Mueller et al. (1976). The Transect external loads included wastewater discharges and Mueller's ungaged runoff loads (Hudson River drainage below Poughkeepsie, New York City area, and New Jersey ungaged area extending north from Sandy Hook along Raritan Bay to the Hackensack River). The New Jersey Coast external loads included wastewater discharges and surface runoff. The Long Island Coast external loads included wastewater discharges, surface runoff, and groundwater mass loads.

The constant external loads were inserted uniformly throughout the 10 layers. The Transect, NJ Coast, and LI Coast loads were distributed uniformly in cells adjacent to the shoreline. Sewage sludge dump site loads were inserted in the cells corresponding to 44°22'30"-40°25'00" N Latitude, 73°41'30"-73°45'00" W Longitude. The dredged material dump site loads were inserted in the cells corresponding to 40°23'38"-40°21'28" N Latitude, 73°51'28"-73°50'00" W Longitude.

Sediment/water column boundary. The sediment/water column interface boundary condition was specified as temporally and spatially constant for SOD and ammonium (NH₄-N) release. Both SOD and NH₄-N releases were modulated through temperature and DO concentration of overlying water. The sediment ammonium release at reference temperature and with overlying oxygenated water was 0.045 g N m⁻² day⁻¹. Ammonium release increased with a decrease in DO. The SOD and ammonium release functions are described in Appendix A.

Table 4
Computed and Reported Hudson River Upstream Loads

Constituent	Loading, tons day[-1]
Computed average loads, 1 Apr through 30 Sep 1976	
DOC	229.98 |
POC	76.66 | sum 306.64
NH$_4$-N	15.06
NO$_3$-N	51.78
DON	18.70 |
PON	12.47 | sum 31.17
Computed average loads, 1 Jan through 31 Dec 1976	
DOC	238.56 |
POC	79.52 | sum 318.01
NH$_4$-N	15.64
NO$_3$-N	53.71
DON	19.40 |
PON	12.93 | sum 32.33
Mass loads reported by Mueller et al. (1976)	
TOC	320.
NH$_4$-N	16.
NO$_3$-N	54.
TON	32.

Note: All units shown as tons and metric tons.

Table 5
Constant External Constituent Loads, tons day[-1]

Zone	DOC	POC	NH$_4$-N	NO$_3$-N	DON	PON
Transect	862.	288.	126.	14.	59.	39.
NJ Coast	9.	26.	6.	13.	3.	2.
LI Coast	12.	4.	6.	2.	2.	1.
Sewage sludge		110.	10.			7.
Dredged material		540.				63.

An examination of available SOD measurements for both 1974 and 1975 revealed that data were spatially limited to collection in the Apex only (Plate 22). The reported SOD data had been normalized to 20 °C. The SOD data were further normalized to nonoxygen limited values by assuming a DO half-saturation constant of 2.0 g O_2 m^{-3} and using recorded overlying water DO concentration values. Table 6 displays the measured SOD values and the number of observations. The rows and columns represent the corresponding HM (i,j) cells. The arithmetic average of all normalized SOD measurements was 0.88 g O_2 m^{-2} day^{-1}. Because of the limited spatial extent of SOD measurements and the feasibility aspect of this study, a spatially and temporally constant SOD value of 1.0 was used. A sensitivity test of SOD is described later in this report.

Table 6
Observed SOD (g M^{-2} day^{-1}) and the Number of Observations for 1974-1975

	20	21	22	23	24	25	26	27	28	29	30	31	32	33	34	35	36	37	38	39	
38												0.97 2									38
37														0.74 4							37
36												1.02 4			0.67 6	1.14 3					36
35										0.48 6		0.61 5	0.85 3			0.38 3		0.73 8			35
34				1.26 1			0.65 5			1.50 3	1.72 4			1.15 8		0.80 5	0.81 3	0.54 1	0.34 1		34
33			0.57 4		0.62 5	1.85 1		1.14 10				1.00 5	1.02 5		0.76 4			0.60 8	0.43 3		33
32		1.48 6			0.62 6			1.08 5		0.89 5	0.95 4		1.19 5	0.82 4		1.11 5	0.87 6			0.43 1	32
31	0.70 5		0.99 4				0.99 1		1.21 9			0.97 5	0.80 4		1.45 1	0.94 5		0.73 5			31
30			0.33 2		0.75 4			1.32 9		0.84 3	0.72 3		1.03 5	1.82 1		0.94 1	0.31 1				30
29				0.92 2		0.76 4	0.71 2		0.54 3	0.46 5		0.87 7			0.60 5						29
28					1.08 2		0.78 4	0.37 1					1.21 1	0.75 1							28
27							0.85 4		0.69 4		0.36 4										27
26							1.72 1			1.02 2											26
25								1.45 2													25
	20	21	22	23	24	25	26	27	28	29	30	31	32	33	34	35	36	37	38	39	

Note: Row and column numbers are HM (i,j) coordinates.

5 Application Results

The summer hypoxia event of 1976 was selected for the WQM application. The 1976 hypoxia event was selected because Dr. Andrew Stoddard (Stoddard 1983) conducted a comprehensive and thorough search and analysis of existing data and literature concerning the eutrophication and oxygen depletion in the New York Bight, and developed and applied a mathematical model of oxygen depletion of the 1976 hypoxic event in the New York Bight. Dr. Stoddard's effort provided a basis for the evaluation of the WQM application. The model was first calibrated (i.e., parameters were adjusted) against observed data for this period. Sensitivity studies were then conducted with the model to investigate the importance of some parameters and boundary conditions. The WQM was run with variations in nutrient loadings to demonstrate model utility and to obtain a better sense of the effect of loads on the system.

The WQM was also used to investigate the causes of the New Jersey nearcoast hypoxia, the event that occurred during the 1976 hypoxia. Finally, LIS external loads were included and results were re-evaluated. Water quality data for LIS external constituent loads were not readily available at the initiation of the study, and observations for calibration within LIS were not provided in the observation data sets. Calibration, sensitivity tests, and load reduction scenarios were conducted without LIS external loads. An investigation was conducted to examine the impact of LIS external loads on the DO resources of the Bight.

The HM simulation extended from 1 Apr through 30 Sep 1976, for 183 days. The HM output was averaged over 12.5-hr intervals beginning 15 Apr and written to a file for subsequent input to the WQM. The 183-day HM simulation required 31 hr of computation time on a CRAY Y-MP. The 168-day (15 Apr through 30 Sep) WQM simulation required 2 hr.

Model-Prototype Calibration

The temporal and spatial sparsity of prototype observations for water quality made model-prototype comparisons difficult. Monthly temporal averaging of all prototype measurements and model simulations was done to mitigate the

temporal sparsity of prototype observations. Several additional techniques were used to provide meaningful model-prototype comparisons:

1. Scatter plots

2. Regional and point comparisons

    a. Spatial average

        (1) Time series plots
        (2) Depth profiles

    b. Depth profiles at specific locations (point comparisons)

3. Transect plots

4. Statistics

An explanation of each of the above comparison methods is discussed in its respective section along with the results. The model-prototype calibration plots are displayed in Appendix D.

Scatter plots

Measured data were aggregated by region (Apex, NJ Coastal Zone, etc.), layer, and month. Each measured datum was associated with the corresponding aggregated simulated result and displayed by plotting. The aggregation procedure is discussed more completely in the next section. The scatter plots display predicted versus observed data for all regions and were effective for gross qualitative calibration.

Plate D1 displays the scatter plots for the calibration run. Examination of Plate D1 provides a quick reference as to how well the model matches observations. Plate D1 indicates that simulated net plankton, DOC, and POC were generally underestimated. However, Appendix B, Initial Conditions Constituent Concentrations, and Appendix C, Boundary Constituent Concentrations, indicate that few net plankton, DOC, and POC measurements were available for initial condition and boundary specification. Future studies should attempt to fill this data gap.

Regional comparison

There were few stations that were frequently sampled at the same location. One technique used to provide meaningful model-prototype comparisons was spatial aggregation to provide larger sample sizes. This technique consisted of computing monthly averages of multiple station values that were contained within a region. The NYB was subdivided into 11 regions as shown in

22

Plate 23. The segmentation scheme is a modification but reflects the segmentation used by NOAA (1979). No data were provided (by Creative Enterprises and Han & Associates 1990) for LIS, and data obtained in the eastern (upcoast) regions were used for upcoast boundary conditions. Therefore, the eastern regions were not included in comparisons of model versus observed data, but LIS results (Region 11) were included in the sensitivity studies to observe the test effects on the Sound. Values for the number of surface cells and average depth of the 11 spatial aggregates are given in Table 7.

Table 7 Regional Spatial Aggregates		
Region	No. Surface Cells	Average Depth, m
1. Apex	184	22.
2. NJ nearshore (<30 m)	213	21.
3. NJ midshelf (30-60 m)	252	42.
4. NJ shelf (>60 m)	123	96.
5. HR midshelf (30-60 m)	119	48.
6. HR shelf (>60 m)	99	152.
7. LI nearshore (<30 m)	80	27.
8. LI midshelf (30-60 m)	382	45.
9. LI shelf (>60 m)	313	134.
10. Transect	77	6.
11. LI Sound	179	17.
Note: NJ is New Jersey, HR is Hudson River, and LI is Long Island.		

The use of regional aggregates can also result in biases that confound model calibration. The model results were averaged for all model time-steps within a given month and for all model cells within the region, thus producing a true monthly, regional average. However, the prototype data are far from representing true monthly, regional averages because of the sparsity of data. Therefore, specific sampling locations were selected to compare measured and simulated data. The sample locations selected for point comparisons were based on the availability of data (e.g., temperature, salinity, and dissolved oxygen). Plate 23 displays the relationship between the spatial regions and selected point comparisons. The regions are outlined with bold lines and the selected points marked with solid circles. Table 8 lists the corresponding surface HM and WQM cell and depth of the selected points.

The ordered (i,j) following the regional name in Table 8 represents the corresponding HM surface cell. The regional spatial comparisons were displayed through depth profiles for various months and time series for a layer

Table 8 Selected Point Comparisons			
Region	HM Cell	WQM Cell	Depth, m
1. Apex	(31,32)	2083	21.
2. NJ nearshore (<30 m)	(4,19)	1261	22.
3. NJ midshelf (30-60 m)	(22,16)	1057	44.
4. NJ shelf (>60 m)	(17, 4)	164	104.
5. HR midshelf (30-60 m)	(30,20)	1361	42.
6. HR shelf (>60 m)	(26,11)	693	66.
7. LI nearshore (<30 m)	(45,25)	1746	34.
8. LI midshelf (30-60 m)	(46,20)	1377	36.
9. LI shelf (>60 m)	(43, 8)	465	73.
10. Transect	(31,38)	2306	9.

(i.e., near surface or near bottom). The point comparisons were displayed through depth profiles at points corresponding to the spatial comparisons.

The depth profiles display simulated and measured constituent values as a function of model layer. It is important to note for plot interpretation that the Tables 7 and 8 list the depths for each region and point that can be used to compute depths. For example, the NJ Nearshore region has an average depth of 21 m while the NJ Shelf region has an average depth of 96 m (Table 7). The WQM vertical grid has 10 equally thick layers; therefore, the center of the bottom layer of the NJ Nearshore represents a depth of 20 m while the center of the bottom layer of the NJ Shelf represents a depth of 91 m. The measured prototype data are presented at the appropriate layer depths. The results of the depth profiles follow the time series plots.

Time series. The time series plots represent the monthly averaged surface and bottom layer model and prototype data for each region between April and September 1976. Plates D2 through D9 display regional time series for constituents as follows:

24

Plate	Constituent
D2	Temperature
D3	Net plankton
D4	Nanoplankton
D5	DOC
D6	POC
D7	Ammonium nitrogen
D8	Nitrate nitrogen
D9	DO

Plate D2 indicates that simulated temperatures approximate measured values. Time series of simulated and measured DO (Plate D9) also indicate relatively close agreement. However, the surface and bottom layer simulated DO exceeded measured values in the Transect region. Furthermore, simulated bottom DO in the Transect region frequently exceeded surface values. The excessive DO computed in the Transect region is attributed to the nanoplankton blooms that occurred in the modeled Transect region. Nanoplankton photosynthesis, with resulting DO production, was high in Raritan Bay and occurred throughout the model depth. The column depths of the cells in Raritan Bay were 3 to 6 m. It is not known how excessive the model algal production is since there are no nanoplankton observations in the Transect region. It is speculated that model production should be decreased in this region through light attenuation associated with suspended solids. It is feasible for surface DO concentrations to be lower than bottom values since the surface layer would rapidly equilibrate toward saturation through release to the atmosphere. A reasonable hypothesis is that prototype bottom layer DO concentration was less than simulated. Suspended solids would attenuate light transmission, resulting in little photosynthetic DO production in the lower layers.

Plates D5 and D6 (DOC and POC time series) indicate temporally sparse measured data. The large average values of POC in the transect are due to the large simulated nanoplankton concentrations (Plate D4). Algal carbon is added to the state variable POC for display since the sum of the state variables POC, net plankton carbon, and nanoplankton carbon approximates the laboratory measurement of POC. Net plankton concentrations were low and visually appear diminutive (Plate D3) because of the selection of the ordinate values for display; the maximum value of 20 mg Chl m^{-3} was selected because of the one measurement observed in May in the bottom layer of the Hudson River Mid-shelf region.

The WQM underpredicted DOC in the Apex yet overpredicted DOC in the Transect. The excessive DOC in the Transect is the result of hydrolysis of the large values of POC computed, due to nanoplankton computed. However, the model underpredicts DOC Bight-wide. The underprediction is reflected in the

DOC scatter plot (Plate D1). It is believed that the ocean contains refractory DOC that degrades very slowly. The model has only one DOC variable. To more accurately simulate DOC, the model should have two DOC variables, labile and refractory. Labile DOC degrades much faster than refractory DOC. Presently, the model DOC degrades at rates more representative of labile DOC.

Examination of Plate D7 indicates a spike in ammonia during May in the Transect. There were no measured ammonia values in the Transect during the period, but examination of Plate D8 reveals a spike in measured nitrate during May, which lends some credibility to an ammonia spike since ammonia oxidizes to nitrate.

Profiles. Plates D10 and D11 display regionally averaged, vertical profiles for temperature and DO, respectively, for the month of August. In the shallow waters, such as the Transect region, both measured and observed temperature and DO indicate a well-mixed water column. In the deeper waters, the vertical profiles of temperature indicate similar surface and bottom temperatures for both measured and simulated data, but the depths of the thermocline are generally deeper for the measured data (e.g., HR Shelf and NJ Shelf). It is hypothesized that these disagreements are the result of too little vertical diffusion in the surface layers in the deeper waters. The vertical diffusion used in the WQM is an output variable from the HM. Earlier HM output had produced too much vertical mixing, whereas these final results seem to produce too little mixing. Clearly, future efforts should focus on more accurate representation of vertical diffusion in the HM through one of the higher order turbulence closure models that are available.

The discrepancies between measured and simulated vertical profiles of temperature and DO were similar (Plates D10 and D11). Notably, the simulated DO was about a factor of two greater than that measured in the Transect, due to excessive algal production in this region. The reason for this problem was discussed above in the explanation of the DO time series plots (Plate D9). Also, as stated earlier, the sparsity of DO observations in the Transect region may make comparisons of regionally averaged DO meaningless for this region.

Vertical profiles in August 1976 were compared to simulated results at specific stations, rather than using regional averages, as shown in Plates D12 and D13 for temperature and DO, respectively. Comparison of the computed area and point profiles indicates similar vertical distributions. However, the computed thermocline depth was deeper at the point (28,11), HR Shelf, than the average over the region, thus comparing more closely with the average measured profile for this region. The simulated bottom DO values for point comparisons were less than the area averages.

Transects

Transect plots are another procedure for comparing model-prototype results. Plate 24 shows the five transects that were used. Their location and width

were selected to maximize the amount of available prototype data. With this technique, model results and observations were averaged over each month and across the transect. The results were plotted as monthly averaged surface and bottom layer concentration versus distance from the seaward boundary along the transect.

Plates D14 and D15 display surface and bottom transect plots for August 1976 for temperature and DO, respectively. The temperature transects indicate that simulated temperatures match well the measured temperatures for August.

Examination of DO transects (Plate D15) reveals that, overall, the computed and observed DO match fairly well except for the bottom layer, nearshore of Transect 1, where computed values exceeded measured values. Several things could have led to this discrepancy, such as monthly averaging of model results and the use of constant shoreline and point source loads and monthly updates for boundary loads. Examination of the submonthly, time-varying simulated DO (at model time-step intervals) for the bottom layer of Transect 1 indicated that simulated DO was less than 1.0 g m^{-3} at times. However, the model results in Plate D15 represent monthly averages. Monthly averaging may provide adequate resolution for the detection of seasonal trends, but it attenuates extremes that occur over a few days and may fail to detect trends occurring on the time scales of days and weeks. The measured data are not a true monthly average since the data are rather sparse in time. Finally, the model may not be fully capturing all the oxygen demand that existed in this part of the Bight, as a result of inadequate depiction of loadings, SOD, or some other process.

Statistics

In addition to the qualitative model-prototype comparisons provided by plots, a suite of statistical measurements were used to compare observed and simulated DO concentrations, since DO is the primary variable of interest in this study. All available DO measurements collected between 15 Apr and 30 Sep 1976 were temporally and spatially associated with simulated predictions and the following statistics were computed:

1. Mean Error, ME

$$ ME = \frac{\sum (P_i - O_i)}{n} \tag{1} $$

where

P = predicted value
O = observed value
n = number of observations

2. Absolute Mean Error, AME

$$AME = \frac{\sum(|P_i - O_i|)}{n}$$ (2)

3. Root-Mean-Square Error, RMS

$$RMS = \sqrt{\frac{\sum(P_i - O_i)^2}{n}}$$ (3)

4. Relative Error, RE

$$RE = \frac{\sum(|P_i - O_i|)}{\sum(O_i)}$$ (4)

The calibration statistics for DO are given in Table 9. A total of 3,664 proto-type observations were available for the calculation of the statistical measures.

Table 9 Calibration Statistics for DO	
Statistic	Value
Mean Error	-0.55 g O_2 m^{-3}
Absolute Mean Error	1.69 g O_2 m^{-3}
Root-Mean-Square Error	2.20 g O_2 m^{-3}
Relative Error	0.09

A mean error of zero is ideal. A negative mean error indicates that on the average the model underpredicts, while a positive mean error indicates over-prediction. Examination of the mean error indicates that overall the model underpredicted measured values on the average by 0.55 g O_2 m^{-3}. Although some of the discussion above focused on areas where the model overpredicted DO, the overall underprediction trend is also evident in the scatter plot of Plate D1. An absolute mean error of zero is ideal. The absolute mean error is a measure of the magnitude of the average deviations between predictions and observations. The calculated absolute mean error of DO for the calibration was 1.69 g O_2 m^{-3}. The root-mean-square error is an indicator of the spread of error between predictions and observations. The relative error is the ratio of the absolute mean error to the mean of the observations. The error statistics are relatively high compared with other modeling studies, such as Chesapeake Bay (Cerco and Cole, in preparation), which underscores the difficulty of mod-

28

eling the NYB. The fact that the sediment quality model was not activated
may have contributed to the error.

Sensitivity Tests

Following preliminary model calibration, the WQM was exercised, as dis-
cussed in this section, to investigate Bight flushing characteristics and
questions concerning input for model boundary conditions. The preliminary
calibration run differs from the current calibration run (presented herein) in the
base sediment NH_4 release rate and the temperature effect on SOD. The pre-
liminary calibration used a base sediment NH_4 rate of 0.1 g N m^{-2} day^{-1} and a
SOD temperature rate coefficient of 1.07. The preliminary calibration run as
well as the sensitivity test runs used equivalent kinetic and boundary values
except for the values being test.

Flushing analysis

A test was conducted to estimate "flushing time" for the NYB. The pur-
pose of the test was an order-of-magnitude evaluation of the time required for
conditions within the Bight to be flushed by flows through the boundaries.
The flushing analysis also provides an estimate of the "memory" time of the
Bight. The test consisted of using a uniform initial conservative tracer con-
centration of 100 units m^{-3} in each WQM cell and tracer boundary condition
concentrations of 0.0. The boundary conditions ensured that any tracer passing
out of the Bight would not return. The WQM simulation extended from
15 Apr through 30 Sep 1976. The number of units remaining at the end of
each month was recorded and used to estimate the flushing time (Table 10).
The number of units, which is in the form of mass, was obtained by multiply-
ing the cell concentration times the cell volume.

Examination of Table 10 reveals that 2.0699×10^{15} units were flushed out
of the NYB in 154 days and that the decrease was exponential with a decay
coefficient of 6.0265×10^{-3} day^{-1}. Using the exponential decrease and the cal-
culated decay coefficient, 50 percent of the tracer is flushed out of the NYB in
115 days; thus, in one year, only about 11 percent of the tracer is remaining.
The flushing analysis therefore indicates that the flushing time of the NYB is
on the order of a year.

Examination of surface and bottom tracer concentrations during the months
of July and August 1976 revealed that transport of tracer was upcoast from the
southwest to the northeast as evidenced by lowest concentrations in the south-
west and highest concentrations in the northeast. The simulated upcoast circu-
lation is consistent with observed hydrographic flow anomalies that occurred

Table 10 Conservative Tracer Flushing Results		
Date	Julian Day	No. Units Remaining x 16⁻¹⁵
30 Apr	121	3.4231
31 May	152	2.5997
30 Jun	182	2.0256
31 Jul	213	1.7627
31 Aug	244	1.5969
30 Sep	274	1.3532

from late spring until mid-August with the passage of Hurricane Belle (NOAA 1979).

Model boundary conditions

Sensitivity tests were conducted to examine the importance of the benthic boundary (i.e., specification of SOD) and ocean nutrient (i.e., nitrogen) boundary conditions. The interest in SOD stems from the fact that the sediment quality model was not activated and SOD had to be specified rather than modeled. The primary data limitation exists along the open-ocean boundaries, thus causing uncertainty in specification of ocean boundary conditions. Since the NYB algae ar primarily nitrogen limited, nitrogen is a primary variable of concern and was the focus of ocean boundary sensitivity tests.

The sensitivity tests consisted of comparing simulation results following each sensitivity change with the calibration results. Comparison plots consisted of scatter plots, regional (e.g., Apex, NJ Nearshore) vertical profiles, and transect plots. Profiles and transects were produced for June and August. Scatter plots were for the entire simulation period of 15 Apr through 30 Sep 1976.

Comparison statistics consisted of volumetrically weighted averages of test and calibration concentrations, volumetrically weighted averages of test and calibration concentration differences, and volumetrically weighted RMS (root mean square) differences. Volumetric weighting was employed to avoid having small and large WQM cells contribute equally to the average. All comparison statistics were computed for the entire simulation; thus, they represent a simulation average. Monthly averages of concentrations were recorded at the end of each month for the serial output of the WQM. The volume-averaged comparison statistics were computed as follows:

$$Calib = \frac{\sum_j \sum_i (vol_{ij} \times c_{ij})}{\sum_j \sum_i vol_{ij}} \qquad (5)$$

where

$c_{ji} = i^{th}$ cell monthly averaged calibration concentration for month j

vol_{ij} = volume of the i cell for month j

$$Test = \frac{\sum_j \sum_i (vol_{ij} \times t_{ij})}{\sum_j \sum_i vol_{ij}} \qquad (6)$$

where

$t_{ij} = i^{th}$ cell monthly averaged test concentration for month j

$$Diff = \frac{\sum_j \sum_i \left[vol_{ij} (t_{ij} - c_{ij}) \right]}{\sum_j \sum_i (vol_{ij})} \qquad (7)$$

and

$$TRMS = \sqrt{\frac{\sum_j \sum_i \left[vol_{ij} (t_{ij} - c_{ij})^2 \right]}{\sum_j \sum_i vol_{ij}}} \qquad (8)$$

SOD boundary condition. For the sensitivity test calibration, a temporally and spatially constant SOD boundary condition of 1.0 g m^{-2} day^{-1} was used because of the limited spatial and temporal extent of the SOD data. A sensitivity study was conducted to evaluate the effect of inaccurate SOD boundary conditions. Two test simulations were conducted: (1) SOD = 0.0 and (2) SOD = 10.0 g m^{-2} day^{-1}. The sensitivity test plots are displayed in Appendix E and consist of the following:

Plate	Plot
E1	DO Scatter Plot, SOD = 0.0
E2	Vertical DO Profile Comparison, Jun, SOD = 0.0
E3	Vertical DO Profile Comparison, Aug, SOD = 0.0
E4	DO Scatter Plot, SOD = 10.0
E5	Vertical DO Profile Comparison, Jun, SOD = 10.0
E6	Vertical DO Profile Comparison, Aug, SOD = 10.0

The effect of setting SOD to zero had a slight effect throughout the modeled system, but more noticeably in the shallower areas of LIS, Apex, and Transect regions (Plates E2 and E3). Table 11 lists, by region, simulation-average comparison statistics for the SOD = 0.0 test. Examination of Table 11

Table 11
Dissolved Oxygen Comparison Statistics, SOD = 0.0 g O_2 m^{-2} day^{-1}

Region	N	Calib g O_2 m^{-3}	Test g O_2 m^{-3}	Diff g O_2 m^{-3}	TRMS g O_2 m^{-3}
1	11040	5.72	6.27	0.55	0.67
2	12780	6.12	6.33	0.12	0.38
3	15120	5.65	5.77	0.12	0.27
4	7380	5.85	5.89	0.04	0.08
5	7140	5.48	5.80	0.32	0.44
6	5940	6.00	6.06	0.06	0.14
7	4800	6.25	6.76	0.51	0.63
8	22920	5.89	6.25	0.36	0.50
9	18780	6.06	6.18	0.12	0.23
10	4620	9.54	10.22	0.68	0.92
11	10740	7.63	8.09	0.46	0.53
NYB	150060	6.13	6.32	0.19	0.35

Note: See Table 8 for Region name. Region 11 is LIS, and NYB is the entire modeled system. N is the number of values used to compute the statistic.

reveals that zero SOD sediment boundary conditions increase the DO for all regions and by 0.19 g O_2 m^{-3}, or 3 percent, for the NYB as a whole. The most notable change was for Region 10, the Transect, where DO increased 7 percent. Examination of Plates E2 and E3 (Vertical DO Profile Comparisons)

reveals that the most detectable increase in DO occurred in the more shallow regions.

Increasing the sediment boundary SOD to 10.0 g m^{-2} day^{-1} (an extremely high and unrealistic value) decreased the Bight-wide DO by only 15 percent (Table 12). However, this value had a substantial effect in terms of concentrations (Plates E5 and E6). The most notable decrease was for the Transect where the DO decreased 3.58 g O$_2$ m^{-3} (from 9.54 g O$_2$ m^{-3} to 5.96 g O$_2$ m^{-3}), a decrease of 38 percent. The high SOD also had a sizeable effect on Regions 7 and 11 (LI Nearshore and LIS). Although the value of 10.0 is unrealistically high, it does demonstrate some potential importance of correctly specifying SOD and the need to use the sediment model in future work.

Table 12 Dissolved Oxygen Comparison Statistics, SOD = 10.0 g O$_2$ m^{-2} day^{-1}					
Region	N	Calib g O$_2$ m^{-3}	Test g O$_2$ m^{-3}	Diff g O$_2$ m^{-3}	TRMS g O$_2$ m^{-3}
1	11040	5l.72	4.09	-1.63	1.92
2	12780	6.12	5.23	-0.89	1.31
3	15120	5.65	5.05	-0.60	1.04
4	7380	5.85	5.52	-0.33	0.62
5	7140	5.48	4.23	-1.25	1.62
6	5940	6.00	5.66	-0.34	0.70
7	4800	6.25	4.21	-2.04	2.33
8	22920	5.89	4.34	-1.55	1.95
9	18780	6.06	5.42	-0.64	1.05
10	4620	9.54	5.96	-3.58	4.14
11	10740	7.63	4.89	-2.74	3.02
NYB	150060	6.13	5.22	-0.21	1.44

Ocean nitrogen BC. A sensitivity study was conducted to investigate the impact of variation in the nitrogen seaward boundary conditions. Two tests were conducted: (1) seaward boundary nitrogen concentrations set to zero (N-BC * 0.0) and (2) an increase of seaward boundary nitrogen concentrations by a factor of two (N-BC * 2.0). Sources of seaward boundary nitrogen consisted of ammonium-nitrogen, nitrate-nitrogen, DON, PON, and algal nitrogen. Algal nitrogen sources, however, were not modified during the sensitivity tests. The plots of these results are presented in Appendix E and are identified as follows:

Plate	Plot
E7	Scatter Plot, N-BC * 0.0
E8	Vertical Nanoplankton Profile Comparison, Jun, N-BC * 0.0
E9	Vertical Nanoplankton Profile Comparison, Aug, N-BC * 0.0
E10	Vertical DO Profile Comparison, Jun, N-BC * 0.0
E11	Vertical DO Profile Comparison, Aug, N-BC * 0.0
E12	Scatter Plot, N-BC * 2.0
E13	Vertical Nanoplankton Profile Comparison, Jun, N-BC * 2.0
E14	Vertical Nanoplankton Profile Comparison, Aug, N-BC * 2.0
E15	Vertical DO Profile Comparison, Jun, N-BC * 2.0
E16	Vertical DO Profile Comparison, Aug, N-BC * 2.0

The time history of monthly averaged, global Bight nitrogen concentrations is shown in Table 13. The flushing study indicated that the memory of the Bight is on the order of a year for a conservative substance. Table 13 indicates a shorter response time for a nonconservative substance such as nitrogen.

Table 13 Bight-Wide Time History for Total Nitrogen, g N m⁻³						
Test	Apr	May	Jun	Jul	Aug	Sep
Calibration	0.1384	0.1532	0.1209	0.1221	0.1367	0.1251
N-BC * 0.0	0.0804	0.0436	0.0362	0.0291	0.0281	0.0312
N-BC * 2.0	0.1967	0.2612	0.2066	0.2162	0.2469	0.2209

The DO comparison statistics for the two nitrogen boundary condition tests are presented in Tables 14 and 15. Examination of Tables 14 and 15 reveals that zero nitrogen seaward boundary conditions result in a slight decrease in DO of 0.5 percent (Bight-wide) while a doubling of the boundary conditions increases Bight DO by 0.3 percent. The WQM DO is relatively insensitive to the nitrogen seaward boundary condition. An increase in the nitrogen boundary condition tends to increase algal productivity, which has the effect of slightly increasing DO overall.

Plates E8 and E9 (Vertical Nanoplankton Profile Comparisons) indicate a decrease in algae for the lower nitrogen boundary condition. Nanoplankton profiles are not evident in Plates E8 and E9 for the Transect region because simulated concentrations exceeded the abscissa maximum of 5.0 mg Chl m⁻³.

34

Table 14
Dissolved Oxygen Comparison Statistics, N-BC * 0.0 * g N m^{-3}

Region	N	Calib g O$_2$ m^{-3}	Test g O$_2$ m^{-3}	Diff g O$_2$ m^{-3}	TRMS g O$_2$ m^{-3}
1	11040	5.72	5.63	-0.08	0.10
2	12780	6.12	6.00	-0.12	0.15
3	15120	5.65	5.58	-0.07	0.12
4	7380	5.85	5.81	-0.04	0.10
5	7140	5.48	5.43	-0.05	0.09
6	5940	6.00	5.98	-0.02	0.05
7	4800	6.25	6.19	-0.06	0.09
8	22920	5.89	5.85	-0.04	0.09
9	18780	6.06	6.04	-0.02	0.06
10	4620	9.54	9.53	-0.01	0.03
11	10740	7.63	7.60	-0.03	0.05
NYB	150060	6.13	6.10	-0.03	0.08

Table 15
Dissolved Oxygen Comparison Statistics, N-BC * 2.0 * g N m^{-3}

Region	N	Calib g O$_2$ m^{-3}	Test g O$_2$ m^{-3}	Diff g O$_2$ m^{-3}	TRMS g O$_2$ m^{-3}
1	11040	5.72	5.80	0.08	0.10
2	12780	6.12	6.20	0.08	0.11
3	15120	5.65	5.69	0.04	0.09
4	7380	5.85	5.87	0.02	0.08
5	7140	5.48	5.52	0.04	0.10
6	5940	6.00	6.01	0.01	0.05
7	4800	6.25	6.30	0.05	0.08
8	22920	5.89	5.92	0.03	0.08
9	18780	6.06	6.07	0.01	0.05
10	4620	9.54	9.56	0.02	0.03
11	10740	7.63	7.66	0.03	0.04
NYB	150060	6.13	6.15	0.02	0.07

The corresponding Vertical Nanoplankton Profile Comparisons (Plates E13 and E14) indicate an increase in algal mass with a doubling of N boundary conditions. However, examination of Vertical DO Profile Comparisons with 0.0 and doubling of the N boundary conditions (Plates E10, E11, E15, and E16) reveals minor deviations in the DO profiles. More impact on DO could be realized with the sediment model activated since the additional algal growth will result in additional organic matter deposited on the bottom, thus increasing SOD.

Demonstration Scenarios

The demonstration scenarios include external load increase and reduction, use of the WQM for the investigation of the cause of the New Jersey near-shore hypoxia, and inclusion of LIS external loads.

External load increase and reduction

Constant external loads were varied for the Transect, NJ Coast, and LI Coast (see Table 5). Two scenario runs were conducted: (1) constant external loads set to zero and (2) constant external loads increased by a factor of 100 (Table 16). The Hudson River loads were abstracted from Table 4. The Hudson River, Sewage Sludge, and Dredged Material zone loadings were not altered for the scenarios. Table 17 displays the percent increase and decrease of the loads for the demonstration scenarios. Setting the constant external loads to zero decreased the carbon and nitrogen loads by a factor of 0.66 and 0.77, respectively. An increase of the constant external loads by a factor of 100 increased the total carbon loads by a factor of 66 and the total nitrogen loads by a factor of 77.

The demonstration scenario plots for external load increase and decrease are displayed in Appendix F as follows:

Table 16
External Loads, tons day^{-1}

Zone	DOC	POC	NH$_4$-N	NO$_3$-N	DON	PON
Calibration Conditions						
Transect	862.	288.	126.	14.	59.	39.
NJ Coast	79.	26.	6.	13.	3.	2.
LI Coast	12.	4.	6.	2.	2.	1.
Sewage Sludge		110.	10.			7.
Dredged Material		540.				63.
Hudson River	230.	77.	15.	52.	19.	12.
Constant External Loads = 0						
Transect	0.	0.	0.	0.	0.	0.
NJ Coast	0.	0.	0.	0.	0.	0.
LI Coast	0.	0.	0.	0.	0.	0.
Sewage Sludge		110.	10.			7.
Dredged Material		540.				63.
Hudson River	230.	77.	15.	52.	19.	12.
Constant External Loads * 100						
Transect	86200.	28800.	12600.	1400.	5900.	3900.
NJ Coast	7900.	2600.	600.	1300.	300.	200.
LI Coast	1200.	400.	600.	200.	200.	100.
Sewage Sludge		110.	10.			7.
Dredged Material		540.				63.
Hudson River	230.	77.	15.	52.	19.	12.

Table 17
Percent Increase and Decrease of Constant External Load Scenarios

Scenario	DOC	POC	NH$_4$-N	NO$_3$-N	DON	PON
External loads set to zero	-81	-30	-85	-36	-77	-34
External loads * 100	7975	3013	8382	3544	7534	3879

Plate	Plot
F1	Scatter Plot, Loads = 0.0
F2	Vertical Nanoplankton Profile Comparison, Jun, Loads = 0.0
F3	Vertical Nanoplankton Profile Comparison, Aug, Loads = 0.0
F4	Vertical DOC Profile Comparison, Jun, Loads = 0.0
F5	Vertical DOC Profile Comparison, Aug, Loads = 0.0
F6	Vertical POC Profile Comparison, Jun, Loads = 0.0
F7	Vertical POC Profile Comparison, Aug, Loads = 0.0
F8	Vertical DO Profile Comparison, Jun, Loads = 0.0
F9	Vertical DO Profile Comparison, Aug, Loads = 0.0
F10	Transect DOC Comparison, Jun, Loads = 0.0
F11	Transect DOC Comparison, Aug, Loads = 0.0
F12	Transect POC Comparison, Jun, Loads = 0.0
F13	Transect POC Comparison, Aug, Loads = 0.0
F14	Scatter Plot, Loads * 100
F15	Vertical Nanoplankton Profile Comparison, Jun, Loads * 100
F16	Vertical Nanoplankton Profile Comparison, Aug, Loads * 100
F17	Vertical DOC Profile Comparison, Jun, Loads * 100
F18	Vertical DOC Profile Comparison, Aug, Loads * 100
F19	Vertical POC Profile Comparison, Jun, Loads * 100
F20	Vertical POC Profile Comparison, Aug, Loads * 100
F21	Vertical DO Profile Comparison, Jun, Loads * 100
F22	Vertical DO Profile Comparison, Aug, Loads * 100
F23	Transect DOC Comparison, Jun, Loads * 100
F24	Transect DOC Comparison, Aug, Loads * 100
F25	Transect POC Comparison, Jun, Loads * 100
F26	Transect POC Comparison, Aug, Loads * 100

In addition, comparison statistics for simulation-averaged DO were computed regional and Bight-wide (i.e., NYB) and are provided in Tables 18 and 19 for loads = 0.0 and loads * 100, respectively.

Decreasing the external loads had the effect of decreasing algal, DOC, and POC concentrations. Although organic carbon decreased, the net effect of these changes resulted in a slight decrease in DO, most noticeable in the Transect region. The decrease in algae had more impact on decreasing DO than the effect of decreasing organic carbon had on increasing DO. Dramatic

38

loading increases caused slight DO decrease Bight-wide and a substantial DO decrease in the Transect region. Nearshore regions (e.g., the Apex) also exhibited substantial decreases. The loading increase also caused high algal and organic carbon concentrations.

Overall, the whole NYB system exhibits little sensitivity to loading changes, especially for DO (see NYB in Tables 18 and 19), demonstrating that the NYB has a tremendous assimilative capacity. The above demonstrations should not be interpreted as what would happen with loading changes. It is pointed out that this model does not include the sediment model that can accumulate organic matter and adjust the SOD accordingly. These simulations merely demonstrate how the model might be used and roughly estimate the sensitivity of the Bight to loading changes. For more definitive estimates of the effects of loading changes on water quality, the sediment model should be activated and calibrated, and long-term (e.g., multiyear) simulations would be required to properly capture sedimentation and mineralization of organic matter in the sediments and the resulting SOD. Additionally, the WQM should be more accurately calibrated for longer periods of time.

The external loads were inserted in cells immediately adjacent to shore. However, both the load comparison statistics and the plots used spatially averaged results (averaged over regions and the Bight). Near-field effects that may occur within meters to a few kilometers of the point of discharge would be attenuated through the averaging process and may not be evident in the regional averages.

Table 18 Dissolved Oxygen Comparison Statistics, Loads = 0.0					
Region	N	Calib g O_2 m^{-3}	Test g O_2 m^{-3}	Diff g O_2 m^{-3}	TRMS g O_2 m^{-3}
1	11040	5.72	5.66	-0.06	0.13
2	12780	6.12	6.12	-0.00	0.01
3	15120	5.65	5.65	-0.00	0.00
4	7380	5.85	5.85	0.00	0.00
5	7140	5.48	5.48	-0.00	0.00
6	5940	6.00	6.00	-0.00	0.00
7	4800	6.25	6.23	-0.02	0.04
8	22920	5.89	5.88	-0.00	0.02
9	18780	6.06	6.06	-0.00	0.00
10	4620	9.54	7.70	-1.84	2.92
11	10740	7.63	7.54	-0.08	0.24
NYB	150060	6.13	6.12	-0.00	0.09

Table 19
Dissolved Oxygen Comparison Statistics, Loads * 100

Region	N	Calib $g O_2 m^{-3}$	Test $g O_2 m^{-3}$	Diff $g O_2 m^{-3}$	TRMS $g O_2 m^{-3}$
1	11040	5.72	5.14	-0.58	1.33
2	12780	6.12	6.13	0.01	0.16
3	15120	5.65	5.65	-0.00	0.06
4	7380	5.85	5.84	-0.00	0.02
5	7140	5.48	5.42	-0.06	0.37
6	5940	6.00	5.99	-0.01	0.12
7	4800	6.25	5.59	-0.66	1.14
8	22920	5.89	5.66	-0.23	0.77
9	18780	6.06	6.02	-0.03	0.37
10	4620	9.54	2.20	-7.34	7.98
11	10740	7.63	7.67	0.04	0.31
NYB	150060	6.13	6.03	-0.10	0.52

New Jersey nearshore hypoxia

The measured bottom layer DO contour shown in Plate 25, which was obtained from the bottom 5-m oxygen distribution presented in Stoddard (1983, 1989), indicates that low DO occurred during July 1976 off the coast of New Jersey. Stoddard's model oxygen budget investigations indicated that transport was a key factor in the onset of hypoxia. The onset of steady southwest winds in latter May resulted in an upcoast northeast flow with upwelling. The upcoast, upwelling flows triggered the accumulation of *Ceratium* off the coast of New Jersey whose respiration and decay contributed to oxygen depletion. However, the NYB WQM simulation predicted small biomass of net plankton, which was not in disagreement with small measured values. Although few measured data were available for net plankton, their magnitude suggested small concentrations for initial and ocean boundary conditions.

The WQM was used to investigate why a DO minimum was correctly simulated (see Plate 25, where "Simulated" results were obtained from the WQM of this present study) off the coast of New Jersey. Plate 26 displays the 4.0-g O_2 m^{-3} contour plot for the calibration run. The 4.0-g O_2 m^{-3} contour was selected for the New Jersey nearshore hypoxia investigation because this contour appeared in all the test investigations.

The first step in the investigation was to examine the magnitude of the source and sink terms in the DO kinetic terms. The DO kinetic terms were recorded for the water column corresponding to WQM cell 1125 (i,j = 16,17).

40

WQM cell 1125 was selected because it occurred in the center of the July minimum. The water column depth was 31.87 m. The kinetic DO fluxes for each layer were typically negative. The DO kinetic fluxes indicated that DOC mineralization was the dominant kinetic DO sink for layers 1-9 and SOD was the dominant sink for layer 10, the bottom layer.

An examination of the kinetic sources and sinks of DOC indicated that the mineralization sink of DOC greatly exceeded algal sources and sources through hydrolysis of POC. Alternative sources of DOC include advection of DOC from the New Jersey coastline (NJ external constituent loads listed in Table 5) and advection from the seaward boundary. The WQM does provide options for recording advective fluxes through cell walls, but identification of the source required examination of the NJ coast external loads and boundary conditions.

A WQM simulation with NJ coast external loads set to zero resulted in no observed difference in DO or DOC in the water column corresponding to WQM cell 1125 or the spatial pattern of the 4.0-g O_2 m^{-3} contour (Plate 27). The northeast flows along the New Jersey coast did not advect the coastal loads to WQM cell 1125. The remaining source of DOC was the ocean boundary conditions. The northeast flows suggest that the southwest boundary conditions for Segments 1, 2, and 3 (Plate 5) could possibly affect WQM cell 1125. A WQM simulation was conducted with Segments 1, 2, and 3 DOC boundary concentrations set to 0.0. A comparison of DO contour plots for the calibration run (Plate 26) and DOC boundary conditions for Segments 1, 2, and 3 set equal to zero (Plate 28) revealed that the patterns of low DO concentrations were similar. However, the spatial extent of low DO was smaller with the DOC boundary condition segments set to zero. The flux of DOC from the ocean boundaries intensified DO depletion off the coast of New Jersey, but it was not the major cause of the hypoxia.

Because SOD was the dominant kinetic sink for DO for the bottom layer, a WQM simulation was conducted with SOD set equal to 0.0 for the NJ Nearshore, NJ Midshelf, and NJ Shelf regions. The pattern of the simulated DO contour off the New Jersey coast is substantially different with the SOD set to zero (Plate 29), indicating that SOD played an important role in the New Jersey nearshore hypoxia. However, there is still a relatively large zone of low DO with the SOD set to zero, indicating other remaining causes of the hypoxia.

The DO ocean boundary conditions were examined. The DO boundary concentrations for Segments 1, 2, and 3 listed in Appendix C are reproduced in Table 20.

The significance of the DO boundary condition was investigated by reflecting the DO boundary condition. Reflection of the DO boundary condition means that the boundary DO concentration was set equal to the immediately interior WQM cell DO concentration from the previous time-step. The DO boundary conditions were thus completely dependent upon transport and

Table 20 Calibration Run DO Ocean Boundary Conditions (g O_2 m^{-3})						
	Seg 1		Seg 2		Seg 3	
Month	Surface	Bottom	Surface	Bottom	Surface	Bottom
Apr	8.57	7.57	8.57	7.57	8.57	7.57
May	7.89	7.43	8.57	7.43	8.57	7.43
Jun	7.94	6.84	8.29	6.26	8.30	5.85
Jul	6.56	3.94	7.43	4.71	7.43	4.71
Aug	7.34	2.54	7.86	4.04	7.29	5.89
Sep	7.01	4.37	6.86	2.19	6.91	5.03
Note: Underlined values are prototype measurements.						

kinetics interior to the boundary. Examination of contour plots of bottom layer DO for July with reflective DO boundaries revealed that DO was greater than 4.0 g O_2 m^{-3} globally (i.e., Bight-wide). In contrast, the calibration bottom DO during July was generally less that 4.0 off the coast of New Jersey with extensive areas of DO less than 3.0. The conclusion of the reflective DO boundary experiment was that low DO concentrations for the southwest ocean boundary were a major contributor to simulated DO depression off the coast of New Jersey.

The New Jersey nearshore hypoxia investigation revealed that low DO simulated off the coast of New Jersey was the result of three major interacting components: (1) the prevailing southwest to northeast residual flows, (2) DOC and DO boundary conditions along the southwest ocean boundary of the model grid, and (3) SOD. The prevailing southwest to northeast residual flows advected the southwest boundary condition constituents upcoast along the New Jersey coast. The southwest boundary provided a source of DOC of larger magnitude than from algae and hydrolysis of POC. The southwest boundary condition for DO was specified using measured prototype data. Measured bottom DO used in the specification of the southwest boundary conditions was frequently less than 3.0 g O_2 m^{-3}. The prevailing residual currents advected the low DO boundary waters along the NJ coastline. The mineralization of the DOC intensified DO depletion. The SOD increased the rate of DO depletion in the bottom layer. This increased rate of DO depletion was manifested through earlier occurrence and greater intensity of low DO concentrations. The New Jersey Coast external constituent loads had little influence on the simulated DO depression off the coast of New Jersey.

42

LIS external loads

As stated earlier, calibrations, sensitivity tests, and load reduction scenarios were conducted without LIS external loads. An investigation was conducted to examine the impact of LIS external loads on the DO resources of the Bight.

The LIS external loads were based on tabulations listed in Wolfe et al. (1991) (Table 21).

Table 21 Constant External Constituent Loads, LIS, tons day^{-1}					
DOC	POC	NH$_4$-N	NO$_3$-N	DON	PON
411.	137.		101.	15.	10.

Table 22 lists by region the simulation-average DO comparison statistics for the LIS external load test.

Table 22 Dissolved Oxygen Comparison Statistics, Long Island Sound External Loads					
Region	N	Calib g O$_2$ m^{-3}	Test g O$_2$ m^{-3}	Diff g O$_2$ m^{-3}	TRMS g O$_2$ m^{-3}
1	11040	6.06	6.06	0.00	0.01
2	12780	6.30	6.30	0.00	0.00
3	15120	5.87	5.87	0.00	0.00
4	7380	6.02	6.02	0.00	0.00
5	7140	5.88	5.88	0.00	0.00
6	5940	6.13	6.13	0.00	0.00
7	4800	6.69	6.69	0.00	0.00
8	22920	6.33	6.33	0.00	0.00
9	18780	6.29	6.29	0.00	0.00
10	4620	9.71	9.82	0.10	0.16
11	10740	7.87	7.99	0.11	0.20
NYB	150060	6.40	6.40	0.00	0.03

Examination of Table 22 reveals that inclusion of LIS external loads increases the regional average DO of the Transect region 0.10 g O$_2$ m^{-3} and of the LIS region 0.11 g O$_2$ m^{-3}. A difference in DO was not detected in other regions or Bight-wide. Examination of the DO vertical profile comparison for August (Plate 30) indicates the small increase in DO in the Transect and LIS.

An additional conclusion from the examination of Plate 30 is that the simulated DO in LIS was uniformly distributed from surface to bottom. The uniform distribution may be due to excessive vertical diffusion and/or inability to capture vertical stratification in LIS using 12.5-hr intertidal hydrodynamic averaging.

The slight increase in DO was the result of an increase in algal photosynthesis, a pattern similar to the sensitivity response due to increased nitrogen boundary concentrations. Dissolved oxygen depletion associated with increased algal growth followed by mortality, settling, and decay of algal carbon in the sediments is not simulated without the inclusion of the sediment diagenesis model. The DO hypoxia in the Western Basin of the Sound (Parker and O'Reilly 1991) was not captured by the model. Possible reasons that the hypoxia was not simulated are (1) the loads were uniformly distributed from East River to Montauk Point and (2) excessive vertical mixing prevented physical stratification.

44

6 Conclusions and Recommendations

Conclusions

This study demonstrates that a water quality model of the NYB is feasible and provides reasonable results. The model simulates the Bight, LIS, harbor, and estuaries as a single, dynamically coupled unit. This approach has much merit for assessing how the various regions interact and for providing a true representation of the real system.

A model such as this provides a strong capability for examining, in a cost-effective manner, a host of questions that could not otherwise be addressed. The present model is not developed to the point that it can be used for determining future nutrient loading goals or waste load allocations (WLAs), but it is a large step toward such a model, which is now considered attainable. In its present state of development, the model is well suited to examining a number of questions, some of which are discussed herein.

The model compared relatively well with observations in the Bight and successfully captured the summer hypoxia of 1976. However, water quality conditions within the Transect region (i.e., in the harbor and estuaries) did not compare well, and improvements are needed if any additional modeling is undertaken. Recommendations for these improvements are discussed below. The primary reasons for the hypoxia off the New Jersey coast during the summer of 1976, as determined by the model, were SOD and the advection of DOC and low DO from the southwest ocean boundary toward the northeast. The advection of low DO had the greatest effect of these three processes.

Loading sensitivity studies indicated that throughout most of the Bight, water quality (e.g., algae and DO) is insensitive to loading decreases, but the Transect region and part of the Apex are sensitive. Extremely large loading increases were required to register effects in the Bight. Although algae, POC, and DOC increased substantially (especially closer to shore and within the Transect) when total loading was increased over 60-fold, DO within the Bight changed little. The effect on SOD of this loading increase was not accounted for since the sediment diagenesis model was not activated. However,

increasing the SOD to 10 g m^{-2} day^{-1} (an unrealistically high value) only moderately reduced DO in Bight bottom waters (e.g., a reduction of about 1 to 3 g DO m^{-3}). It appears that the tremendous volume of the Bight provides a great assimilative capacity for DO, which tends to increase in the seaward direction. Setting the SOD to zero only slightly increased bottom water DO by about 1.0 g DO m^{-3} in nearshore regions, and even less farther offshore. Sensitivity tests on the ocean boundary condition for nitrogen indicated that, although algae responded, DO of the NYB system was insensitive to changes in nutrients introduced from the ocean.

Modeling Recommendations

The model results point out several deficiencies that should be overcome if the model is to be used for establishing nutrient reduction goals and WLAs. Several steps should be taken to obtain a more accurate WQM as discussed below. These recommendations are not necessarily in order of priority.

a. The sediment diagenesis/flux model should be activated and calibrated. Recent sediment flux measurements from LIS could be used to assist in this calibration. Activation of the sediment model may also require activation of additional water quality state variables.

b. Additional data sources should be sought for better defining loadings and boundary conditions and for making calibration comparisons. Insufficient water quality data were utilized in this study for the Transect region and LIS, which makes it difficult to draw meaningful conclusions about model accuracy in these areas. More accurate loading estimates for the Hudson River should also be sought.

c. More frequent update intervals for loadings and boundary conditions should be used. For example, daily or weekly Hudson River flows and concentrations (or loads) should be used. At least monthly updates should be used for external loads.

d. The excessive algal concentration computed within the Transect region should be investigated further and remedied. The most probable solution to this problem is to include the effect of suspended solids on light attenuation. If there are insufficient data to include suspended solids as a model state variable, it may be possible to indirectly relate light attenuation to suspended solids through a relationship to Hudson River flow discharge.

e. Refractory DOC can be added to the model to better match measured DOC.

46

f. Multiyear (e.g., 2 years or more) calibration/verification simulations should be conducted to obtain a more accurate model and more fully demonstrate the accuracy.

g. A primary deficiency concerns the difficulty in representing the proper vertical mixing. During the course of the study, the parameters that affect the vertical eddy diffusivity calculations in the HM were varied, causing WQM results for temperature and DO to range from well-mixed to overly stratified. A higher order closure algorithm for vertical eddy diffusivity, such as transport equations for kinetic energy and dissipation, may be required to properly simulate vertical mixing.

There are at least two investigations that should be undertaken to improve confidence in the model. These investigations may lead to additional model improvements or modifications as explained below.

a. Investigate transport in more detail. Vertical diffusion is computed as a simple arithmetic mean in the intertidal averaging procedure. This procedure may not be adequate in the more dynamic regions of the harbors, estuaries, and LIS. The proper preservation of vertical mixing with intertidal transport was not investigated in this study. This was found not to be a problem in the Chesapeake Bay model study (Dortch 1990), but that estuary is weakly nonlinear whereas the inner regions of this study site are much more nonlinear. In any future modeling of this system, this aspect should be studied more closely. It may be possible to still use intertidal currents, but the vertical diffusion may have to be handled differently. Additionally, tests should be conducted to ensure that mass flux through the Transect is properly represented with intertidal transport. This test can be accomplished by comparing HM mass or salt flux through the Transect with that of the WQM using intertidal hydrodynamic updates.

b. Conduct additional investigations of the sensitivity of ocean boundary conditions. Further development of the model for determining nutrient reduction goals would subsequently involve simulating various proposed nutrient reduction strategies to evaluate their effectiveness. As discussed earlier, the investigation of the cause of the hypoxia revealed the importance of ocean boundary conditions for DO and DOC. This brings up a question: How can water quality with future loading conditions be predicted if the results depend on ocean boundary conditions which could depend on the future loadings? Fortunately, the results of this study generally support the idea that loadings from the land boundaries have minimal effect on conditions near the ocean boundaries. However, this idea should be more thoroughly investigated to ensure that nutrient loading strategies are simulated properly.

If future modeling must address WLAs and their impacts within the Transect region, a fine-grid model of the inner harbors and bays is recommended. It is not possible to accurately resolve conditions inside the Transect with the

present grid. The simplest approach would be to construct a separate model of the inner harbors and bays which extends into the Apex and LIS so that it can be interfaced with the NYB model (i.e., the grid of the present model). The models would not have to be dynamically coupled; rather, results from the NYB model could be used to set boundary conditions for the fine-scale harbor/estuaries model.

Water Quality Monitoring Recommendations

This section provides general recommendations for water quality monitoring for two purposes: to support a future comprehensive eutrophication model and to monitor future water quality/eutrophication trends. The first purpose requires detailed, synoptic sampling over a rather short time frame, while the second purpose requires much less detailed sampling over a long time frame. These two approaches to monitoring are referred to here as *synoptic monitoring for modeling* and *long-term monitoring*. Both types of monitoring are for general water quality (e.g., nutrients and DO) and do not address contaminants (e.g., trace metals, hydrocarbons, and synthetic organics).

Neither monitoring purpose would be used for real-time water quality modeling. Real-time modeling is defined here as trying to predict conditions in the near future based on recent observations. Eutrophication/general water quality models of large water bodies such as this are not used for real-time water quality prediction, but rather for planning and evaluating future management strategies (e.g., evaluating the effects of reducing nutrient loadings). The water quality observed at a particular location may be the result of months (even years) of previous conditions because of the long memory of large water bodies. For example, low DO observed during August may be the result of loadings and algal blooms that occurred in the spring. Therefore, it is unreasonable to expect such water quality models to predict what the water quality will be next month based on the observed water quality this month. With this in mind, water quality monitoring should not be conducted to support real-time water quality modeling.

The discussion below provides general guidance for conducting the two types of monitoring programs. The details for these monitoring programs are not provided since formulation of such details would depend on logistical capabilities of the parties that would collect these data and other conditions discussed below. Additionally, the effort required to formulate the details of the monitoring programs is beyond the scope of this study.

Synoptic monitoring for modeling

The water quality model feasibility study described herein was constrained because of data limitations. The constraint was in part based on the study period selected, i.e., DO hypoxia event during summer 1976. There may be

48

years where more complete data were obtained (such as monitoring of additional nutrient forms). If a comprehensive eutrophication model is performed, more complete data will be required to ensure proper model implementation. Such data sets are referred to as synoptic and would be used primarily for water quality model calibration and verification.

Before a synoptic water quality monitoring program is developed and executed, the existing database should be examined more closely. Stoddard and Han (1989) reviewed and assessed field data available for use in this study. Their inventory of available data indicated that an enormous amount of water quality data was readily available from databases to characterize the water quality of the New York Bight. They provided WES with data from the period of study (i.e., 1976). Relatively complete data sets may exist for other periods as well, in addition to more recently collected data, e.g., sediment flux data collected in Long Island Sound.

The first step in a comprehensive eutrophication model study should be to collate and study the existing database and to select study years where the data are most complete. Data gaps should be identified to help determine what, if any, additional data are required for a comprehensive eutrophication model study. Problems may be encountered with the historical data, such as changes in collection and analytical techniques that occurred over the last two decades. If the existing data are deemed adequate, a synoptic monitoring program is not needed. However, if the existing data are considered inadequate to support such a modeling effort, a synoptic data set based on current Bight conditions and analytical techniques should be considered as described below.

A 3-year data collection program would be adequate for establishment of a synoptic data set. The constituents measured should include salinity, temperature, chlorophyll and algal quantification and speciation, multiple forms of organic carbon, multiple forms of organic and inorganic nitrogen and phosphorus, multiple forms of silica, and dissolved oxygen. Additionally, some work on partitioning of labile and refractory organic components is recommended.

Year-round, bimonthly sampling stations should be located in the Hudson, Raritan, and Passaic Rivers just upstream of their fall lines. Bimonthly sampling should also be conducted between April and October for stations in Long Island Sound, Newark and Raritan Bays, the Kills, and the Sandy Hook-Rockaway transect. Monthly sampling should be conducted at these stations during winter months. Three to six stations are needed in Long Island Sound. Newark and Raritan Bays and the Kills should have one or two stations each. Approximately three stations should be located across the transect.

Monthly sampling should be conducted on the seaward boundaries with a station for each of the seven boundary segments shown in Plate 21. Monthly-to-seasonal (about every 2 months) sampling should be conducted in the remaining extent of the Bight at approximately nine stations which represent the nine regions outside the transect in Plate 23. For these nine Bight stations,

monthly sampling should occur from April through October with sampling
every 2 months during the winter.

All sampling, except the fall lines, should be conducted over the water col-
umn, i.e., at multiple depths for each station. A minimum of two depths (i.e.,
near-surface and near-bottom) are required, but additional depths between these
two are highly desirable, such as within the pycnocline.

A comprehensive eutrophication model study will require activation of the
sediment diagenesis/flux model. The sediment model oxygen and nitrogen
parameters measured for Chesapeake Bay were transferable to Long Island
Sound and Narragansett Bay applications; however, the phosphorus parameters
were not transferable. Sediment water fluxes of oxygen, nitrogen, phosphorus,
silicon, and sulfide should be measured for the Bight at multiple locations. A
sediment sampling station should be established in each of the major interior
areas, i.e., Hudson River, Raritan Bay, Newark Bay, the Kills, and within the
transect region (see Plate 23). Nine sites should also be located throughout the
Bight to cover the nine regions shown outside the transect in Plate 23. Sedi-
ment sampling for flux measurements should be conducted four times a year
(winter, spring, summer, and fall) throughout the 3-year synoptic monitoring
study. Each sample should be extracted as an intact core of about 30-cm
length. The flux measurements should be conducted immediately onboard the
survey ship following collection. The same procedures used in the Chesapeake
Bay and Long Island Sound studies should be followed.

The above synoptic monitoring program would cost several million dollars.
This is not a firm cost proposal, but rather a rough estimate for planning pur-
poses. This work would most likely be contracted to an organization that does
estuarine and oceanographic monitoring routinely and has the capability to
cover extensive geographic areas in a relatively short time frame.

It is emphasized that the final monitoring recommendations would depend
on the results of a data compilation and synthesis effort and budgetary con-
straints. The final recommendations could extend from initiating few, if any,
of the items in the above plan to all of the items in the above plan.

Long-term monitoring

A separate and very different monitoring plan would be used to track long-
term water quality trends. Water quality is also constrained here to nutrients,
DO, and phytoplankton (i.e., eutrophication). This type of data would be used
to monitor the health of the Bight and how that health might be changing with
time. Such data would not be fully adequate for modeling future water
quality/eutrophication.

Several monitoring programs are ongoing, as summarized by Waste Man-
agement Institute (1991). However, most of these programs cover only near-
shore areas, usually extending no more than 3 miles offshore. Of the ongoing

50

monitoring efforts, the only program that comes close to fulfilling the requirements for long-term water quality monitoring of the Bight is EPA's New York Bight Water Quality Monitoring Program. The following variables are routinely measured: DO, salinity, temperature, fecal coliform bacteria, phytoplankton abundance and species composition, and chlorophyll. Additionally, sediment and benthic samples are analyzed for viruses and other pathogens and heavy metals. Sampling is conducted from May through October. The EPA monitoring program contains many stations along the Long Island and New Jersey coasts and within the Apex. Several transects included in this sampling program extend to about 15 miles offshore. Additionally, sediment samples are collected in a transect along the Hudson Canyon.

If long-term monitoring for status and trends of hypoxia and eutrophication is pursued, then the following recommendations are made. These recommendations are driven by the need to minimize costs. Thus, a small number of water quality variables would be sampled at select locations. Any new monitoring program should be conducted in conjunction with the existing EPA New York Bight Water Quality Monitoring Program to reduce costs. Total nitrogen and phosphorus should be added to the EPA program at a few select stations representative of the New York/New Jersey nearshore and Apex regions. Total N and P, chlorophyll, and DO should also be monitored at new stations representative of the midshelf and shelf regions (i.e., the six regions shown in Plate 23). Thus, the sampling program would basically consist of three transects (i.e., New Jersey coast, Apex/Hudson Canyon, and Long Island coast) extending from nearshore to the shelf with a minimum of three stations along each transect. Each station should be sampled at near surface and near bottom for total N and P, chlorophyll, DO, salinity, and temperature, as a minimum. Additionally, information on phytoplankton abundance and species composition is desirable.

Chlorophyll has been monitored through remote sensing. This approach requires some surface measurements for calibration. NOAA is one Federal agency that has used remote sensing within the Bight for chlorophyll analyses. Remote sensing could be designed into a future monitoring program to reduce costs while increasing coverage.

Before a new long-term water quality monitoring program is developed, various agencies and other participating parties should convene to scope such an effort, to avoid duplication while trying to meet the needs of all participants. Several other related, ongoing efforts could influence the direction of any future monitoring program. For example, NOAA and EPA are conducting ecosystem monitoring, which includes nutrient analyses, along the northeast shelf as part of the Marine Monitoring, Analysis, and Prediction Program. Additionally, these two agencies are jointly evaluating the existing monitoring programs nationwide to recommend future direction in coastal monitoring under the National Coastal Monitoring Program, which resulted from the 1992 Act of the same name. New, related programs might be under way by universities in the region (such as the Long-Term Ecosystem Observation Program recently initiated by Rutgers University). The specifics of any additional,

future long-term monitoring for eutrophication would depend on the opportunities for cooperation with these other monitoring efforts.

References

Ambrose, R. B., Jr., Vandergrift, S. B., and Wool, T. A. (1986). "WASP3, a hydrodynamic and water quality model--Model theory, user's manual, and programmer's guide," Report EPA/600/3-86/034, Environmental Research Laboratory, U.S. Environmental Protection Agency, Athens, GA.

American Society of Civil Engineers (ASCE). (1961). "Effect of water temperature on stream reaeration," *Journal of the Sanitary Engineering Division*, 87(SA6):59-71.

Bird, D., and Kalff, J. (1984). "Empirical relationships between bacterial abundance and chlorophyll concentration in fresh and marine waters," *Canadian Journal of Fisheries and Aquatic Science*, 41:1015-23.

Cerco, C. C., and Cole T. (1989). "Calibrating the Chesapeake Bay water quality model." *Proceedings of the Conference on Estuarine and Coastal Modeling, Newport, Rhode Island, November 15-17, 1989*, 192-99.

_____. (1992). "Thirty year simulation of Chesapeake Bay eutrophication." *Proceedings of the 2nd International Conference on Estuarine and Coastal Modeling, Tampa, Florida, November 13-15, 1992*, 116-26.

_____. "Application of the three-dimensional eutrophication model CE-QUAL-ICM to Chesapeake Bay," Technical Report (in preparation), U.S. Army Engineer Waterways Experiment Station, Vicksburg, MS.

Cole, J., Findlay, S., and Pace, M. (1988). "Bacterial production in fresh and saltwater ecosystems: a cross-system overview," *Marine Ecology Progress Series*, 43:1-10.

Creative Enterprises, Inc., and Han & Associates, Inc. (1990). "Hydrodynamic and water quality data compilation for the New York Bight," prepared for the U.S. Army Engineer Waterways Experiment Station, Vicksburg, MS, and U.S. Army Engineer District, New York, New York.

DiToro, D. M., and Fitzpatrick, J. J. (1992). "Chesapeake Bay sediment flux model," prepared for the U.S. Army Engineer Waterways Experiment Station, Vicksburg, MS.

DiToro, D., O'Connor, S., and Thomann, R. (1971). "A dynamic model of the phytoplankton population in the Sacramento-San Jaoquin Delta," in *Nonequilibrium Systems in Water Chemistry*, American Chemical Society, Washington, DC, pp 131-80.

Dortch, M. S. (1990). "Three-dimensional, Lagrangian residual transport computed from an intratidal hydrodynamic model," Technical Report EL-90-11, U.S. Army Engineer Waterways Experiment Station, Vicksburg, MS.

Edinger, J. E., Brady, D. K., and Geyer, J. C. (1974). "Heat exchange and transport in the environment," Report 14, EPRI Publication No. 74-049-00-3, prepared for Electric Power Research Institute, Palo Alto, CA.

Eiker, E. E. (1977). "Heat exchange programs," *Thermal simulation of lakes, user's manual*, U.S. Army Engineer District, Baltimore, Baltimore, MD.

Genet, L., Smith, D., and Sonnen, M. (1974). *Computer program documentation for the dynamic estuary model*. U.S. Environmental Protection Agency, Systems Development Branch, Washington, DC.

Hall, R. W. (1990). "Los Angeles and Long Beach Harbors model enhancement programs; numerical water quality Model study of harbor enhancements," Technical Report EL-90-6, U.S. Army Engineer Waterways Experiment Station, Vicksburg, MS.

Hall, R. W., and Chapman, R. S. (1982). "Comparison of third-order transport schemes." *Proceedings of the Conference on Applying Research to Hydraulic Practice*, HD, ASCE, Jackson, MS., August 17-20, 1982, 510-19.

_____. (1985). "Two-dimensional QUICKEST; solution of the depth-averaged transport-dispersion equation," Technical Report EL-85-3, U.S. Army Engineer Waterways Experiment Station, Vicksburg, MS.

Johnson, B. H., Heath, R. E., Hsieh, B. B., Kim, K. W., and Butler, H. L. (1991a). "Development and verification of a three-dimensional numerical hydrodynamic, salinity, and temperature model of Chesapeake Bay; Vol I, main text and appendix D," Technical Report HL-91-7, U.S. Army Engineer Waterways Experiment Station, Vicksburg, MS.

Johnson, B. H., Heath, R. E., Hsieh, B. B., Kim, K. W., and Butler, H. L. (1991b). "User's guide for the Chesapeake Bay three-dimensional numerical hydrodynamic model," Technical Report HL-91-1, U.S. Army Engineer Waterways Experiment Station, Vicksburg, MS.

Kremer, J., and Nixon, S. (1978). *A coastal marine ecosystem simulation and analysis*. Springer Verlag, New York.

Leonard, B. P. (1979). "A stable and accurate convective modelling procedure based on quadratic upstream interpolation," *Computer Methods in Applied Mechanics and Engineering*, Vol 19, 59-98.

Monod, J., (1949). "The growth of bacterial cultures," *Annual review of microbiology*, 3:371-94.

Morel, F. (1983). *Principles of aquatic chemistry*. John Wiley and Sons, New York.

Mueller, J. A., Jeris, J. S., Anderson, A. R., and Hughes, C. F. (1976). "Contaminant inputs to the New York Bight," NOAA Technical Memorandum ERL MESA-6, Marine EcoSystem Analysis Program Office, Boulder, CO.

National Oceanic and Atmospheric Administration. (1979). "Oxygen depletion and associated benthic mortalities in New York Bight, 1976," NOAA Professional Paper 11, Rockville, MD.

O'Connor, D. (1983). "Wind effects on gas-liquid transfer coefficients," *Journal of the Environmental Engineering Division*, 190:731-52.

O'Connor, D., and Dobbins, W. (1958). *Mechanisms of reaeration in natural streams*. Transactions of the American Society of Civil Engineers, 123:641-666.

Parker, C. A., and O'Reilly, J. E. (1991). "Oxygen depletion in Long Island Sound: A historical perspective," *Estuaries*, Vol 14, No. 3, 248-64.

Parsons, T., Takahashi, M., and Hargrave, B. (1984). *Biological oceanographic processes*. Pergamon Press, Oxford.

Ray Chapman and Associates. (1988). "Analysis and improvement of the numerical and physical mixing characteristics of the WASP box model," prepared for the U.S. Army Engineer Waterways Experiment Station, Vicksburg, MS.

Scheffner, N. W., Vemulakonda, S. R., Kim, K. W., Mark, D. J., and Butler, H. L. "New York Bight Study; Report 1, Hydrodynamic modeling" (in preparation), Technical Report CERC-94-4, U.S. Army Engineer Waterways Experiment Station.

Sheng, Y. P. (1986). "A three-dimensional mathematical model of coastal, estuarine and lake currents using boundary fitted grid," Report No. 585, A.R.A.P. Group of Titan Systems, New Jersey, Princeton, NJ.

Steele, J. (1962). "Environmental control of photosynthesis in the sea," *Limnology and Oceanography*, 7:137-50.

Stoddard, A. (1983). "Mathematical model of oxygen depletion in the New York Bight: An analysis of physical, biological, and chemical factors in 1975 and 1976," Ph.D. diss., University of Washington, Seattle, WA.

_____. (1989). "Eutrophication and recurrent hypoxia in the New York Bight: A synthesis of historical data and numerical model of the 1976 anoxic event." *Estuarine and Coastal Proceedings*, WW Div, ASCE, Newport R.I., November 15-17, 1989, 361-70.

Stoddard, A., and Han, G. (1989). "Review and assessment of prototype data available for use in studying hydrodynamic/water quality interactions in the New York Bight," prepared for Evans-Hamilton, Inc., Rockville, MD.

Thomann, R., and Fitzpatrick, J. (1982). "Calibration and verification of a mathematical model of the eutrophication of the Potomac Estuary," Hydro-Qual, Inc., Mahwah, NJ.

Wen C., Kao, J.,. Wang, L., and Liaw, C. (1984). "Effects of salinity of reaeration coefficient of receiving waters," *Water Science and Technology*, 16:139-54.

Wezernak, C., and Gannon, J., (1968). "Evaluation of nitrification in steams," *Journal of the Sanitary Engineering Division*, 94(SA):883-95.

Wolfe, D. A., Monahan, R., Stacey, P. E., Farrow, D. R. G., and Robertson, A. (1991). "Environmental quality of Long Island Sound: assessment and management issues," *Estuaries*, Vol 14, No. 3, 224-36.

WMI. (1989). "Workshop on hydro-environmental monitoring and modeling in the New York Bight: program and abstracts," Waste Management Institute, Marine Sciences Research Center, State University of New York, Stony Brook, NY.

_____. (1991). "Workshop on hydro-environmental monitoring and modeling in the New York Bight: Program and abstracts," Marine Sciences Research Center, State University of New York, Stony Brook, NY.

NEW YORK BIGHT

Initial HM Grid used for WQM and HM Transport Comparison
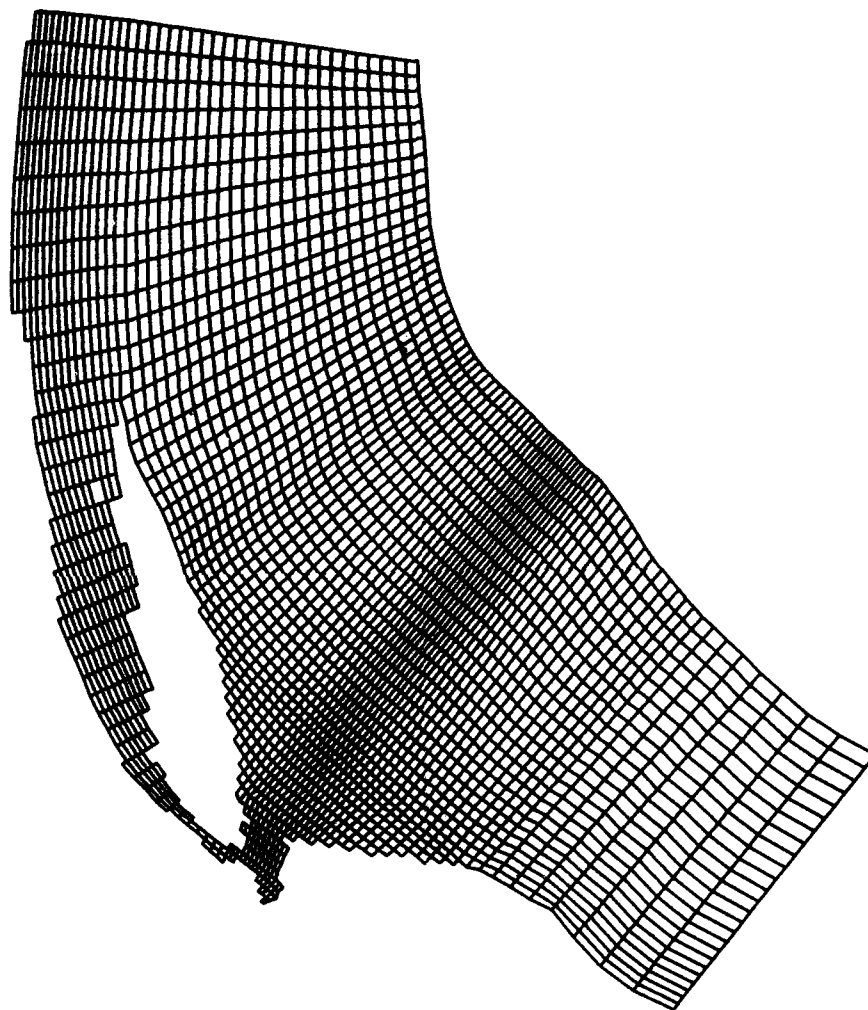
Plate 1

NEW YORK BIGHT

Final Hydrodynamic Model Grid

Plate 2

Hudson River Continuous Release
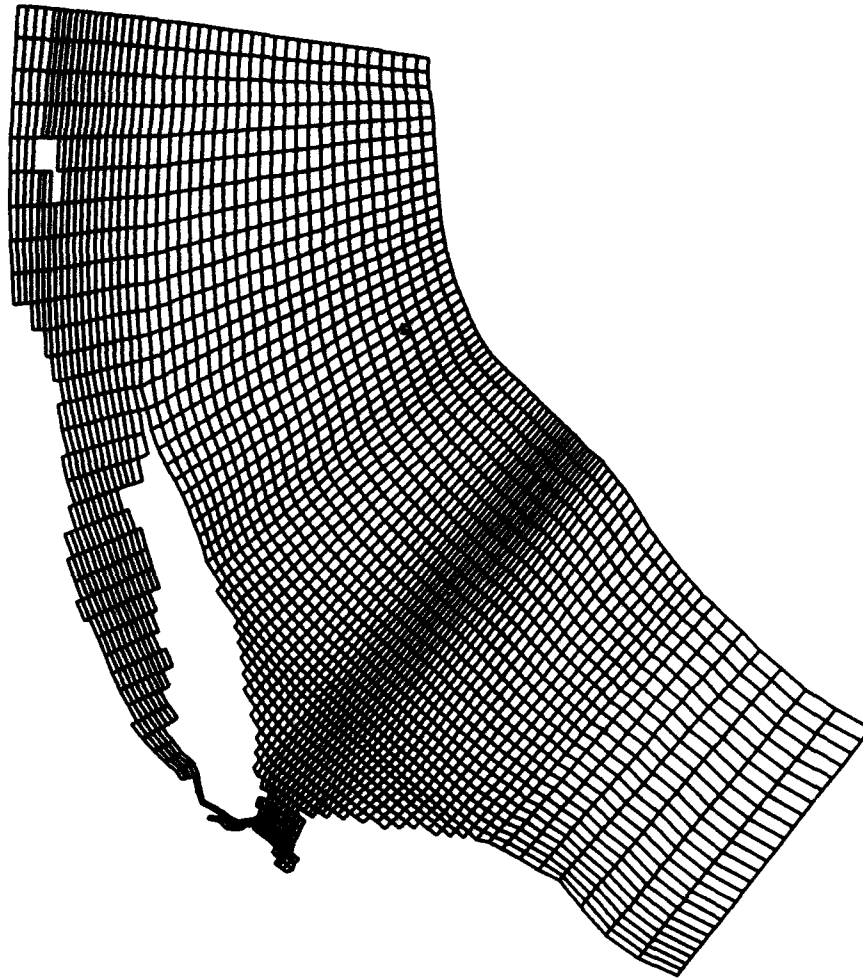
■ Release
○ Sample
— Transect
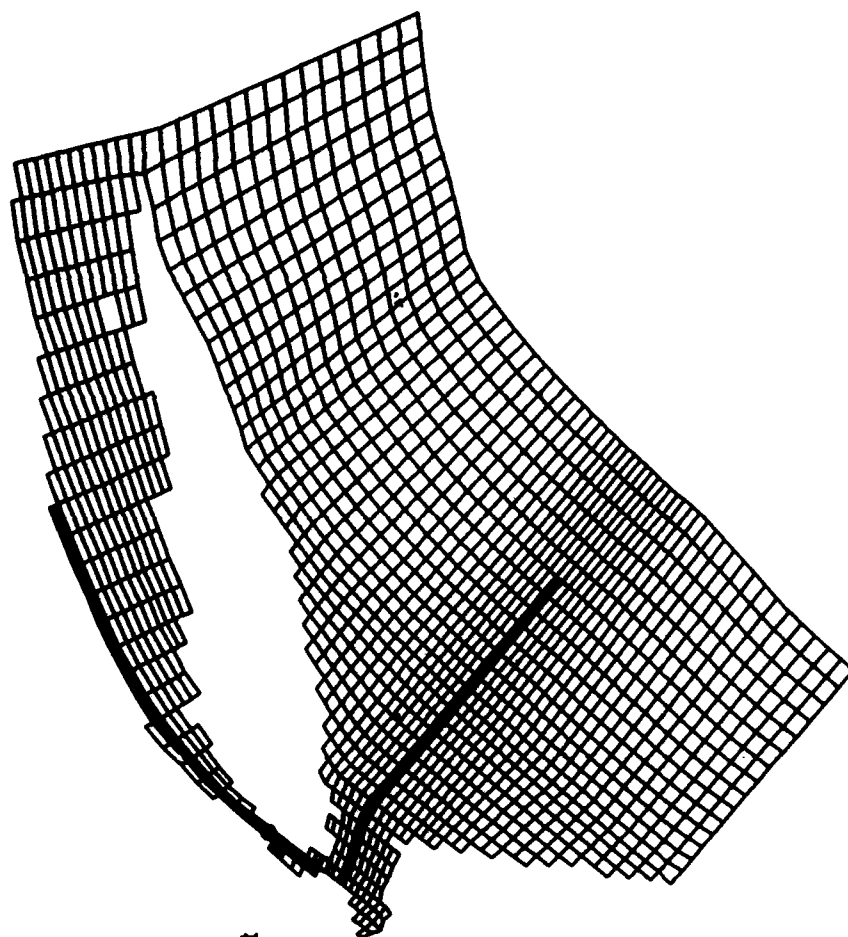
Plate 3

HM Versus WQM Transport Comparison
Hudson River Continuous Release

WQM Cell 2422, HM Cell (40,42,5)

WQM Cell 2394, HM Cell (34,41,5)

Legend
WQM
HM - - - -

Plate 4

HM Versus WQM Transport Comparison
Hudson River Continuous Release

Time =   5.00 days

Legend
WQM ———
HM ┄┄┄

Transect 2

Transect 1

Plate 5

Bight Continuous Release

■ Release
O Sample

Plate 6
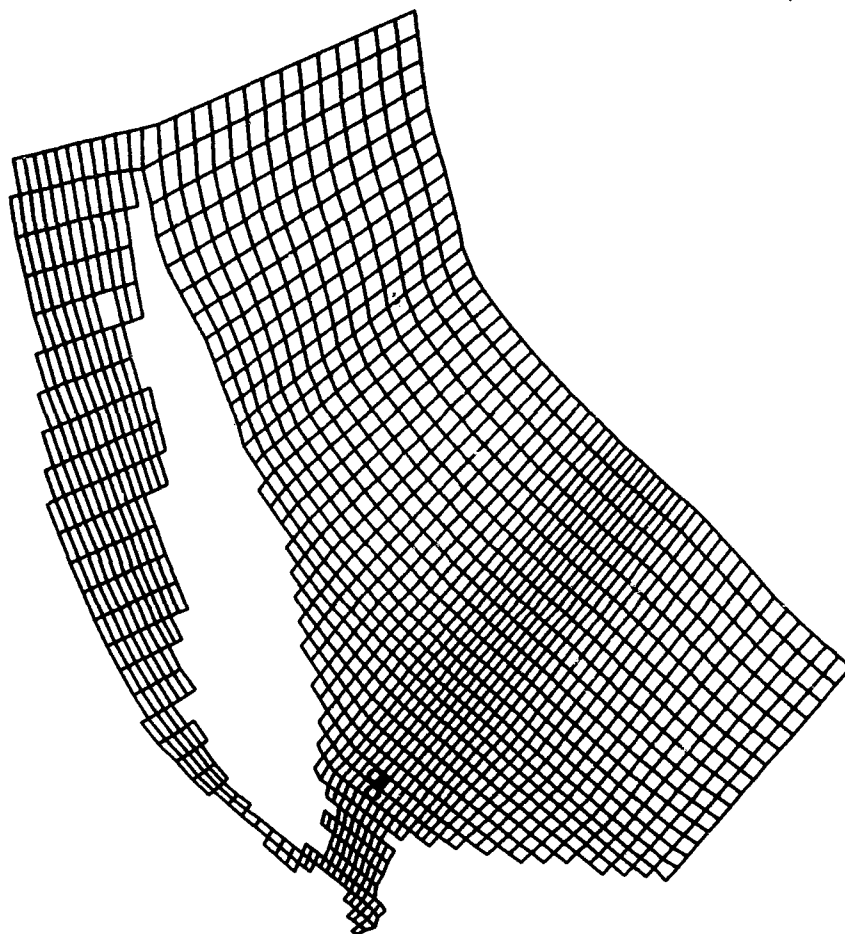
HM Versus WQM Transport Comparison
Bight Contiuous Release

UPWIND Solution Scheme

WQM Cell 2167, HM Cell (31,34,5)
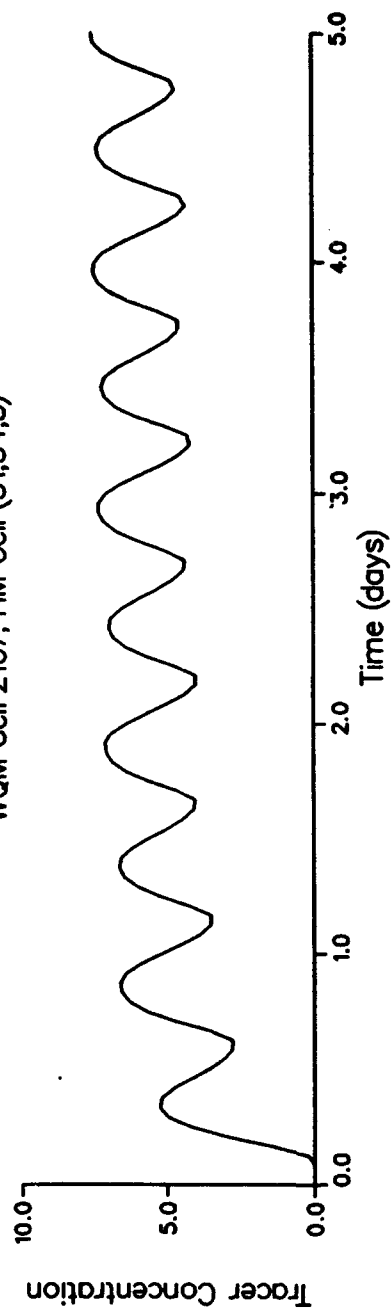
WQM Cell 2126, HM Cell (32,33,5)
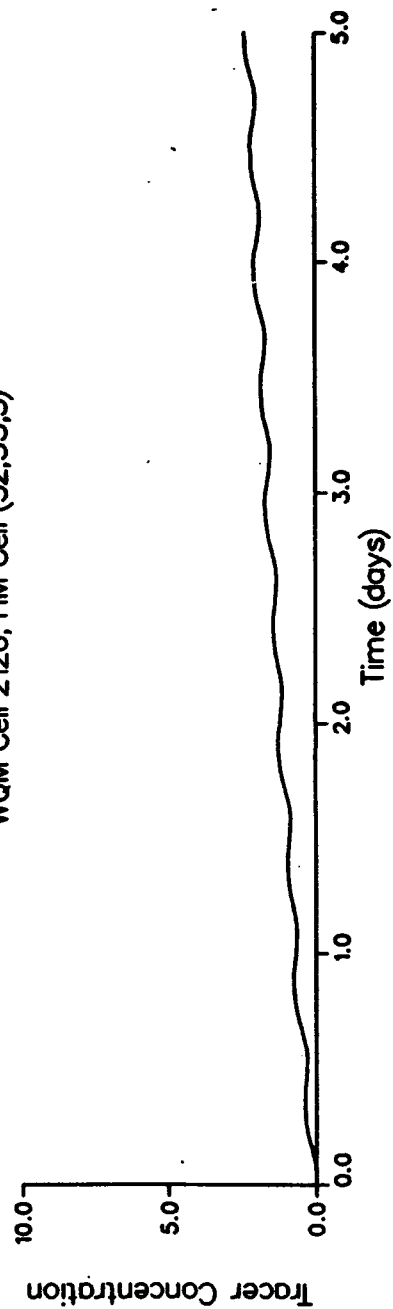
Legend
WQM ───
HM ─ ─ ─

Plate 7

HM Versus WQM Transport Comparison
Bight Contiuous Release

QUICKEST Solution Scheme

WQM Cell 2167, HM Cell (31,34,5)

WQM Cell 2126, HM Cell (32,33,5)

Legend
WQM
HM

Plate 8

Bight Spot Dump

■ Release
—— Transect
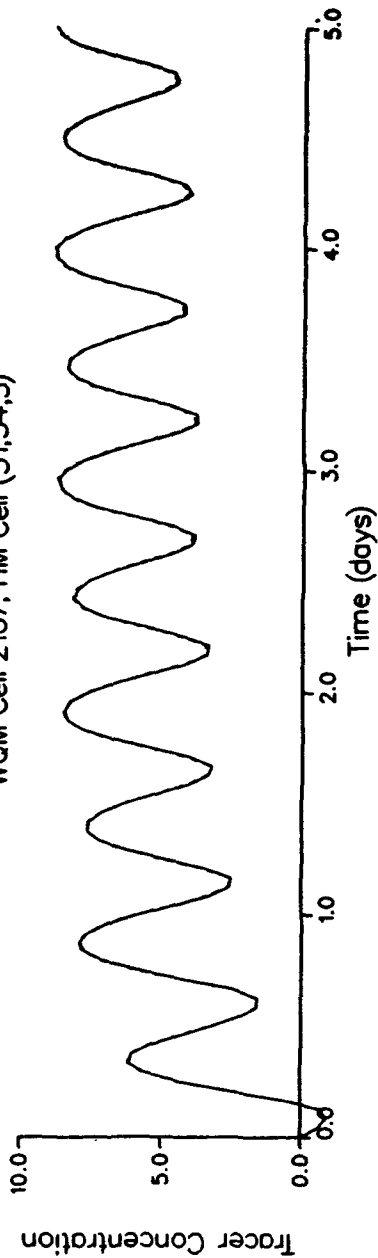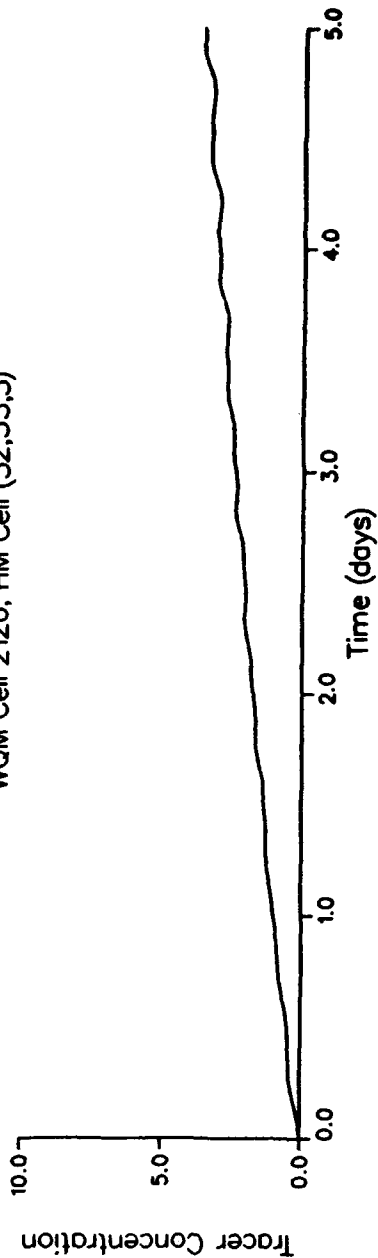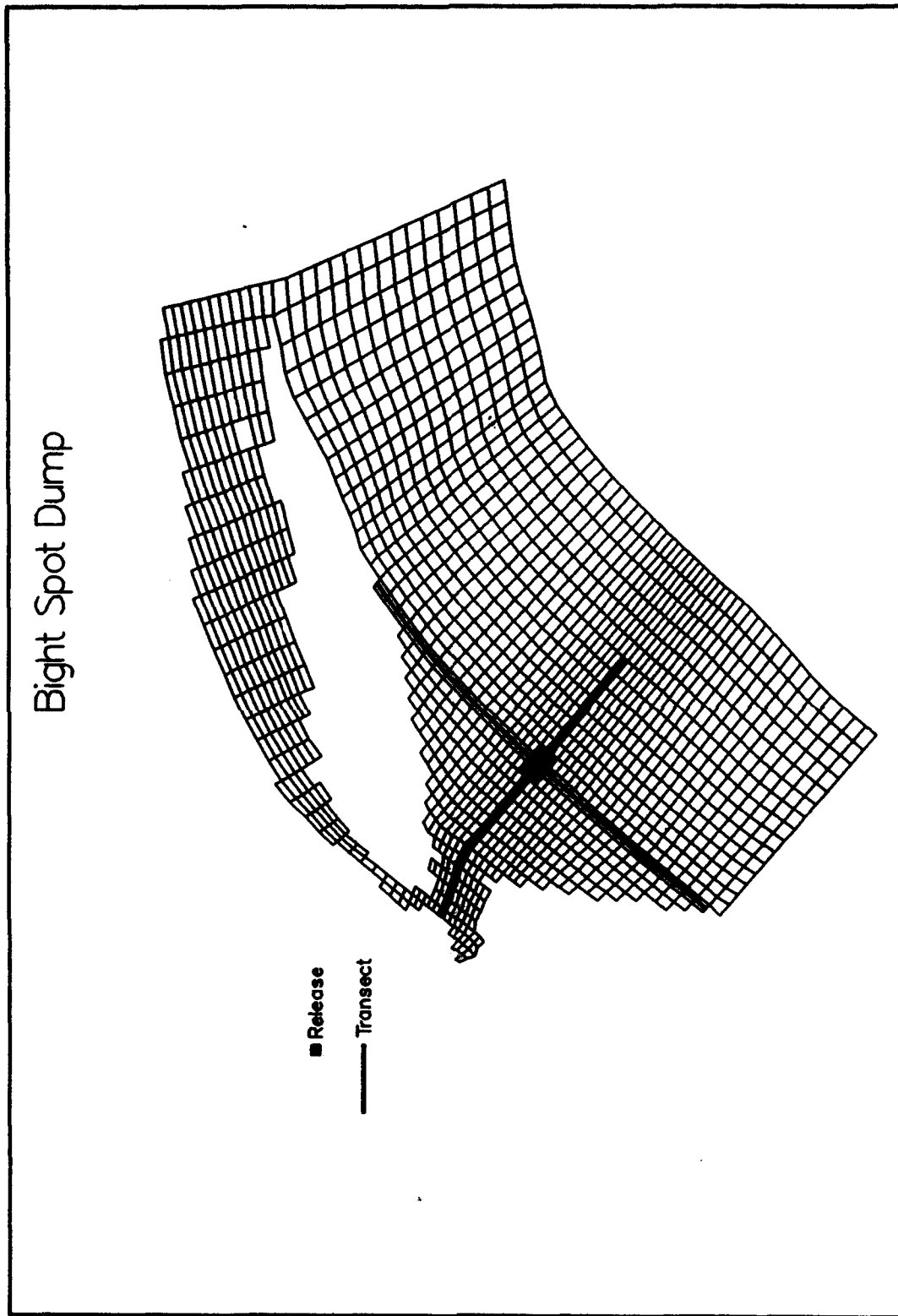
Plate 9

Intratidal and Intertidal Transport Comparison
Bight Spot Dump

1-hr Intratidal Averaging

Time = 20.00 days

Legend
WQM ———
HM - - - - -

Transect.2

Transect 1
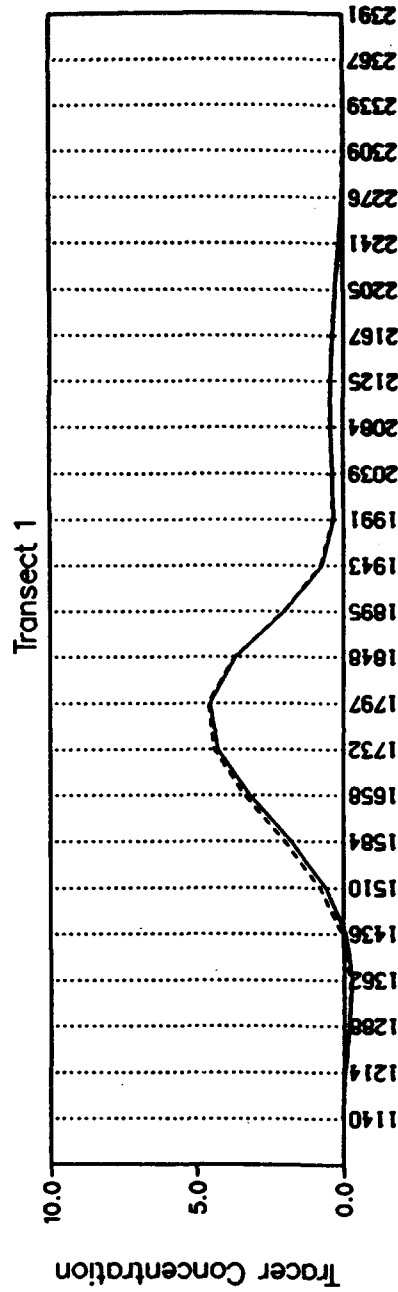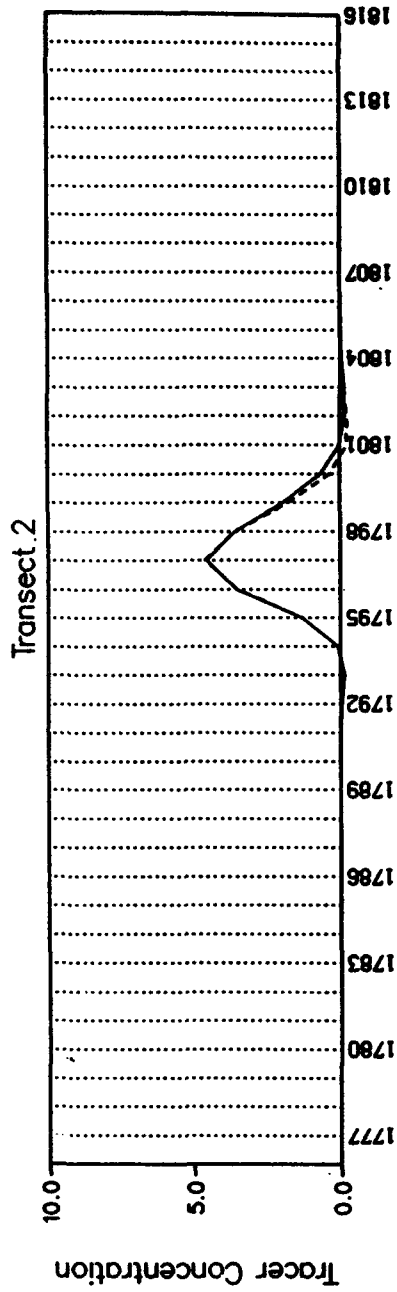
Plate 10

Intratidal and Intertidal Transport Comparison
Bight Spot Dump

12.5-hr Intertidal Averaging

Time = 20.03 days

Plate 11
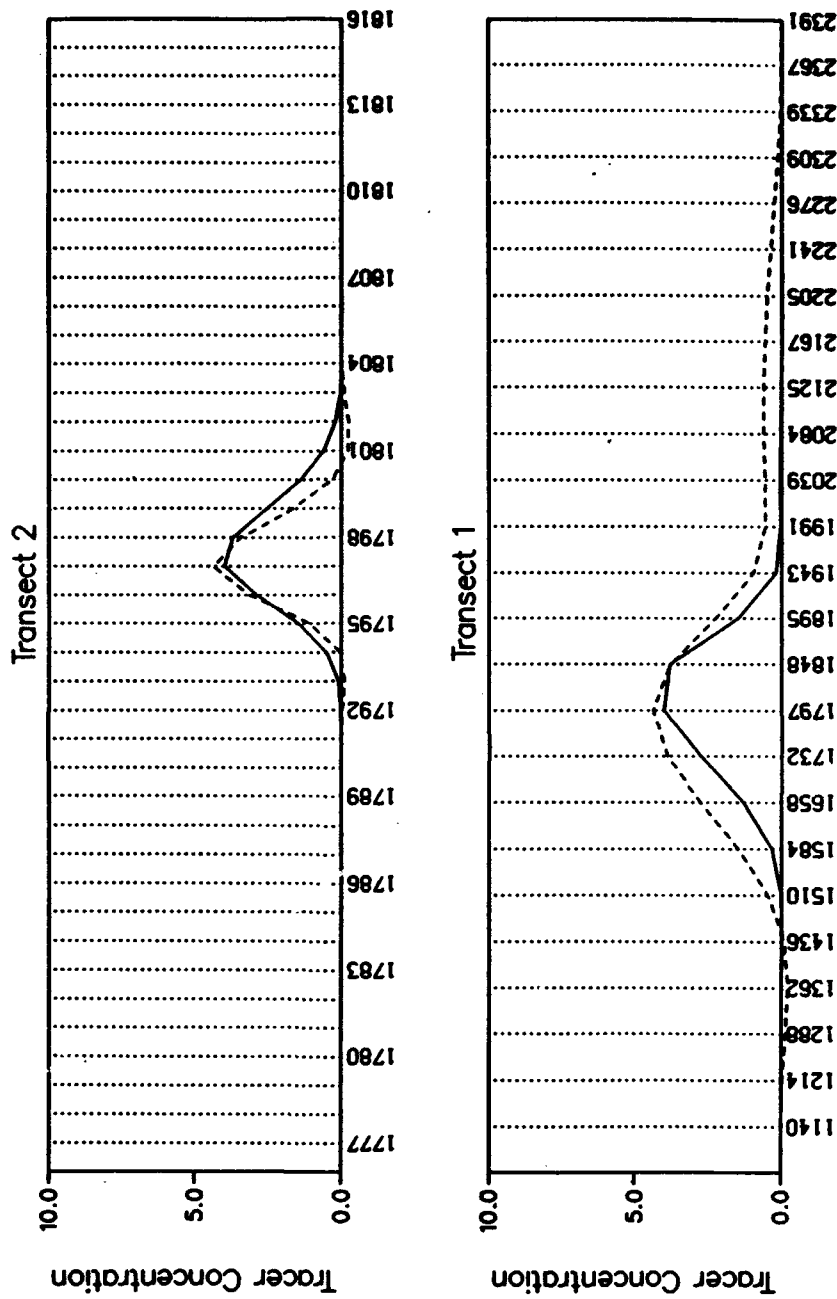
Intratidal and Intertidal Transport Comparison
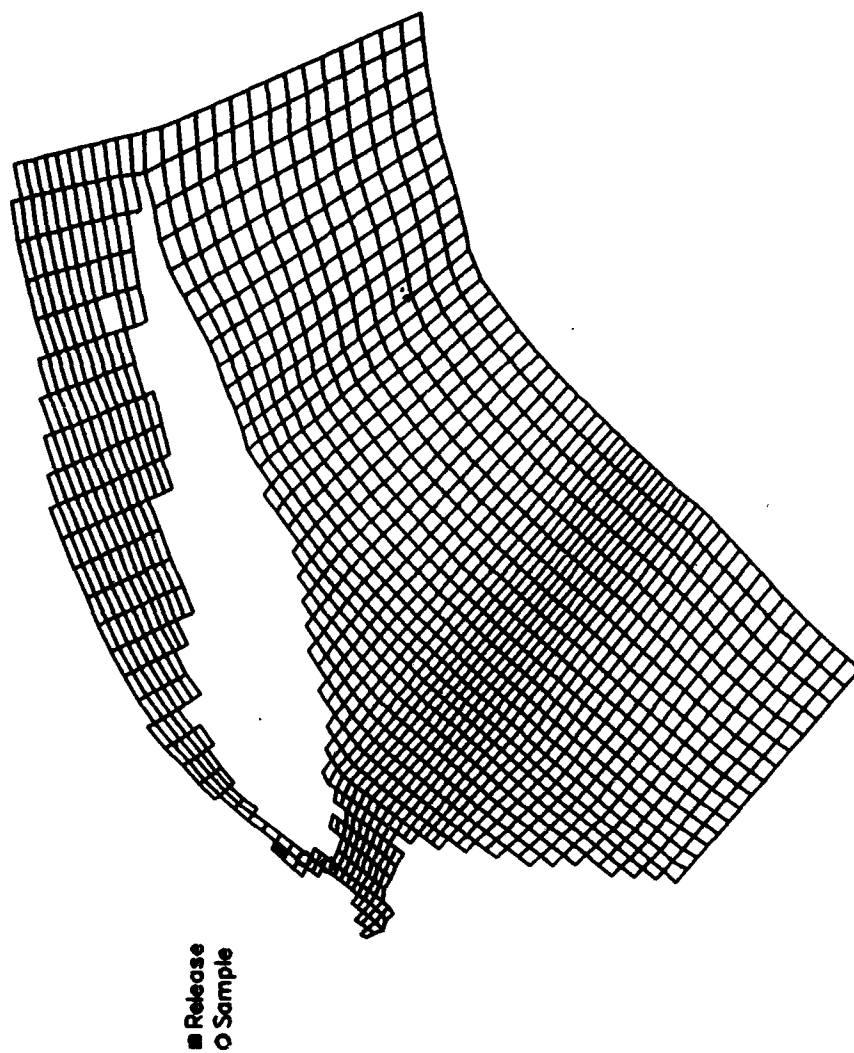
■ Release
○ Sample

Plate 12

Intratidal and Intertidal Transport Comparison
Hudson River Continuous Release

1-hr Intratidal Averaging

WQM Cell 2419, HM Cell (43,43,5)

WQM Cell 2394, HM Cell (34,41,5)

Plate 13

Intratidal and Intertidal Transport Comparison
Hudson River Continuous Release

4-hr Intratidal Averaging

WQM Cell 2419, HM Cell (43,43,5)

WQM Cell 2394, HM Cell (34,41,5)

Legend
WQM

Plate 14

Intratidal and Intertidal Transport Comparison
Hudson River Continuous Release

8-hr Intratidal Averaging

WQM Cell 2419, HM Cell (43,43,5)

WQM Cell 2394, HM Cell (34,41,5)

Legend
WQM

Plate 15

Intratidal and Intertidal Transport Comparison
Hudson River Continuous Release

12-hr Intratidal Averaging

WQM Cell 2419, HM Cell (43,43,5)

WQM Cell 2394, HM Cell (34,41,5)

Legend
WQM

Plate 16

Intratidal and Intertidal Transport Comparison
Hudson River Continuous Release

Plate 17
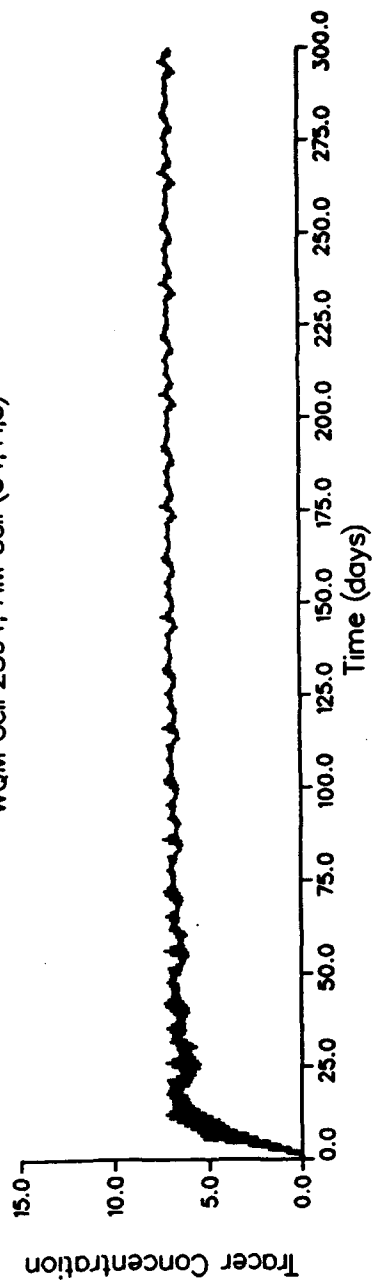
NEW YORK BIGHT

74x48 Water Quality Model Grid
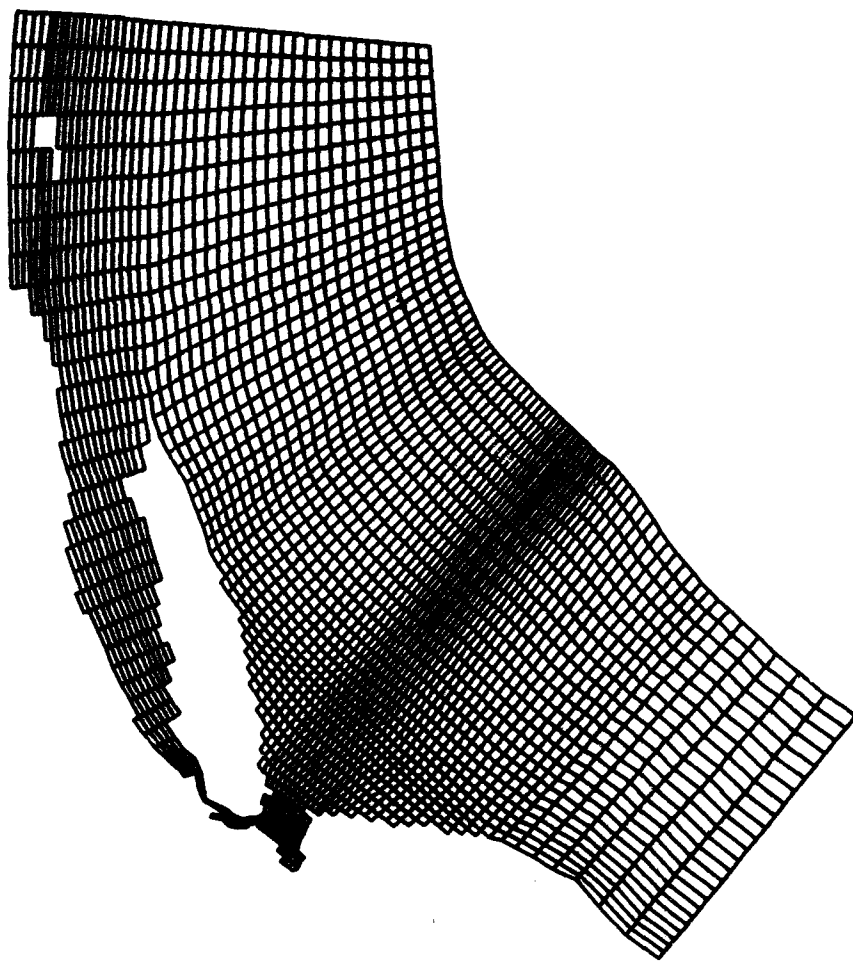
Plate 18

NEW YORK BIGHT

78x44 Transformed Hydodynamic Model Grid

Plate 19
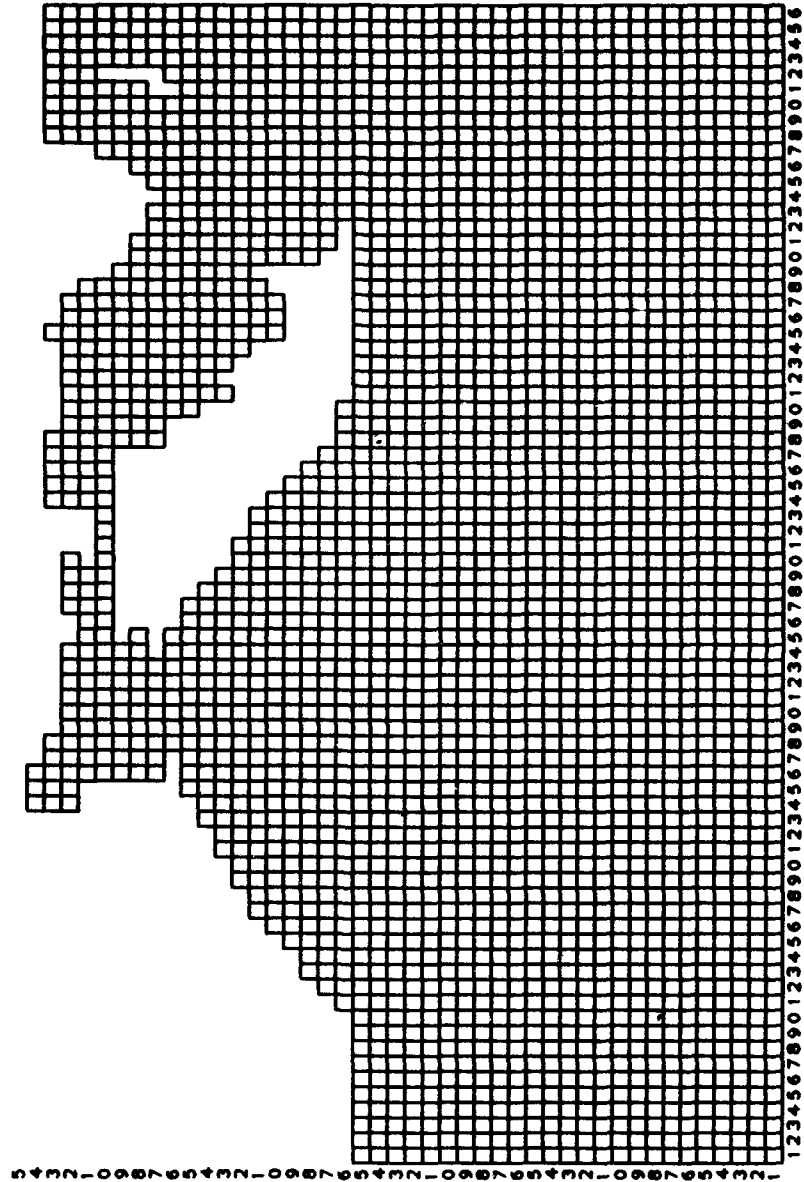
IC Coarse Grid
Overlaid 74x43 Transformed WQM Grid

Plate 20

BOUNDARY CONDITION SEGMENTS

Plate 21

SOD : 1974-1975

Plate 22
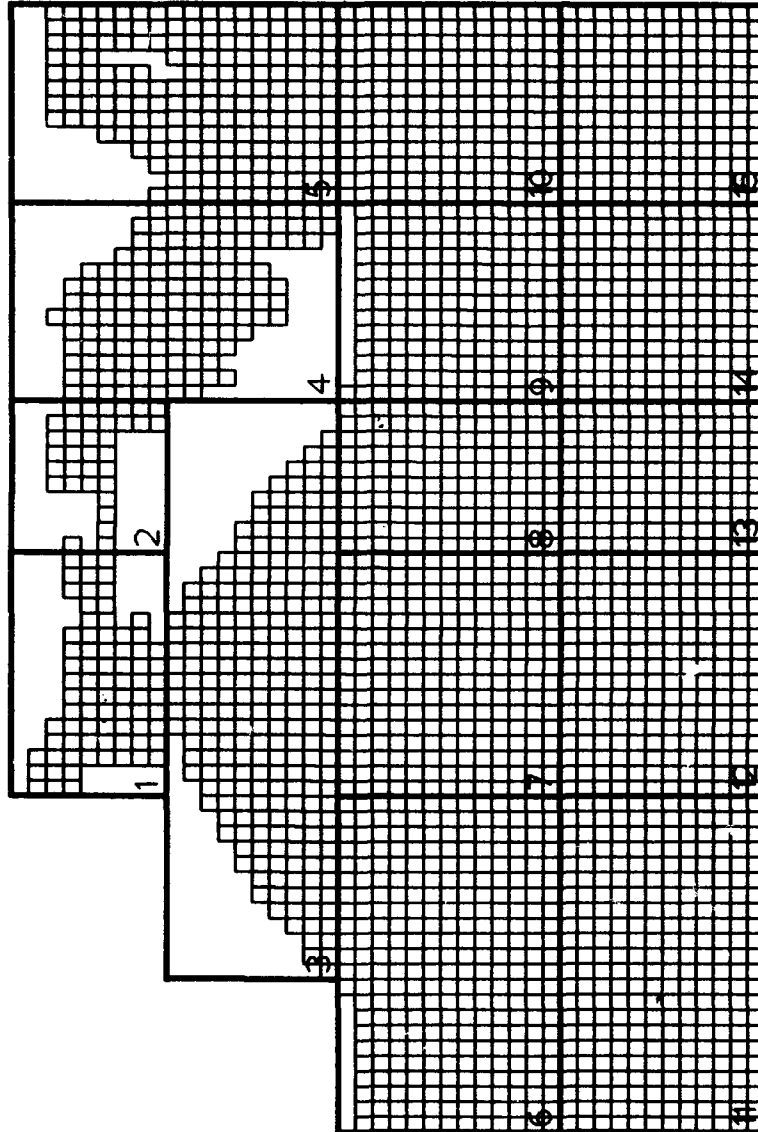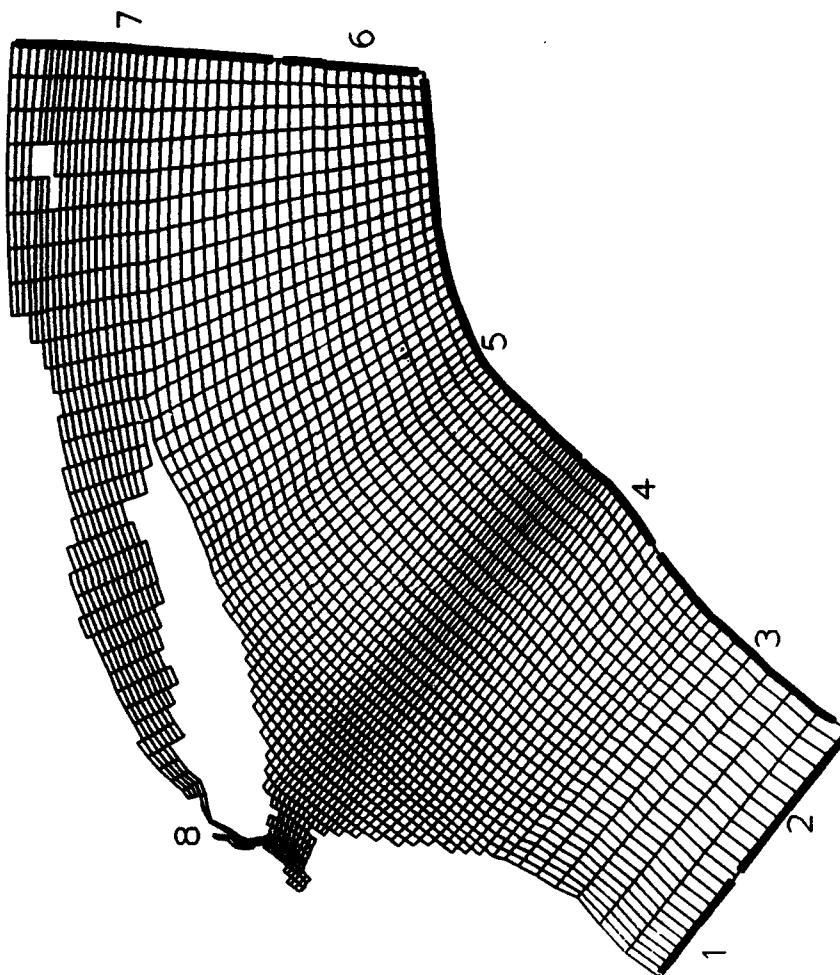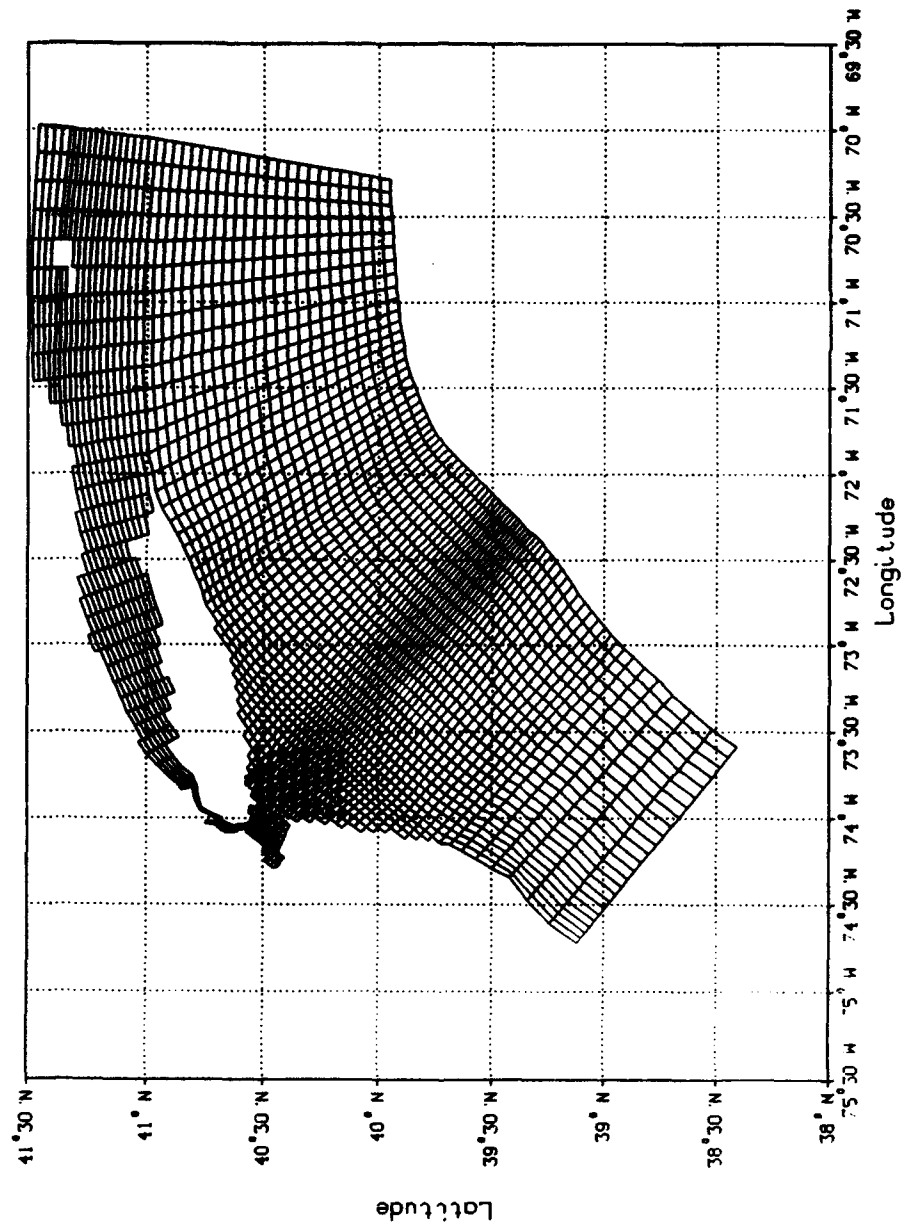
MEASURED AND SIMULATED COMPARISONS

Spatial Regions and Specific Locations

Plate 23

WQM Transects

Plate 24
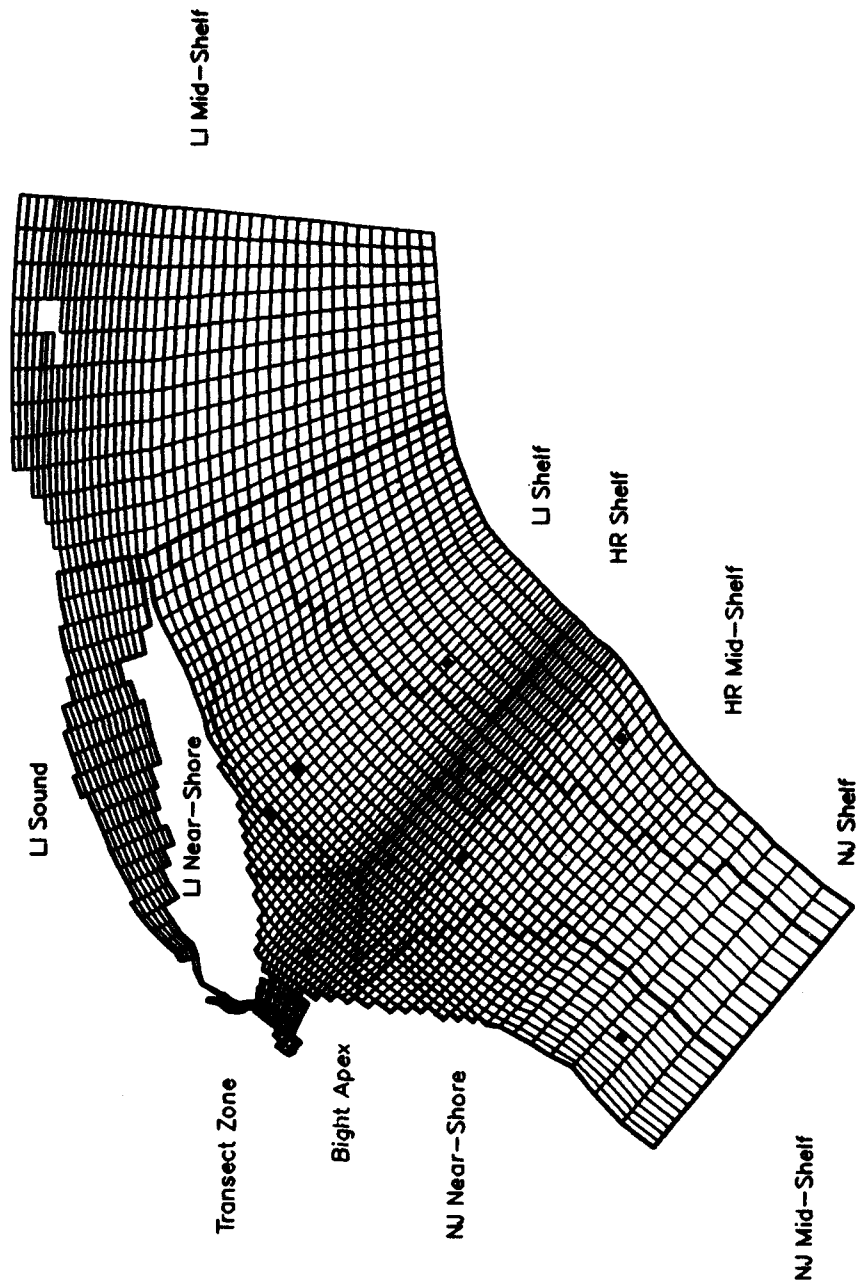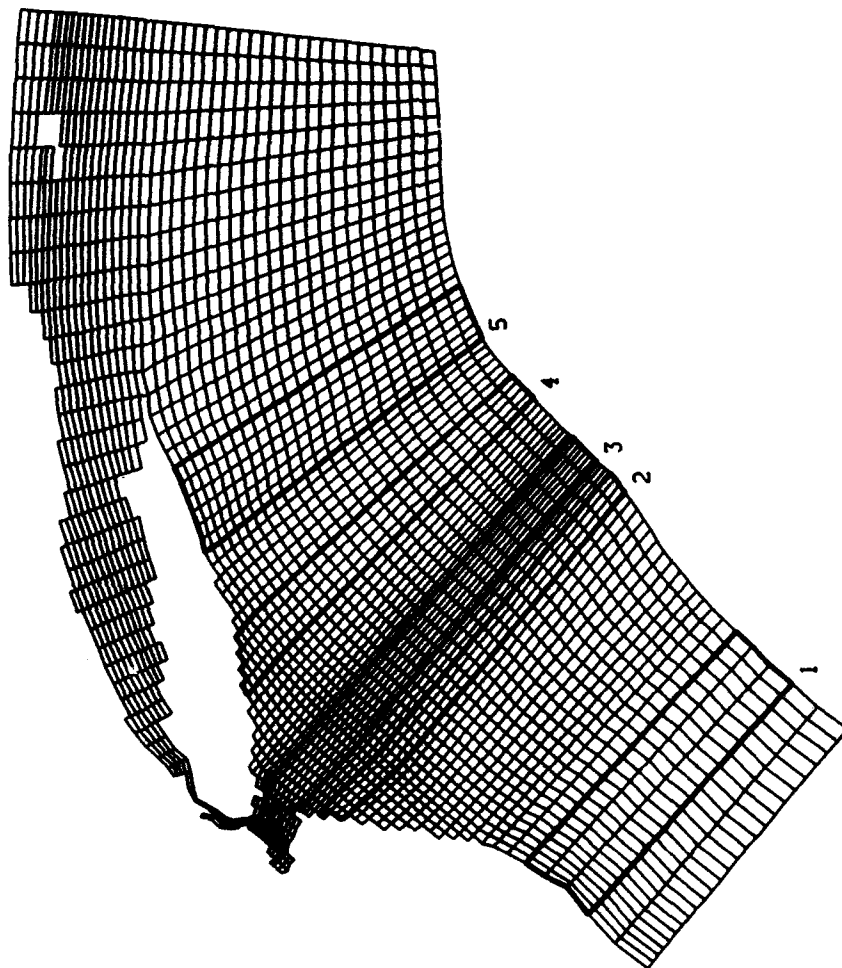
New York Bight

Dissolved Oxygen (2.0 ml l^{-1})

Bottom – July 1976

Legend

Simulated ——————

Measured ▪ ▪ ▪ ▪

Plate 25
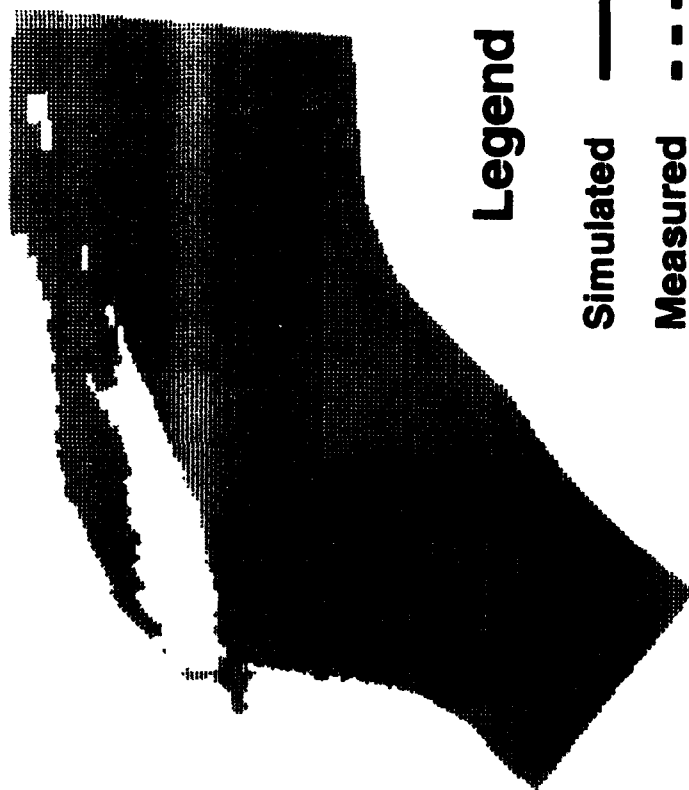
Dissolved Oxygen (4.0 g DO m^{-3})
Bottom Layer – July 1976
Calibration Run

Plate 26

Dissolved Oxygen (4.0 g DO m^{-3})
Bottom Layer – July 1976
New Jersey External Loads = 0.0

Plate 27
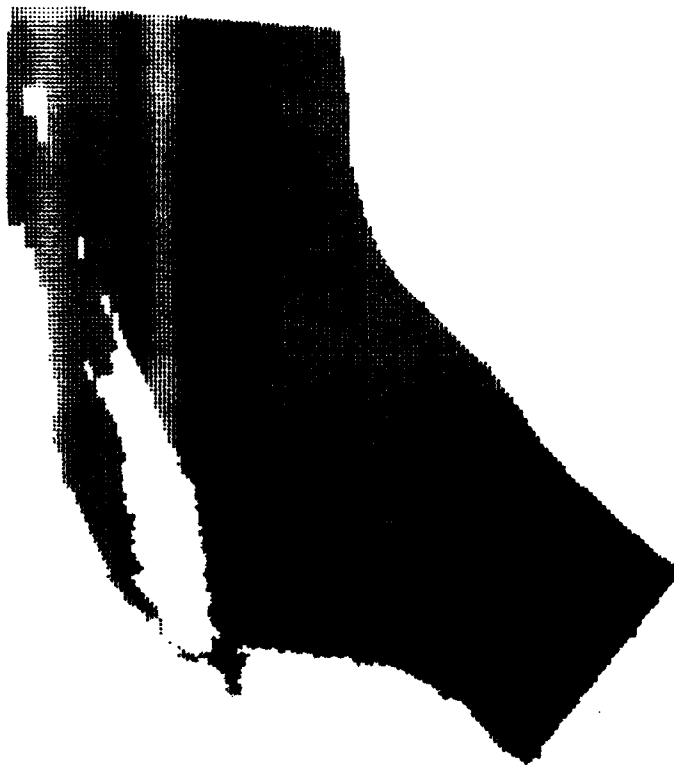
Dissolved Oxygen (4.0 g DO m^{-3})

Bottom Layer – July 1976

DOC Boundary Conditions = 0.0

Plate 28
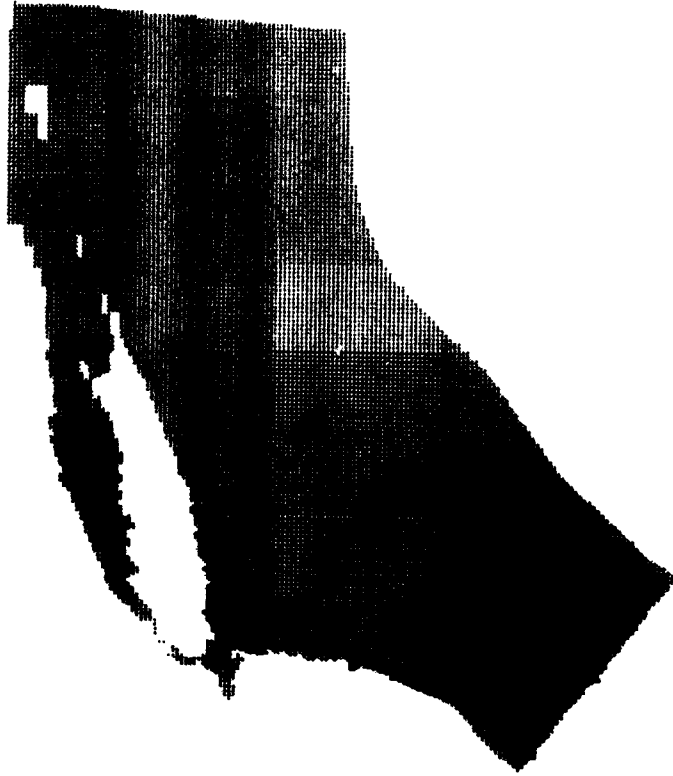
Dissolved Oxygen (4.0 g DO m^{-3})

Bottom Layer – July 1976

New Jersey Near–Shore, Mid–Shelf, and Shelf SOD = 0.0

Plate 29

Sensitivity: LIS External Loads

Month: Aug

LEGEND
Calibration
LIS External Loads
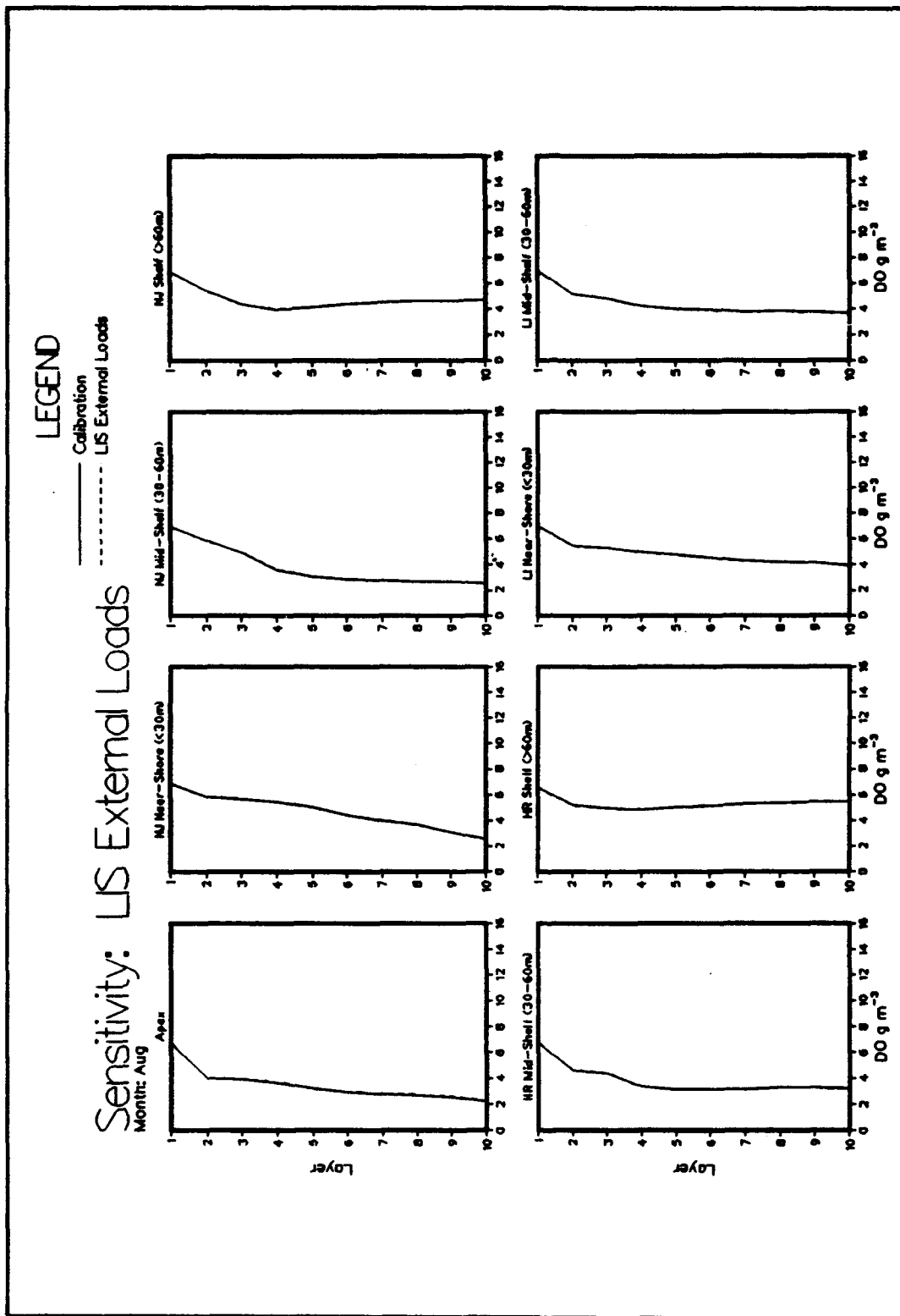
Plate 30.   (Sheet 1 of 2)

Sensitivity: LIS External Loads

Month: Aug

LEGEND
Calibration
LIS External Loads

Plate 30.   (Sheet 2 of 2)
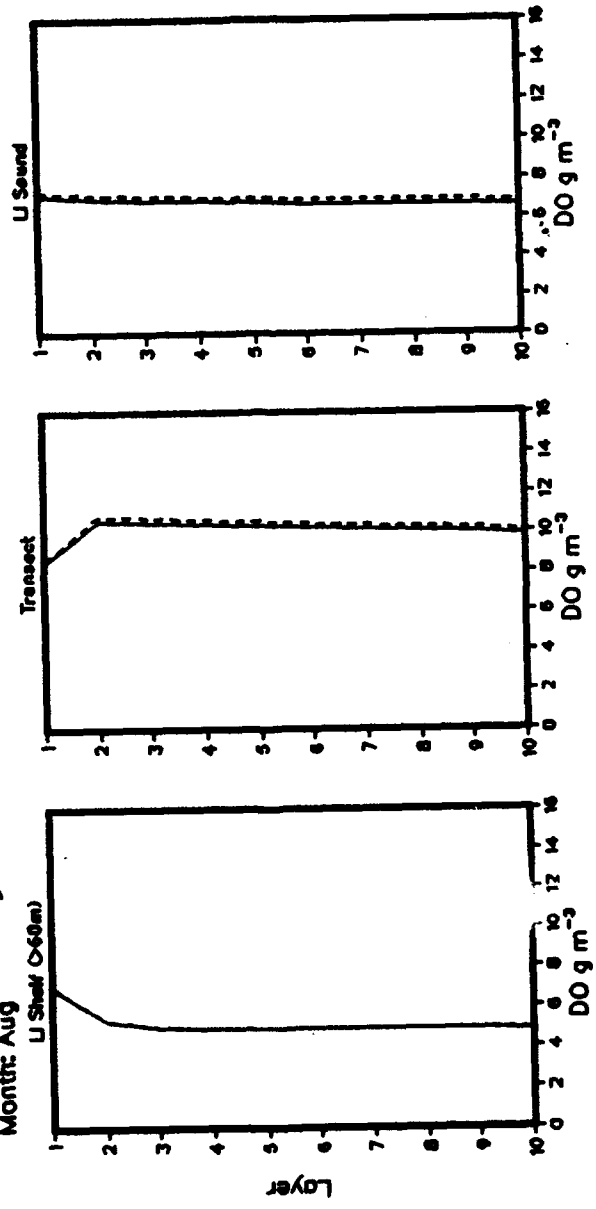
Appendix A
Water Quality Model Kinetic Formulations and Coefficients

Draft text from Chapter 4 (The Water Quality Model) of the Chesapeake Bay Water Quality Model (Cerco and Cole, in preparation)[1] is extracted and reproduced in this appendix to relate the water quality model (WQM) kinetic coefficients selected and to clarify the New York Bight (NYB) model adaptations. The major NYB kinetic adaptations that included sediment oxygen demand (SOD) and ammonia (NH_4-N) sediment-water column fluxes and bottom layer denitrification are also presented. A tabulation of the kinetic coefficient values used in the NYB water quality model is presented at the conclusion of this appendix.

Sediment Oxygen Demand (SOD)

Sediment oxygen demand was specified as temporally and spatially constant (SOD_{base}). The SOD was modulated through temperature and DO concentration of overlying water. The SOD formulation was

$$SOD = SOD_{base} \exp{(KSO\,(T - TRSO))}\,DO/(KHSO + DO) \qquad \text{(A1)}$$

where

KSO = effect of temperature on SOD, $°C^{-1}$

$TRSO$ = reference temperature for SOD, $°C$

$KHSO$ = half-saturation concentration of DO for SOD, $g\,O_2\,m^{-3}$

---

[1] See References at the end of the main text.

Sediment Ammonia Release

The formulation for sediment NH_4-N release was similar to that for SOD:

$$NH_4 \; release = NH_{4 \; base} \; \exp(KSNH4 \; (T - TRSNH4)$$

$$KHSNH4/(KHSNH4 + DO) \qquad \text{(A2)}$$

where

$KSNH4$ = effect of temperature on NH_4-N sediment release, $°C^{-1}$

$TRSNH4$ = reference temperature for sediment NH_4-N release, $°C$

$KHSNH4$ = half-saturation concentration DO for sediment NH_4-N release, $g \; O_2 \; m^{-3}$

Bottom Layer Denitrification

Nitrate transfer across the sediment-water interface is proportional to the concentration difference between sediment interstitial water and the water column.

$$Flux = RKSED \; (NO_{3 \; sed} - NO_{3 \; water}) \qquad \text{(A3)}$$

In systems such as the NYB, $NO_{3 \; water} >> NO_{3 \; sed}$ so that

$$Flux = -RKSED \; NO_3 \qquad \text{(A4)}$$

$RKSED$ = sediment-water mass transfer rate, $m \; day^{-1}$

The following text was extracted from Chapter 4 of the Chesapeake Bay Water Quality Model (Cerco and Cole, in preparation) and modified to reflect the NYB application.

State Variables

Algae

Algae are grouped into two size-fractionated classes: net plankton ($>20 \; \mu m$) and nanoplankton ($<20 \; \mu m$).

Organic carbon

Two organic carbon state variables are considered: dissolved (DOC) and particulate (POC).

Nitrogen

Nitrogen is divided into organic and mineral fractions. Organic nitrogen state variables are dissolved organic nitrogen (DON) and particulate organic nitrogen (PON). Two mineral nitrogen forms are considered: ammonia (NH_4) and nitrate (NO_3). The nitrate state variable represents the sum of nitrate plus nitrite.

Dissolved oxygen

Dissolved oxygen is a central component of the water quality model.

Salinity

Salinity is a conservative tracer that allows for verification of the transport component of the model and facilitates examination of conservation of mass. Salinity also influences the saturation concentration of DO.

Temperature

Temperature is a primary determinant of the rate of biochemical reactions.

Conservation Of Mass Equation

The Chesapeake Bay water quality model, CE-QUAL-ICM, is an integrated compartment box model. The box structure was selected to allow maximum flexibility for adaptation of the model to alternate hydrodynamic models. Boxes in CE-QUAL-ICM correspond to cells in X-Y-Z space on the CH3D grid. CE-QUAL-ICM solves, for each grid cell and for each state variable, the conservation of mass equation:

$$\frac{\delta V_i C_i}{\delta t} = \sum_{j=1}^{n} Q_j C_j^* + \sum_{j=1}^{n} A_j D_j \frac{\delta C}{\delta x_j} + \Sigma \ S_i \qquad (A5)$$

where

V_i = volume of ith compartment (m^3)

C_i = concentration in ith compartment (g m^{-3})

Q_j = volumetric flow across flow face j of ith compartment (m^3 sec^{-3})

C^e_j = concentration in flow across flow face j (g m^{-3})

A_j = area of flow face j (m^2)

D_j = diffusion coefficient at flow face j (m^2 sec^{-1})

n = number of flow faces attached to ith compartment

S_i = external loads and kinetic sources and sinks in ith compartment (g sec^{-1})

t, x = temporal and spatial coordinates, respectively

This appendix focuses on the portion of the temporal derivative attributed to internal sources and sinks (kinetics). Within the model, kinetics are computed using a temporal dimension of days, for consistency with reported rate coefficients. Kinetic sources and sinks are converted within CE-QUAL-ICM to a dimension of seconds before employment in the mass-balance equation.

Algae

Algae play a central role in the carbon and nitrogen cycles that comprise the model ecosystem. Equations governing the two algal groups are largely the same. Differences among groups are expressed through the magnitudes of parameters in the equations. In describing the parameters, the letter "x" is used as a "wild card." As needed in this text, and within the model code, the wild card is replaced with a letter that indicates a specific algal group. Characters that indicate each algal group are:

d = net plankton

g = nanoplankton

Sources and sinks of algae are:

Sources: Growth (production)

Sinks: Settling
        Basal metabolism
        Predation

The last two sinks of algae are grouped under the heading mortality. The governing equation for algal biomass is

A4

$$\frac{\partial}{\partial t} Bx = \left(Px - Mx - WSx \frac{\partial}{\partial z}\right) Bx \qquad \text{(A6)}$$

where

Bx = biomass, expressed as carbon (g C m^{-3})

Px = production (day^{-1})

Mx = mortality (day^{-1})

WSx = settling velocity (m day^{-1})

z = vertical coordinate (m)

Production

Production by phytoplankton is determined by the availability of nutrients, by the intensity of light, and by the ambient temperature. The effects of each are considered to be multiplicative:

$$Px = PMx \ f(N) \ f(I) \ f(T) \qquad \text{(A7)}$$

where

PMx = production under optimal conditions (day^{-1})

$f(N)$ = effect of suboptimal nutrient concentration ($0 \leq f \leq 1$)

$f(I)$ = effect of suboptimal illumination ($0 \leq f \leq 1$)

$f(T)$ = effect of suboptimal temperature ($0 \leq f \leq 1$)

Nutrients

Carbon, nitrogen, and phosphorus are the primary nutrients required for algal growth. Carbon is usually available in excess, and nitrogen was assumed the limiting nutrient in the NYB. Therefore, carbon and phosphorus were not considered. The effect of nitrogen on growth is described by the formulation commonly referred to as "Monod kinetics" (Monod 1949) in which growth is dependent upon nitrogen availability at low nitrogen concentrations but independent of nitrogen at high concentrations:

$$f(N) = \frac{NH4 + NO3}{KHNx + NH4 + NO3} \qquad (A8)$$

where

$KHNx$ = half-saturation constant for nitrogen uptake (g N m^{-3})

Light

Algal production increases as a function of light intensity until an optimal intensity is reached. Beyond the optimal intensity, production declines as intensity increases. Steele's equation (DiToro, O'Connor, and Thomann 1971) describes this phenomenon:

$$f(I) = \frac{I}{IS} \exp\left(1 - \frac{I}{IS}\right) \qquad (A9)$$

where

I = illumination rate (Langleys day^{-1})

IS = optimal illumination (Langleys day^{-1})

Steele's equation describes the instantaneous light limitation at a point in space. The model, however, computes processes integrated over discrete time intervals and aggregated spatially into model segments. Therefore, Steele's equation must be integrated over an appropriate time interval and averaged over the thickness of each model segment. The integration interval selected is 1 day. This interval does not preclude computation steps less than a day but frees the model from accounting for illumination in "real time." The price paid is that diurnal fluctuations in algae are not computed. Assuming light intensity declines exponentially with depth, the integrated, averaged form of Steele's equation is:

$$f(I) = \frac{2.72\ FD}{KESS\ H} [\exp(\alpha b) - \exp(\alpha t)] \qquad (A10)$$

$$\alpha b = - \frac{Io}{FD\ IS} \exp[-KESS\ (ZD + H)] \qquad (A10a)$$

$$\alpha t = - \frac{Io}{FD\ IS} \exp(-KESS\ ZD) \qquad (A10b)$$

A6

where

Io = daily illumination at water surface (Langleys day^{-1})

FD = fractional daylength ($0 \leq FD \leq 1$)

$KESS$ = total light attenuation coefficient (m^{-1})

ZD = distance from water surface to top of layer (m)

Light attenuation in the water column is composed of two fractions: a background value dependent on water color and concentration of suspended particles, and extinction due to light absorption by ambient chlorophyll:

$$KESS = KE + KECHL \frac{1}{CCHLx} \sum_{x=1_e} Bx \qquad (A11)$$

where

$KESS$ = total attenuation affecting algal growth (m^{-1})

KE = background light attenuation (m^{-1})

$KECHL$ = light attenuation coefficient for chlorophyll a (m^2 mg^{-1})

$CCHLx$ = carbon-to-chlorophyll ratio of algal group x (g C mg^{-1} chl)

Optimal illumination for photosynthesis depends on algal taxonomy, duration of exposure, temperature, nutritional status, and previous acclimation. Variations in optimal illumination are largely due to adaptations by algae intended to maximize production in a variable environment. Steele (1962) noted the result of adaptations is that optimal illumination is a consistent fraction ($\approx$ 50 percent) of daily illumination. Kremer and Nixon (1978) reported an analogous finding that maximum algal production occurs at a constant depth ($\approx$1 m) in the water column. Their approach is adopted here so that optimal illumination is expressed:

$$ISx = IOAVG \exp (-KESS\ DOPTx) \qquad (A12)$$

where

$IOAVG$ = adjusted surface illumination (Langleys day^{-1})

$DOPTx$ = depth of maximum algal production (m)

A minimum, $ISMIN$, is specified for optimal illumination so that algae do not thrive at extremely low light levels. The time required for algae to adapt

to changes in illumination is recognized by computing ISx based on a time-weighted average of daily illumination:

$$IOAVG = 0.7 \, Io + 0.2 \, I1 + 0.1 \, I2 \qquad (A13)$$

where

$I1$ = daily illumination 1 day preceding model day (Langleys day^{-1})

$I2$ = daily illumination 2 days preceding model day (Langleys day^{-1})

Temperature

Algal production increases as a function of temperature until an optimum temperature or temperature range is reached. Above the optimum, production declines until a temperature lethal to the organisms is attained. Numerous functional representations of temperature effects are available. Inspection of growth versus temperature curves indicates that a function similar to a Gaussian probability curve provides a good fit to observations:

$$F(T) = \begin{cases} \exp\left[-KTGx1 \, (T - TMx)^2\right] & when \ T \leq TMx \\ \\ \exp\left[-KTGx2 \, (TMx - T)^2\right] & when \ T > TMx \end{cases} \qquad (A14)$$

where

TMx = optimal temperature for algal growth (°C)

$KTGx1$ = effect of temperature below TMx on growth (°C^{-2})

$KTGx2$ = effect of temperature above TMx on growth (°C^{-2})

Settling

Separate settling velocities are specified for each algal group.

Mortality

Mortality of phytoplankton is the sum of two processes:

$$Mx = BMx + PRx + BGx \qquad (A15)$$

where

BMx = basal metabolism (day^{-1})

PRx = predation by zooplankton (day^{-1})

Basal metabolism

As employed here, basal metabolism is the sum of all internal processes that decrease algal biomass. A portion of the metabolism is respiration and may be viewed as a reversal of production. In respiration, carbon and nutrients are returned to the environment accompanied by the consumption of DO. A second internal sink of biomass is the excretion (exudation) of dissolved organic carbon.

Respiration cannot proceed in the absence of DO. Basal metabolism cannot decrease in proportion to oxygen availability, however, or algae would approach immortality under anoxic conditions. To solve this dilemma, basal metabolism is considered to be independent of DO but the distribution of metabolism between respiration and excretion is DO dependent. When oxygen is freely available, respiration is a large fraction of the total. When oxygen is restricted, excretion becomes dominant. Formulation of this process is detailed in the text that describes algal effects on carbon and DO.

Basal metabolism is commonly considered to be an exponentially increasing function of temperature:

$$BMx = BMRx \ exp \ [KTBx \ (T - TRx)] \tag{A16}$$

where

$BMRx$ = metabolic rate at TRx (day^{-1})

$KTBx$ = effect of temperature on metabolism (°C^{-1})

TRx = reference temperature for metabolism (°C)

Predation

The predation formulation is identical to that for basal metabolism. The difference in predation and basal metabolism lies in the distribution of the end products of these processes.

$$PRx = BPRx \ exp \ [KTBx \ (T - TRx)] \tag{A17}$$

where $BPRx$ is the predation rate at TRx (day^{-1}).

Effect of algae on organic carbon

During production and respiration, algae primarily take up and produce carbon dioxide, an inorganic form not considered in the model. A small fraction of basal metabolism is exuded as DOC, however, and in the model this fraction increases as DO becomes deficient. Algae also produce organic carbon through the effects of predation. Zooplankton take up and redistribute algal carbon through grazing, assimilation, respiration, and excretion. Since zooplankton are not included in the model, routing of algal carbon through zooplankton is simulated by empirical distribution coefficients. The effects of algae on organic carbon are expressed as

$$\frac{\partial}{\partial t} DOC = \left\{ \left[FCDx + (1 - FCDx) \frac{KHRx}{KHRx + DO} \right] - BMx + FCDP\ PRx \right\} Bx$$

(A18)

$$\frac{\partial}{\partial t} POC = FCLP\ PRx\ Bx$$

(A19)

where

$FCDx$ = fraction of basal metabolism exuded as DOC

$KHRx$ = half-saturation concentration for algal DOC excretion (g DO m^{-3})

$FCDP$ = fraction of dissolved organic carbon produced by predation

$FCLP$ = fraction of particulate carbon produced by predation

The sum of the two predation fractions must equal unity.

Effect of algae on nitrogen

Algae take up NH$_4$ and NO$_3$ during production and release NH$_4$ and organic nitrogen through mortality. NO$_3$ taken up is reduced internally to NH$_4$ before synthesis into biomass occurs (Parsons, Takahashi, and Hargrave 1984). Trace concentrations of NH$_4$ inhibit reduction of NO$_3$ so that, in the presence of NH$_4$ and NO$_3$, NH$_4$ is utilized first. The "preference" of algae for NH$_4$ can be expressed empirically (Thomann and Fitzpatrick 1982):

A10

$$PNx = NH4 \left[\frac{NO3}{(KHNx + NH4) \ (KHNx + NO3)} \right.$$

$$\left. + \frac{KHNx}{(NH4 + NO3) \ (KHNx + NO3)} \right] \qquad \text{(A20)}$$

where

    PNx = algal preference for NH4 uptake $(0 \le PNx \le 1)$

    Algal biomass is expressed in units of carbon. Algal uptake and release of nitrogen are quantified through a proportionality constant that represents the average ratio of nitrogen to carbon in algal biomass. As with carbon, routing of algal nitrogen through zooplankton is represented by distribution coefficients. The effects of algae on the nitrogen state variables are expressed as

$$\frac{\partial}{\partial t} NH4 = (BMx \ FNIx + PRx \ FNIP - PNx \ px) \ ANCx \ Bx \qquad \text{(A21)}$$

$$\frac{\partial}{\partial t} NO3 = (PNx - 1) \ pX \ ANCx \ Bx \qquad \text{(A22)}$$

$$\frac{\partial}{\partial t} DON = (BMx \ FNDx + PRx \ FNDP) \ ANCx \ Bx \qquad \text{(A23)}$$

$$\frac{\partial}{\partial t} PON = (BMx \ FNLx + PRx \ FNLP) \ ANCx \ Bx \qquad \text{(A24)}$$

where

    $ANCx$ = nitrogen-to-carbon ratio of algae (g N g^{-1} C)

    $FNIx$ = fraction of inorganic nitrogen produced by metabolism

    $FNDx$ = fraction of dissolved organic nitrogen produced by metabolism

    $FNLx$ = fraction of particulate nitrogen produced by metabolism

    $FNIP$ = fraction of inorganic nitrogen produced by predation

    $FNDP$ = fraction of dissolved organic nitrogen produced by predation

    $FNLP$ = fraction of particulate nitrogen produced by predation

The sums of the metabolism fractions and the predation fractions must each equal unity.

Effect of algae on dissolved oxygen

Algae produce oxygen during photosynthesis and consume oxygen through respiration. The quantity produced depends on the form of nitrogen taken up. Since oxygen is released in the reduction of NO_3, more oxygen is produced, per unit of carbon fixed, when NO_3 is the algal nitrogen source than when NH_4 is the source. Equations describing algal uptake of carbon and nitrogen and production of DO are (Morel 1983):

$$106\ CO_2 + 16\ NH_4^+ + H_2PO_4^- + 106\ H_2O$$

$$\rightarrow protoplasm + 106\ O_2 + 15\ H^+$$

(A25)

$$106\ CO_2 + 16\ NO_3^+ + H_2PO_4^- + 122\ H_2O + 17\ H^+$$

$$\rightarrow protoplasm + 138\ O_2$$

(A26)
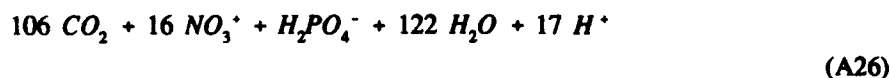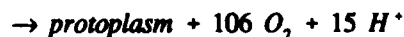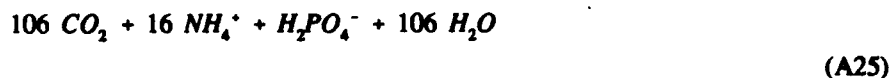
When NH_4 is the nitrogen source, 1 mole oxygen is produced per mole carbon dioxide fixed. When NO_3 is the nitrogen source, 1.3 moles oxygen are produced per mole carbon dioxide fixed.

The equation that describes the effect of algae on DO in the model is

$$\frac{\partial}{\partial t}\ DO = \left[(1.3 - 0.3\ PNx)\ Px - \frac{DO}{KHRx + DO}\ BMx\right] AOCR\ Bx \qquad (A27)$$

where $AOCR$ is the dissolved oxygen-to-carbon ratio in respiration (2.67 g DO g^{-1} C).

The quantity $(1.3 - 0.3\ PNx)$ is the photosynthesis ratio and expresses the molar quantity of oxygen produced per mole carbon fixed. The photosynthesis ratio approaches unity as the algal preference for NH_4 approaches unity.

Organic Carbon

Carbon fixed by primary producers undergoes innumerable transformations in the water column. Particulate organic carbon is converted to dissolved organic carbon, DOC and POC are incorporated into heterotrophic biomass,

A12

and organic carbon is respired to inorganic carbon. A detailed representation of the carbon cycle is not required to achieve the objectives of this model. A reduced system is conceived consisting of the following elements:

Phytoplankton exudation
Predation on phytoplankton
Dissolution of particulate carbon
Heterotrophic respiration
Denitrification
Settling

In the reduced system, POC and DOC are produced by predation on phytoplankton. The POC undergoes first-order dissolution to DOC. DOC produced by phytoplankton exudation, predation, and dissolution is respired or denitrified at a first-order rate to inorganic carbon.

Dissolution and respiration rates

Dissolution and respiration rates depend on the availability of carbonaceous substrate and on heterotrophic activity. Heterotrophic activity and biomass have been correlated with algal activity and biomass across a wide range of natural systems (Bird and Kalff 1984; Cole, Findlay, and Pace 1988). Consequently, algal biomass can be incorporated into dissolution and respiration rate formulations as a surrogate for heterotrophic activity. The correlation between algae and heterotrophs occurs because algae produce labile carbon that fuels heterotrophic activity. Dissolution and respiration processes do not require the presence of algae, however, and may be fueled entirely by allochthonous carbon inputs. Representation of dissolution and respiration in the model allows specification of algal-dependent and algal-independent rates:

$$KDOC = KDC + KDCALG \sum_{x=1_s} Bx \qquad (A28)$$

where

$KDOC$ = respiration rate of dissolved organic carbon (day^{-1})

KDC = minimum respiration rate (day^{-1})

$KDCALG$ = constant that relates respiration to algal biomass (m^3 g^{-1} C day^{-1})

$$KLPOC = KLC + KLCALG \sum_{x=1_s} Bx \qquad (A29)$$

where

$KLPOC$ = dissolution rate of particulate organic carbon (day^{-1})

KLC = minimum dissolution rate (day^{-1})

$KLCALG$ = constant that relates dissolution to algal biomass (m^3 g^{-1} C day^{-1})

Temperature has a multiplicative effect on dissolution and respiration as expressed by Equation A16 with appropriate changes in notation.

Denitrification

As oxygen is depleted from natural systems, oxidation of organic matter is effected by the reduction of alternate oxidants (in standard terminology referred to as "alternate electron acceptors"). The sequence in which alternate acceptors are employed is determined by the thermodynamics of oxidation-reduction reactions. The first substance reduced in the absence of oxygen is nitrate. One representation of the denitrification reaction is

$$4NO_3^- + 4H^+ + 5CH_2O = 2N_2 + 7H_2O + 5CO_2 \qquad (A30)$$
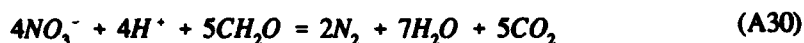
The model representation of the denitrification reaction differs from the balanced redox equation since only NO_3^- and CH_2O (as DOC) are model state variables. The model representation incorporates a temperature-dependent reaction rate and notes that significant denitrification occurs only when nitrate is freely available and dissolved oxygen is depleted:

$$DENIT = \frac{KHODOC}{KHODOC + DO} \ \frac{NO3}{KHNDN + NO3} \ AANOX \ KDOC \qquad (A31)$$

where

$DENIT$ = denitrification rate of dissolved organic carbon (day^{-1})

$AANOX$ = ratio of denitrification to oxic carbon respiration rate

$KHODOC$ = half-saturation concentration of DO required for oxic respiration (g DO m^{-3})

$KHNDN$ = half-saturation concentration of nitrate required for denitrification (g N m^{-3})

Temperature has a multiplicative effect on denitrification as expressed by Equation A16 with appropriate changes in notation.

A14

Equations follow that sum all organic carbon sources and sinks in the model ecosystem.

Dissolved organic carbon

$$\frac{\partial}{\partial t} DOC = \sum_{x=d,g} \left\{ \left[FCDx + (1 - FCDx) \frac{KHRX}{KHRX + DO} \right] BMx + FCDP\, PRx \right\} BX$$

$$+ KLPOC\, f(T)\, LPOC + KRPOC\, f(T)\, RPOC \qquad \text{(A32)}$$

$$- \frac{DO}{KHODOC + DO} KDOC\, f(T)\, DOC - DENIT\, f(T)\, DOC$$

Particulate organic carbon

$$\frac{\partial}{\partial t} POC = \sum_{x=d,g} FCLP\, PRx\, Bx$$

$$\text{(A33)}$$

$$- KLPOC\, f(t)\, LPOC - WSL\, \frac{\partial}{\partial z} LPOC$$

where *WSL* is the settling velocity of labile particles (m day^{-1}).

Nitrogen

Nitrogen undergoes innumerable transformations in the water column. A reduced system is conceived that includes the following processes:

Algal production and metabolism
Predation
Hydrolysis of particulate organic nitrogen
Mineralization of dissolved organic nitrogen
Settling
Nitrification
Denitrification

Effects of nitrogen of algal production, metabolism, and predation have already been detailed. Descriptions of hydrolysis, mineralization, nitrification and denitrification follow.

Hydrolysis and mineralization

For purposes of this model, hydrolysis is defined as the process by which particulate organic nitrogen (PON) is converted to the dissolved organic form. Mineralization is defined as the process by which DON is converted to NH_4. Conversion of PON to NH_4 proceeds through the sequence of hydrolysis and mineralization. Direct mineralization of PON does not occur. Formulations for hydrolysis and mineralization are based on the following assumptions:

    a. Rates of hydrolysis and mineralization are proportional to available substrate.

    b. Rates of hydrolysis and mineralization are proportional to algal biomass.

    c. Hydrolysis and mineralization are accelerated when inorganic nitrogen is insufficient to supply algal demand.

Assumption *a* states that hydrolysis and mineralization cannot proceed in the absence of PON or DON. The assumption is a restatement of first-order kinetics. Assumption *b* recognizes that nitrogen transformation rates are influenced by the biomass of heterotrophic organisms that mediate the transformations. While bacteria and zooplankton are not quantified in the model, observations in numerous systems (Bird and Kalff 1984; Cole, Findlay, and Pace 1988) indicate their biomass is proportional to algal biomass. Consequently, algal biomass is an indicator of heterotrophic biomass and relation of nitrogen transformations to algal biomass is appropriate. Assumption *c* is based largely on analogy to phosphorus mineralization for which low phosphate concentration stimulates production of an enzyme that mineralizes organic phosphorus to phosphate.

Formulations for the mineralization and hydrolysis rates, consistent with the three assumptions, are

$$KDON = KDN + \frac{KHN}{KHN + NH4 + NO3} \, KDNALG \sum_{x=d_g} Bx \qquad (A34)$$

where

    $KDON$ = mineralization rate of dissolved organic nitrogen (day^{-1})

    KDN = minimum mineralization rate (day^{-1})

    KHN = mean half-saturation constant for algal nitrogen uptake (g N m^{-3})

    $KDNALG$ = constant that relates mineralization to algal biomass (m^3 g^{-1} C day^{-1})

and

$$KLPON = KLN + \frac{KHN}{KHN + NH\$ + NO3} \; KLNALG \sum_{x=1}^{4} Bx \qquad \text{(A35)}$$

where

$KLPON$ = hydrolysis rate of labile particulate nitrogen (day^{-1})

KLN = minimum hydrolysis rate (day^{-1})

$KLNALG$ = constant that relates hydrolysis to algal biomass (m^3 g^{-1} C day^{-1})

Mineralization and hydrolysis rates are a function of temperature as expressed by Equation A16 with appropriate changes in notation.

Nitrification

Nitrification is a process mediated by specialized groups of autotrophic bacteria that obtain energy through the oxidation of ammonium to nitrite and oxidation of nitrite to nitrate. A simplified expression for complete nitrification is

$$NH_4^+ + 2O_2 \rightarrow NO_3^- + H_2O + 2H^+ \qquad \text{(A36)}$$
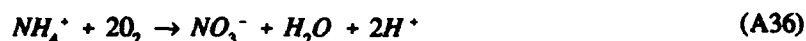
The equation indicates that 2 moles of oxygen are required to nitrify 1 mole of ammonium into nitrate. The simplified equation is not strictly true, however. Cell synthesis by nitrifying bacteria is accomplished by the fixation of carbon dioxide so that less than 2 moles of oxygen are consumed per mole ammonium utilized (Wezemak and Gannon 1968).

In this study, nitrification is modeled as a function of available ammonium, dissolved oxygen, and temperature:

$$NT = \frac{DO}{KHONT + DO} \; \frac{NH_4}{KHNNT + NH_4} \; f(TJ) \; NTM \qquad \text{(A37)}$$

where

NT = nitrification rate (g N m^{-3} day^{-1})

NTM = maximum nitrification rate at optimal temperature (g N m^{-3} day^{-1})

$KHONT$ = half-saturation constant of DO required for nitrification (g DO m^{-3})

$KHNNT$ = half-saturation constant of $NH4$ required for nitrification (g N m^{-3})

The optimal temperature for nitrification may be less than peak temperatures that occur in coastal waters. To allow for a decrease in nitrification at superoptimal temperature, the effect of temperature on nitrification is modeled in the Gaussian form of Equation A14 with appropriate changes in notation.

Effect of nitrification on ammonium

$$\frac{\partial}{\partial t} NH4 = -NT \qquad\qquad (A38)$$

Effect of nitrification on nitrate

$$\frac{\partial}{\partial t} NO3 = NT \qquad\qquad (A39)$$

Effect of nitrification on dissolved oxygen

$$\frac{\partial}{\partial t} DO = -AONT\ NT \qquad\qquad (A40)$$

where $AONT$ is the mass DO consumed per mass NH_4-N nitrified (4.33 g $\ldots$ g^{-1} N).

Effect of denitrification on nitrate

The effect of denitrification on DOC has been detailed. Denitrification removes nitrate from the system in stoichiometric proportion to DOC removal as determined by Equation A31:

$$\frac{\partial}{\partial t} = -ANDC\ DENIT\ f(T)\ DOC \qquad\qquad (A41)$$

where $ANDC$ is the mass NO3-N reduced per mass DOC oxidized (0.933 g N g^{-1} C).

Ammonia

The equation is written by summing all previously described sources and sinks:

A18

$$\frac{\partial}{\partial t} NH4 = \sum_{x=l_s} (BMx\ FNIx + PRx\ FNIP - PNx\ Px)\ ANCx\ Bx$$

(A42)

$$+ KDON\ f(T)\ DON - NT$$

Dissolved organic nitrogen

$$\frac{\partial}{\partial t} DON = \sum_{x=l_s} (BMx\ FNDx + PRx\ FNDP)\ ANCx\ Bx$$

(A43)

$$- KDON\ f(T)\ DON + KLPON\ f(T)\ LPON$$

$$+ KRPON\ f(T)\ RPON$$

Particulate organic nitrogen

$$\frac{\partial}{\partial t} PON = \sum_{x=l_s} (BMx\ FNLx + PRx\ FNLP)\ ANCx\ Bx$$

(A44)

$$- KLPON\ f(T)\ LPON - WSL\ \frac{\partial}{\partial z} LPON$$

Nitrate

$$\frac{\partial}{\partial t} NO3 = \sum_{x=l_s} (PNx - 1)\ px\ ANCx\ Bx$$

(A45)

$$+ NT - ANDC\ DENIT\ f(TP)\ DOC$$

Dissolved Oxygen

Sources and sinks of DO in the water column include:

Sources: Algal photosynthesis
Atmospheric reaeration

Sinks: Algal respiration
Heterotrophic respiration
Nitrification

Reaeration

Reaeration occurs only in the model segments that form the air-water interface. The effect of reaeration is

$$\frac{\partial}{\partial t} DO = \frac{KR}{H} (DOs - DO) \tag{A46}$$

where

KR = reaeration coefficient (m day^{-1})

DOs = dissolved oxygen saturation concentration (g DO m^{-3})

The surface renewal concept, attributed to Danckwerts by O'Connor and Dobbins (1958), indicates

$$KR = (DL\ R)^{1/2} \tag{A47}$$

where

DL = molecular diffusivity of oxygen in water ($\approx 1.7 \times 10^{-4}$ m^2 day^{-1})

R = surface renewal rate

Specification of the surface renewal rate is the fundamental problem in reaeration theory. O'Connor and Dobbins (1958) state that, in isotropic turbulence, surface renewal can be approximated as the ratio of stream velocity to depth. The renewal rate is also influenced by wind, however (O'Connor 1983). Influences on reaeration of temperature (ASCE 1961) and salinity (Wen et al. 1984), most likely effected through changes in diffusivity, have been measured. No single theory that unites all these factors into a formulation of reaeration in an estuary is available. The surface renewal concept is retained in this study with the renewal rate treated as a calibration parameter.

Saturation dissolved oxygen concentration is computed (Genet, Smith, and Sonnen 1974):

$$DOs = 14.5532 - 0.38217\ T + 0.0054258\ T^2$$

$$- CL\ (1.665 \times 10^{-4} - 5.866 \times 10^{-6}\ T \tag{A48}$$

$$+ 9.796 \times 10^{-8}\ T^2$$

where CL is the chloride concentration (= salinity/1.80655).

Summary of *DO* sources and sinks

The complete kinetics for *DO* are

$$\frac{\partial}{\partial t} DO = \sum_{x=a}^{} \left[(1.3 - 0.3\ PNx)\ Px - \frac{DO}{KHRx + DO}\ BMx \right] AOCR\ Bx$$

$$- AONT\ NT - \frac{DO}{KHODOC + DO}\ f(T)\ AOCR\ KDOC\ DOC \qquad \text{(A49)}$$

$$- \frac{KR}{H}\ (DOs - DO)$$

Salinity

No internal sources or sinks of salinity exist.

Temperature

A conservation of internal energy equation can be written analogous to the conservation of mass equation. The only source or sink of internal energy considered is exchange with the atmosphere. Although solar radiation can penetrate several meters into the water column, radiation-induced increases in internal energy are here assigned entirely to the surface model layer.

For practical purposes, the internal-energy equation can be written as a conservation of temperature equation. Change of temperature due to atmospheric exchange is considered proportional to the temperature difference between the water surface and a theoretical equilibrium temperature (Edinger, Brady, and Geyer 1965):

$$\frac{\partial}{\partial t} T = \frac{KT}{\rho\ CP\ H}\ (TE - T) \qquad \text{(A50)}$$

where

TE = equilibrium temperature (C°)

KT = heat exchange coefficient (watt m^{-2} °C^{-1})

CP = specific heat of water (4,200 watt sec kg^{-1} °C^{-1})

ρ = density of water (1,000 kg m^{-3})

Kinetic Coefficient Values Used in the NYB Application

The coefficients labeled "Hardwired" were coded, and the coefficients labeled "Input" were specified in input files.

Hardwired:

KE	=	0.15	light attenuation coefficient, m^{-1}
PMd	=	2.0	maximum net plankton production, day^{-1}
PMg	=	2.3	maximum nanoplankton production, day^{-1}
BMRd	=	0.2	metabolic rate net plankton at reference temperature, day^{-1}
BMRg	=	0.23	metabolic rate nanoplankton at reference temperature, day^{-1}
BPRd	=	0.0	predation rate net plankton at reference temperature, day^{-1}
BPRg	=	0.08	predation rate nanoplankton at reference temperature, day^{-1}
WSd	=	5.0	settling rate net plankton, m day^{-1}
WSg	=	0.1	settling rate nanoplankton, m day^{-1}
WSL	=	2.0	settling rate labile particulates, m day^{-1}
RKSED	=	0.5	bottom layer denitrification rate, m day^{-1}

Input:

KSO	=	0.07	effect of temperature on SOD, $°C^{-1}$
KSNH4	=	0.07	effect of temperature on NH_4-N sediment release, $°C^{-1}$
KHSO	=	2.0	half-saturation concentration of DO for SOD, g O_2 m^{-3}
KHSNH4	=	2.0	half-saturation concentration DO for sediment NH_4-N release, g O_2 m^{-3}
TRSO	=	20.0	reference temperature for SOD, °C
TRSNH4	=	20.0	reference temperature for sediment NH_4-N release, °C
TMd	=	20.0	optimal temperature for net plankton growth, °C
KTGd1	=	0.004	effect of temperature on net plankton growth below TMd
KTGd2	=	0.006	effect of temperature on net plankton growth above TMd
TMg	=	20.0	optimal temperature for nanoplankton growth, °C
KTGg1	=	0.008	effect of temperature on nanoplankton growth below TMg
KTGg2	=	0.010	effect of temperature on nanoplankton growth above TMg
CCHLd	=	80.0	C/Chl ratio for net plankton
CCHLg	=	80.0	C/Chl ratio for nanoplankton

KTGg1	=	0.008	effect of temperature on nanoplankton growth below TMg
KTGg2	=	0.010	effect of temperature on nanoplankton growth above TMg
CCHLd	=	80.0	C/Chl ratio for net plankton
CCHLg	=	80.0	C/Chl ratio for nanoplankton
KECHL	=	17.0	algal self-shading, m^2 $(g\ Chl)^{-1}$
DOPTd	=	1.0	depth maximum net plankton production, m
DOPTg	=	1.0	depth maximum nanoplankton production, m
ISMIN	=	40.0	minimum optimal illumination rate, Langleys day^{-1}
I0WT	=	0.7	weight current illumination
I1WT	=	0.2	weight illumination one preceding day
I2WT	=	0.1	weight illumination two preceding days
KHNd	=	0.01	half-saturation concentration of N for net plankton N uptake, $g\ N^{-3}$
KHNg	=	0.001	half-saturation concentration of N for nanoplankton N uptake, $g\ N^{-3}$
TRd	=	20.0	reference temperature for base net plankton metabolism, °C
TRg	=	20.0	reference temperature for base nanoplankton metabolism, °C
KTBd	=	0.069	effect of temperature on base net plankton metabolism, $°C^{-1}$
KTBg	=	0.069	effect of temperature on base nanoplankton metabolism, $°C^{-1}$
FCDd	=	0.1	fraction net plankton metabolism excreted as DOC
FCDg	=	0.1	fraction nanoplankton metabolism excreted as DOC
KHRd	=	0.5	half-saturation concentration of DO for net plankton DOC excretion, $g\ O_2\ m^{-3}$
KHRg	=	0.5	half-saturation concentration of DO for nanoplankton DOC excretion, $g\ O_2\ m^{-3}$
FCDP	=	0.1	fraction algal predation excreted as DOC
KHODOC	=	0.5	half-saturation concentration of DO for heterotrophic respiration, $g\ O_2\ m^{-3}$
FCLP	=	0.45	fraction algal predation excreted as POC
KDC	=	0.01	minimum mineralization rate for DOC, day^{-1}
KDCALG	=	0.0	constant that relates respiration to algal biomass, $m^3\ g^{-1}\ C\ day^{-1}$
KLC	=	0.035	minimum hydrolysis rate for POC, day^{-1}
KLCALG	=	0.0	constant that relates dissolution to algal biomass, $m^3\ g^{-1}\ C\ day^{-1}$
KTMNL	=	0.069	effect of temperature on mineralization, $°C^{-1}$
TRMNL	=	20.0	reference temperature for mineralization, °C
KTHDR	=	0.069	effect of temperature on hydrolysis, $°C^{-1}$
TRHDR	=	20.0	reference temperature for hydrolysis, °C
AANOX	=	0.5	ratio of denitrification to oxic carbon respiration rate
KHNDN	=	0.1	half-saturation concentration of NO_3-N for denitrification, $g\ N\ m^{-3}$
TMNT	=	30.0	optimal temperature for nitrification, °C

KTMT1	=	0.09	effect of temperature on nitrification below TMNT, $°C^{-1}$
KTMT2	=	0.09	effect of temperature on nitrification above TMNT, $°C^{-1}$
KHONT	=	1.0	half-saturation concentration of DO for nitrification, $g\ O_2\ m^{-3}$
KHNNT	=	1.0	half-saturation concentration of NH_4-N for nitrification, $g\ N\ m^{-3}$
NTM	=	0.05	maximum nitrification rate, day^{-1}
KHNd	=	0.01	half-saturation concentration of N for net plankton N uptake, $g\ N\ m^{-3}$
KHNg	=	0.001	half-saturation concentration of N for nanoplankton N uptake, $g\ N\ m^{-3}$
FNId	=	0.25	fraction NH_4-N produced by net plankton metabolism
FNIg	=	0.25	fraction NH_4-N produced by nanoplankton metabolism
ANCd	=	0.167	net plankton N/C ratio
ANCg	=	0.167	nanoplankton N/C ratio
FNIP	=	0.10	fraction NH_4-N produced by algal predation
KDN	=	0.04	mineralization rate for DON, day^{-1}
KLN	=	0.10	hydrolysis rate for PON, day^{-1}
FNDd	=	0.75	fraction of DON produced by net plankton metabolism
FNDg	=	0.75	fraction of DON produced by nanoplankton metabolism
FNLd	=	0.0	fraction of PON produced by net plankton metabolism
FNLg	=	0.0	fraction of PON produced by nanoplankton metabolism
FNDP	=	0.0	fraction of DON produced by algal predation
FNLP	=	0.45	fraction of PON produced by algal predation

Appendix B
Initial Conditions Constituent Concentrations

Grid	Surface	Middle	Bottom
Temperature, °C			
1	6.9		7.2
2	7.0		7.0
3	6.9		6.7
4	7.0		7.0
5	7.5		8.1
6	7.6		6.9
7	6.9		7.0
8	7.5		7.0
9	8.5		7.0
10	8.5		6.1
11	7.9		7.6
12	7.7		7.4
13	8.4		9.2
14	10.0		8.9
15	8.7		7.8
Salinity, ‰			
1	26.1		26.3
2	30.0		30.0
3	30.4		32.1
4	30.0		30.0
5	30.7		31.9
6	31.9		32.3
7	32.0		33.4
8	32.4		33.2
9	31.6		33.3
10	31.7		32.8
11	32.4		33.3
12	33.1		33.4
13	32.8		34.0
14	32.4		33.9
15	32.7		33.6
Netplankton, mg chl m^3			
1	0.5	2.0	0.2
2	0.5	2.0	0.2
3	0.5	2.0	0.2
4	0.5	2.0	0.2
5	0.5	2.0	0.2
6	0.5	2.0	0.2
7	0.5	2.0	0.2
8	0.5	2.0	0.2
9	1.0	3.9	0.3
10	0.3	1.8	0.2
11	0.5	2.0	0.2
12	0.5	2.0	0.2
13	0.5	2.0	0.2
14	0.3	0.8	0.1
15	0.2	2.1	0.6

Note: Underlined values are measured values.

Grid	2

Nanoplankton, mg ch
1
2
3
4
5
6
7
8
9
10
11
12
13
14
15

Dissolved Organic C
1
2
3
4
5 .
6
7
8
9
10
11
12
13
14
15

Particulate Organic
1
2
3
4
5
6
7
8
9
10
11
12
13
14
15

Appendix B Initial Conditions

Grid	Surface	Middle	Bottom
Ammonia, g N m⁻³			
1	0.007		0.014
2	0.007		0.014
3	0.007		0.014
4	0.007		0.014
5	0.014		0.010
6	0.007		0.014
7	0.007		0.014
8	0.007		0.014
9	0.006		0.025
10	0.004		0.028
11	0.004		0.028
12	0.004		0.028
13	0.006		0.007
14	0.004		0.028
15	0.004		0.025
Nitrate, g N m⁻³			
1	0.140		0.140
2	0.014		0.007
3	0.011		0.004
4	0.014		0.007
5	0.018		0.004
6	0.006		0.007
7	0.001		0.004
8	0.001		0.003
9	0.001		0.053
10	0.001		0.039
11	0.001		0.022
12	0.003		0.014
13	0.003		0.109
14	0.001		0.101
15	0.003		0.125
Dissolved Organic Nitrogen, g N m⁻³			
1	0.014		0.014
2	0.014		0.014
3	0.014		0.014
4	0.014		0.014
5	0.014		0.014
6	0.014		0.014
7	0.014		0.014
8	0.014		0.014
9	0.014		0.014
10	0.014		0.014
11	0.014		0.014
12	0.014		0.014
13	0.014		0.014
14	0.014		0.014
15	0.014		0.014

Grid	Surface	Middle	Bottom

Particulate Organic Nitrogen, g N m^{-3}

Grid	Surface	Middle	Bottom
1	0.014		0.014
2	0.014		0.014
3	0.014		0.014
4	0.014		0.014
5	0.014		0.014
6	0.014		0.014
7	0.014		0.014
8	0.014		0.014
9	0.014		0.014
10	0.014		0.014
11	0.014		0.014
12	0.014		0.014
13	0.014		0.014
14	0.014		0.014
15	0.014		0.014

Dissolved Oxygen, g O$_2$ m^{-3}

Grid	Surface	Middle	Bottom
1	9.9		10.1
2	10.3		10.0
3	10.3		8.9
4	10.3		10.0
5	10.3		10.0
6	10.3		9.7
7	9.7		8.6
8	10.6		8.7
9	10.6		8.9
10	10.6		8.9
11	10.6		8.9
12	10.4		8.6
13	10.4		8.7
14	10.4		8.6
15	10.4		8.6

Appendix C
Boundary Condition Constituent Concentrations

Temperature, °C

Date: 092 (Apr)

	Surf	Bot
seg 1	12.5	7.5
seg 2	12.5	7.5
seg 3	12.5	7.5
seg 4	12.5	7.5
seg 5	12.5	7.5
seg 6	8.7	7.8
seg 7	8.4	6.4
seg 8	10.0	10.0

Date: 122 (May)

	Surf	Bot
seg 1	11.4	8.4
seg 2	11.5	8.5
seg 3	11.6	8.6
seg 4	11.7	8.4
seg 5	11.7	8.0
seg 6	10.0	8.0
seg 7	9.4	6.7
seg 8	14.2	14.2

Date: 153 (Jun)

	Surf	Bot
seg 1	16.9	11.7
seg 2	16.6	8.5
seg 3	16.6	9.7
seg 4	16.3	8.0
seg 5	13.6	4.0
seg 6	13.0	7.0
seg 7	12.5	7.0
seg 8	19.7	19.7

Date: 183 (Jul)

	Surf	Bot
seg 1	19.3	13.6
seg 2	19.0	9.0
seg 3	19.0	9.0
seg 4	18.7	8.0
seg 5	15.0	7.0
seg 6	15.4	7.0
seg 7	14.9	7.0
seg 8	23.6	23.6

Note: Underlined values are measured values.

Date: 214 (Aug)

		Surf	Bot
seg	1	23.2	16.5
seg	2	22.0	9.7
seg	3	22.7	10.5
seg	4	22.3	7.9
seg	5	21.2	7.8
seg	6	21.0	7.5
seg	7	19.5	7.5
seg	8	23.2	23.2

Date: 245 (Sep)

		Surf	Bot
seg	1	20.0	17.2
seg	2	21.8	10.4
seg	3	21.8	11.0
seg	4	21.5	10.0
seg	5	21.1	8.8
seg	6	20.6	11.6
seg	7	18.6	13.0
seg	8	21.2	21.2

Date: 275 (Oct)

		Surf	Bot
seg	1	17.1	16.7
seg	2	16.8	12.2
seg	3	16.8	12.0
seg	4	16.5	11.5
seg	5	16.0	8.5
seg	6	15.8	10.0
seg	7	14.0	10.0
seg	8	16.0	16.0

Salinity, %o

Date: 092 (Apr)

	Surf	Bot
seg 1	31.9	32.3
seg 2	32.4	33.3
seg 3	33.1	33.4
seg 4	34.0	34.8
seg 5	34.8	35.0
seg 6	32.7	33.6
seg 7	31.6	32.6
seg 8	20.0	20.0

Date: 122 (May)

	Surf	Bot
seg 1	32.0	32.5
seg 2	33.5	33.8
seg 3	33.0	34.0
seg 4	33.2	35.2
seg 5	33.8	35.1
seg 6	33.5	34.0
seg 7	32.7	32.8
seg 8	20.0	20.0

Date: 153 (Jun)

	Surf	Bot
seg 1	32.0	32.4
seg 2	32.1	33.1
seg 3	32.4	34.9
seg 4	35.0	35.3
seg 5	34.4	35.0
seg 6	34.0	35.0
seg 7	33.5	34.0
seg 8	20.0	20.0

Date: 183 (Jul)

	Surf	Bot
seg 1	32.0	32.4
seg 2	32.1	33.1
seg 3	32.4	34.9
seg 4	35.0	35.3
seg 5	34.4	35.0
seg 6	34.0	35.0
seg 7	33.5	34.0
seg 8	20.0	20.0

Date: 214 (Aug)

		Surf	Bot
seg	1	32.0	32.4
seg	2	32.2	33.2
seg	3	33.8	34.5
seg	4	34.7	34.8
seg	5	32.8	34.5
seg	6	32.5	33.5
seg	7	32.0	32.5
seg	8	20.0	20.0

Date: 245 (Sep)

		Surf	Bot
seg	1	32.1	32.3
seg	2	32.8	32.9
seg	3	34.0	35.2
seg	4	34.6	35.2
seg	5	34.4	35.2
seg	6	34.0	34.1
seg	7	31.8	32.4
seg	8	20.0	20.0

Date: 275 (Oct)

		Surf	Bot
seg	1	33.0	33.5
seg	2	33.5	34.0
seg	3	34.0	34.5
seg	4	34.5	35.0
seg	5	34.5	35.0
seg	6	34.0	34.5
seg	7	34.0	34.5
seg	8	20.0	20.0

Whl-net-nanoplankton, mg chl m^{-3}

Date: 092 (Apr)

seg	Whl Surf	Whl Mid	Whl Bot	Net Surf	Net Mid	Net Bot	Nan Surf	Nan Mid	Nan Bot
seg 1				0.50	3.00	0.25	0.50	1.00	0.10
seg 2				0.50	3.00	0.25	0.50	1.00	0.10
seg 3				0.20	2.00	0.10	0.20	0.75	0.05
seg 4				0.20	2.00	0.10	0.60	1.00	0.10
seg 5	1.74	0.08		0.23	1.39	0.31	0.62	1.21	0.10
seg 6	1.25	3.57	0.52	0.19	2.07	0.56	0.60	1.50	0.40
seg 7	1.26	2.70	0.43	0.32	1.76	0.24	0.66	1.25	0.47
seg 8				0.00	0.00	0.00	0.00	0.00	0.00

Date: 122 (May)

seg	Whl Surf	Whl Mid	Whl Bot	Net Surf	Net Mid	Net Bot	Nan Surf	Nan Mid	Nan Bot
seg 1				0.50	3.00	0.25	0.50	1.00	0.10
seg 2				0.50	3.00	0.25	0.50	1.00	0.10
seg 3				0.20	2.00	0.10	0.20	0.75	0.05
seg 4	0.59	0.02		0.10	2.00	0.10	0.20	0.75	0.05
seg 5	1.12	0.05		0.32	2.00	0.10	0.20	0.75	0.05
seg 6				0.20	2.00	0.10	0.20	0.75	0.05
seg 7	1.08	3.89	0.12	0.20	2.00	0.10	0.20	0.75	0.05
seg 8				0.00	0.00	0.00	0.00	0.00	0.00

Date: 153 (Jun)

seg	Whl Surf	Whl Mid	Whl Bot	Net Surf	Net Mid	Net Bot	Nan Surf	Nan Mid	Nan Bot
seg 1				0.20	2.00	0.10	0.20	0.75	0.05
seg 2				0.20	2.00	0.10	0.20	0.75	0.05
seg 3				0.50	5.00	0.10	0.20	0.75	0.05
seg 4	0.50			0.50	5.00	0.10	0.20	0.75	0.05
seg 5	0.68		0.02	0.50	5.00	0.10	0.20	0.75	0.05
seg 6				0.20	2.00	0.10	0.20	0.75	0.05
seg 7				0.20	2.00	0.10	0.20	0.75	0.05
seg 8				0.00	0.00	0.00	0.00	0.00	0.00

Date: 183 (Jul)

seg	Whl Surf	Whl Mid	Whl Bot	Net Surf	Net Mid	Net Bot	Nan Surf	Nan Mid	Nan Bot
seg 1				0.20	2.00	0.10	0.20	0.75	0.05
seg 2				0.20	2.00	0.10	0.20	0.75	0.05
seg 3				0.20	2.00	0.10	0.20	0.75	0.05
seg 4				0.50	5.00	0.10	0.20	0.75	0.05
seg 5				0.50	5.00	0.10	0.20	0.75	0.05
seg 6				0.50	5.00	0.10	0.20	0.75	0.05
seg 7				0.20	2.00	0.10	0.20	0.75	0.05
seg 8				0.00	0.00	0.00	0.00	0.00	0.00

Date: 214 (Aug)

	Whl			Met			Man		
	Surf	Mid	Bot	Surf	Mid	Bot	Surf	Mid	Bot
seg 1				0.20	2.00	0.10	0.20	0.75	0.05
seg 2				0.20	2.00	0.10	0.20	0.75	0.05
seg 3				0.10	1.00	0.05	0.10	0.25	0.01
seg 4				0.10	1.00	0.05	0.10	0.25	0.01
seg 5				0.10	1.00	0.05	0.10	0.25	0.01
seg 6				0.10	1.00	0.05	0.10	0.25	0.01
seg 7				0.20	2.00	0.10	0.20	0.75	0.05
seg 8				0.00	0.00	0.00	0.00	0.00	0.00

Date: 245 (Sep)

	Whl			Met			Man		
	Surf	Mid	Bot	Surf	Mid	Bot	Surf	Mid	Bot
seg 1				0.04	1.35	1.28	0.79	2.17	1.22
seg 2				0.04	0.34	0.24	0.16	0.27	0.17
seg 3				0.04	0.34	0.24	0.16	0.27	0.17
seg 4				0.03	0.22	0.01	0.16	0.27	0.17
seg 5				0.02	0.09	0.01	0.10	0.25	0.00
seg 6				0.02	0.10	0.01	0.10	0.25	0.00
seg 7				0.02	0.10	0.01	0.10	0.25	0.00
seg 8				0.00	0.00	0.00	0.00	0.00	0.00

Date: 275 (Oct)

	Whl			Met			Man		
	Surf	Mid	Bot	Surf	Mid	Bot	Surf	Mid	Bot
seg 1				0.05	0.50	0.25	0.15	0.25	0.10
seg 2				0.05	0.50	0.25	0.15	0.25	0.10
seg 3				0.03	0.25	0.15	0.15	0.25	0.10
seg 4				0.02	0.10	0.01	0.10	0.25	0.00
seg 5				0.02	0.10	0.01	0.10	0.25	0.00
seg 6				0.02	0.10	0.01	0.10	0.25	0.00
seg 7				0.02	0.10	0.01	0.10	0.25	0.00
seg 8				0.00	0.00	0.00	0.00	0.00	0.00

```
Dissolved Organic Carbon, g C m³

Date: 092 (Apr)

                Surf        Bot
    seg 1       2.00        1.00
    seg 2       2.00        1.00
    seg 3       2.00        1.00
    seg 4       2.00        1.00
    seg 5       2.00        1.00
    seg 6       2.00        1.00
    seg 7       2.00        1.00
    seg 8       0.00        0.00

Date: 122 (May)

                Surf        Bot
    seg 1       2.00        1.00
    seg 2       2.00        1.00
    seg 3       2.00        1.00
    seg 4       2.00        1.00
    seg 5       2.00        1.00
    seg 6       2.00        1.00
    seg 7       2.00        1.00
    seg 8       0.00        0.00

Date: 153 (Jun)

                Surf        Bot
    seg 1       2.00        1.00
    seg 2       2.00        1.00
    seg 3       2.00        1.00
    seg 4       2.00        1.00
    seg 5       2.00        1.00
    seg 6       2.00        1.00
    seg 7       2.00        1.00
    seg 8       0.00        0.00

Date: 183 (Jul)

                Surf        Bot
    seg 1       2.00        1.00
    seg 2       2.00        1.00
    seg 3       2.00        1.00
    seg 4       2.00        1.00
    seg 5       2.00        1.00
    seg 6       2.00        1.00
    seg 7       2.00        1.00
    seg 8       0.00        0.00
```

```
Date: 214 (Aug)

              Surf        Bot
    seg 1     2.95        1.76
    seg 2     2.62        1.38
    seg 3     2.62        1.38
    seg 4     2.62        1.38
    seg 5     2.00        1.00
    seg 6     2.00        1.00
    seg 7     2.00        1.00
    seg 8     0.00        0.00

Date: 245 (Sep)

              Surf        Bot
    seg 1     2.95        1.76
    seg 2     2.62        1.38
    seg 3     2.62        1.38
    seg 4     2.62        1.38
    seg 5     2.00        1.00
    seg 6     2.00        1.00
    seg 7     2.00        1.00
    seg 8     0.00        0.00

Date: 275 (Oct)

              Surf        Bot
    seg 1     2.00        1.00
    seg 2     2.00        1.00
    seg 3     2.00        1.00
    seg 4     2.00        1.00
    seg 5     2.00        1.00
    seg 6     2.00        1.00
    seg 7     2.00        1.00
    seg 8     0.00        0.00
```

Particulate Organic Carbon, g C m^3

Date: 092 (Apr)

	Surf	Bot
seg 1	0.10	0.10
seg 2	0.10	0.10
seg 3	0.10	0.10
seg 4	0.10	0.10
seg 5	0.10	0.10
seg 6	0.10	0.14
seg 7	0.10	0.12
seg 8	0.00	0.00

Date: 122 (May)

	Surf	Bot
seg 1	0.10	0.10
seg 2	0.10	0.10
seg 3	0.10	0.10
seg 4	0.10	0.10
seg 5	0.10	0.10
seg 6	0.10	0.10
seg 7	0.10	0.10
seg 8	0.00	0.00

Date: 153 (Jun)

	Surf	Bot
seg 1	0.10	0.10
seg 2	0.10	0.10
seg 3	0.10	0.10
seg 4	0.10	0.10
seg 5	0.10	0.10
seg 6	0.10	0.10
seg 7	0.10	0.10
seg 8	0.00	0.00

Date: 183 (Jul)

	Surf	Bot
seg 1	0.10	0.10
seg 2	0.10	0.10
seg 3	0.10	0.10
seg 4	0.10	0.10
seg 5	0.10	0.10
seg 6	0.10	0.10
seg 7	0.10	0.10
seg 8	0.00	0.00

```
Date: 214 (Aug)

                  Surf        Bot
    seg 1         0.25        0.33
    seg 2         0.05        0.14
    seg 3         0.10        0.10
    seg 4         0.10        0.10
    seg 5         0.18        0.11
    seg 6         0.10        0.14
    seg 7         0.10        0.08
    seg 8         0.00        0.00

Date: 245 (Sep)

                  Surf        Bot
    seg 1         0.25        0.33
    seg 2         0.05        0.14
    seg 3         0.10        0.10
    seg 4         0.10        0.10
    seg 5         0.18        0.11
    seg 6         0.10        0.14
    seg 7         0.10        0.08
    seg 8         0.00        0.00

Date: 275 (Oct)

                  Surf        Bot
    seg 1         0.10        0.10
    seg 2         0.10        0.10
    seg 3         0.10        0.10
    seg 4         0.10        0.10
    seg 5         0.10        0.10
    seg 6         0.10        0.10
    seg 7         0.10        0.10
    seg 8         0.00        0.00
```

Ammonia - g N m^3

Date: 092 (Apr)

	Surf	Bot
seg 1	0.004	0.004
seg 2	0.004	0.004
seg 3	0.004	0.004
seg 4	0.004	0.004
seg 5	0.012	0.010
seg 6	0.005	0.023
seg 7	0.005	0.025
seg 8	0.000	0.000

Date: 122 (May)

	Surf	Bot
seg 1	0.004	0.004
seg 2	0.004	0.004
seg 3	0.004	0.004
seg 4	0.005	0.005
seg 5	0.006	0.008
seg 6	0.004	0.004
seg 7	0.005	0.022
seg 8	0.000	0.000

Date: 153 (Jun)

	Surf	Bot
seg 1	0.019	0.033
seg 2	0.017	0.024
seg 3	0.017	0.023
seg 4	0.003	0.015
seg 5	0.004	0.004
seg 6	0.004	0.004
seg 7	0.004	0.004
seg 8	0.000	0.000

Date: Jul (183)

	Surf	Bot
seg 1	0.004	0.004
seg 2	0.004	0.004
seg 3	0.004	0.004
seg 4	0.004	0.004
seg 5	0.004	0.004
seg 6	0.004	0.004
seg 7	0.004	0.004
seg 8	0.000	0.000

Date: Aug (214)

	Surf	Bot
seg 1	0.004	0.004
seg 2	0.004	0.004
seg 3	0.004	0.004
seg 4	0.004	0.004
seg 5	0.004	0.004
seg 6	0.004	0.004
seg 7	0.004	0.004
seg 8	0.000	0.000

Date: 245 (Sep)

	Surf	Bot
seg 1	0.004	0.004
seg 2	0.004	0.004
seg 3	0.004	0.004
seg 4	0.004	0.004
seg 5	0.008	0.004
seg 6	0.004	0.004
seg 7	0.004	0.004
seg 8	0.000	0.000

Date: 275 (Oct)

	Surf	Bot
seg 1	0.004	0.004
seg 2	0.004	0.004
seg 3	0.004	0.004
seg 4	0.004	0.004
seg 5	0.004	0.004
seg 6	0.004	0.004
seg 7	0.004	0.004
seg 8	0.000	0.000

Nitrite plus Nitrate, g N m^{-3}

Date: 092 (Apr)

	Surf	Bot
seg 1	0.014	0.042
seg 2	0.014	0.042
seg 3	0.042	0.280
seg 4	0.042	0.280
seg 5	0.039	0.280
seg 6	0.003	0.126
seg 7	0.003	0.035
seg 8	0.000	0.000

Date: 122 (May)

	Surf	Bot
seg 1	0.014	0.042
seg 2	0.014	0.042
seg 3	0.014	0.280
seg 4	0.021	0.420
seg 5	0.006	0.392
seg 6	0.014	0.042
seg 7	0.002	0.046
seg 8	0.000	0.000

Date: 153 (Jun)

	Surf	Bot
seg 1	0.022	0.032
seg 2	0.010	0.042
seg 3	0.006	0.224
seg 4	0.064	0.164
seg 5	0.051	0.336
seg 6	0.014	0.042
seg 7	0.014	0.042
seg 8	0.000	0.000

Date: 183 (Jul)

	Surf	Bot
seg 1	0.007	0.021
seg 2	0.007	0.021
seg 3	0.007	0.140
seg 4	0.007	0.140
seg 5	0.007	0.140
seg 6	0.007	0.021
seg 7	0.007	0.021
seg 8	0.000	0.000

```
Date: 214 (Aug)

                Surf        Bot
    seg 1       0.003       0.009
    seg 2       0.002       0.062
    seg 3       0.003       0.133
    seg 4       0.003       0.224
    seg 5       0.003       0.224
    seg 6       0.001       0.042
    seg 7       0.001       0.042
    seg 8       0.000       0.000

Date: 245 (Sep)

                Surf        Bot
    seg 1       0.007       0.014
    seg 2       0.009       0.046
    seg 3       0.005       0.226
    seg 4       0.014       0.224
    seg 5       0.018       0.273
    seg 6       0.004       0.042
    seg 7       0.004       0.042
    seg 8       0.000       0.000

Date: 275 (Oct)

                Surf        Bot
    seg 1       0.007       0.014
    seg 2       0.007       0.014
    seg 3       0.007       0.140
    seg 4       0.007       0.140
    seg 5       0.007       0.140
    seg 6       0.004       0.042
    seg 7       0.004       0.042
    seg 8       0.000       0.000
```

```
Dissolved Organic Nitrogen, g N m³
  no measurements on boundary or in interior
Date: 092 (Apr)

                 Surf        Bot
    seg 1        0.014       0.014
    seg 2        0.014       0.014
    seg 3        0.014       0.014
    seg 4        0.014       0.014
    seg 5        0.014       0.014
    seg 6        0.014       0.014
    seg 7        0.014       0.014
    seg 8        0.000       0.000

Date: 122 (May)

                 Surf        Bot
    seg 1        0.014       0.014
    seg 2        0.014       0.014
    seg 3        0.014       0.014
    seg 4        0.014       0.014
    seg 5        0.014       0.014
    seg 6        0.014       0.014
    seg 7        0.014       0.014
    seg 8        0.000       0.000

Date: 153 (Jun)

                 Surf        Bot
    seg 1        0.014       0.014
    seg 2        0.014       0.014
    seg 3        0.014       0.014
    seg 4        0.014       0.014
    seg 5        0.014       0.014
    seg 6        0.014       0.014
    seg 7        0.014       0.014
    seg 8        0.000       0.000

Date: 183 (Jul)

                 Surf        Bot
    seg 1        0.014       0.014
    seg 2        0.014       0.014
    seg 3        0.014       0.014
    seg 4        0.014       0.014
    seg 5        0.014       0.014
    seg 6        0.014       0.014
    seg 7        0.014       0.014
    seg 8        0.000       0.000
```

Date: 214 (Aug)

	Surf	Bot
seg 1	0.014	0.014
seg 2	0.014	0.014
seg 3	0.014	0.014
seg 4	0.014	0.014
seg 5	0.014	0.014
seg 6	0.014	0.014
seg 7	0.014	0.014
seg 8	0.000	0.000

Date: 245 (Sep)

	Surf	Bot
seg 1	0.014	0.014
seg 2	0.014	0.014
seg 3	0.014	0.014
seg 4	0.014	0.014
seg 5	0.014	0.014
seg 6	0.014	0.014
seg 7	0.014	0.014
seg 8	0.000	0.000

Date: 275 (Oct)

	Surf	Bot
seg 1	0.014	0.014
seg 2	0.014	0.014
seg 3	0.014	0.014
seg 4	0.014	0.014
seg 5	0.014	0.014
seg 6	0.014	0.014
seg 7	0.014	0.014
seg 8	0.000	0.000

Particulate Organic Nitrogen, g N m⁻³

Date: 092 (Apr)

	Surf	Bot
seg 1	0.014	0.014
seg 2	0.014	0.014
seg 3	0.014	0.014
seg 4	0.014	0.014
seg 5	0.010	0.014
seg 6	0.010	0.014
seg 7	0.013	0.011
seg 8	0.000	0.000

Date: 122 (May)

	Surf	Bot
seg 1	0.014	0.014
seg 2	0.014	0.014
seg 3	0.014	0.014
seg 4	0.014	0.014
seg 5	0.014	0.014
seg 6	0.014	0.014
seg 7	0.014	0.014
seg 8	0.000	0.000

Date: 153 (Jun)

	Surf	Bot
seg 1	0.014	0.014
seg 2	0.014	0.014
seg 3	0.014	0.014
seg 4	0.014	0.014
seg 5	0.014	0.014
seg 6	0.014	0.014
seg 7	0.014	0.014
seg 8	0.000	0.000

Date: 183 (Jul)

	Surf	Bot
seg 1	0.014	0.014
seg 2	0.014	0.014
seg 3	0.014	0.014
seg 4	0.014	0.014
seg 5	0.014	0.014
seg 6	0.014	0.014
seg 7	0.014	0.014
seg 8	0.000	0.000

```
Date: 214 (Aug)

                   Surf          Bot
        seg 1      0.014         0.014
        seg 2      0.014         0.014
        seg 3      0.014         0.014
        seg 4      0.014         0.014
        seg 5      0.014         0.014
        seg 6      0.014         0.014
        seg 7      0.014         0.014
        seg 8      0.000         0.000

Date: 245 (Sep)

                   Surf          Bot
        seg 1      0.014         0.014
        seg 2      0.014         0.014
        seg 3      0.014         0.014
        seg 4      0.014         0.014
        seg 5      0.014         0.014
        seg 6      0.014         0.014
        seg 7      0.014         0.014
        seg 8      0.000         0.000

Date: 275 (Oct)

                   Surf          Bot
        seg 1      0.014         0.014
        seg 2      0.014         0.014
        seg 3      0.014         0.014
        seg 4      0.014         0.014
        seg 5      0.014         0.014
        seg 6      0.014         0.014
        seg 7      0.014         0.014
        seg 8      0.000         0.000
```

```
Dissolved Oxygen, g O₂ m⁻³

Date: 092 (Apr)

                    Surf        Bot
    seg 1           8.57        7.57
    seg 2           8.57        7.57
    seg 3           8.57        7.57
    seg 4           8.57        7.57
    seg 5           8.57        7.57
    seg 6           9.43        7.57
    seg 7           9.43        7.57
    seg 8          12.86       12.86

Date: 122 (May)

                    Surf        Bot
    seg 1           7.89        7.43
    seg 2           8.57        7.43
    seg 3           8.57        7.43
    seg 4           8.57        7.43
    seg 5           8.57        7.43
    seg 6           9.00        7.57
    seg 7           9.00        7.57
    seg 8          11.71       11.71

Date: 153 (Jun)

                    Surf        Bot
    seg 1           7.94        6.84
    seg 2           8.29        6.26
    seg 3           8.39        5.86
    seg 4           8.43        6.00
    seg 5           8.43        6.57
    seg 6           8.43        6.00
    seg 7           8.43        6.00
    seg 8          10.43       10.43

Date: 183 (Jul)

                    Surf        Bot
    seg 1           6.56        3.94
    seg 2           7.43        4.71
    seg 3           7.43        4.71
    seg 4           7.43        4.71
    seg 5           8.14        4.86
    seg 6           8.14        4.86
    seg 7           8.14        4.86
    seg 8           9.57        9.57
```

```
Date: 214 (Aug)

                    Surf        Bot
        seg 1       7.34        2.54
        seg 2       7.66        4.04
        seg 3       7.29        5.89
        seg 4       6.97        5.24
        seg 5       7.29        4.71
        seg 6       7.29        4.71
        seg 7       7.29        4.71
        seg 8       9.86        9.86

Date: 245 (Sep)

                    Surf        Bot
        seg 1       7.01        4.37
        seg 2       6.86        2.19
        seg 3       6.91        5.03
        seg 4       6.00        5.93
        seg 5       7.39        6.10
        seg 6       6.86        4.99
        seg 7       7.41        5.13
        seg 8      10.14       10.14

Date: 275 (Oct)

                    Surf        Bot
        seg 1       7.50        6.93
        seg 2       7.86        6.29
        seg 3       7.86        6.86
        seg 4       7.86        6.86
        seg 5       8.00        7.29
        seg 6       8.00        7.29
        seg 7       8.14        7.29
        seg 8      11.29       11.29
```

Appendix D
Model-Prototype Calibration
Plots

NEW YORK BIGHT

Aggregated by Area, Layer, and Month - 1976
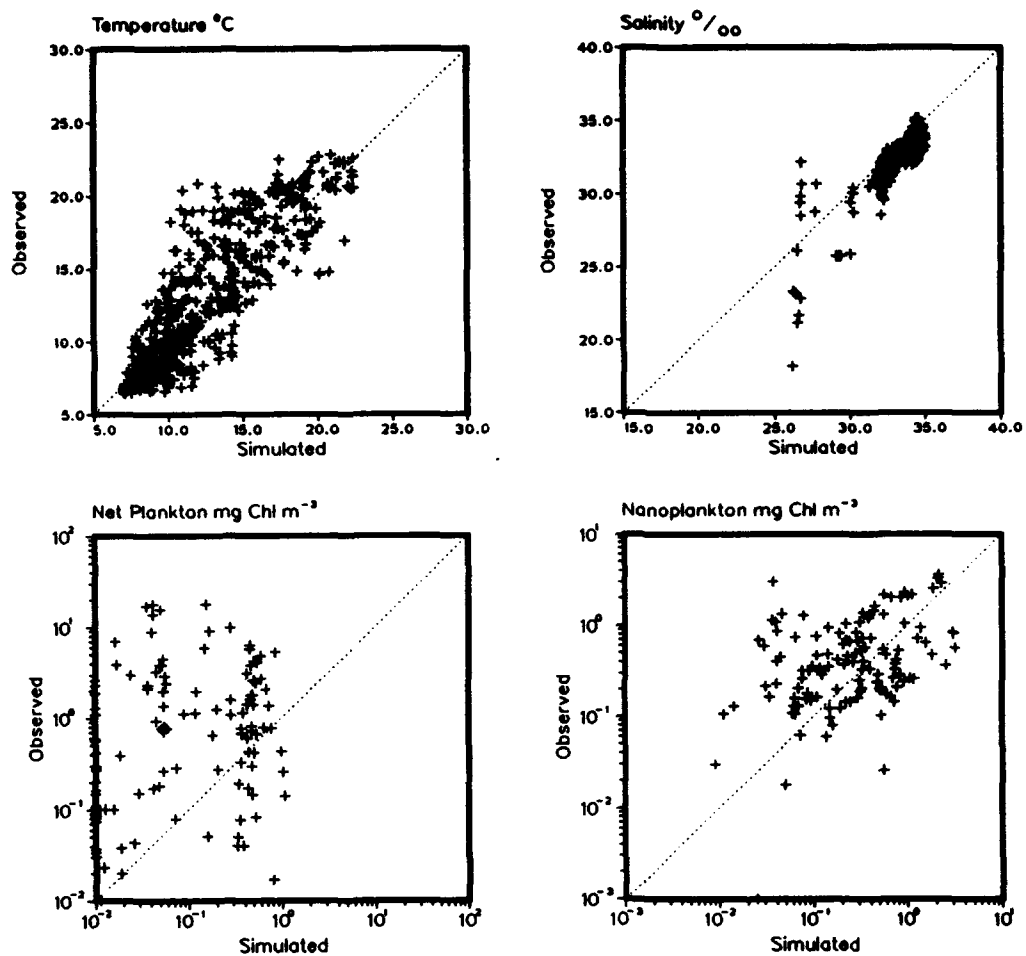
Calibration

Plate D1. (Sheet 1 of 3)

NEW YORK BIGHT
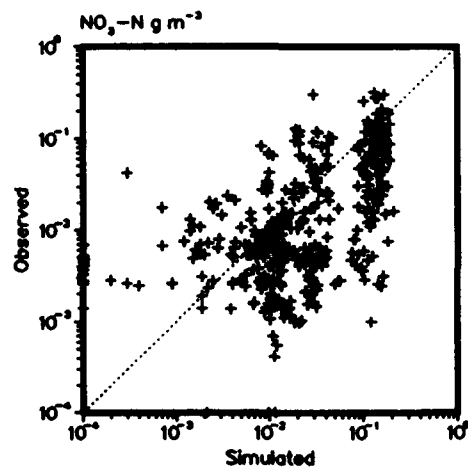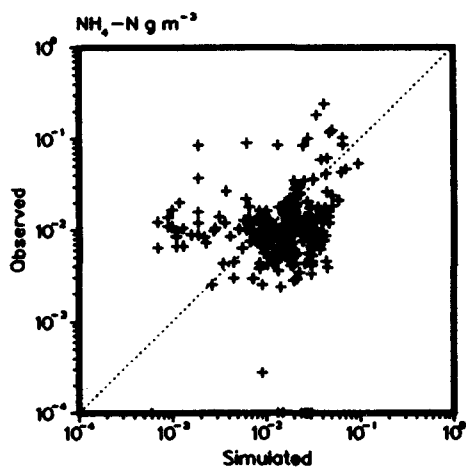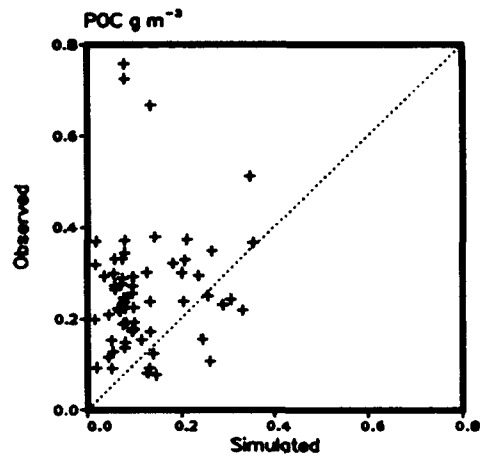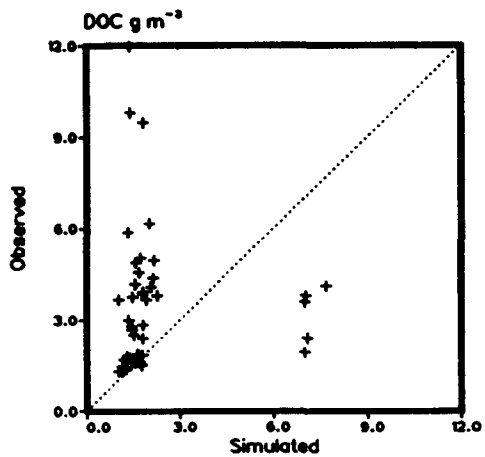
Aggregated by Area, Layer, and Month - 1976

Calibration

NEW YORK BIGHT

Aggregated by Area, Layer, and Month - 1976
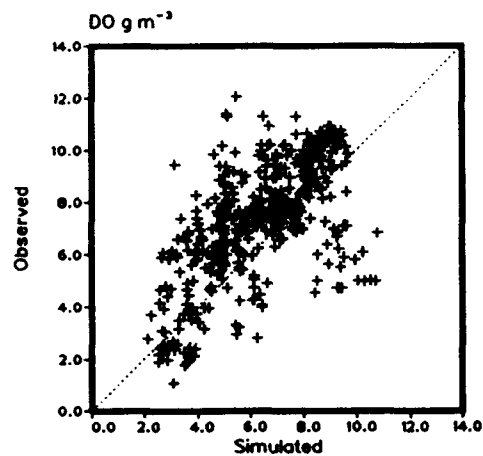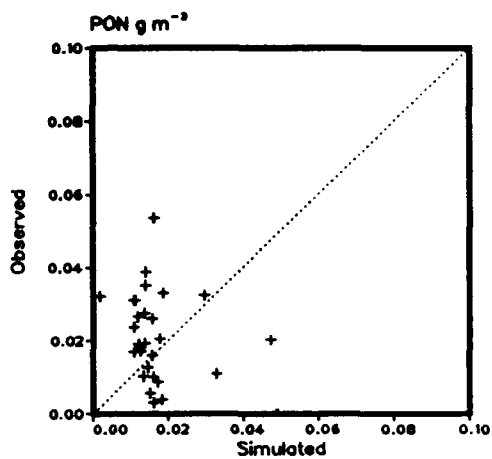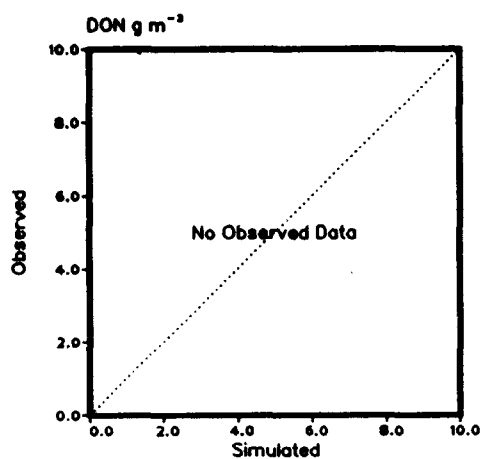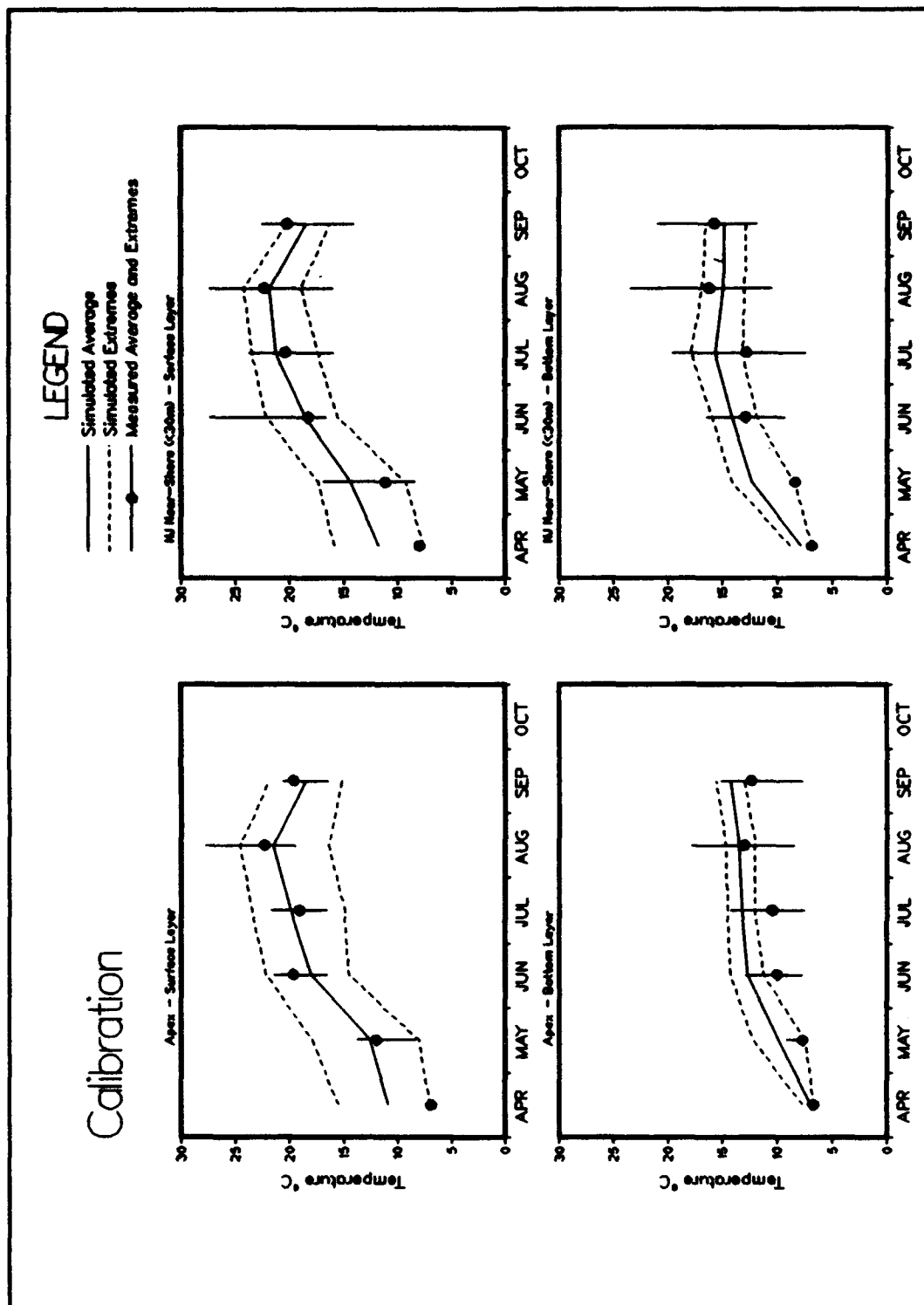
Calibration

Plate D2. (Sheet 1 of 6)

Calibration

Plate D2. (Sheet 3 of 6)

Calibration

LEGEND

— Simulated Average
----- Simulated Extremes
—●— Measured Average and Extremes

Plate D2.   (Sheet 4 of 6)

D8

Plate D2. (Sheet 5 of 6)

Calibration

LEGEND
Simulated Average
Simulated Extremes
Measured Average and Extremes
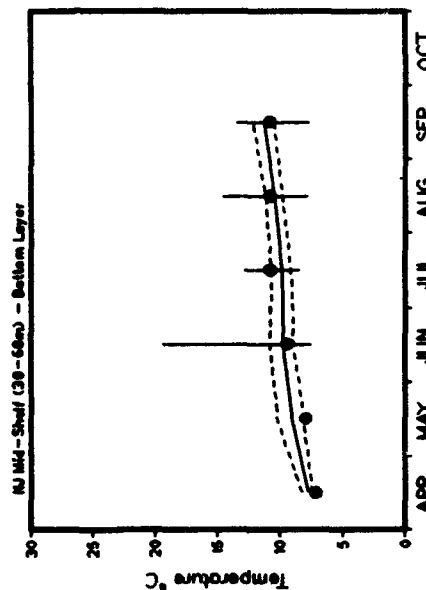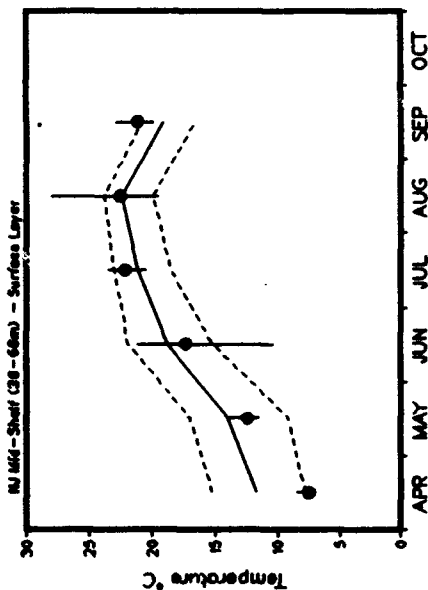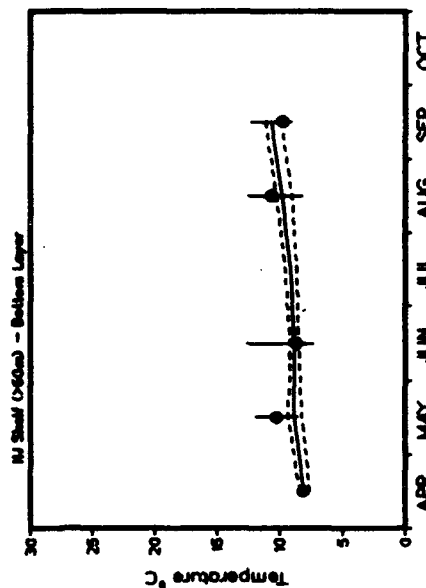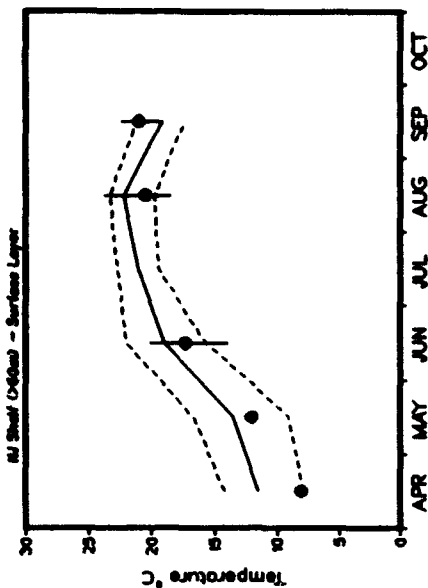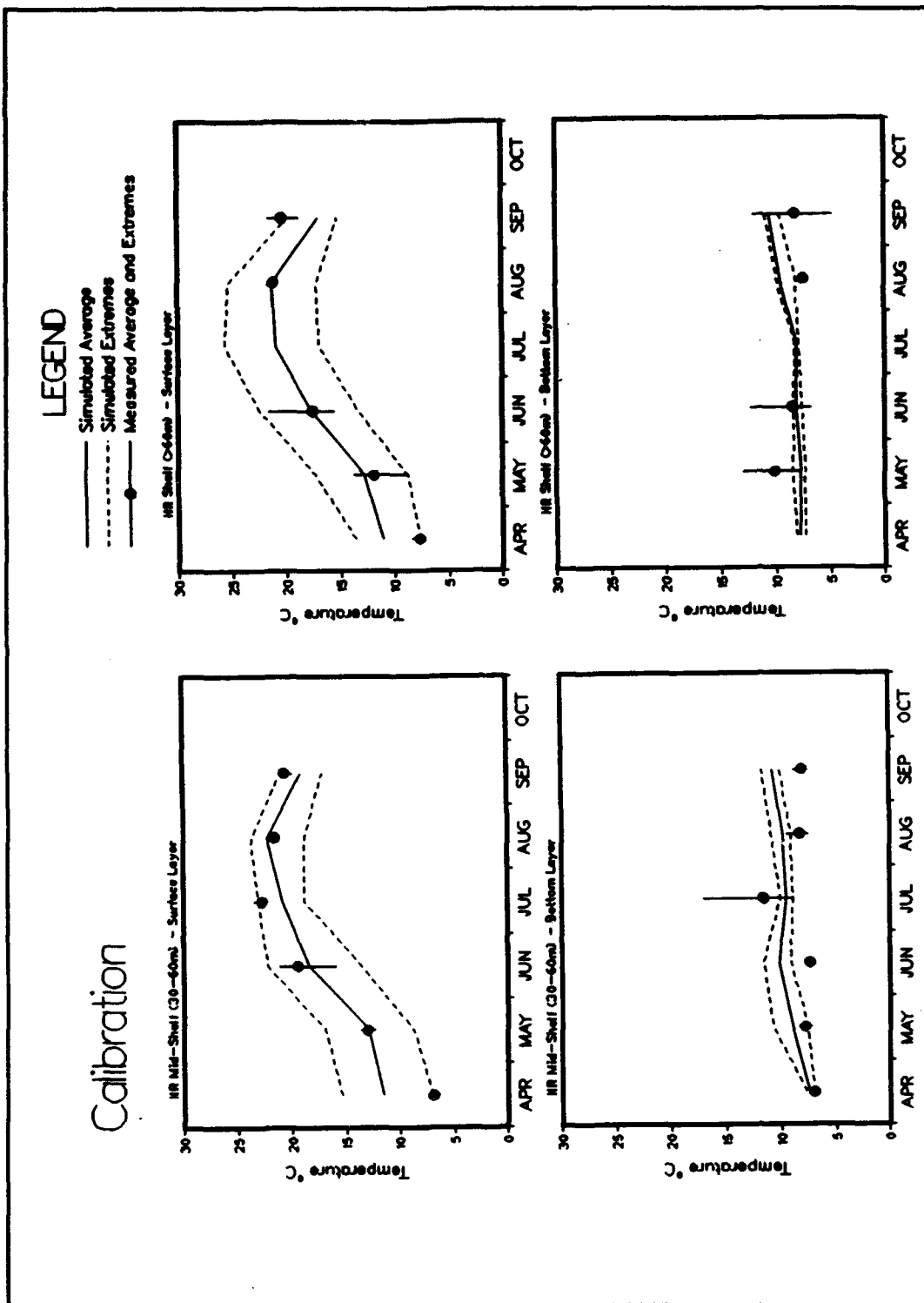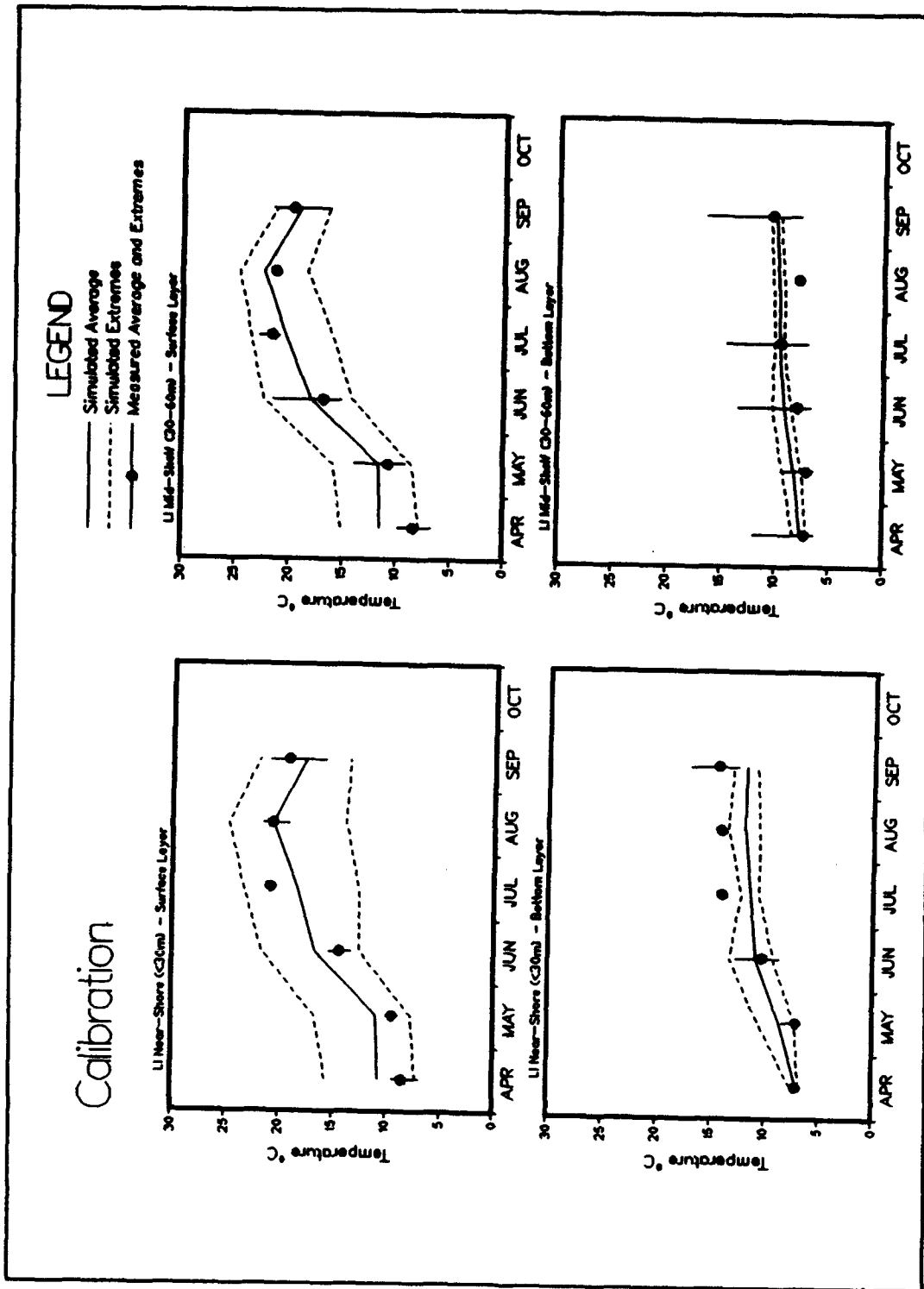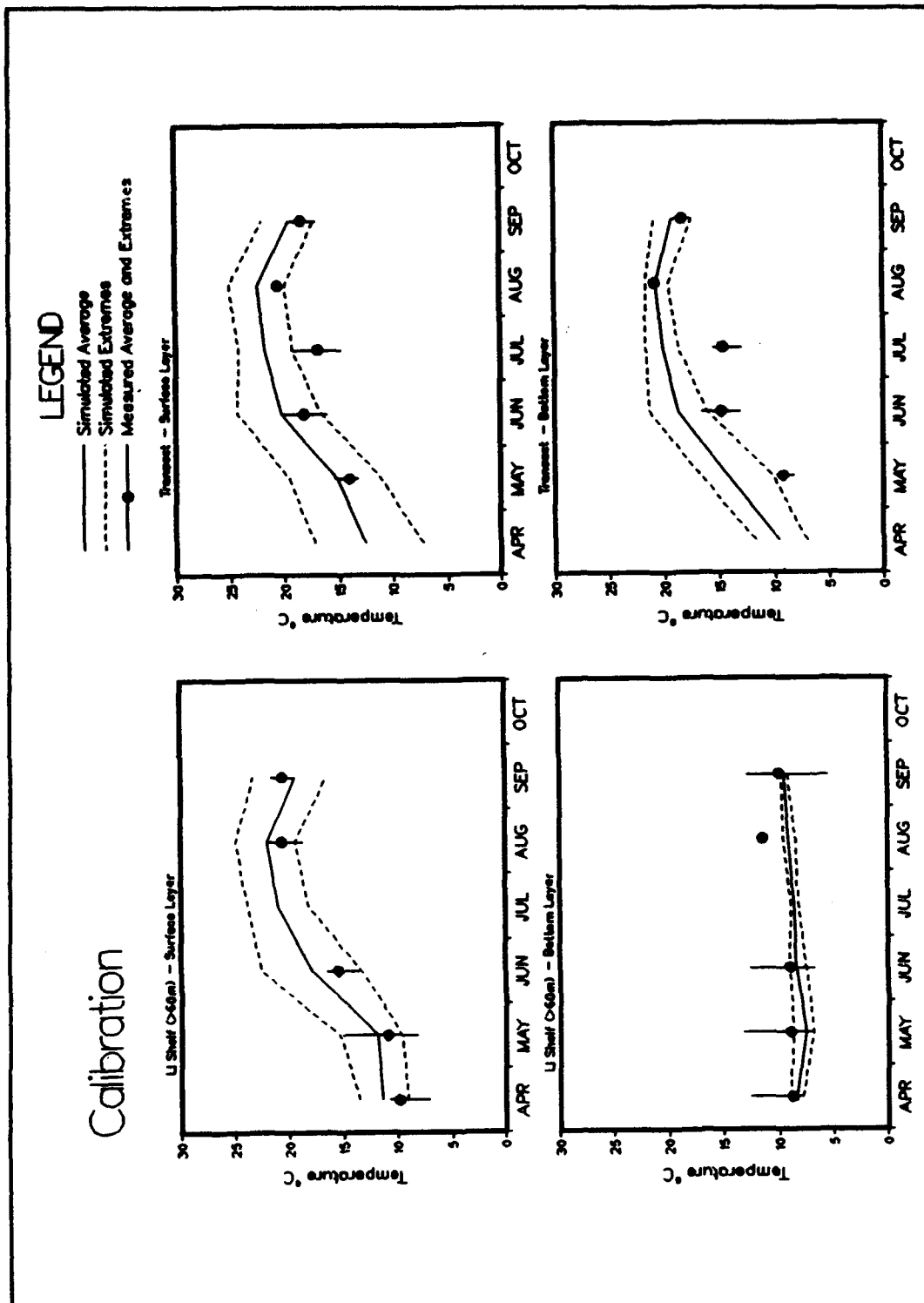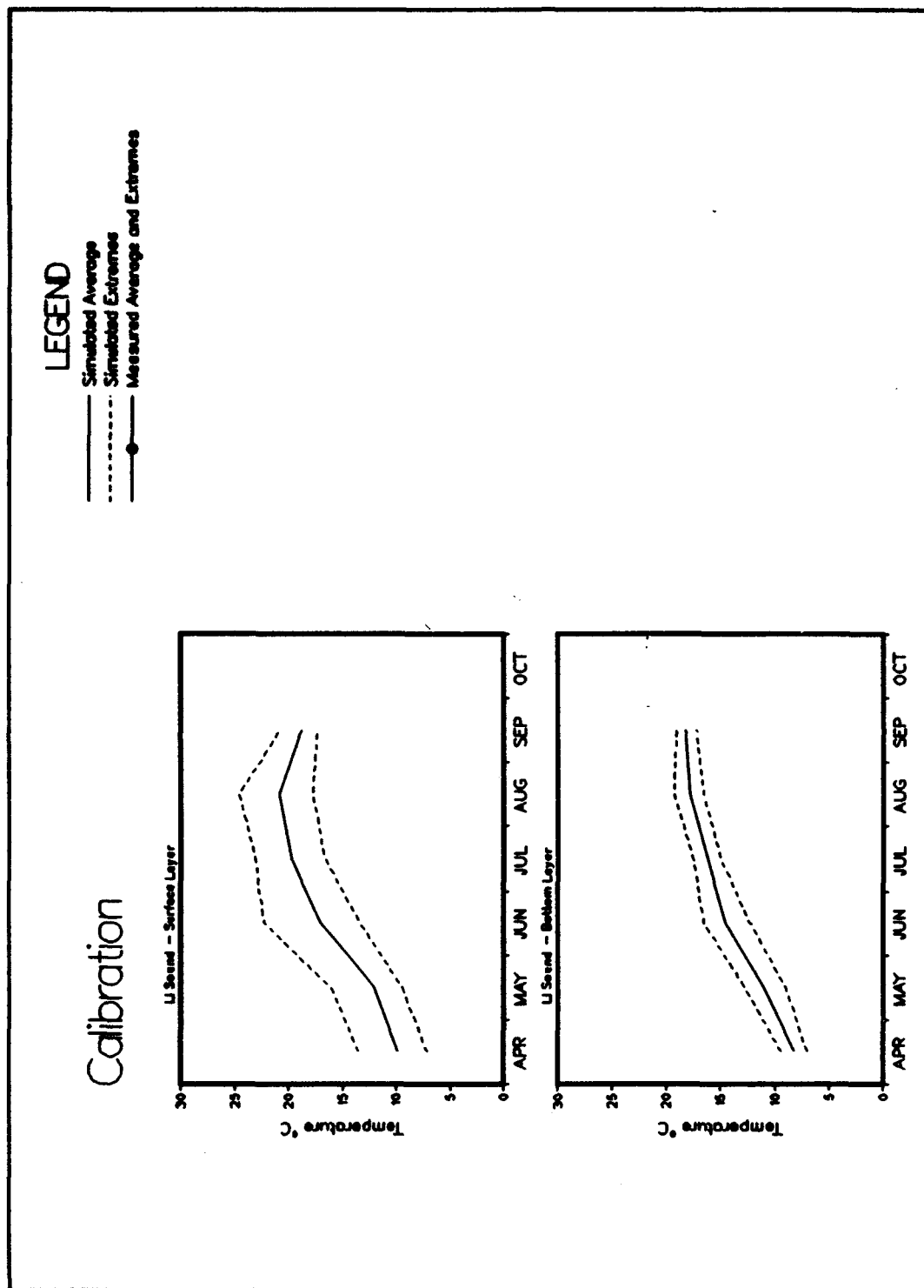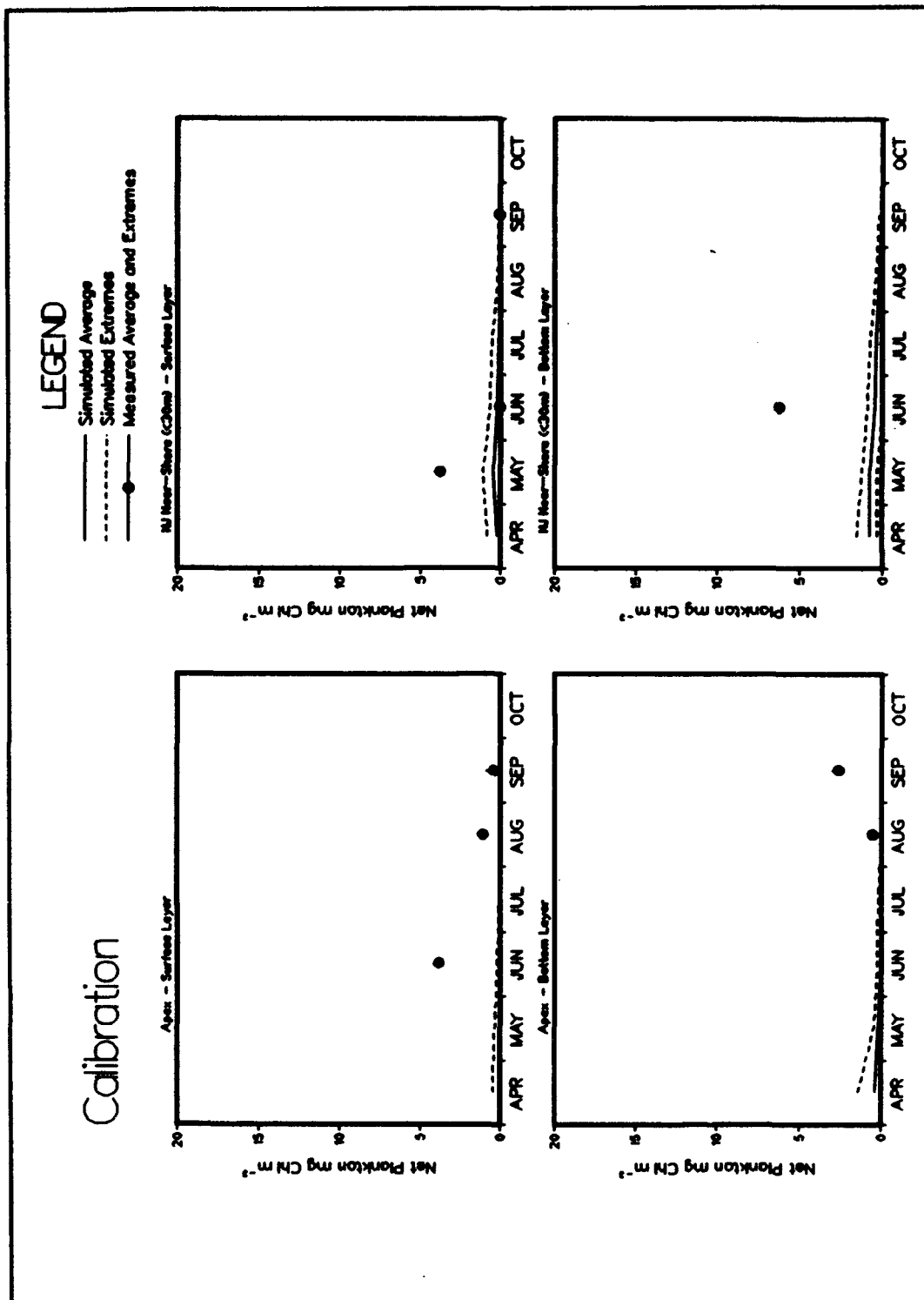
Plate D2. (Sheet 6 of 6)
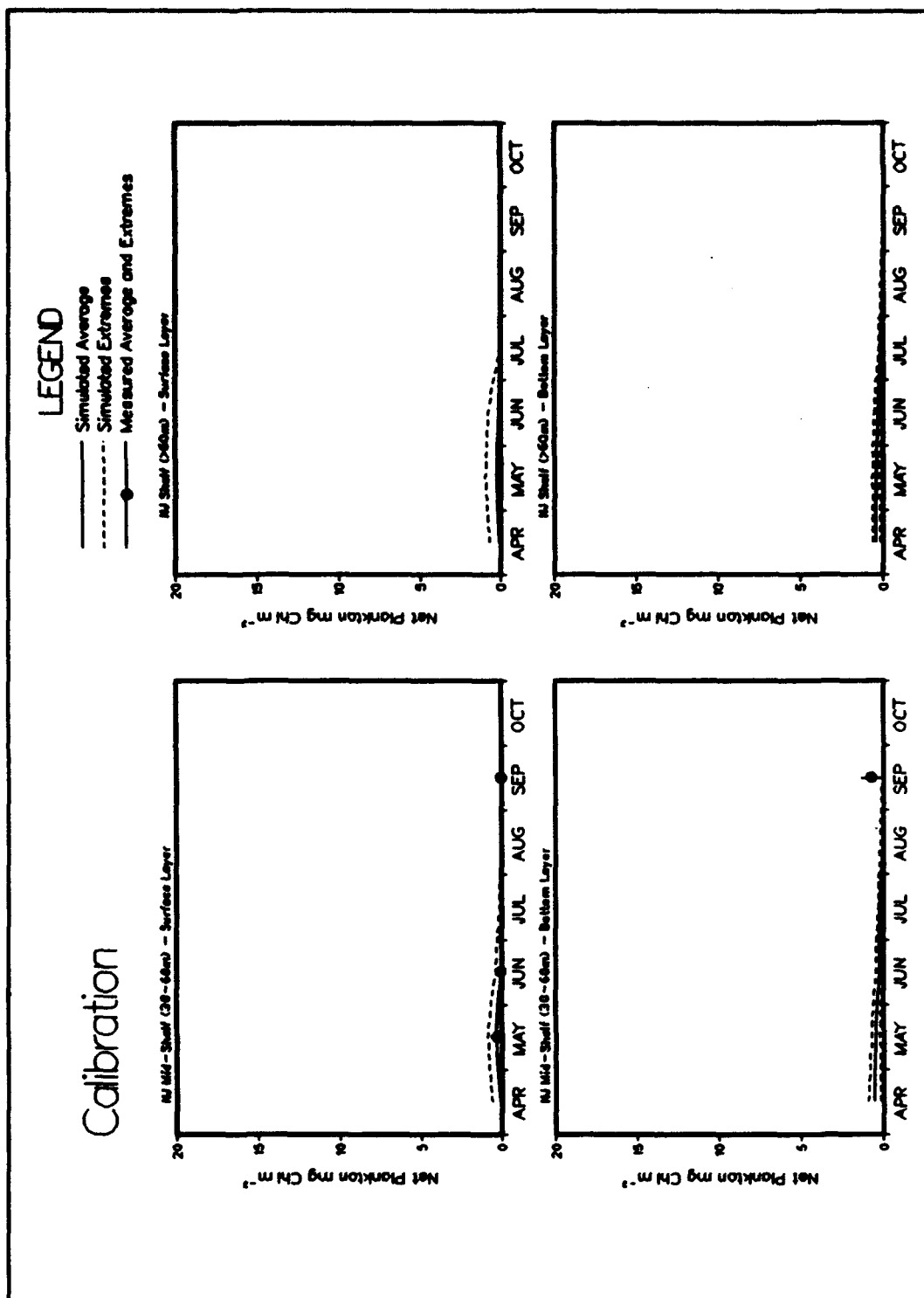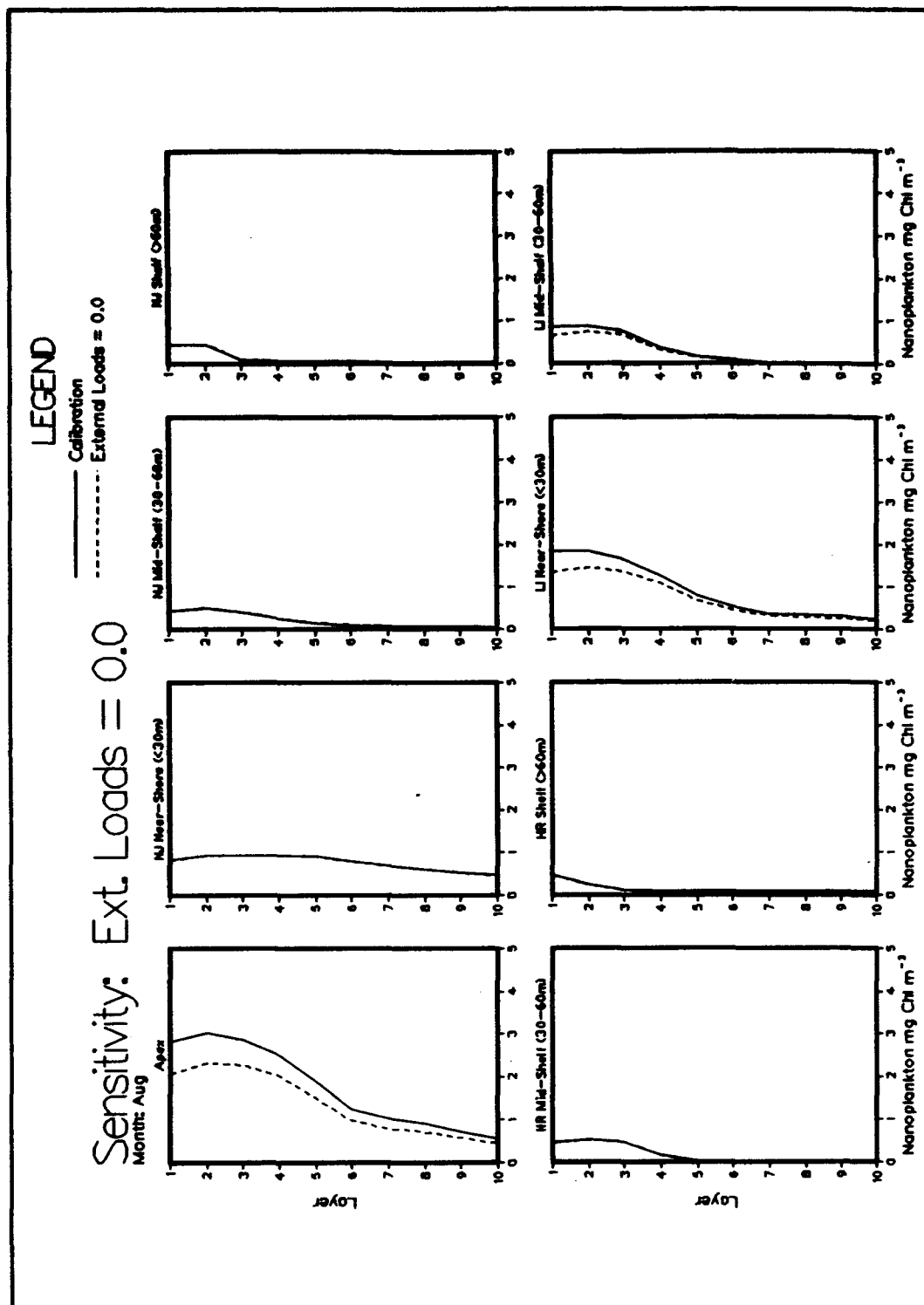
Plate D3. (Sheet 1 of 6)

Plate D3. (Sheet 2 of 6)
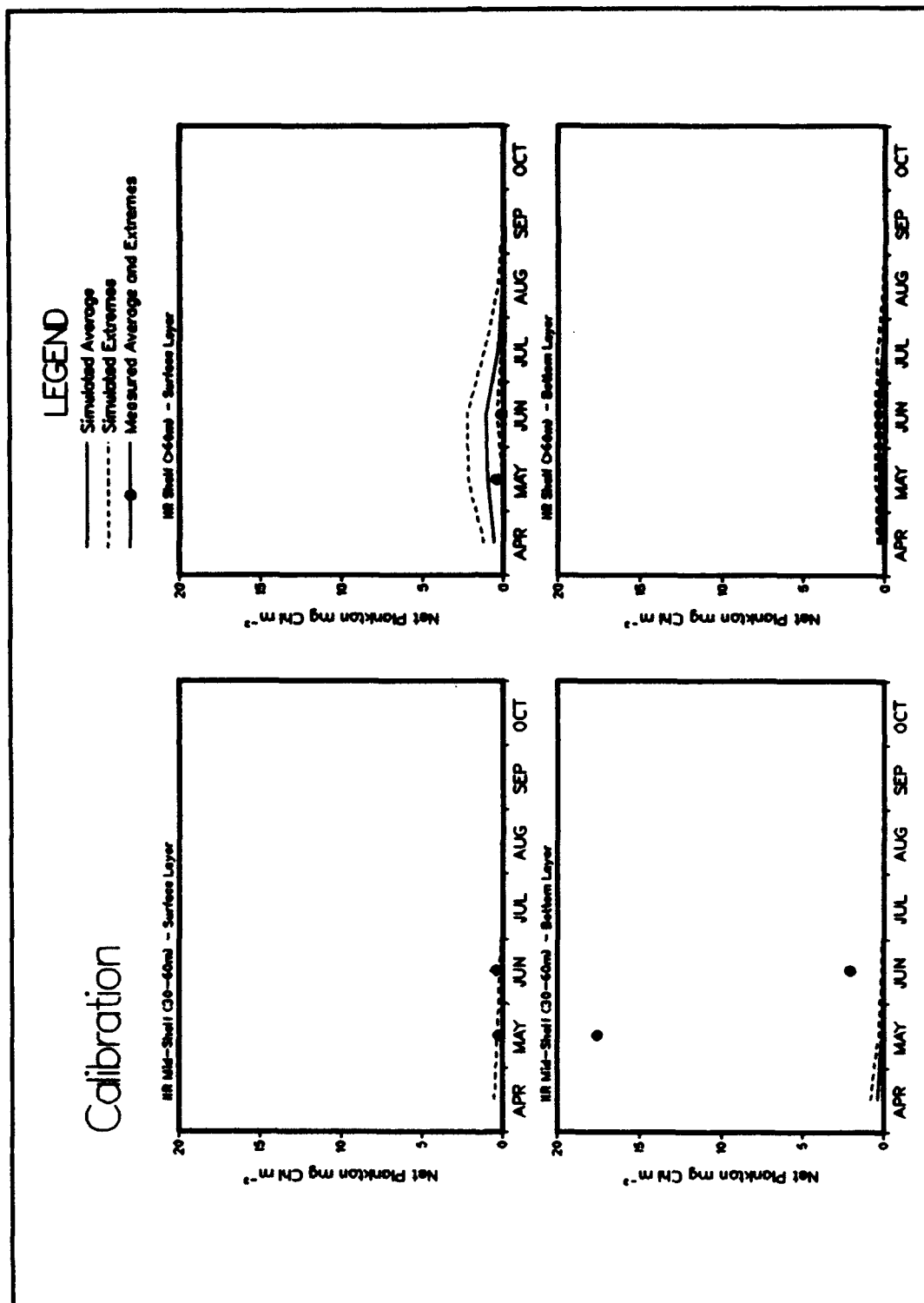
Plate D3. (Sheet 3 of 6)
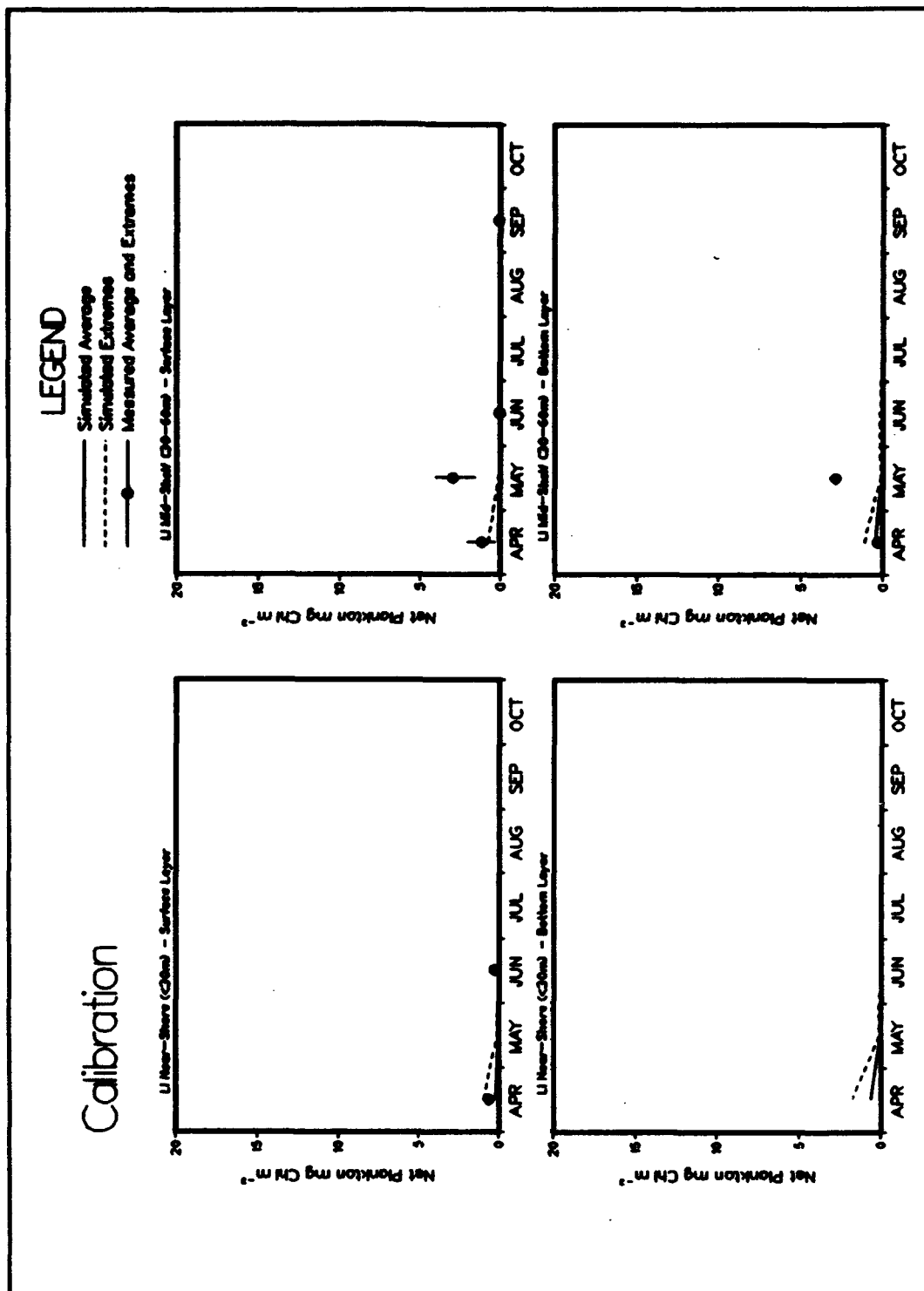
Plate D3. (Sheet 4 of 6)

Plate D3. (Sheet 5 of 6)

Calibration

LEGEND
Simulated Average
Simulated Extremes
Measured Average and Extremes
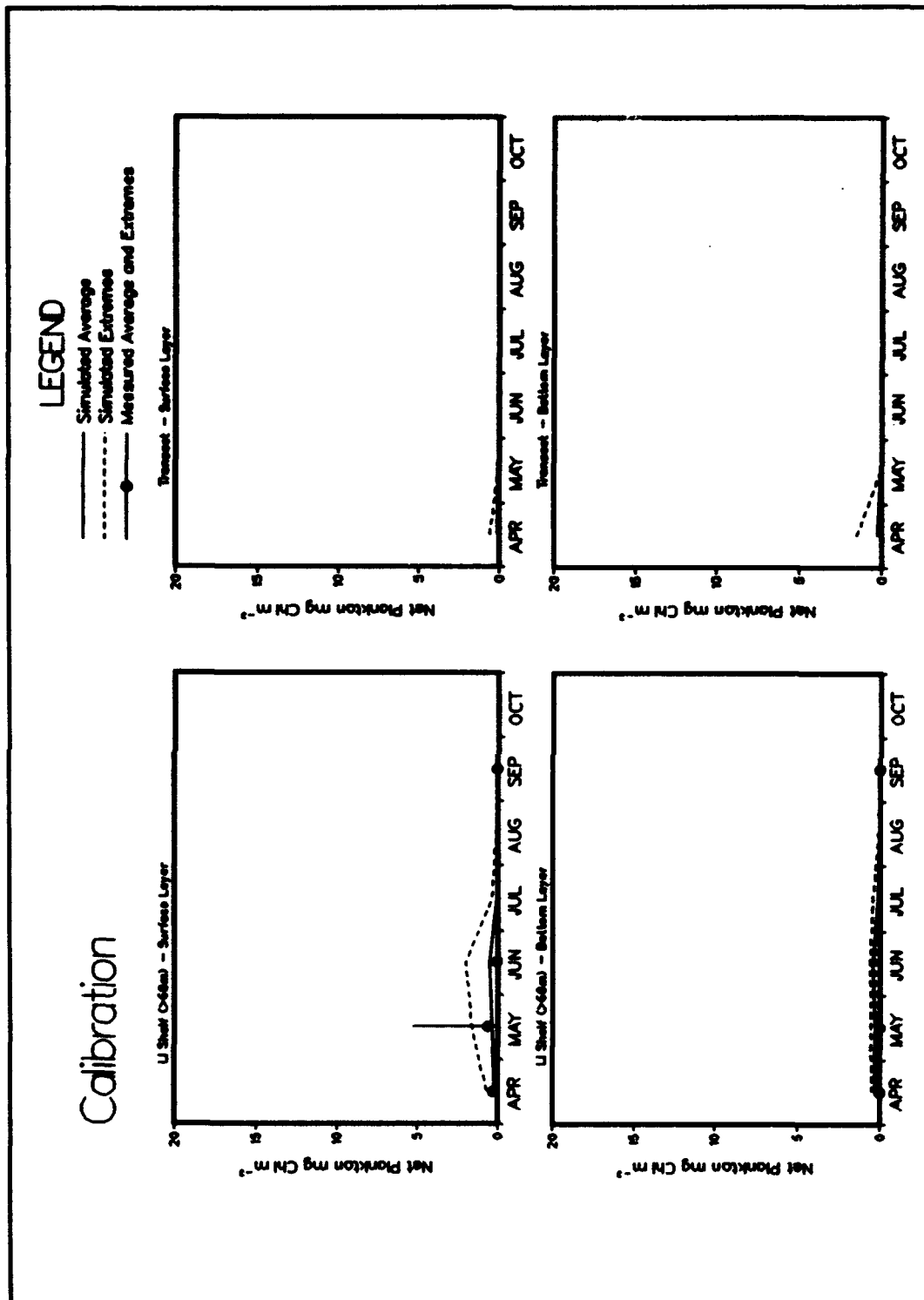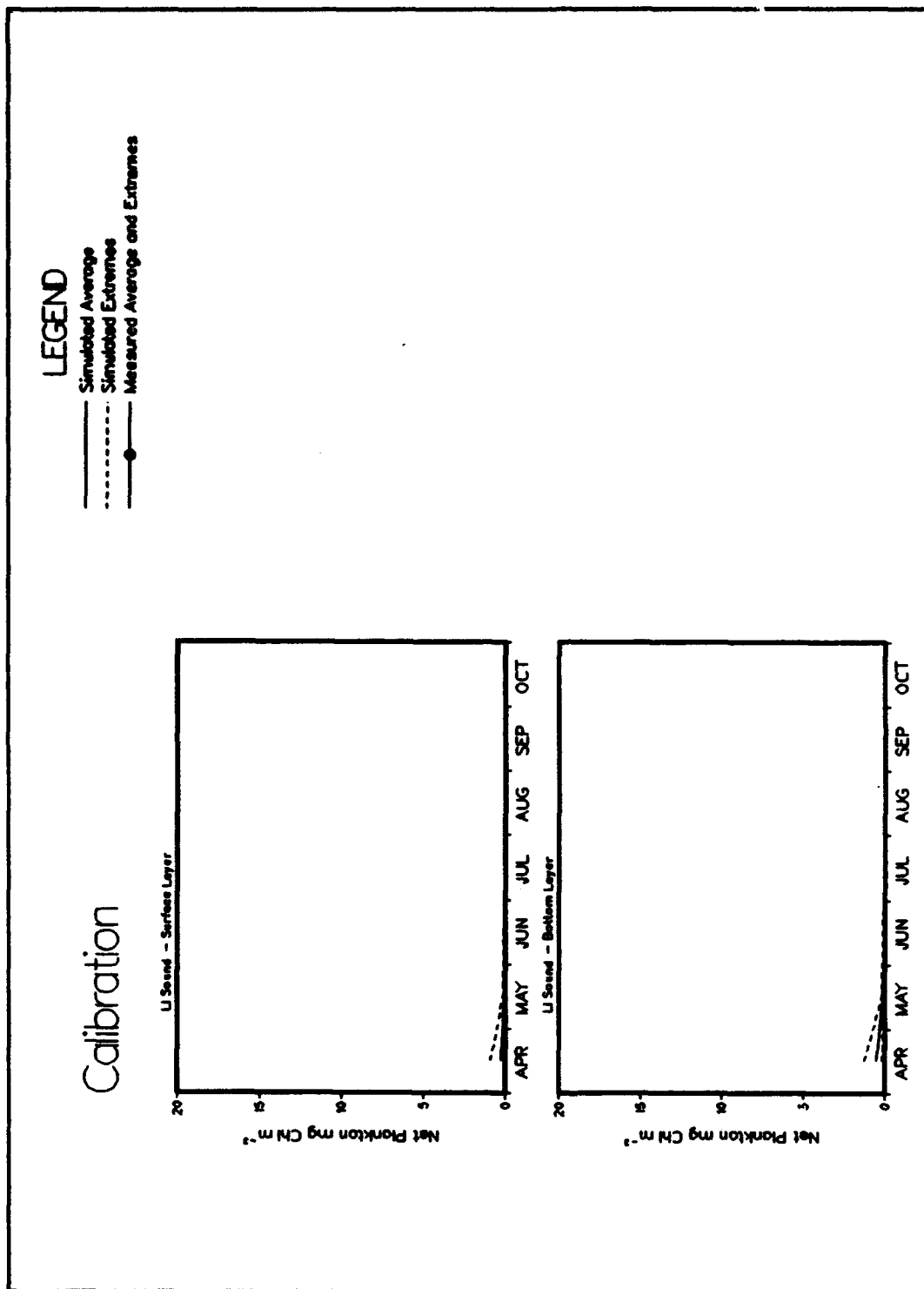
Plate D3. (Sheet 6 of 6)

D16
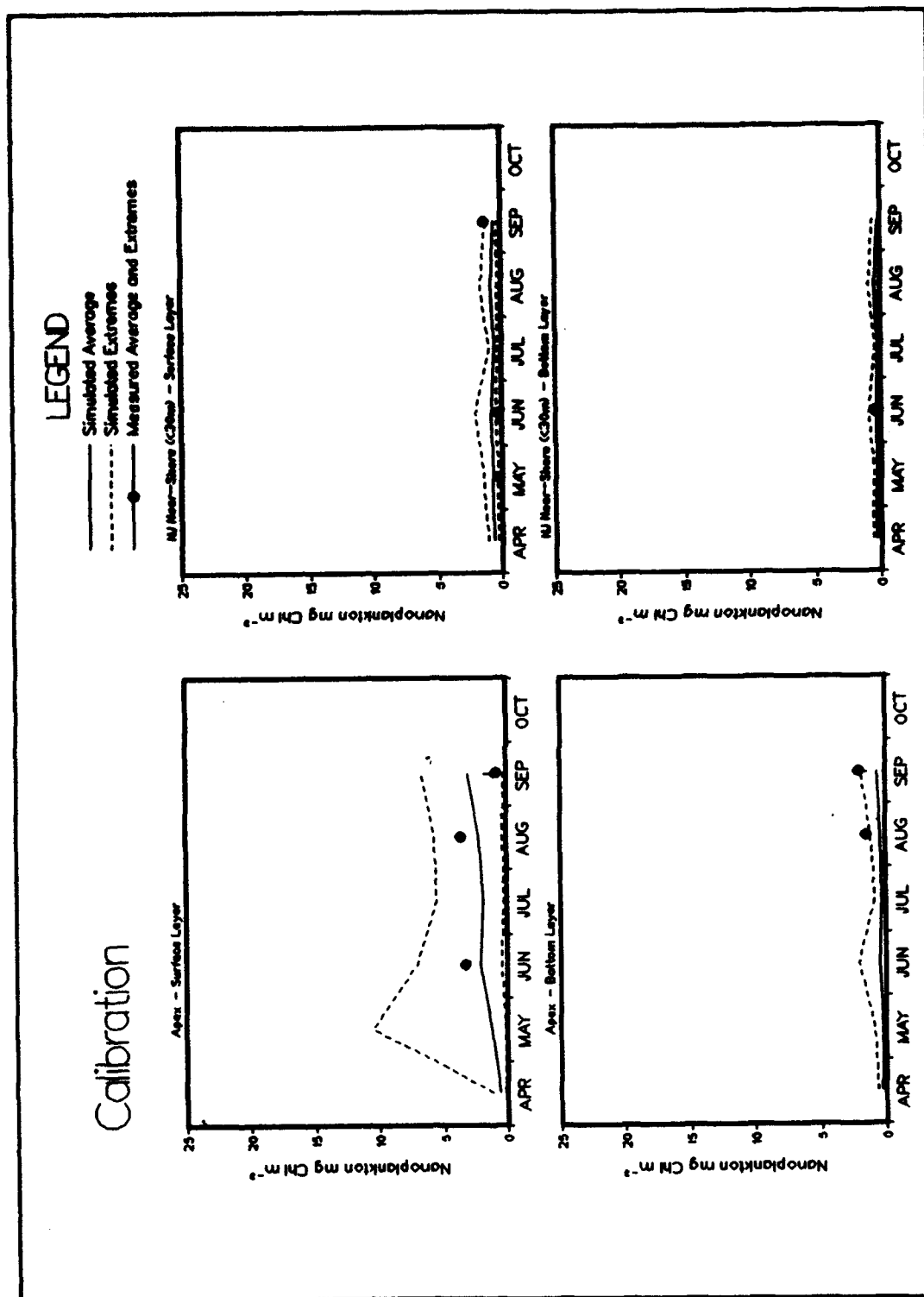
Plate D4. (Sheet 1 of 6)

Plate D4. (Sheet 2 of 6)

D18

Plate D4. (Sheet 3 of 6)

Appendix D   Calibration Plots

Plate D4. (Sheet 4 of 6)

Calibration

Plate D4. (Sheet 5 of 6)

Plate D4.   (Sheet 6 of 6)

Calibration

LEGEND

Simulated Average
Simulated Extremes
Measured Average and Extremes
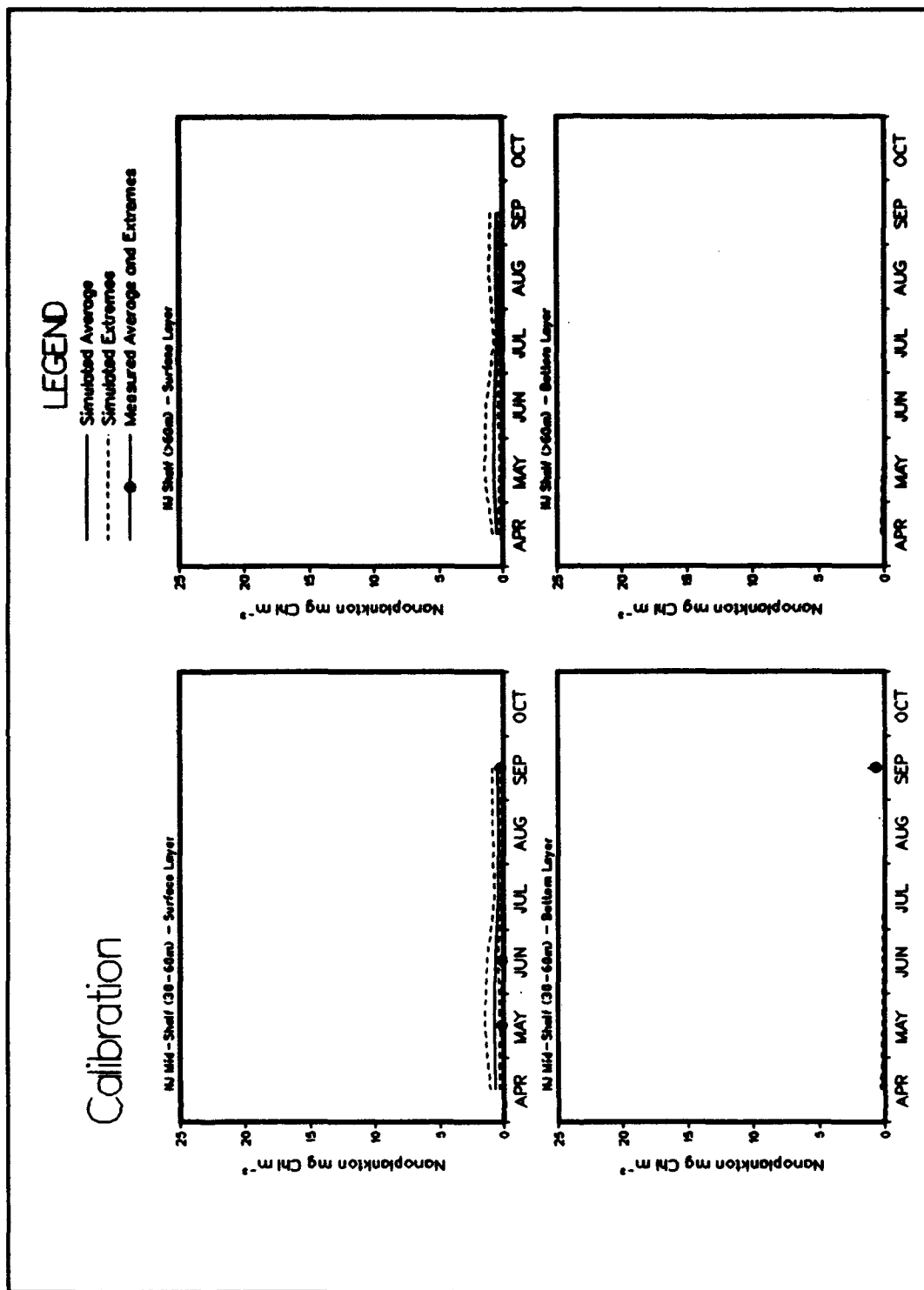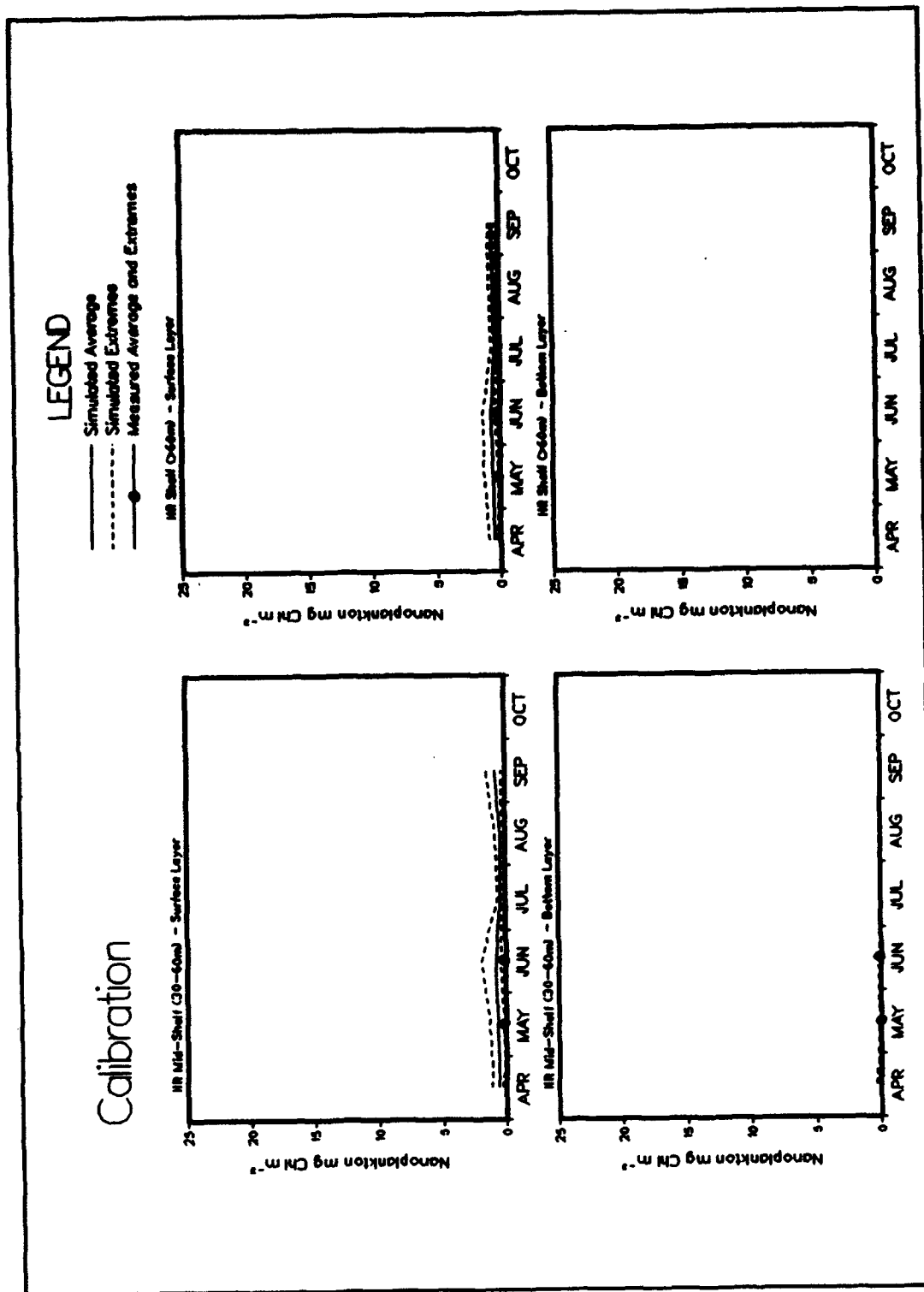
Plate D5. (Sheet 1 of 6)

LEGEND

Simulated Average
Simulated Extremes
Measured Average and Extremes

Calibration
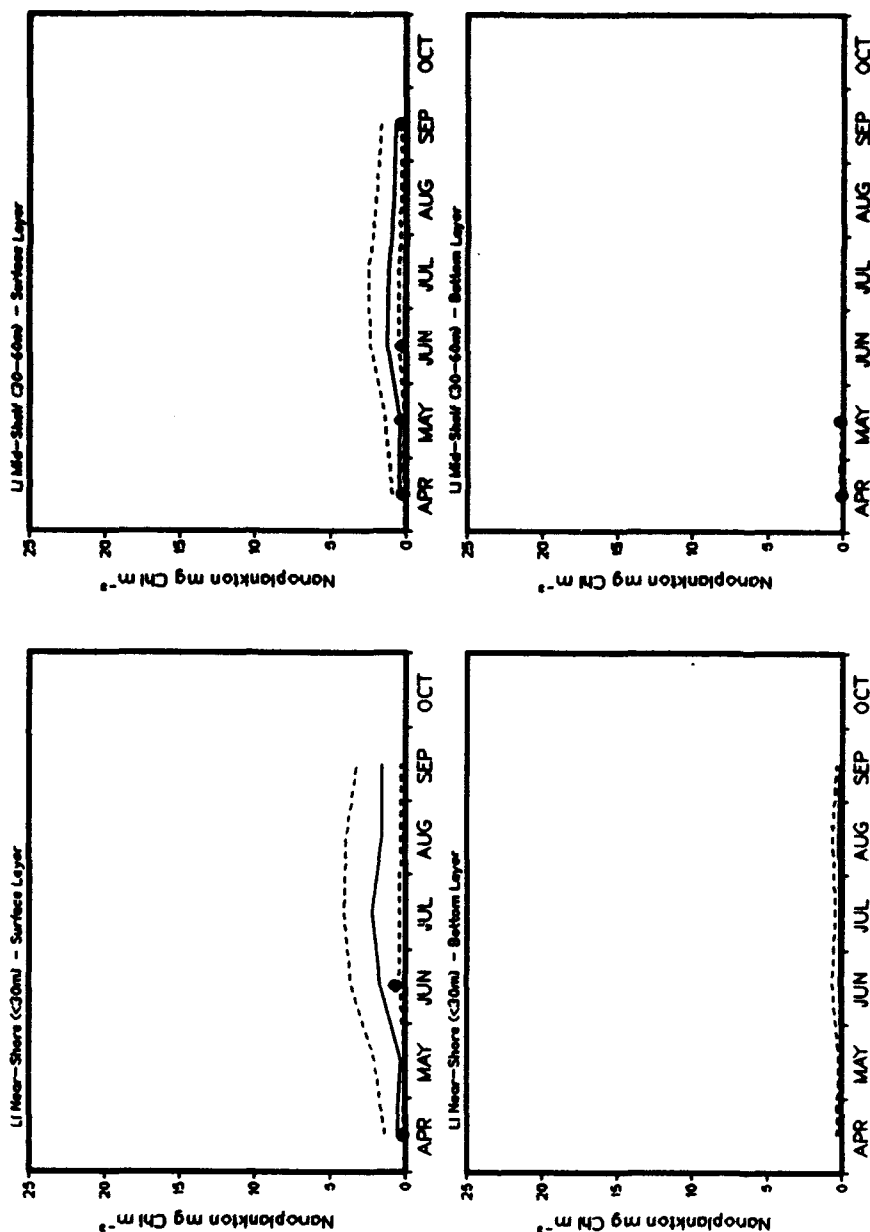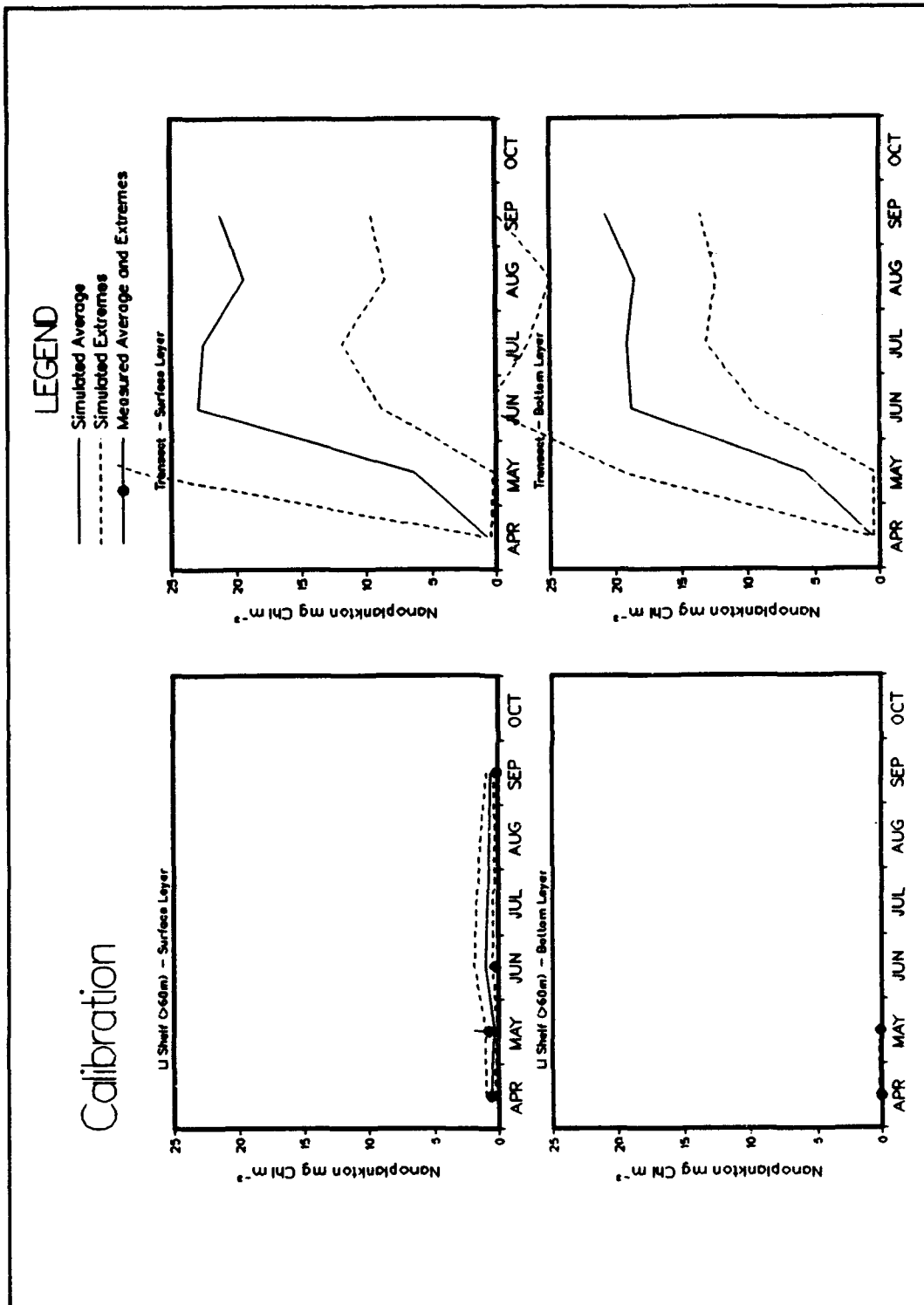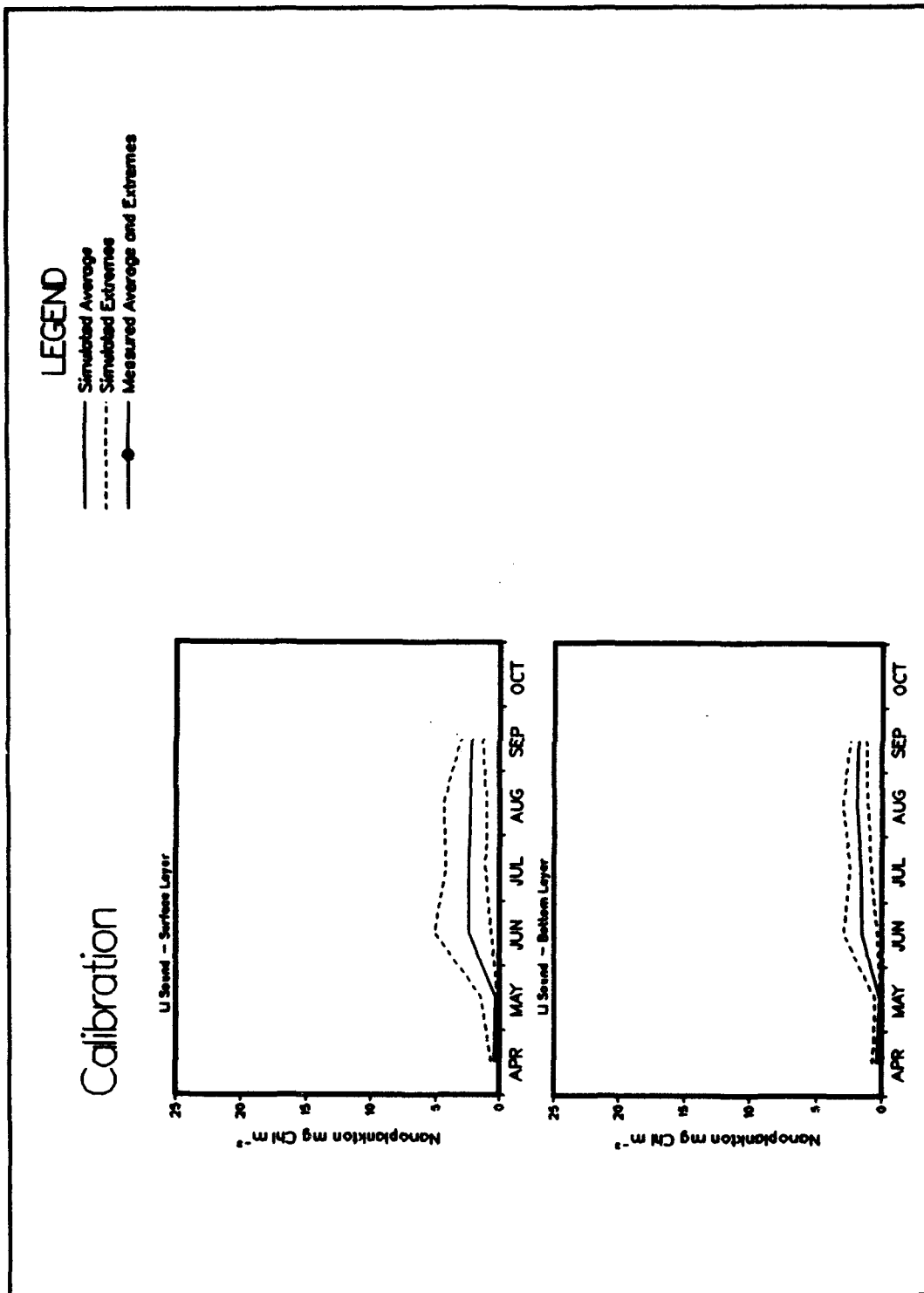
Plate D5. (Sheet 2 of 6)

D24
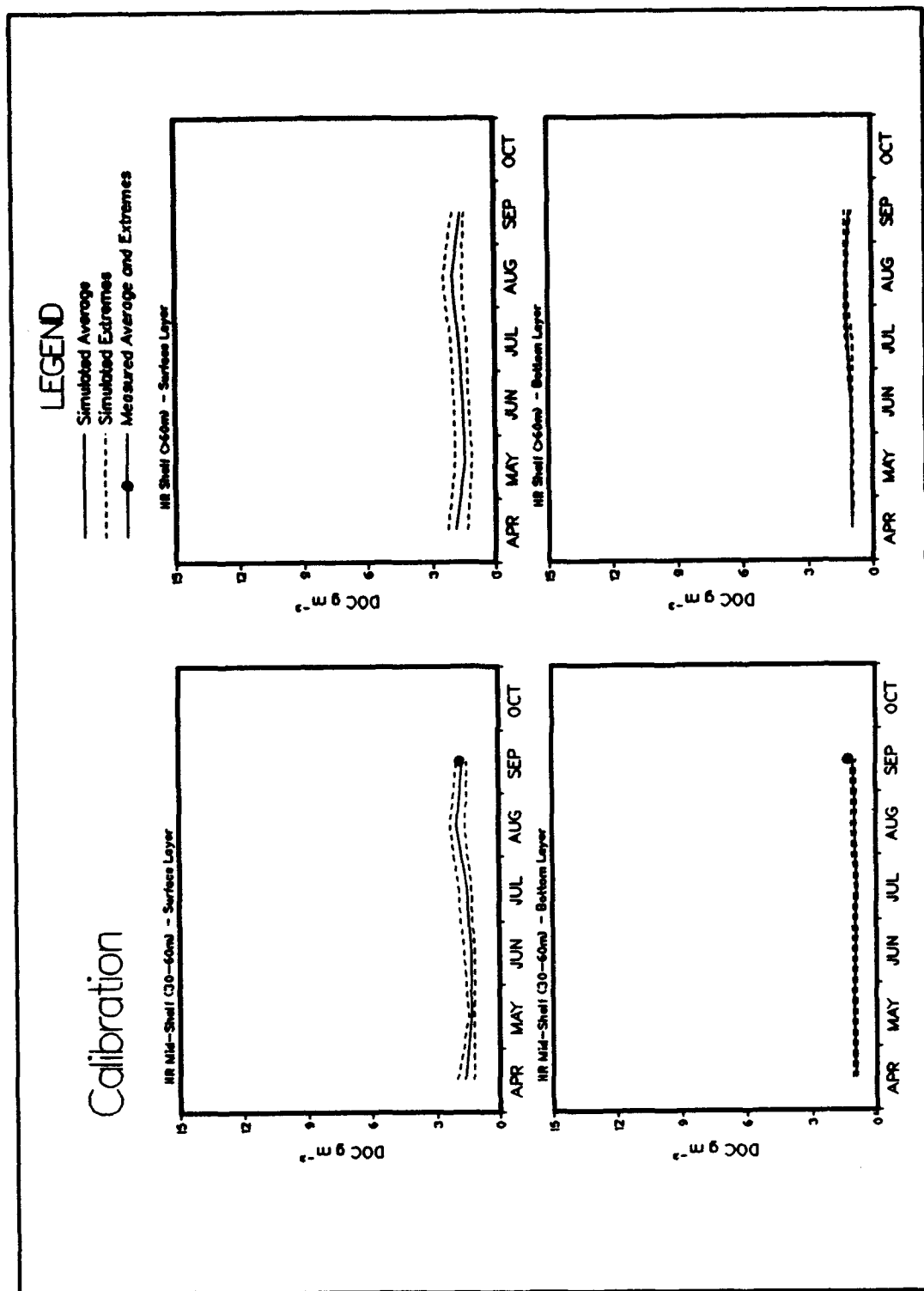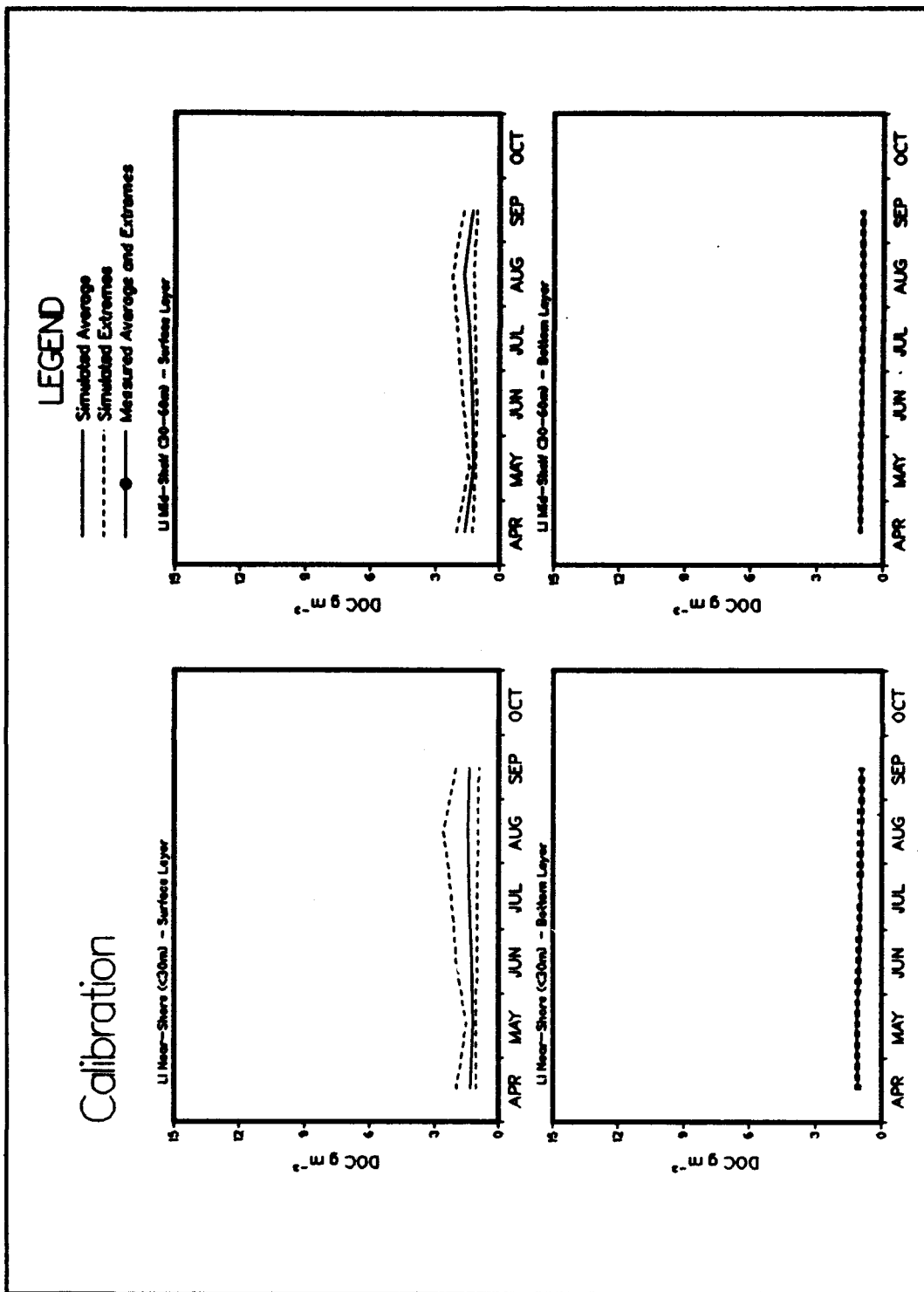
Plate D5. (Sheet 3 of 6)

Plate D5.   (Sheet 4 of 6)

Plate D5.   (Sheet 5 of 6)

Calibration

LEGEND
Simulated Average
Simulated Extremes
Measured Average and Extremes
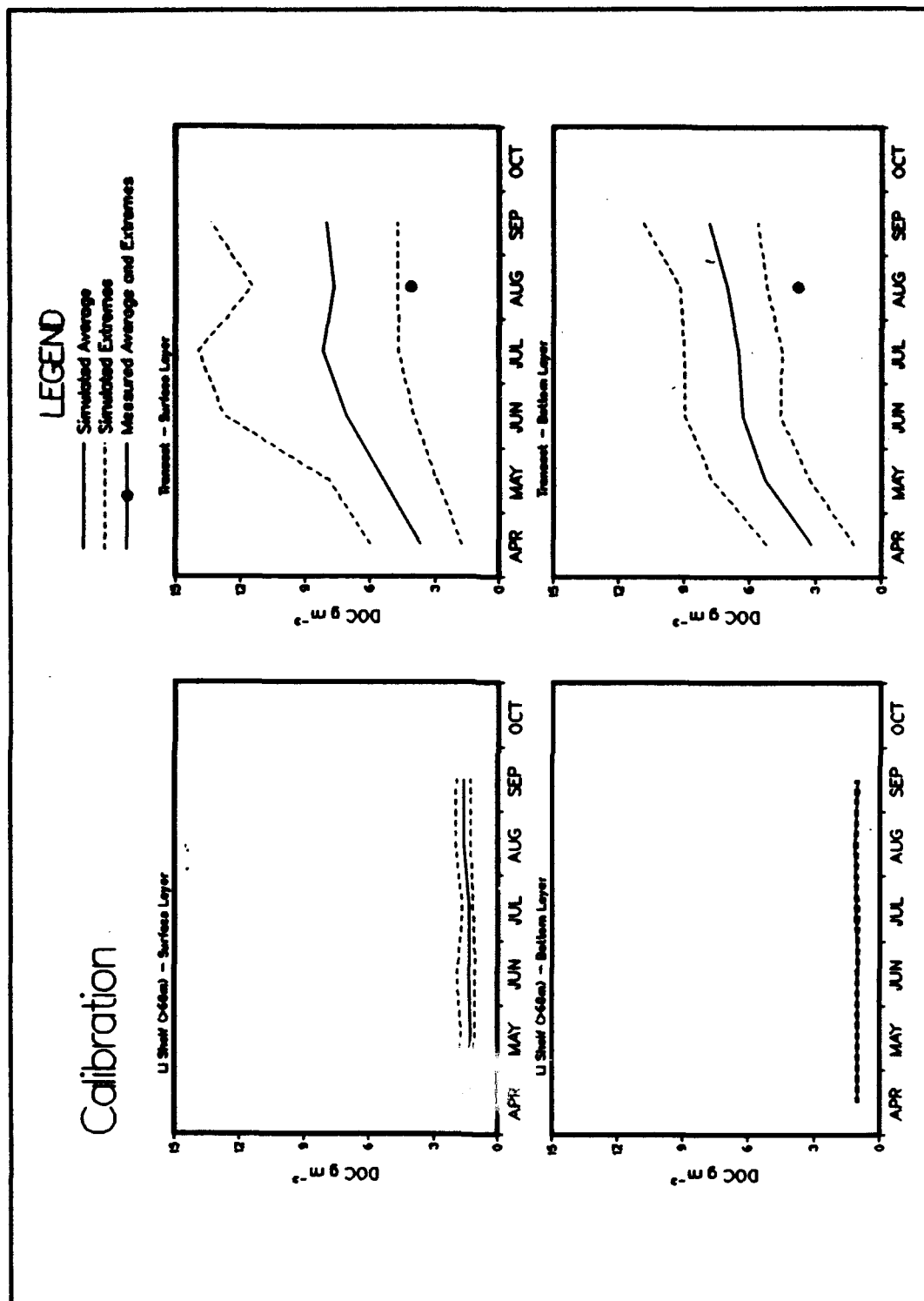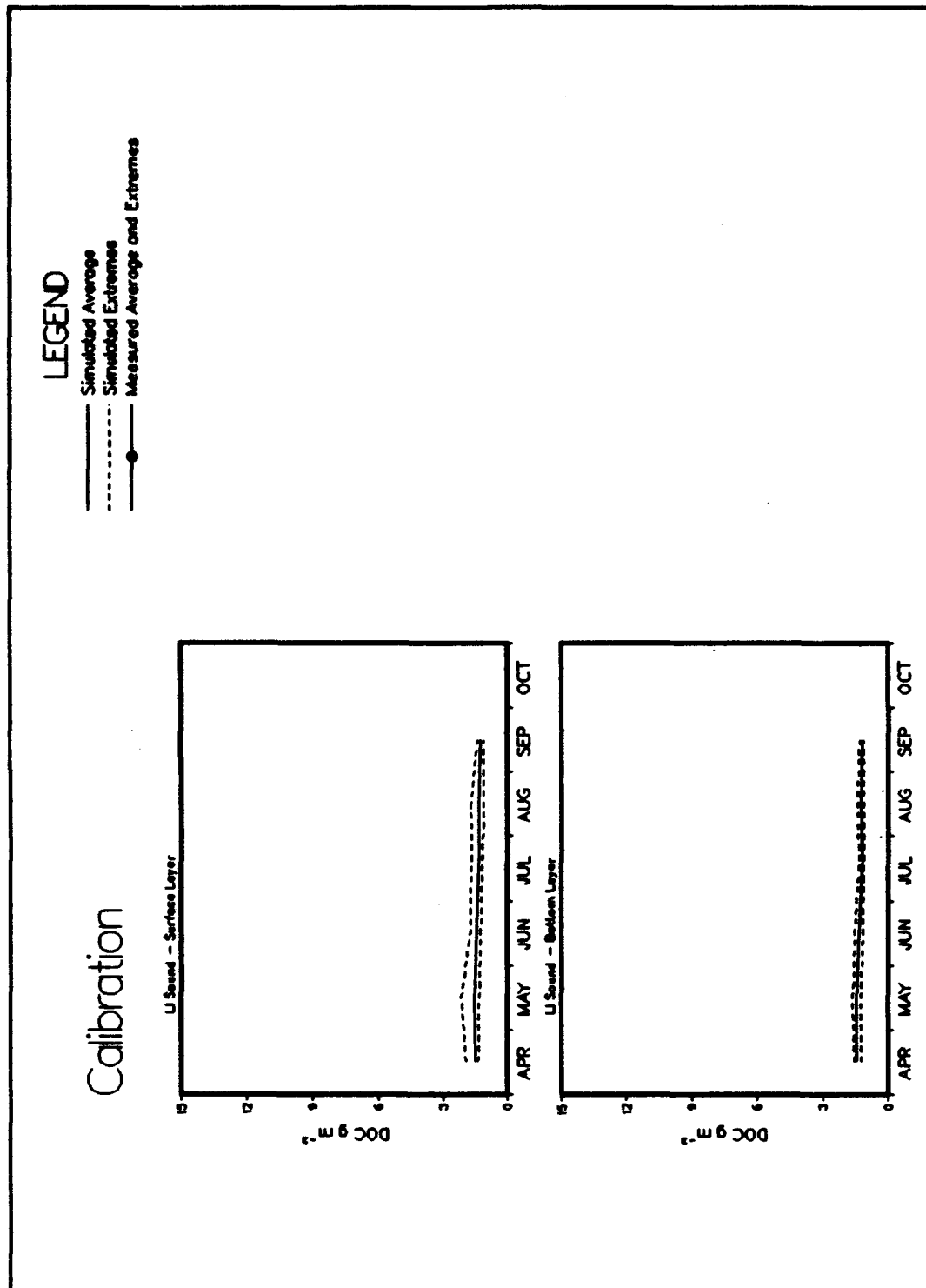
Plate D5. (Sheet 6 of 6)

D28
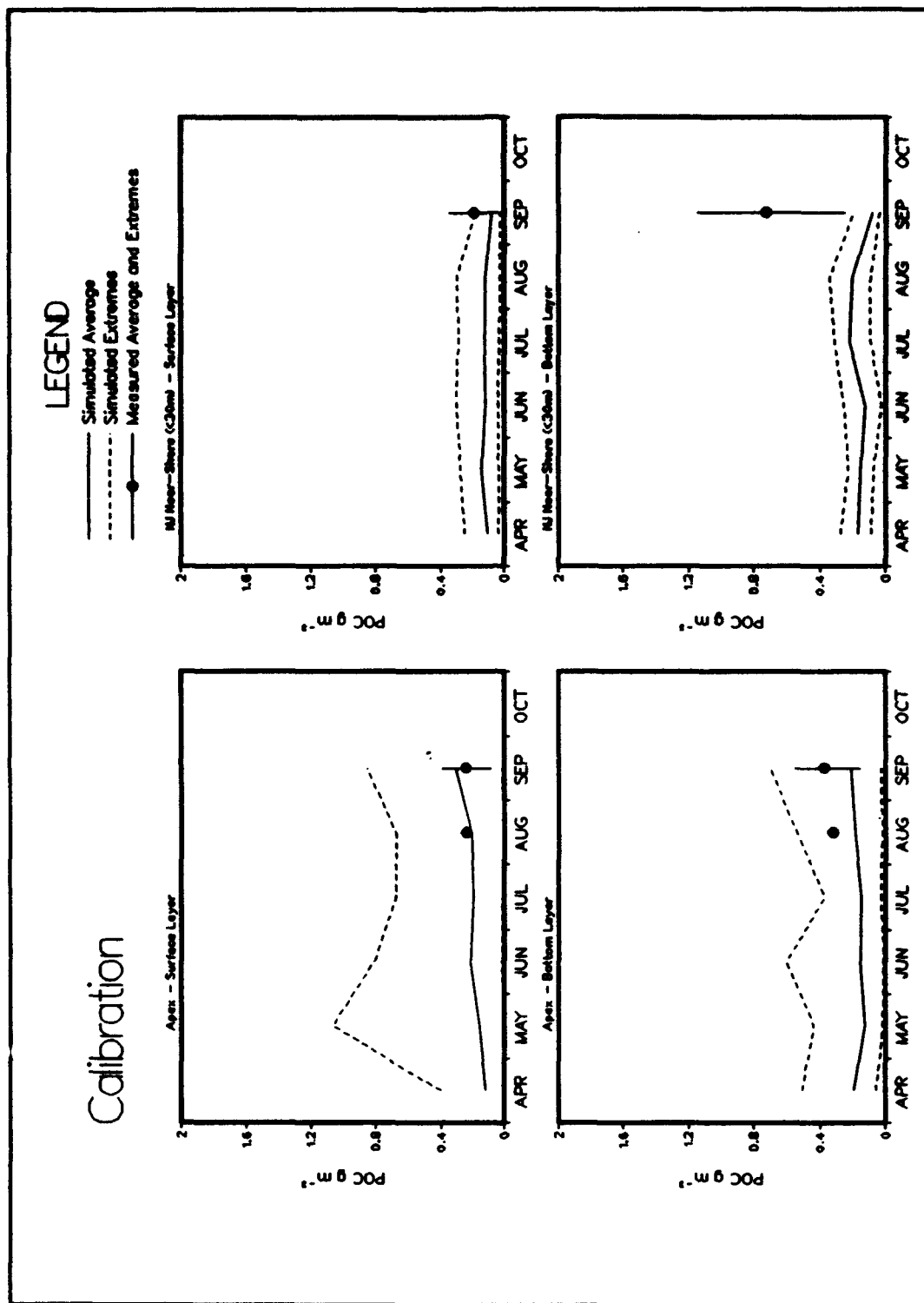
Calibration
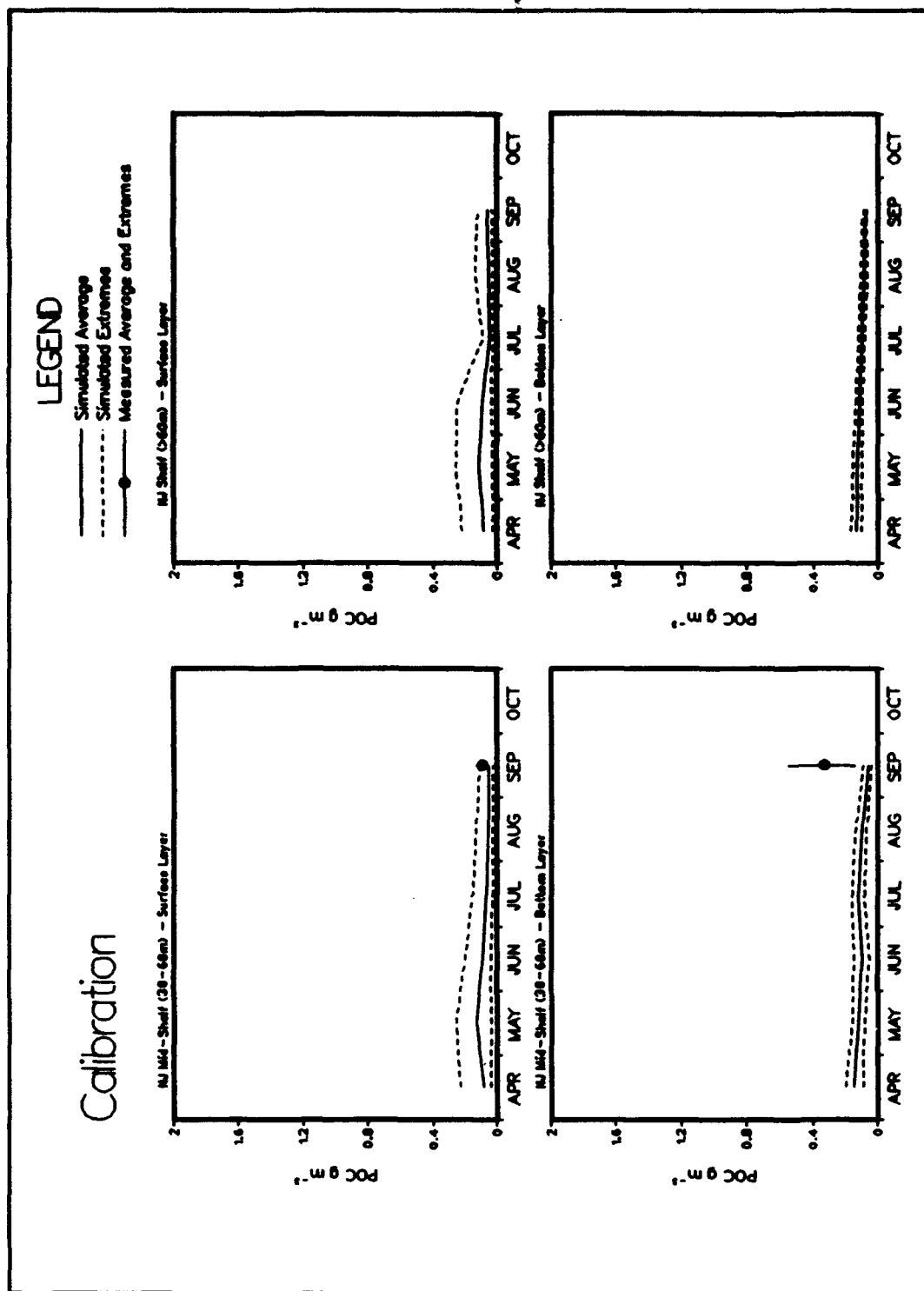
Plate D6. (Sheet 1 of 6)

Plate D6. (Sheet 2 of 6)
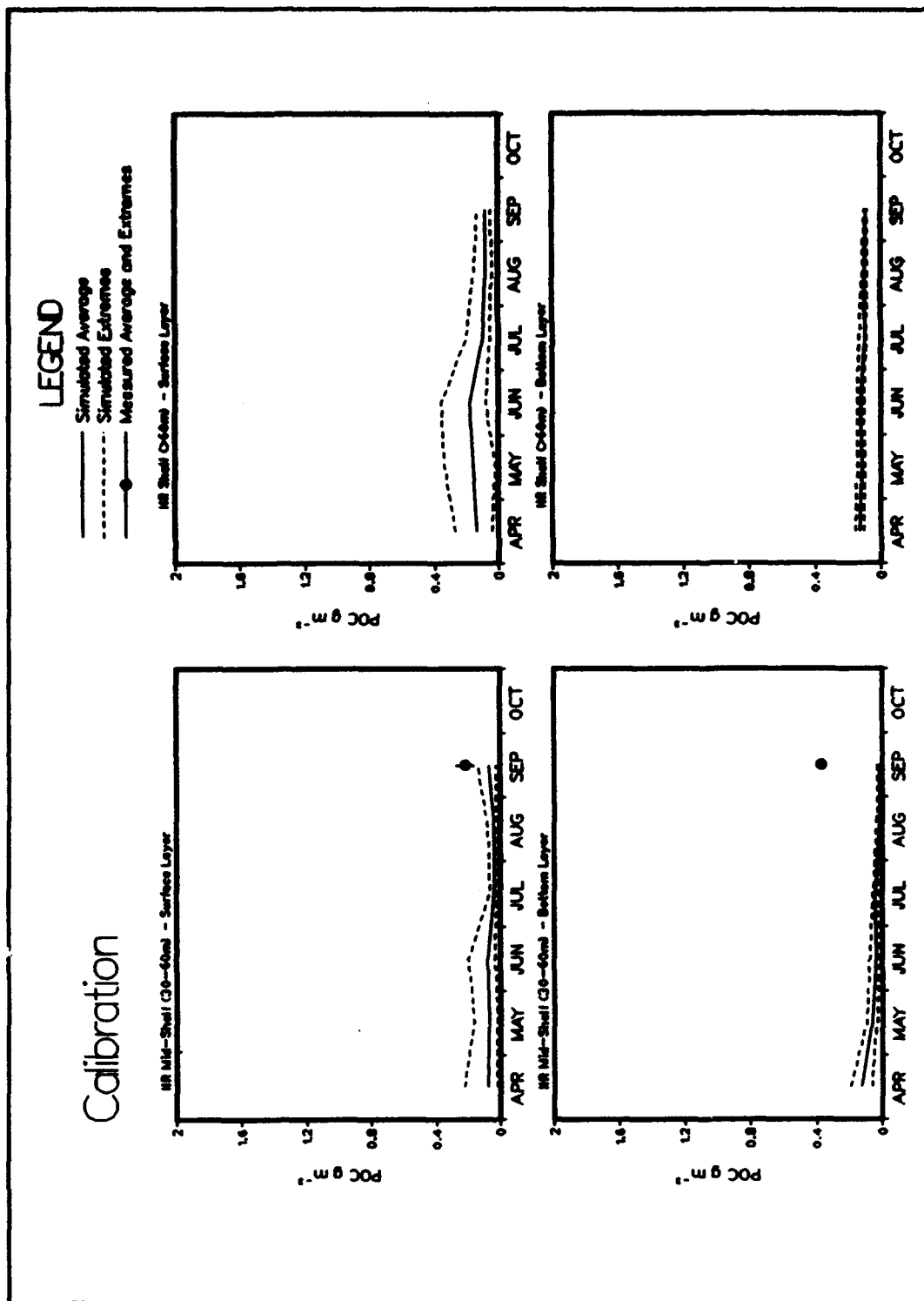
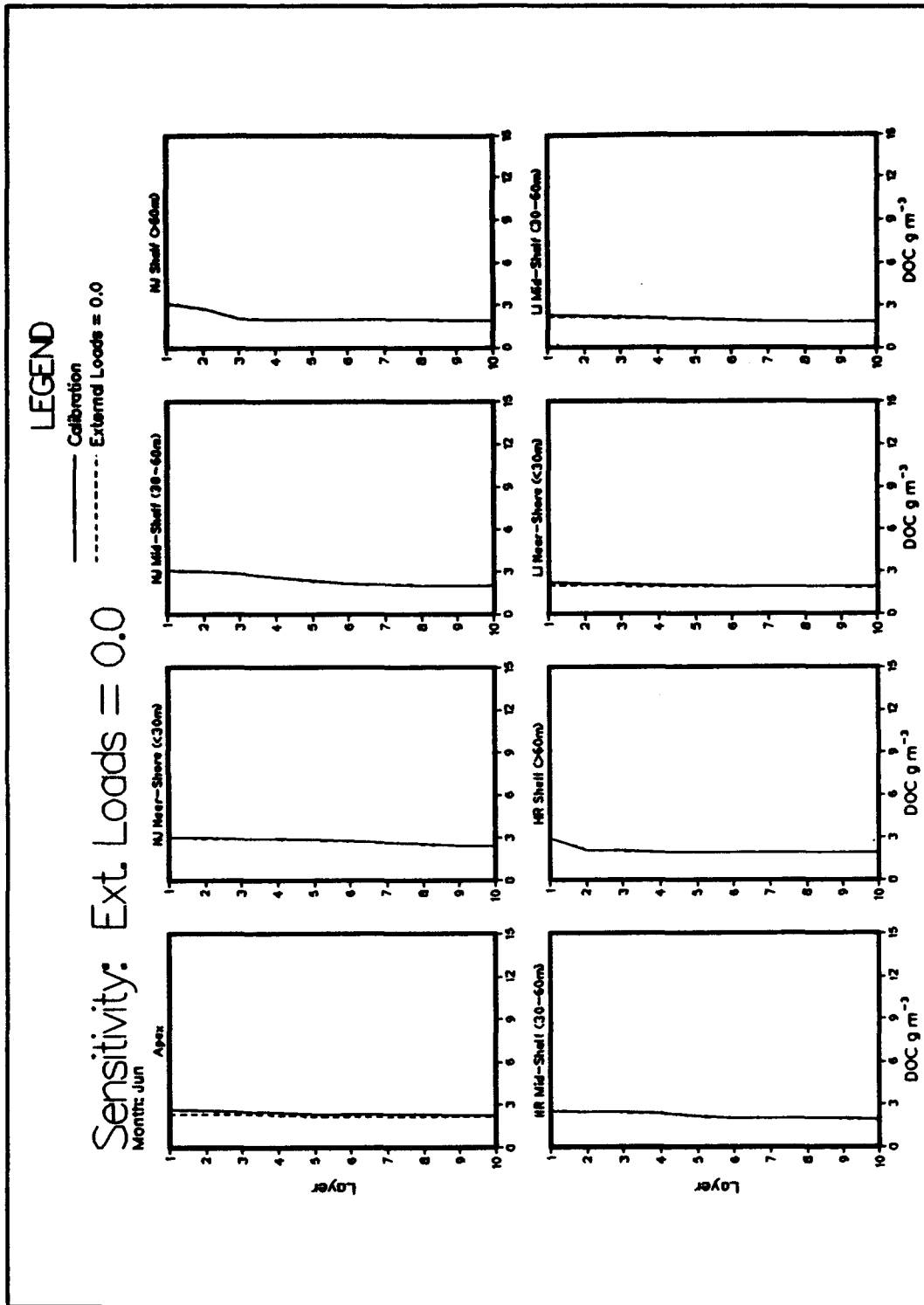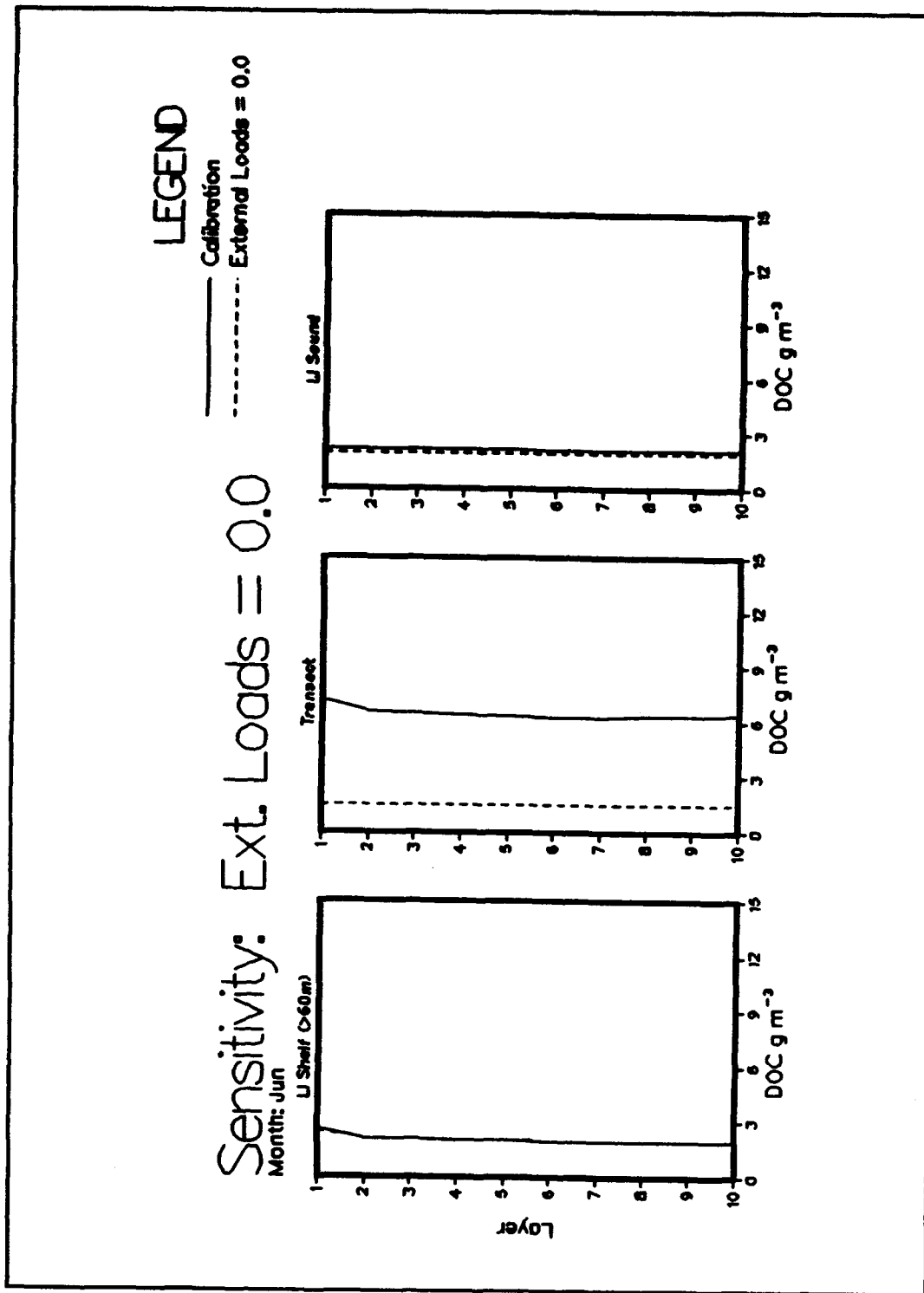Plate D6. (Sheet 3 of 6)
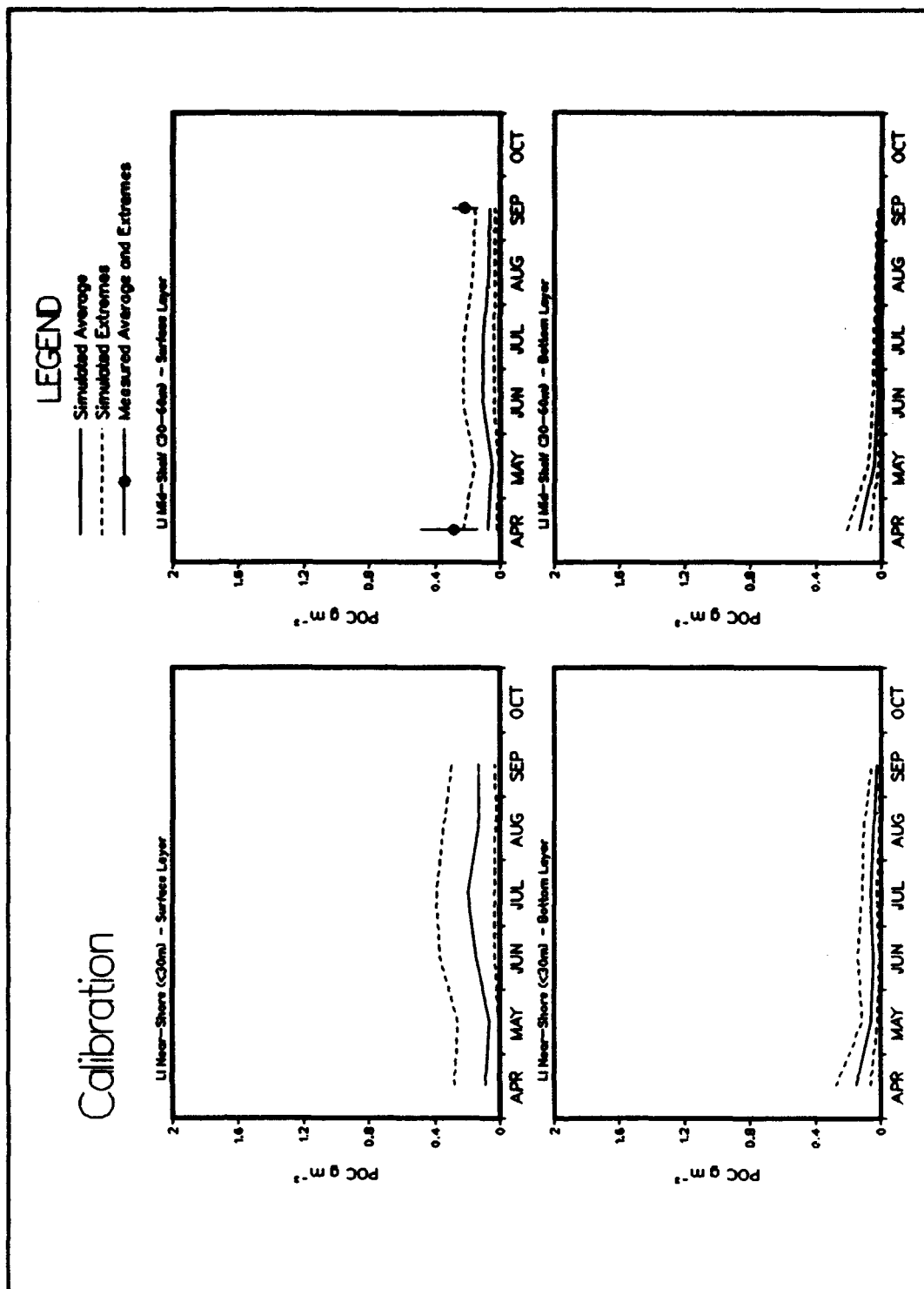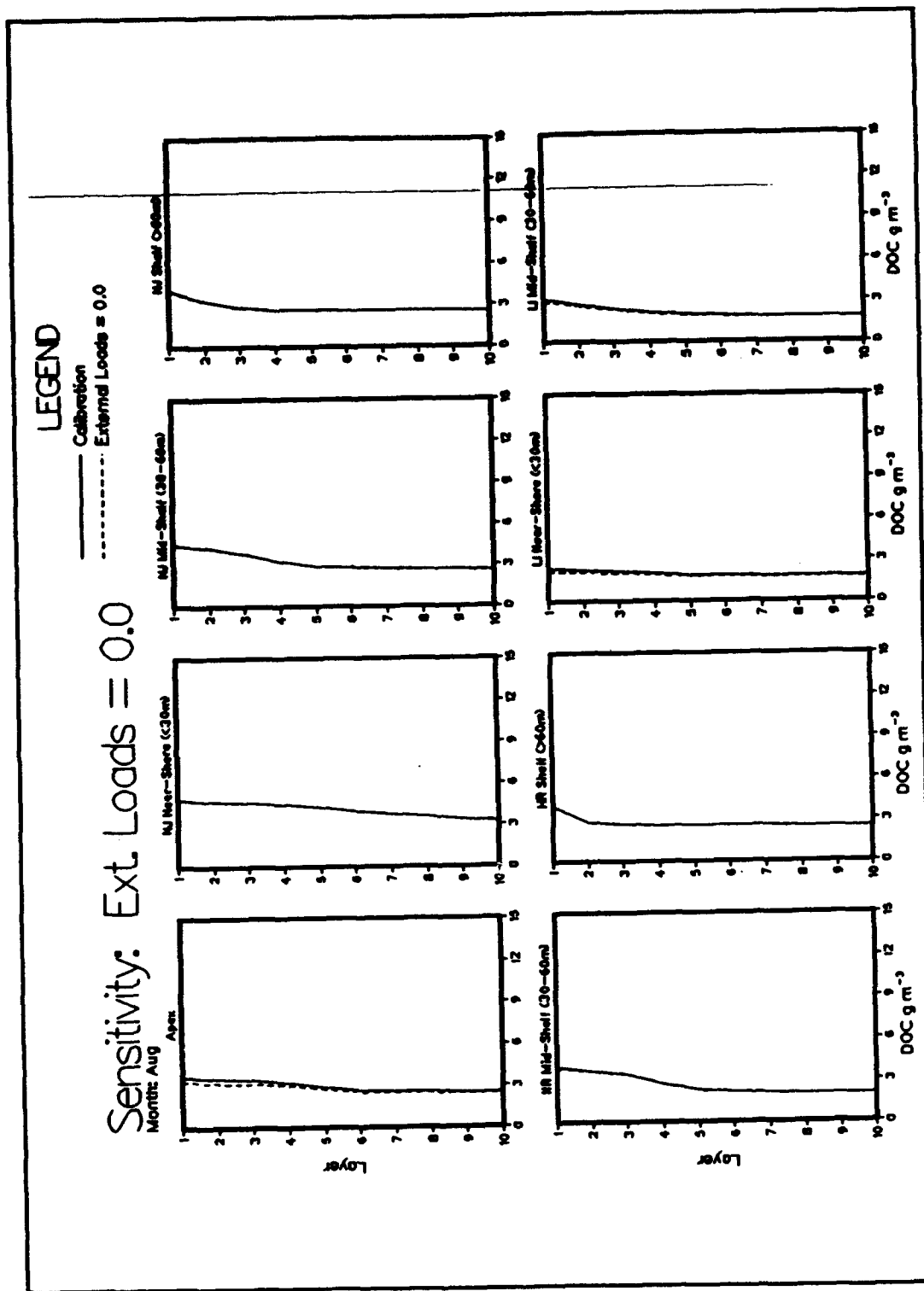
Plate D6.   (Sheet 4 of 6)
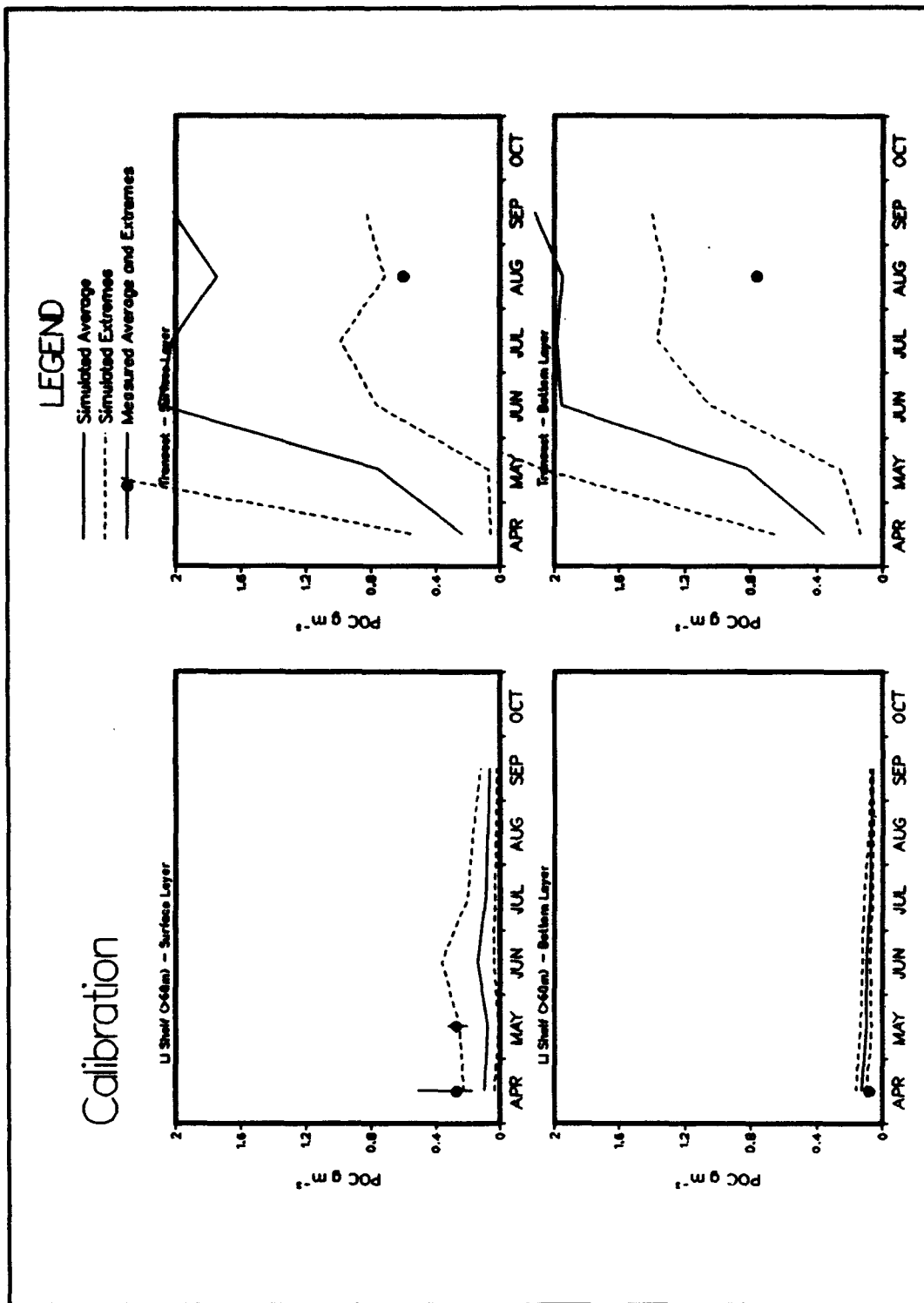
Plate D6. (Sheet 5 of 6)

Calibration

LEGEND
Simulated Average
Simulated Extremes
Measured Average and Extremes
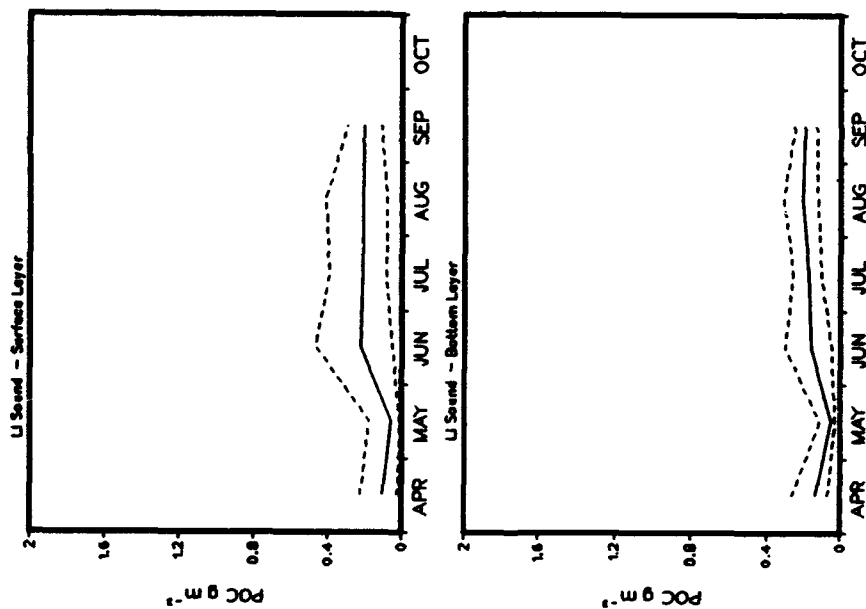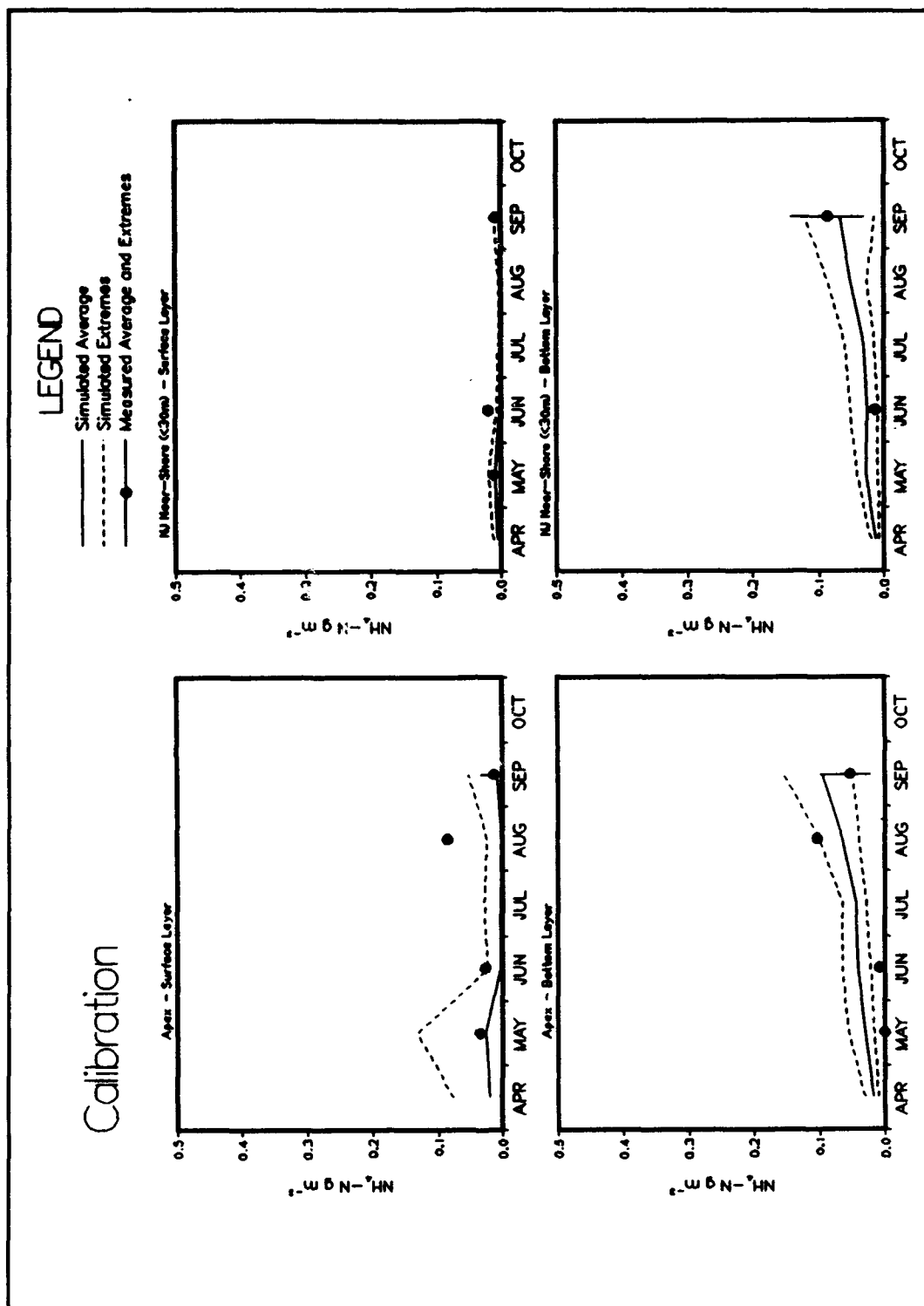
Plate D6. (Sheet 6 of 6)

Plate D7.   (Sheet 1 of 6)

Plate D7.   (Sheet 2 of 6)

Calibration

LEGEND
— Simulated Average
--- Simulated Extremes
•— Measured Average and Extremes
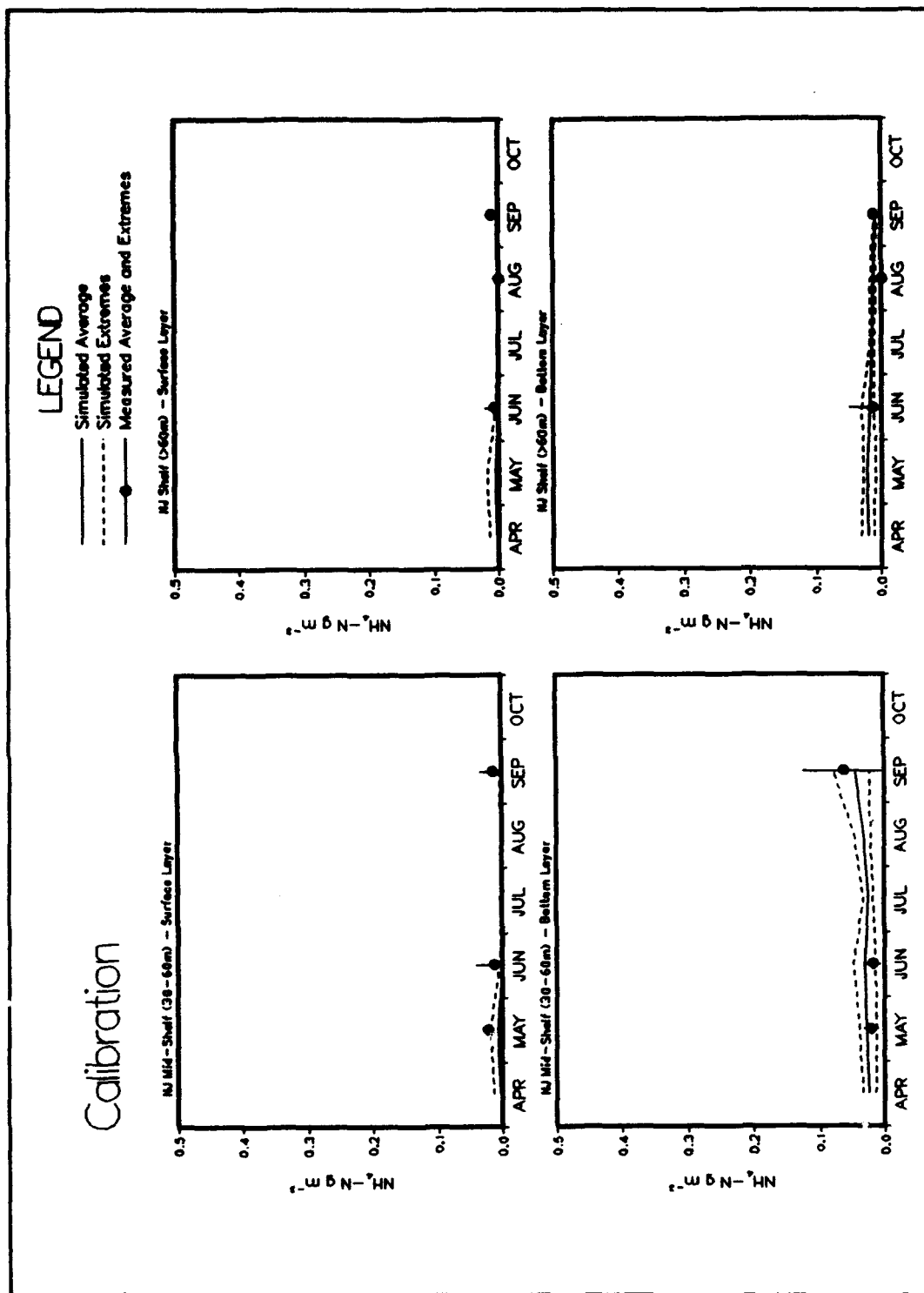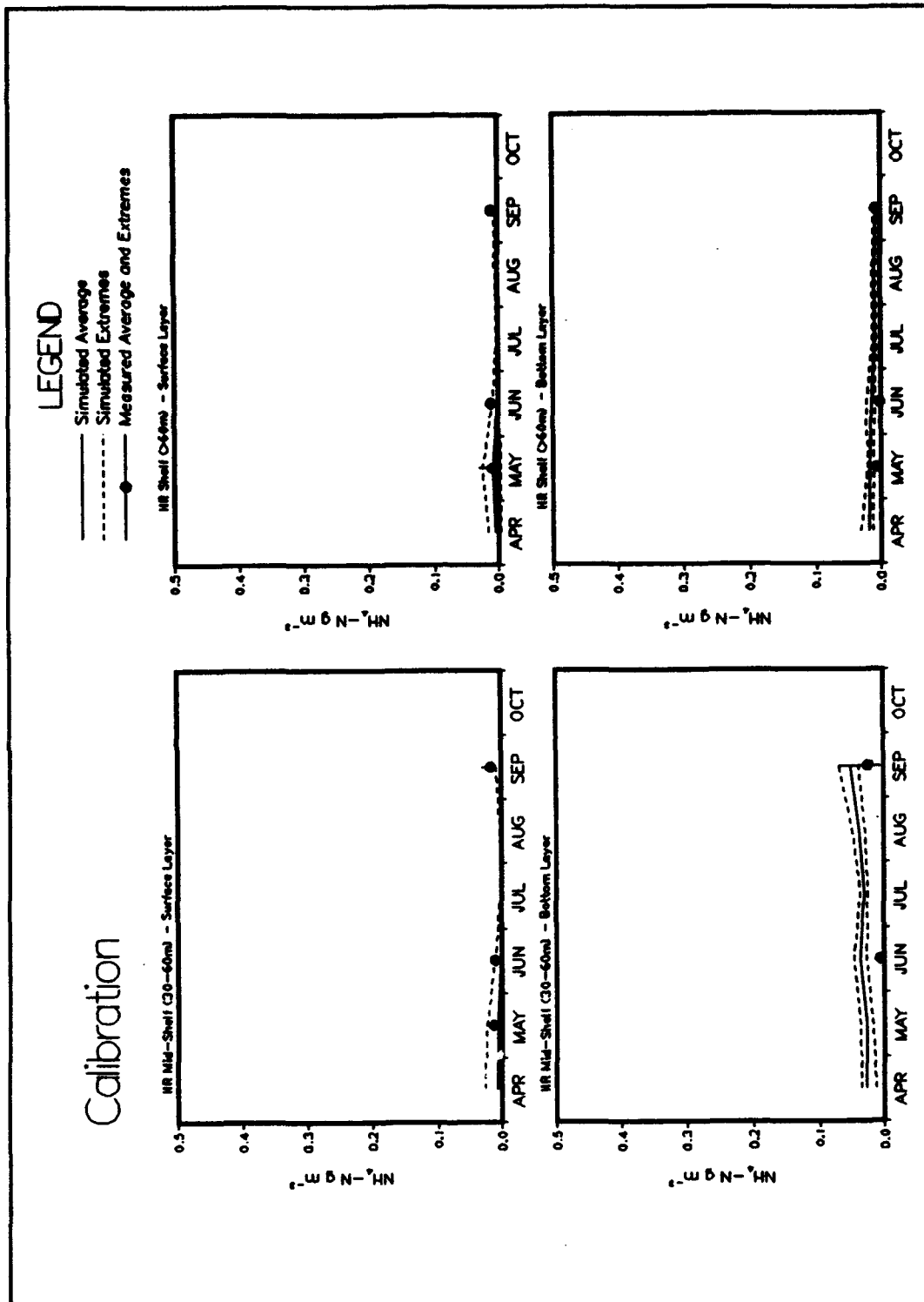
Plate D7. (Sheet 3 of 6)

Plate D7.   (Sheet 4 of 6)

Calibration

Plate D7. (Sheet 5 of 6)

Calibration

LEGEND
Simulated Average
Simulated Extremes
Measured Average and Extremes

LI Seed – Surface Layer

LI Seed – Bottom Layer
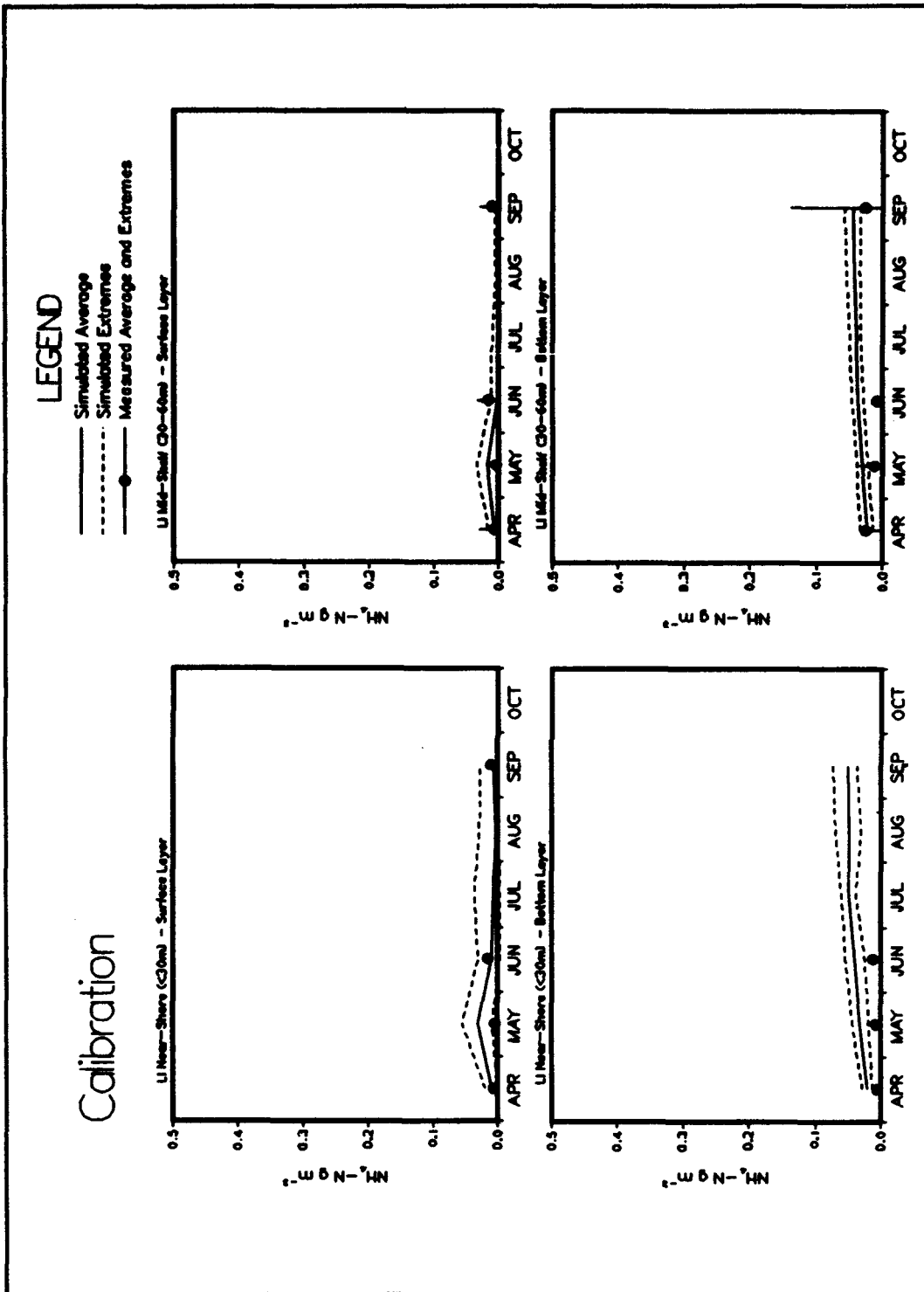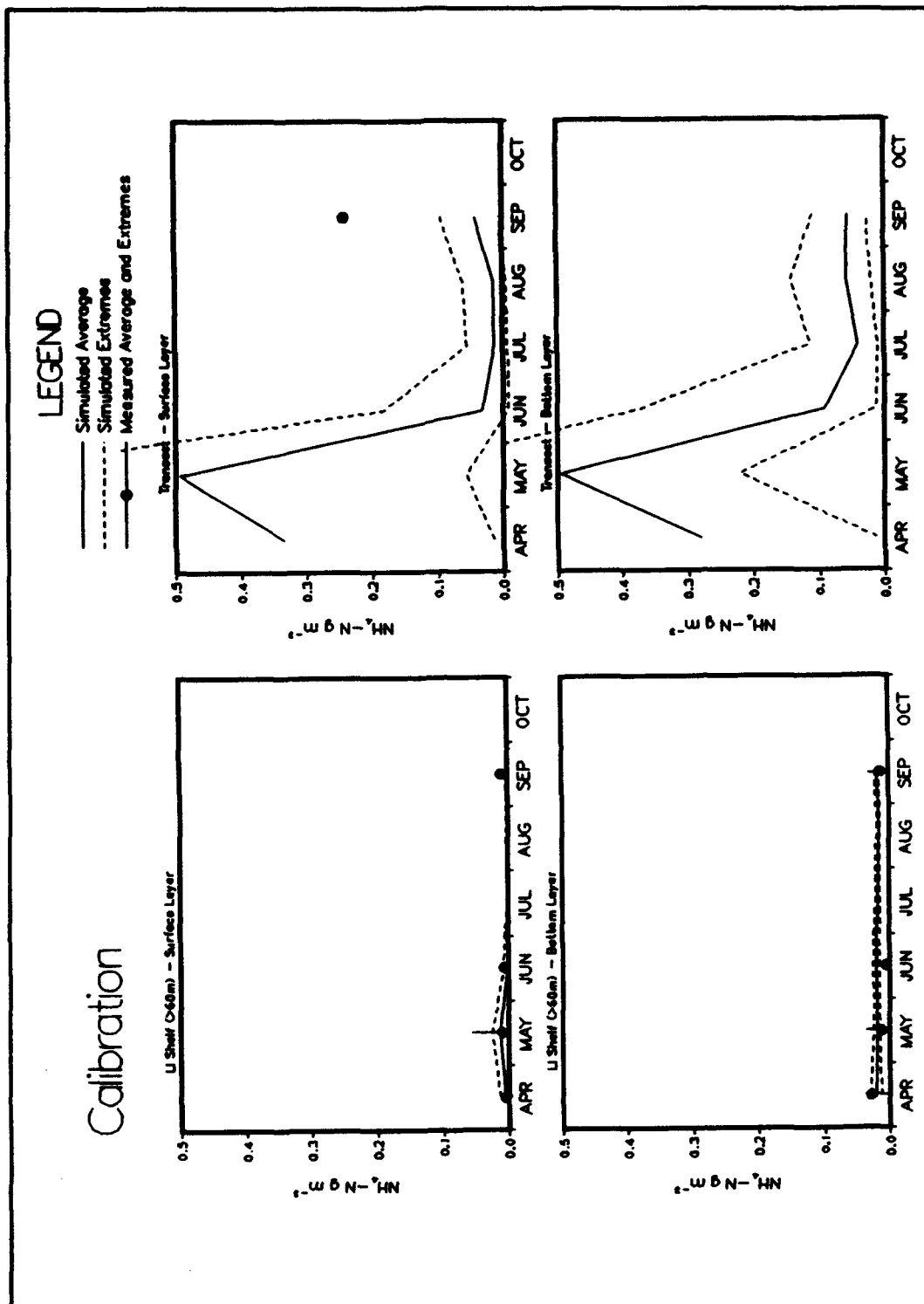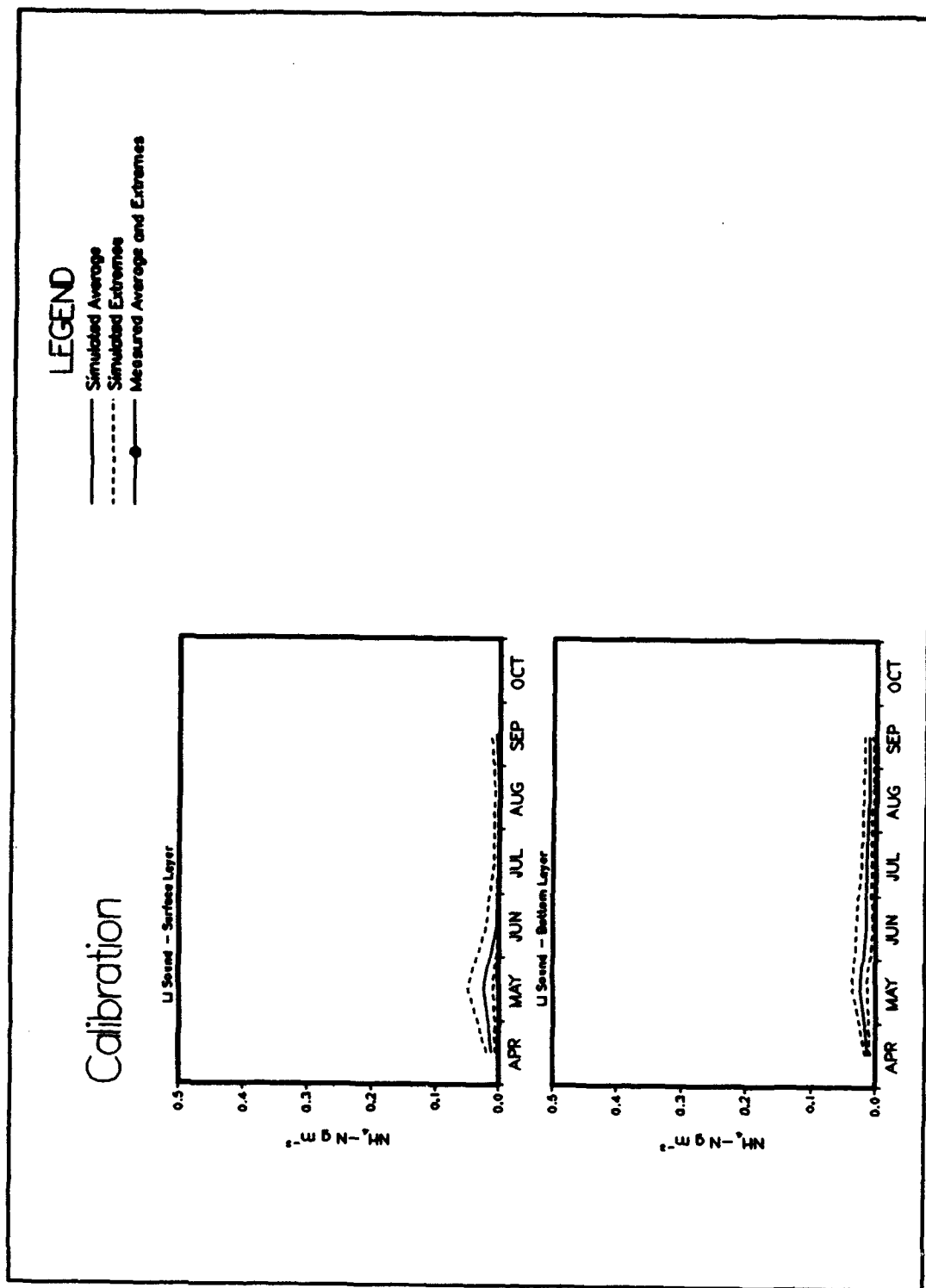
Plate D7.   (Sheet 6 of 6)

D40
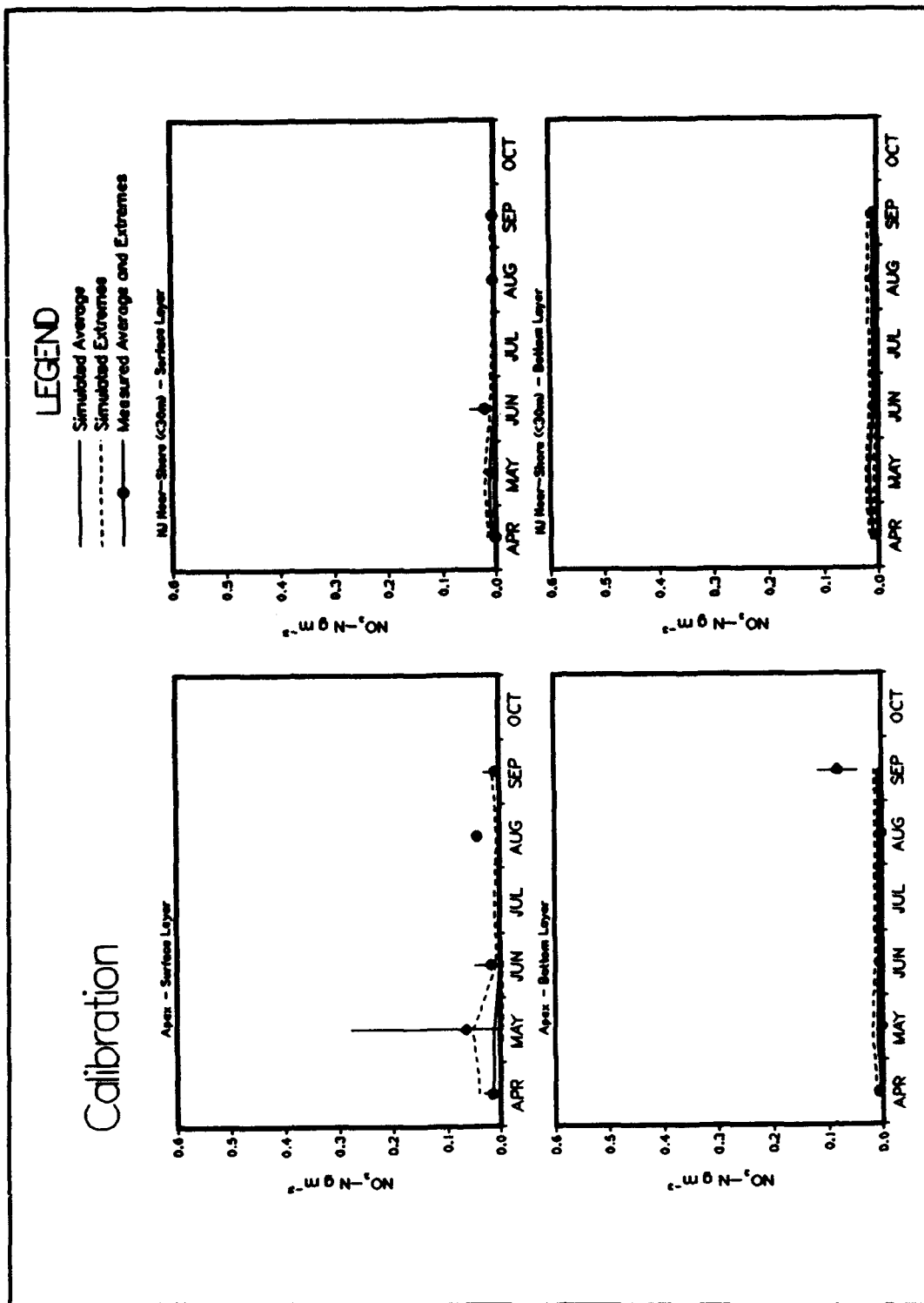
Plate D8. (Sheet 1 of 6)
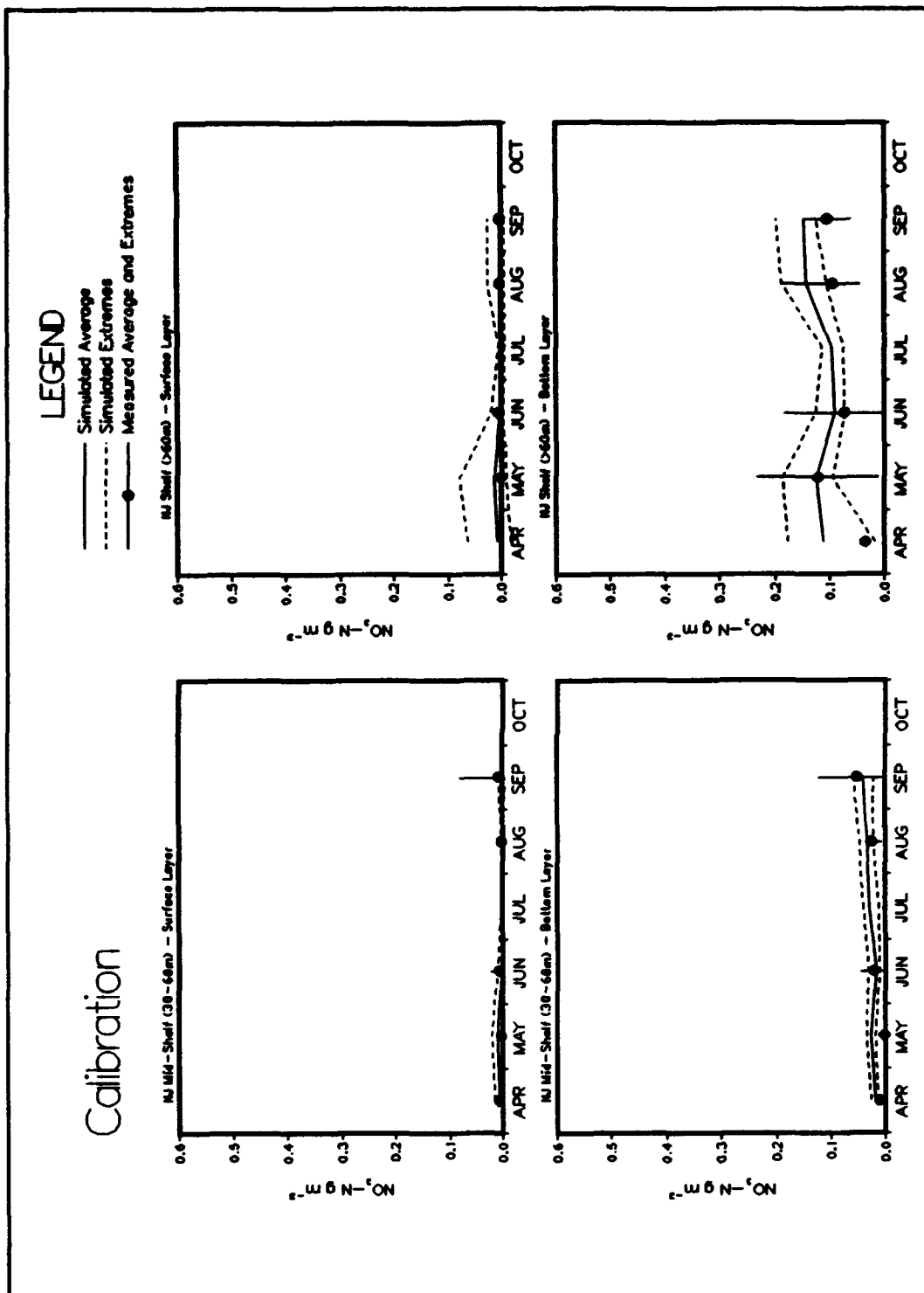
Plate D8. (Sheet 2 of 6)
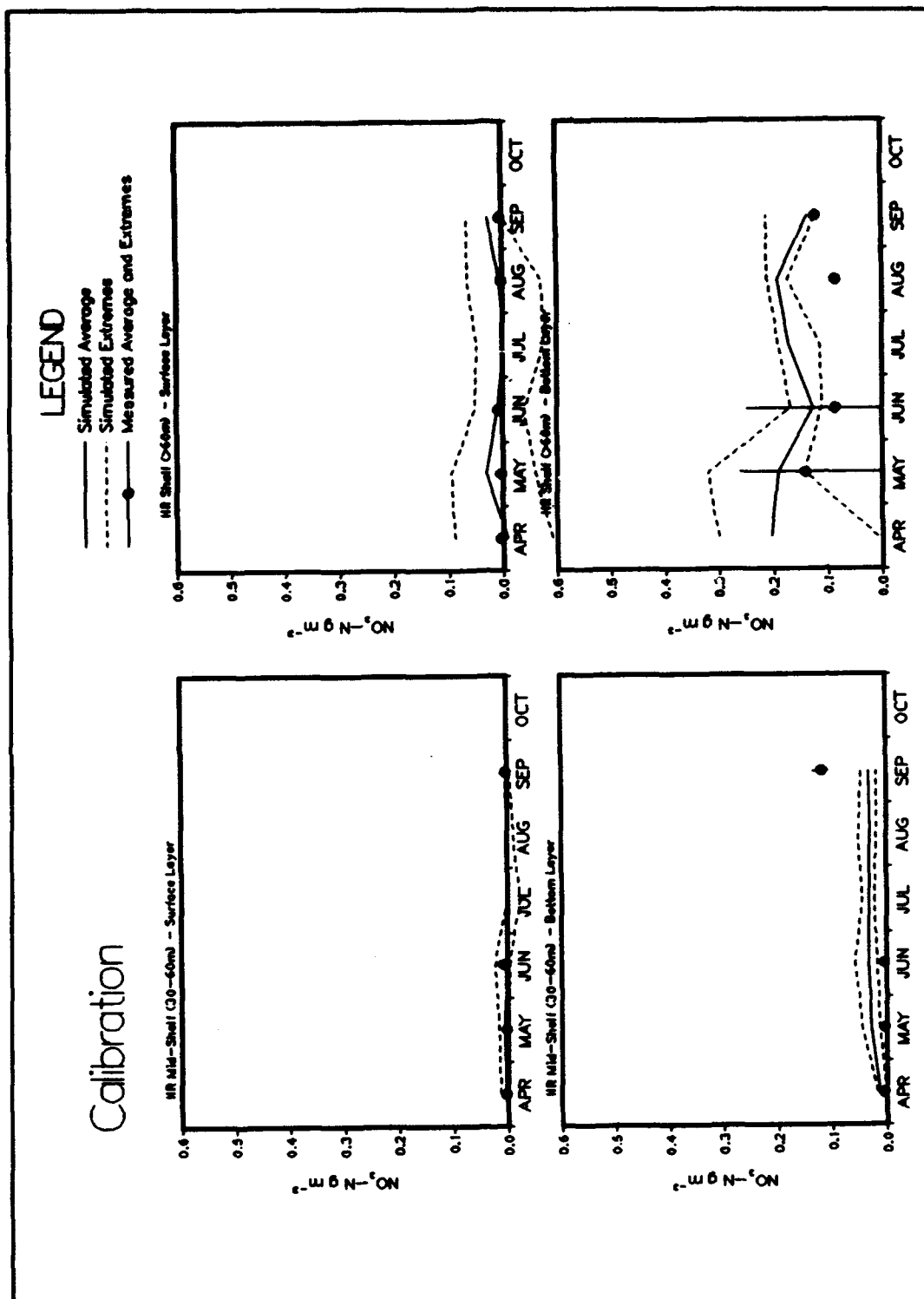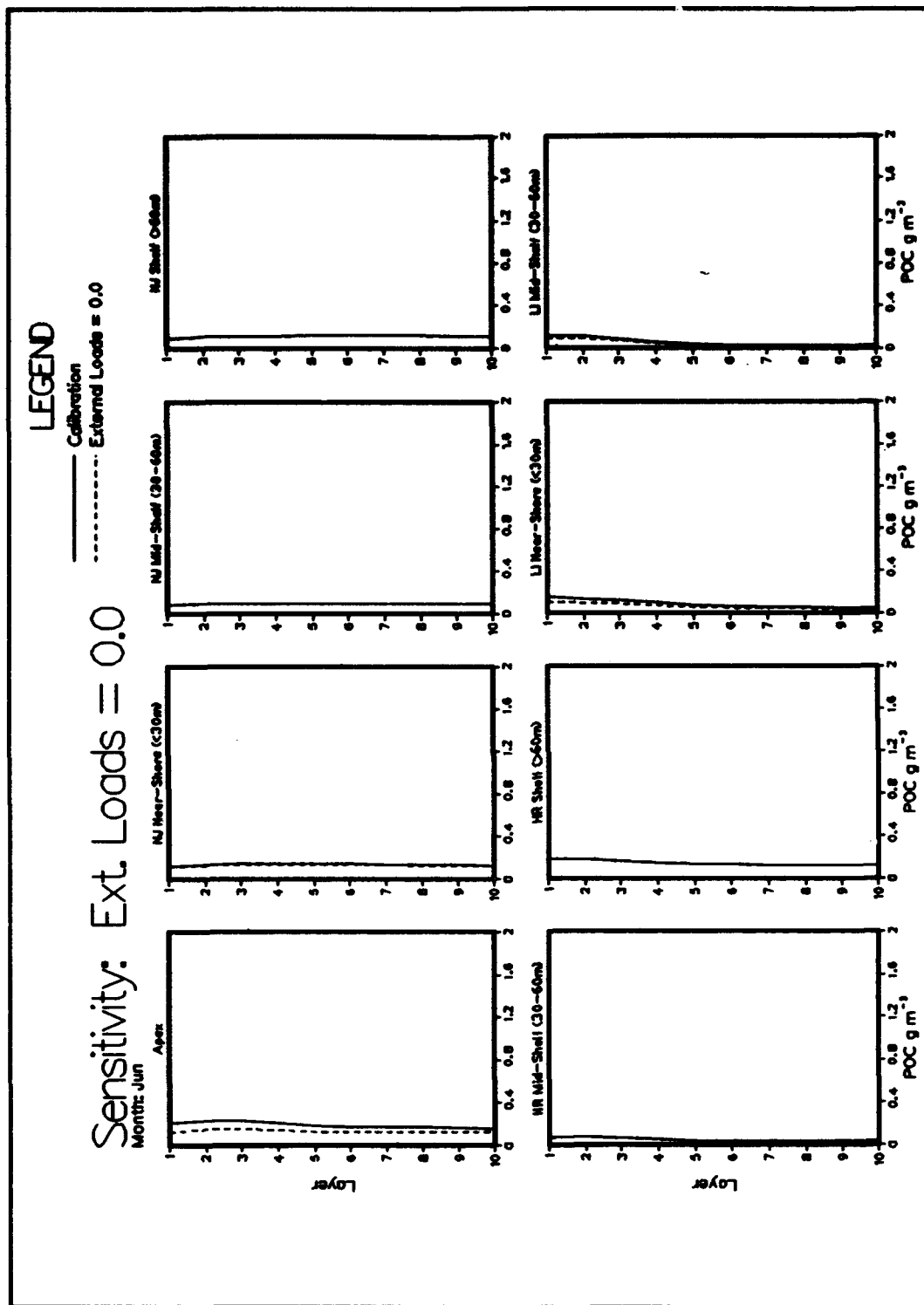
Plate D8. (Sheet 3 of 6)

Plate D8. (Sheet 4 of 6)

D44

Calibration

Plate D8. (Sheet 5 of 6)

Calibration

LEGEND

—————— Simulated Average
------------ Simulated Extreme
———•——— Measured Average and Extremes

U Seed – Surface Layer

U Seed – Bottom Layer

NO_3–N g m^{-3}

NO_3–N g m^{-3}

Plate D8. (Sheet 6 of 6)

Appendix D   Calibration Plots
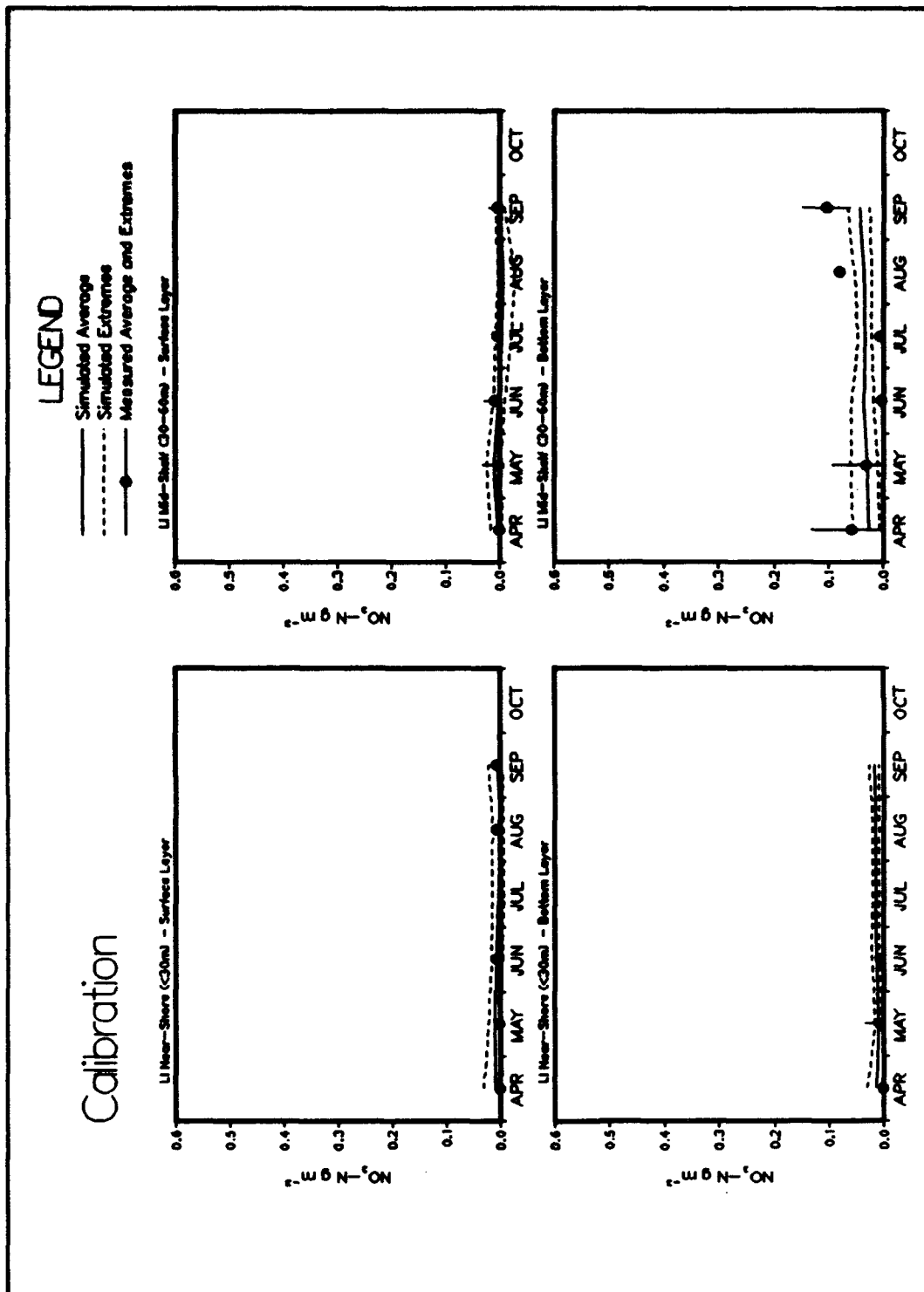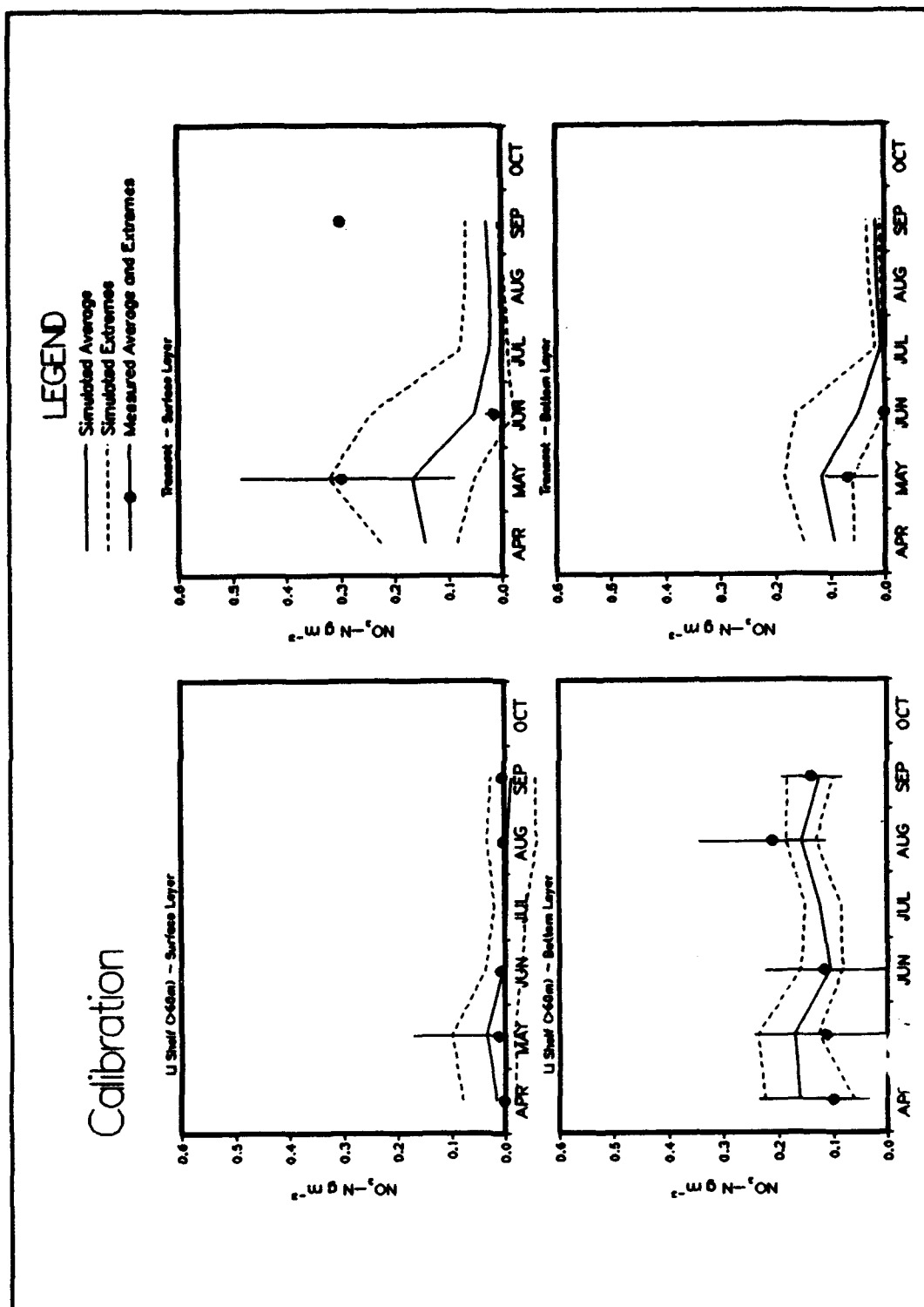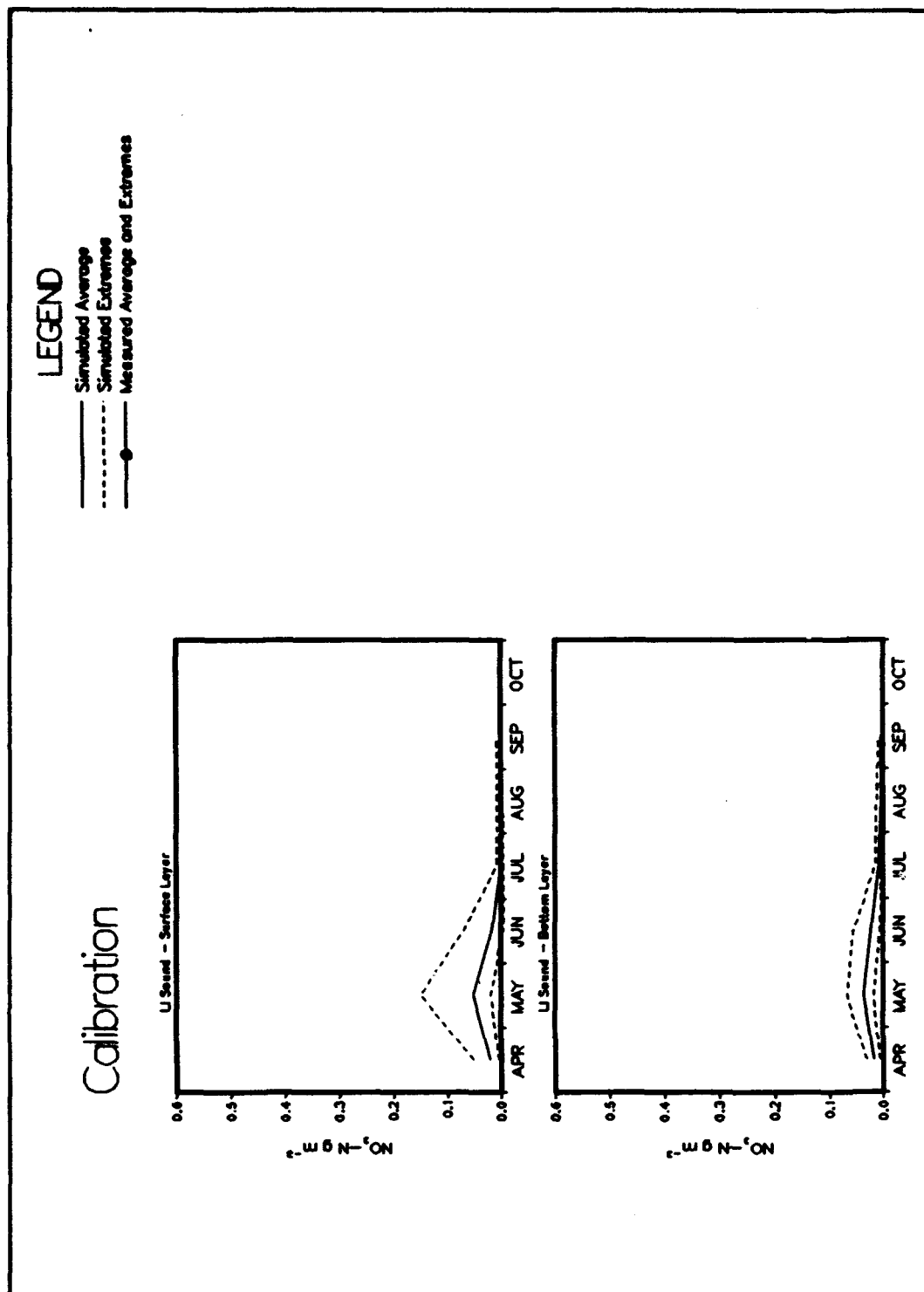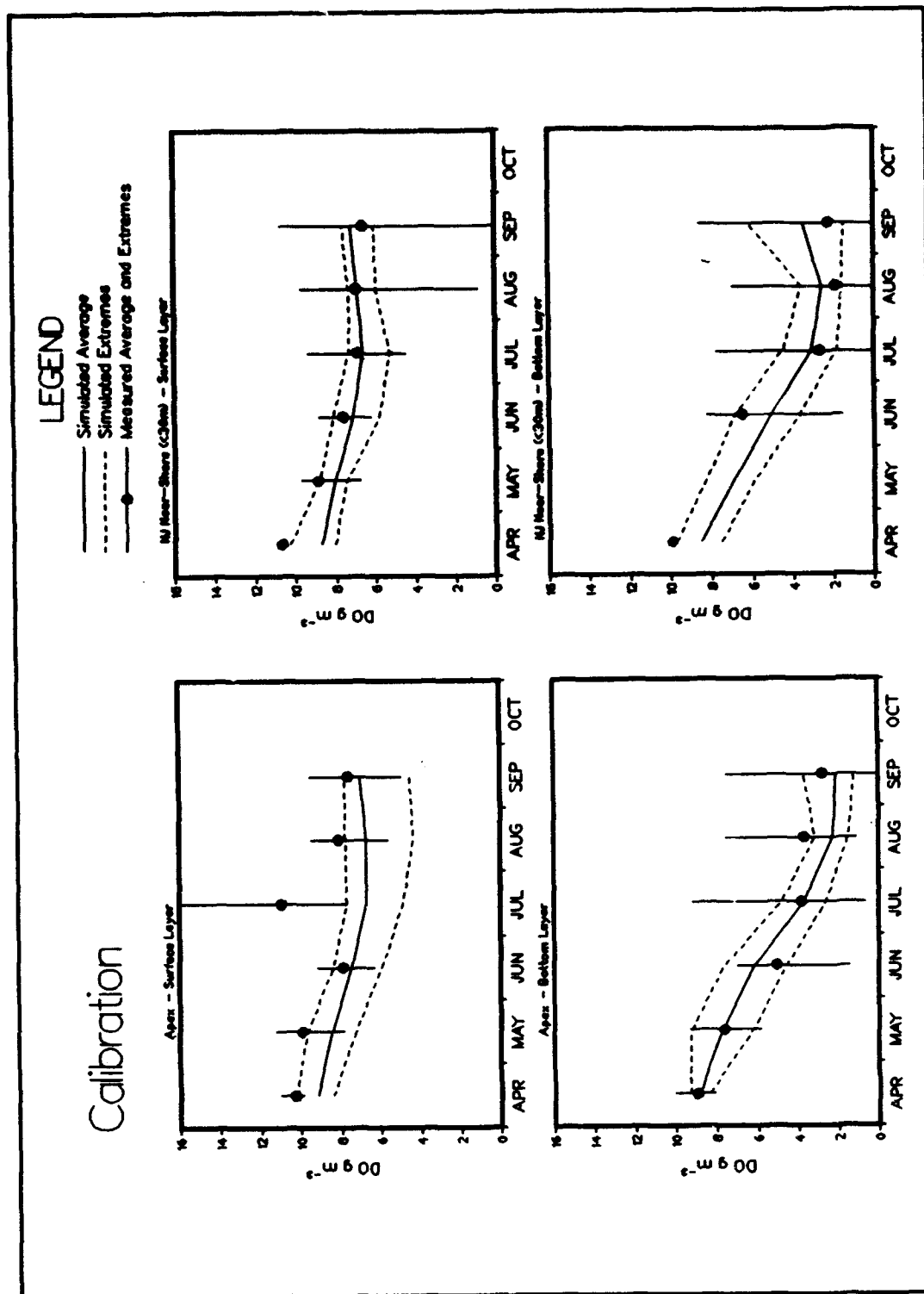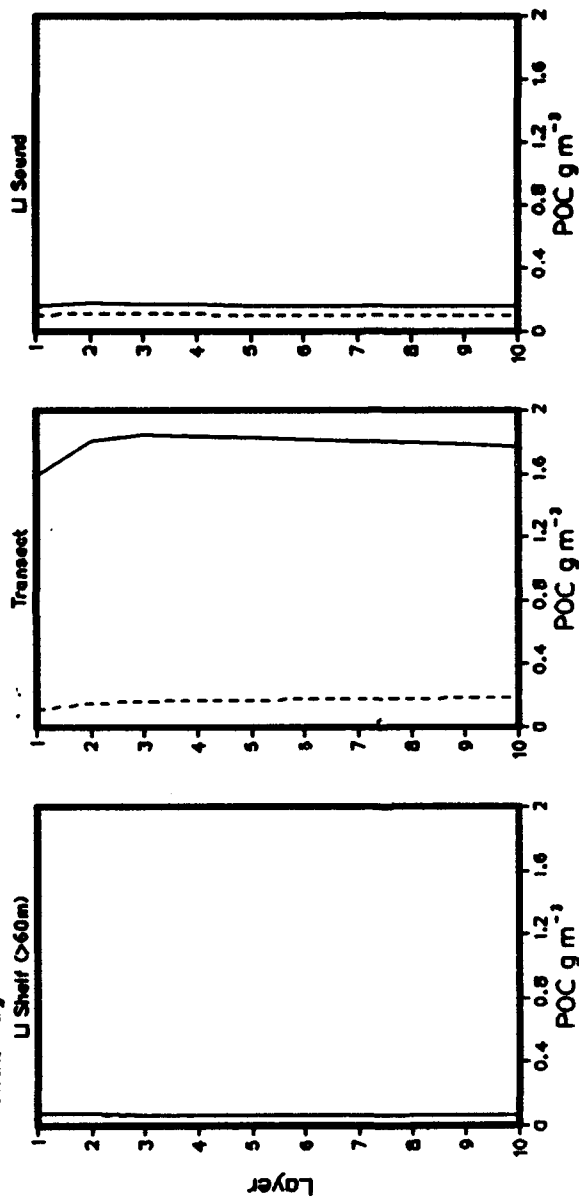
Plate D9.   (Sheet 1 of 6)
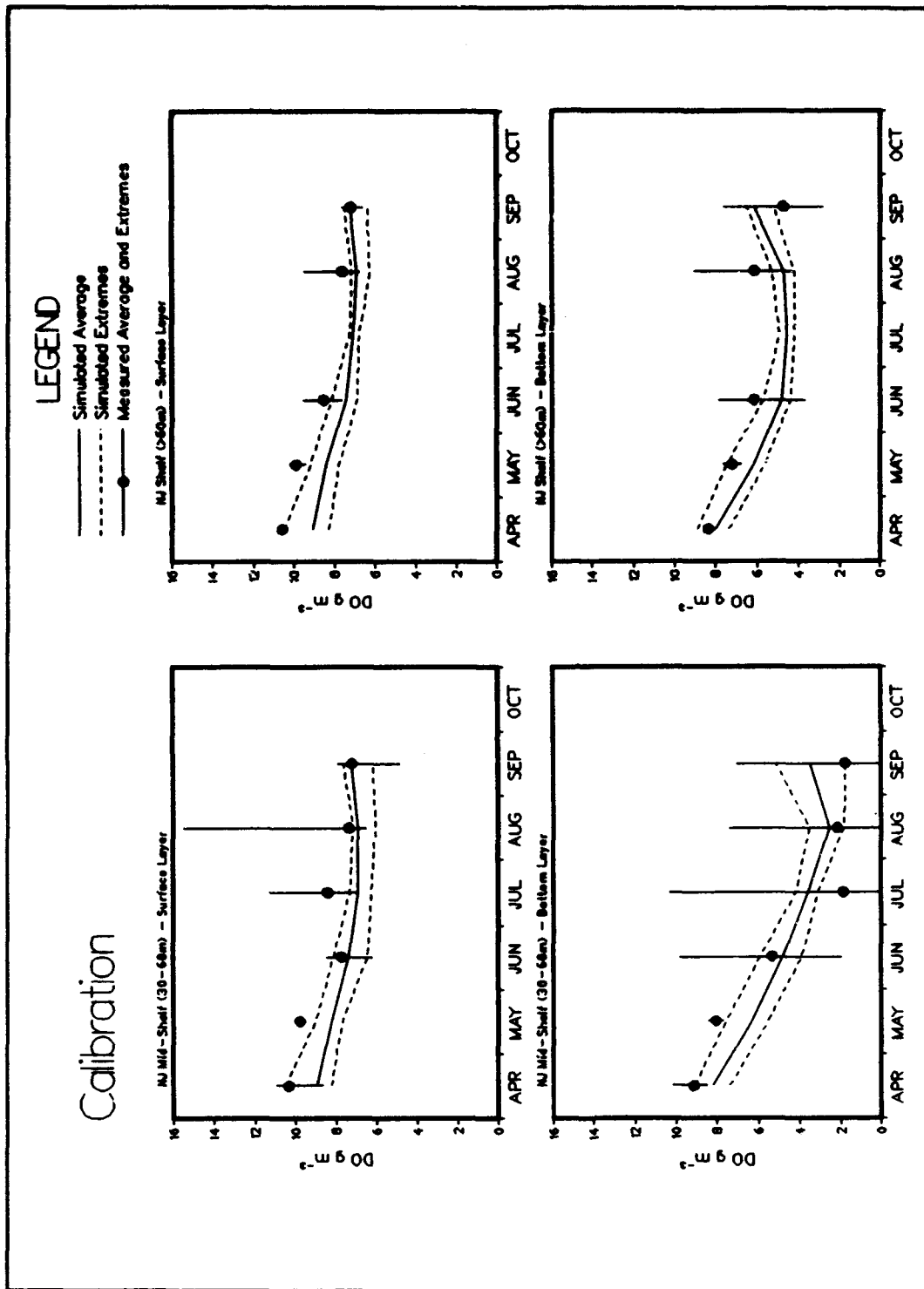
Calibration
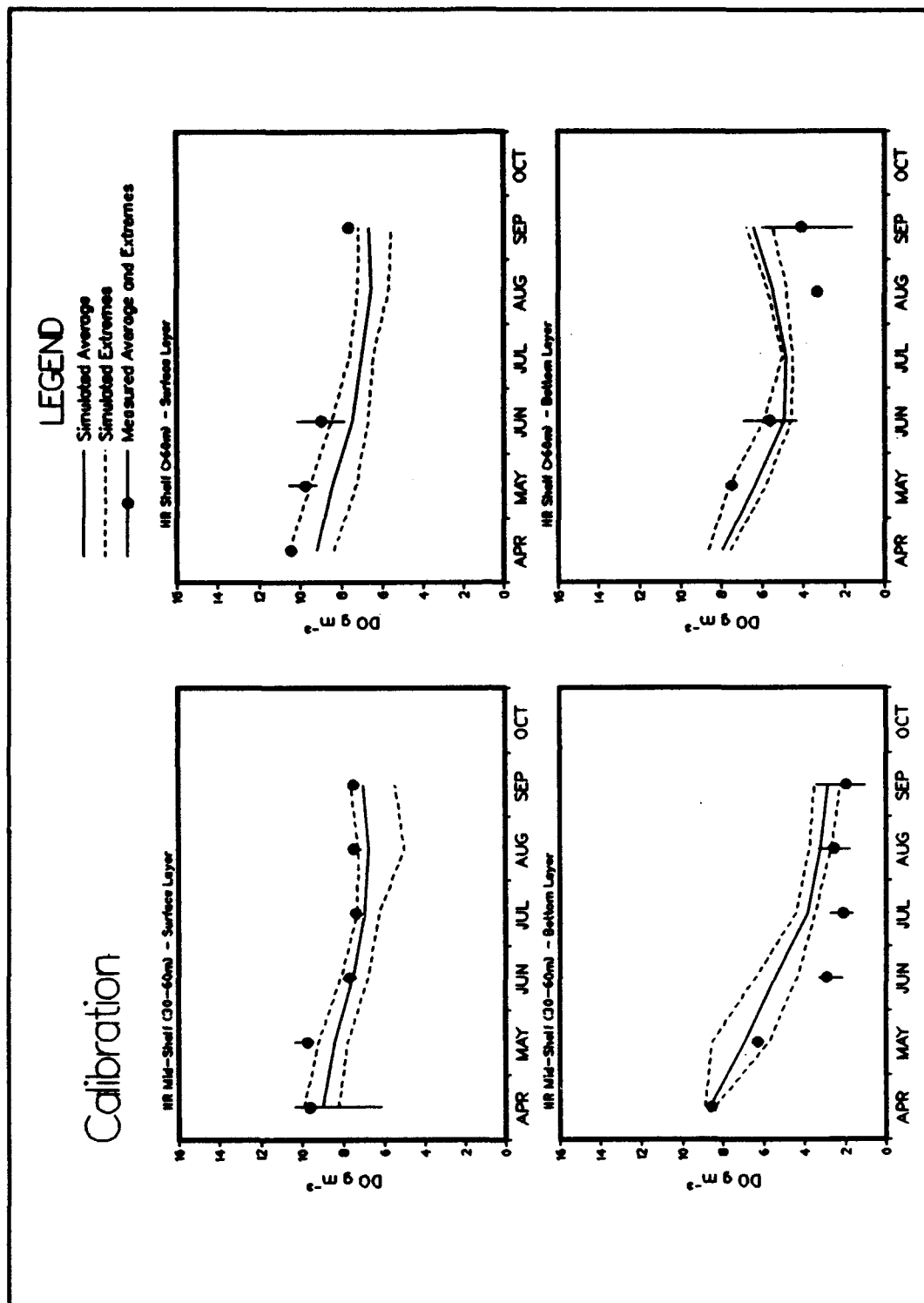
Plate D9.   (Sheet 2 of 6)

Plate D9. (Sheet 3 of 6)
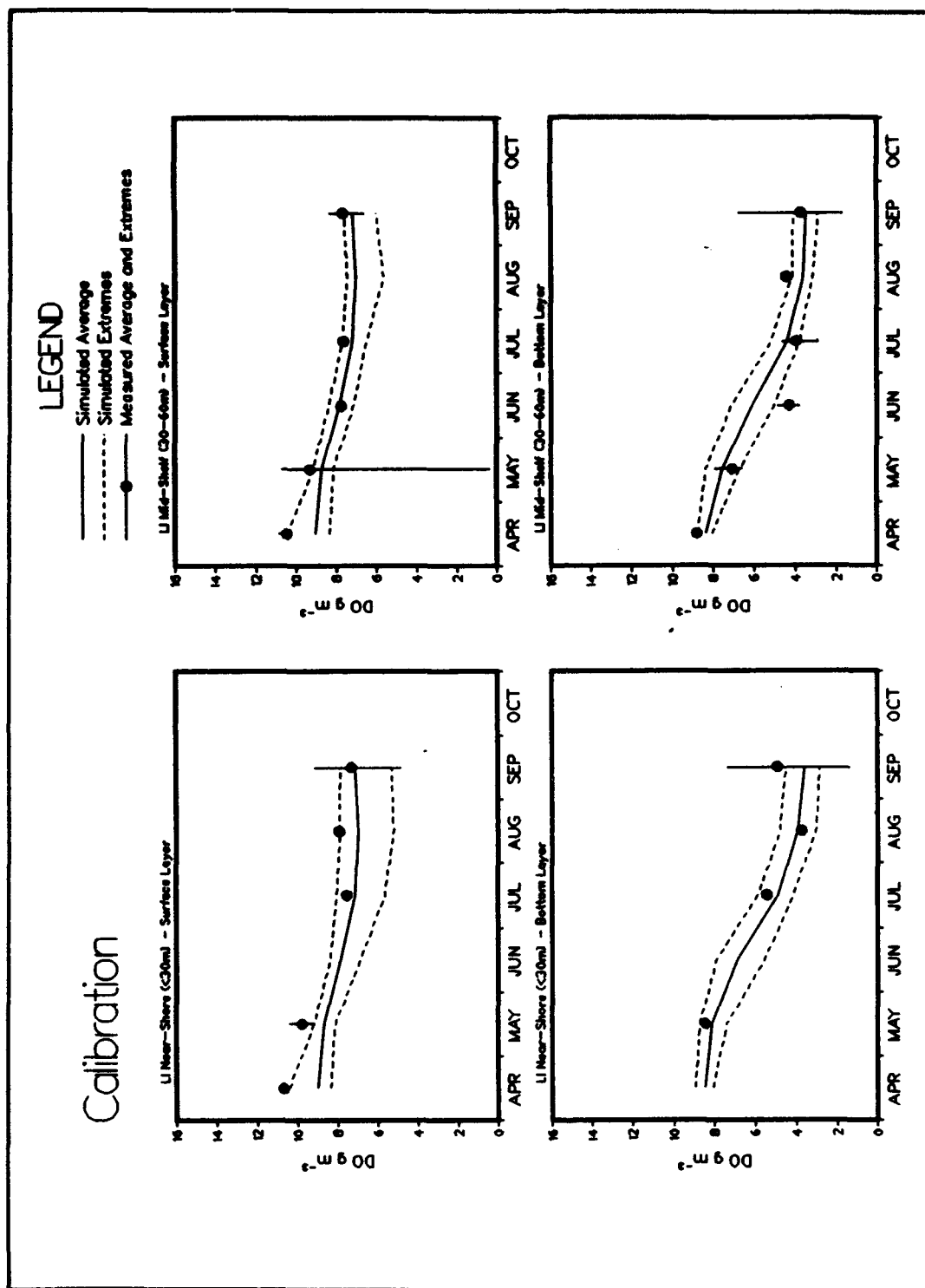
Plate D9. (Sheet 4 of 6)
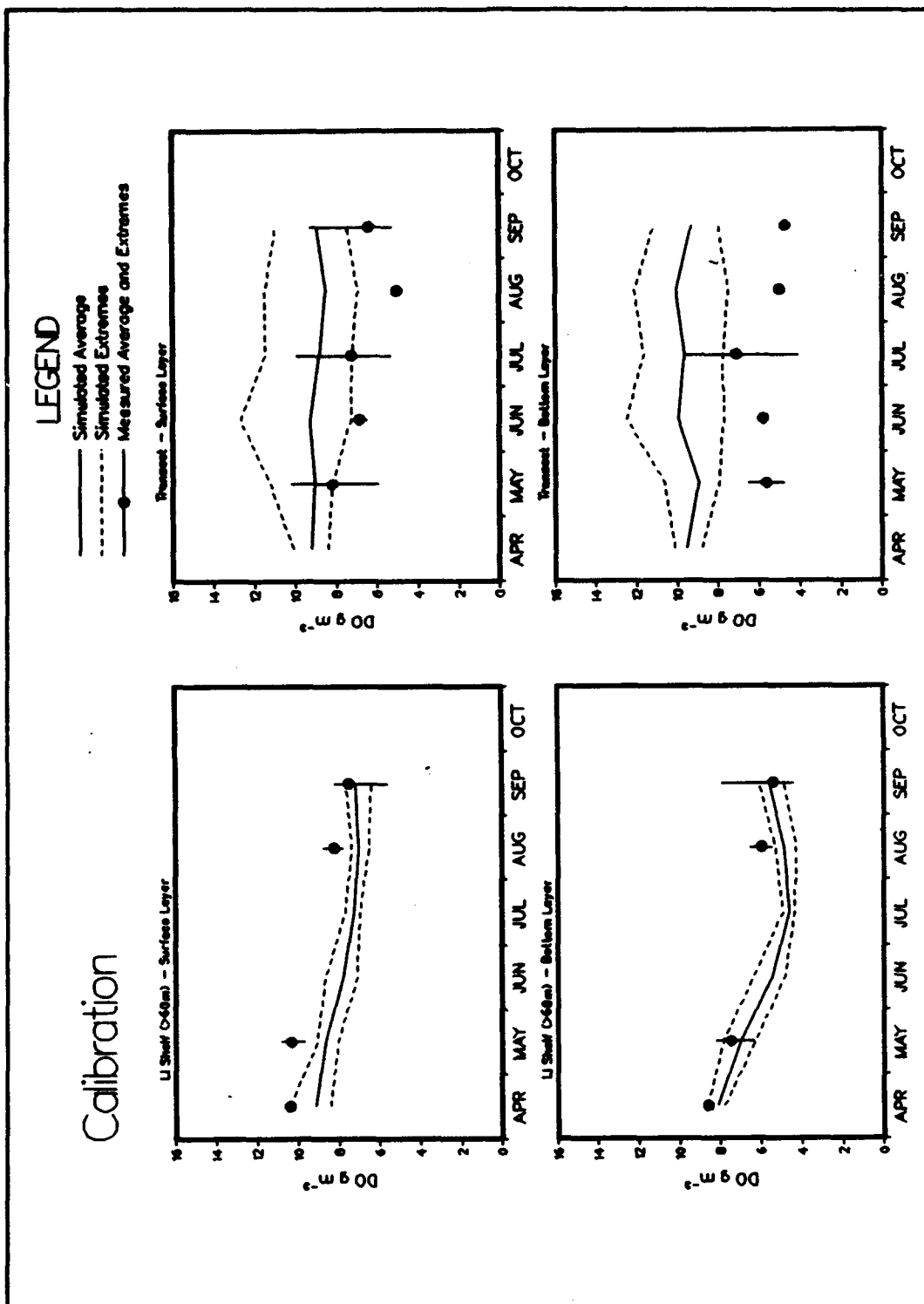
Plate D9. (Sheet 5 of 6)
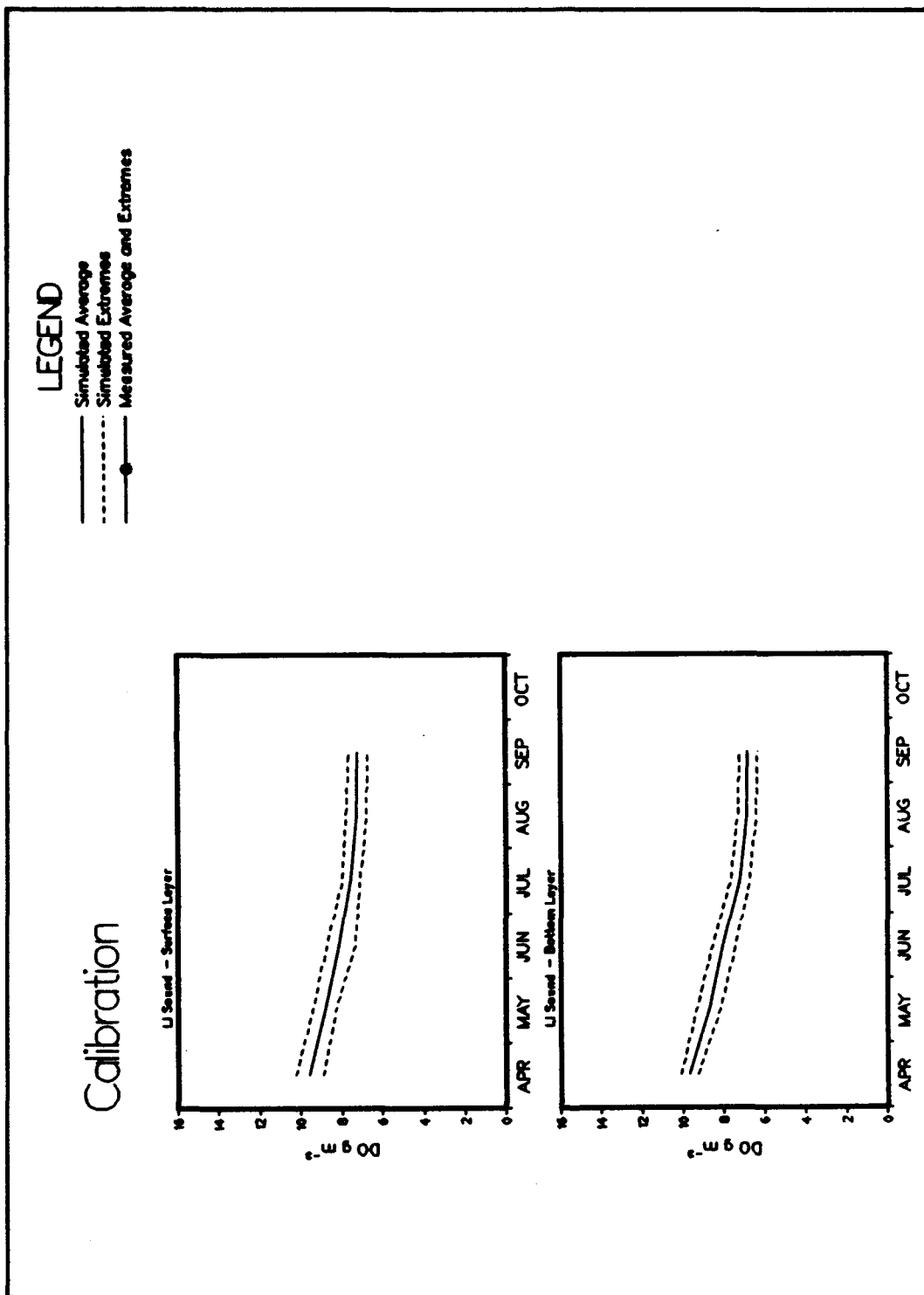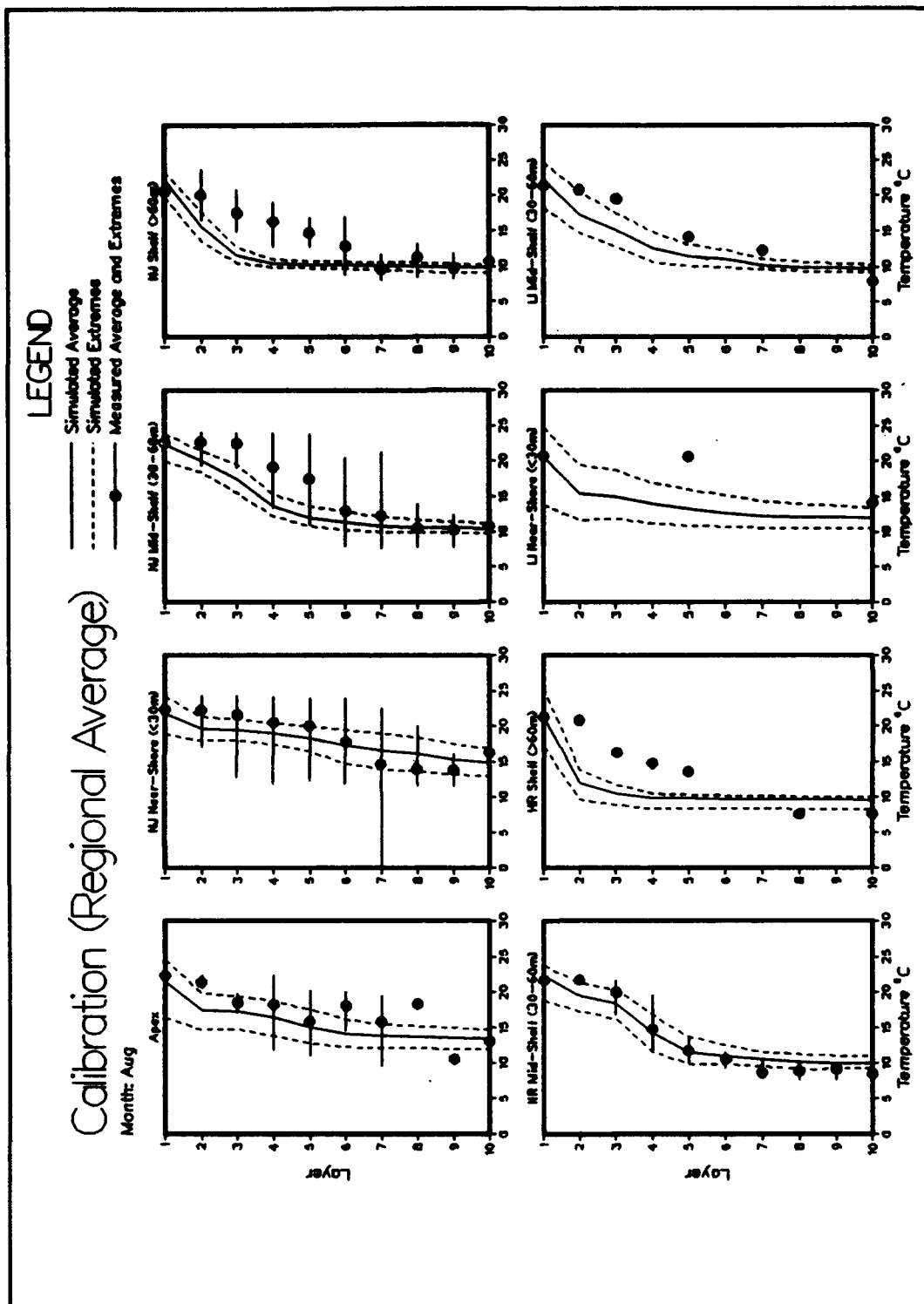
Calibration

LEGEND

Simulated Average
Simulated Extremes
Measured Average and Extremes

Plate D9.   (Sheet 6 of 6)

D52

Calibration (Regional Average)

Plate D10. (Sheet 1 of 2)

Calibration (Regional Average)

Plate D10. (Sheet 2 of 2)

Calibration (Regional Average)

Plate D11. (Sheet 1 of 2)

Calibration (Regional Average)

LEGEND
Simulated Average
Simulated Extremes
Measured Average and Extremes

Plate D11.   (Sheet 2 of 2)

D56

Calibration (Point Comparison)

Plate D12.   (Sheet 1 of 2)

Calibration (Point Comparison)

LEGEND

Simulated Average
Simulated Extremes
Measured Average and Extremes

Month: Aug

U Shell (>60m) (43, 80)

Transect (31, 30)

Plate D12.   (Sheet 2 of 2)

Calibration (Point Comparison)

Plate D13. (Sheet 1 of 2)

Calibration (Point Comparison)
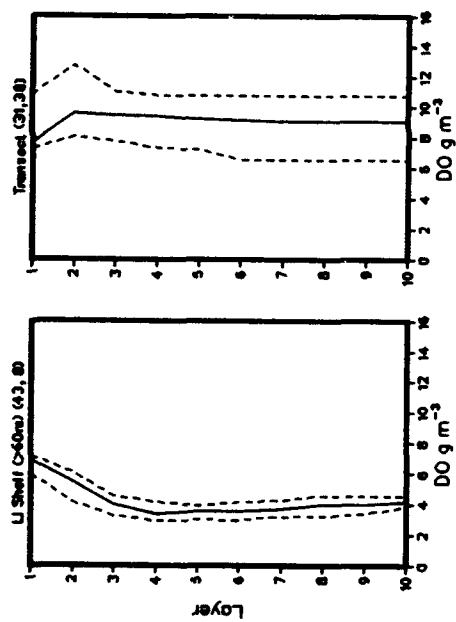
LEGEND
Simulated Average
Simulated Extremes
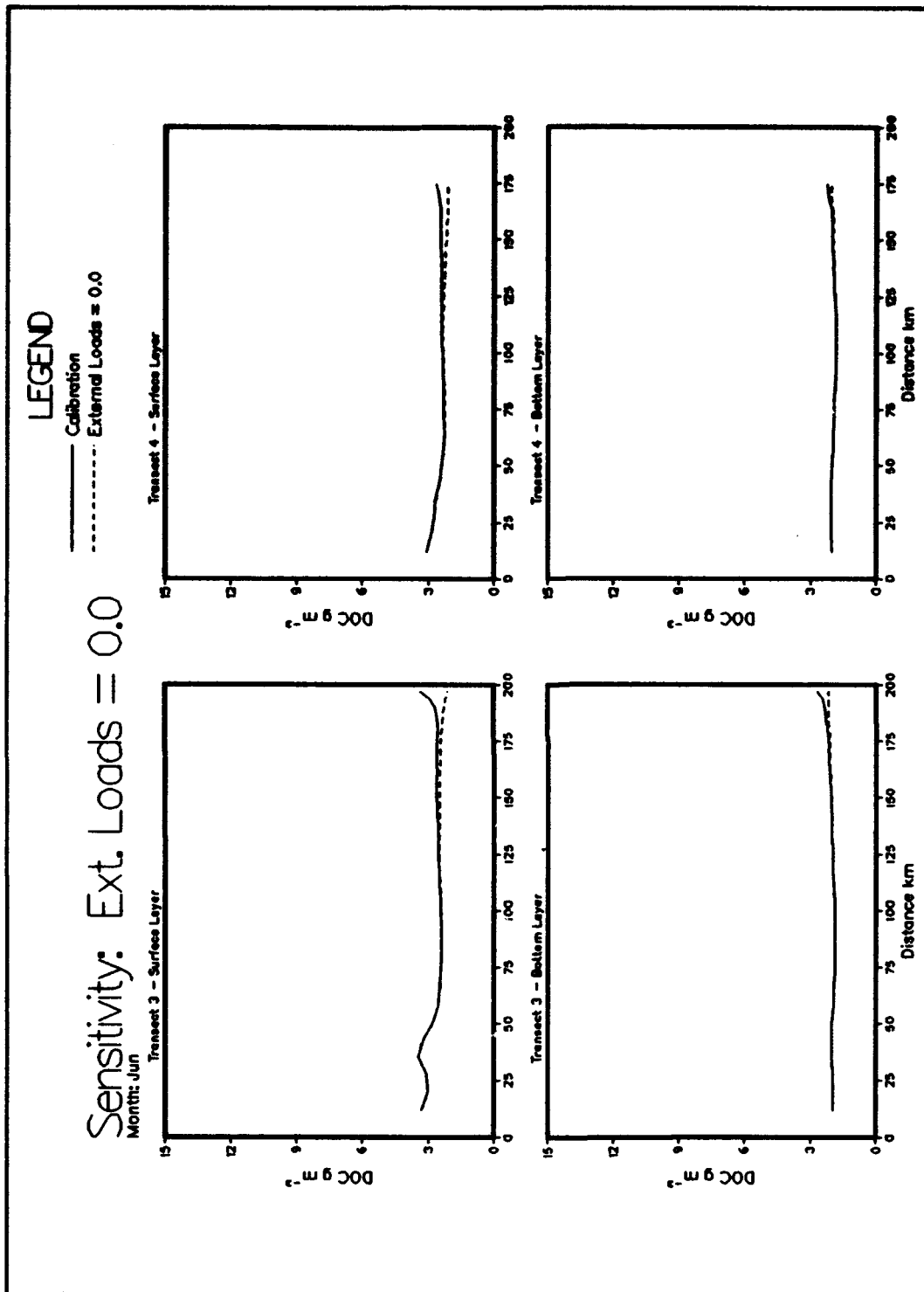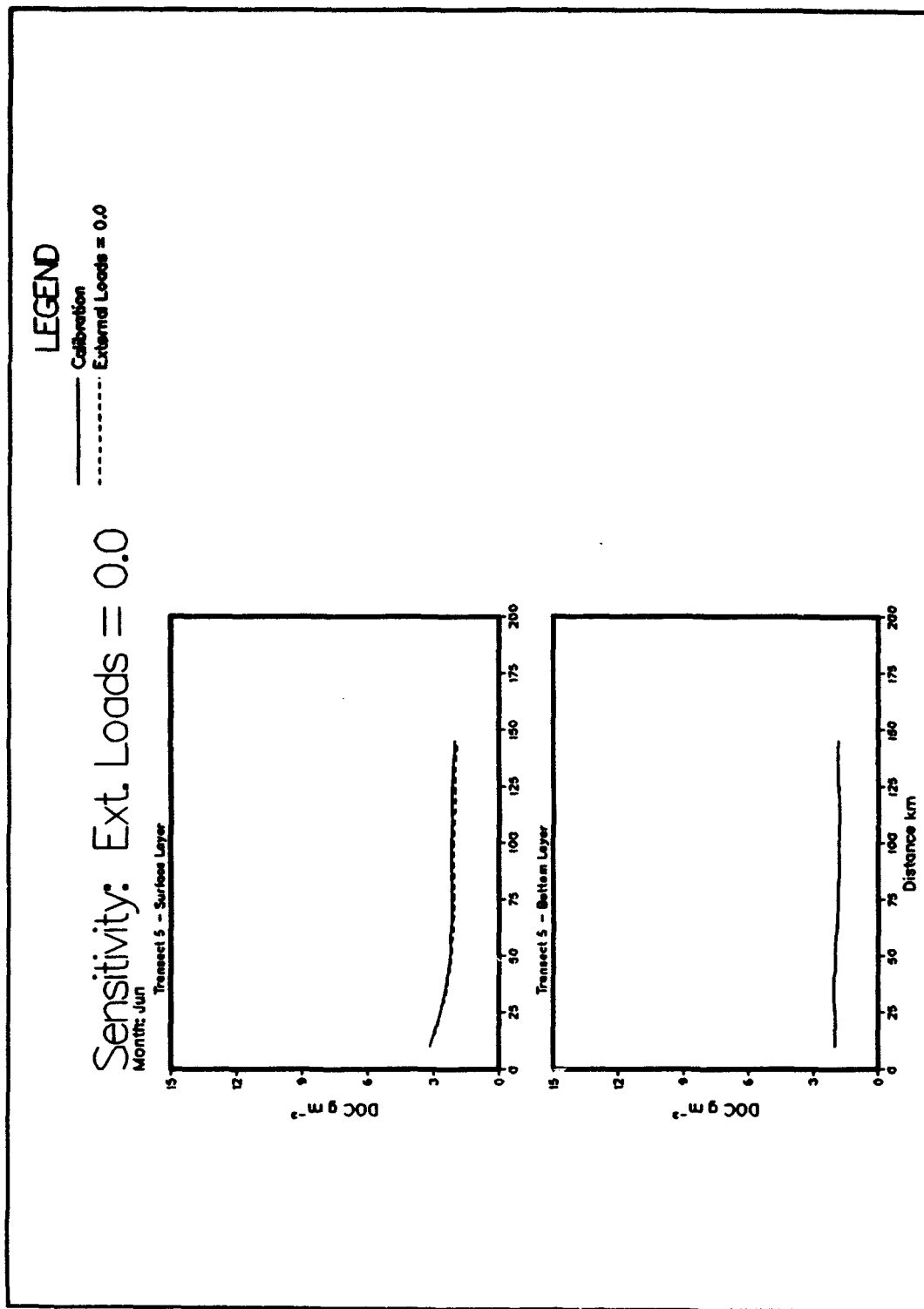Measured Average and Extremes

Plate D13.   (Sheet 2 of 2)
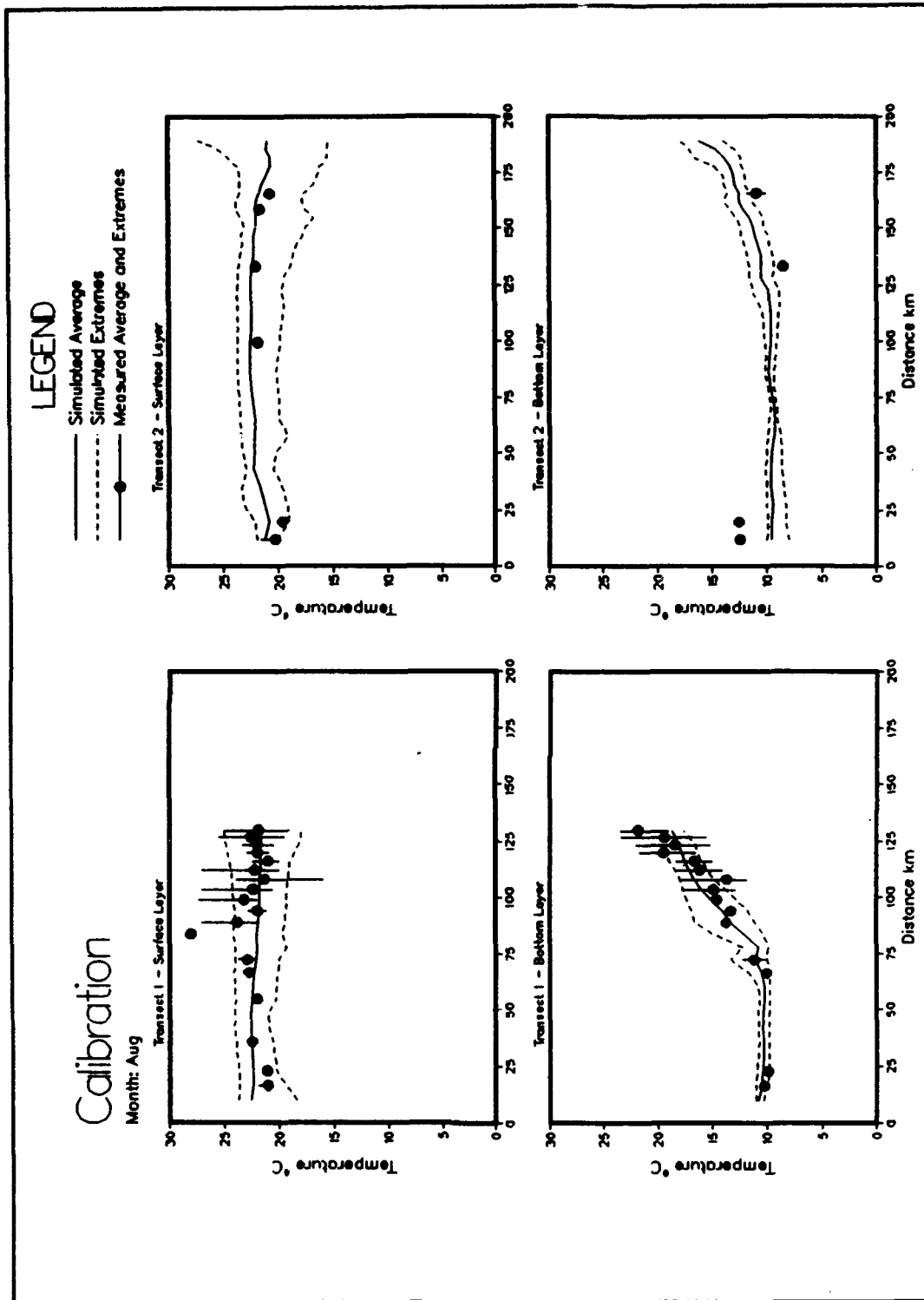
Plate D14. (Sheet 1 of 3)
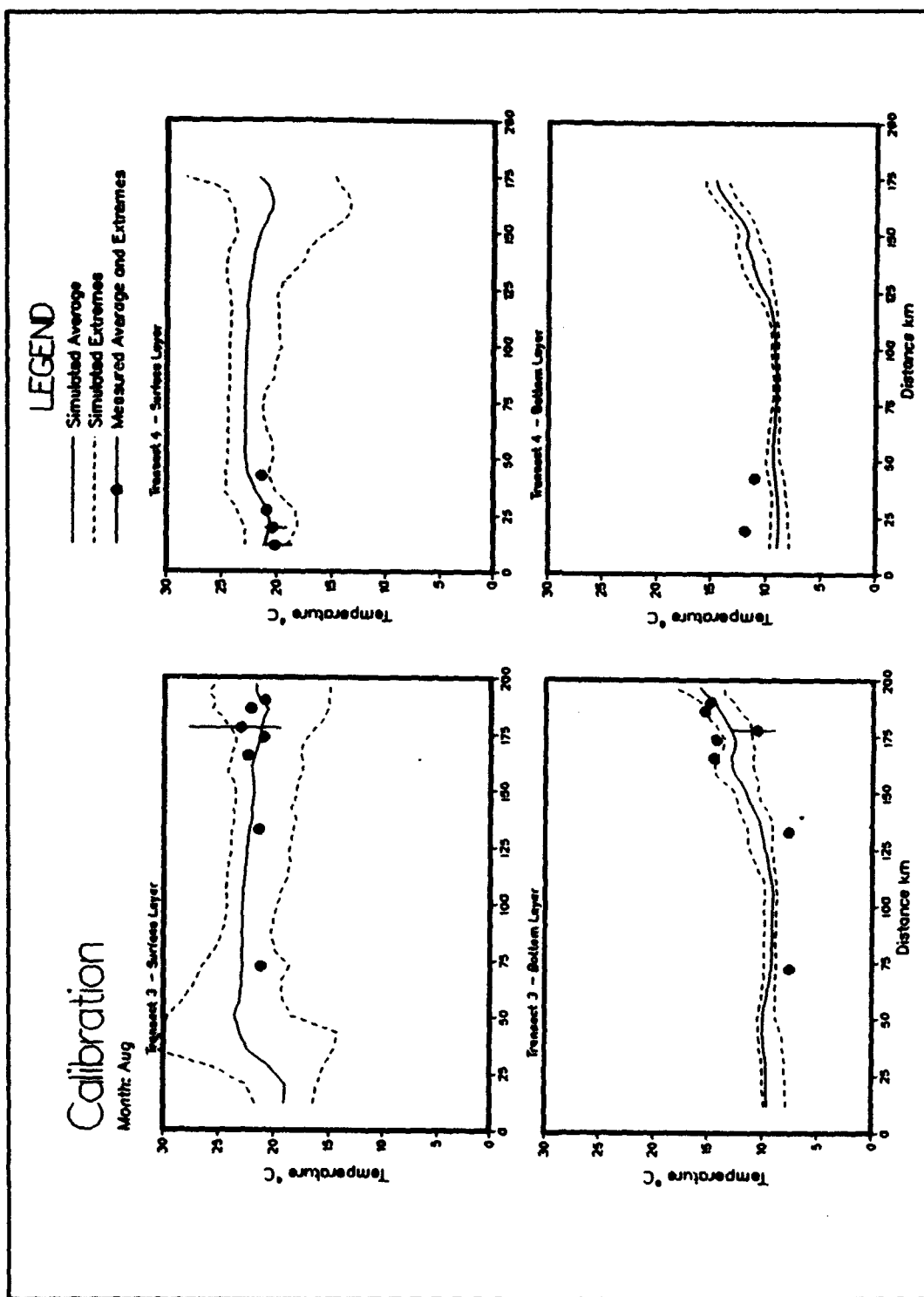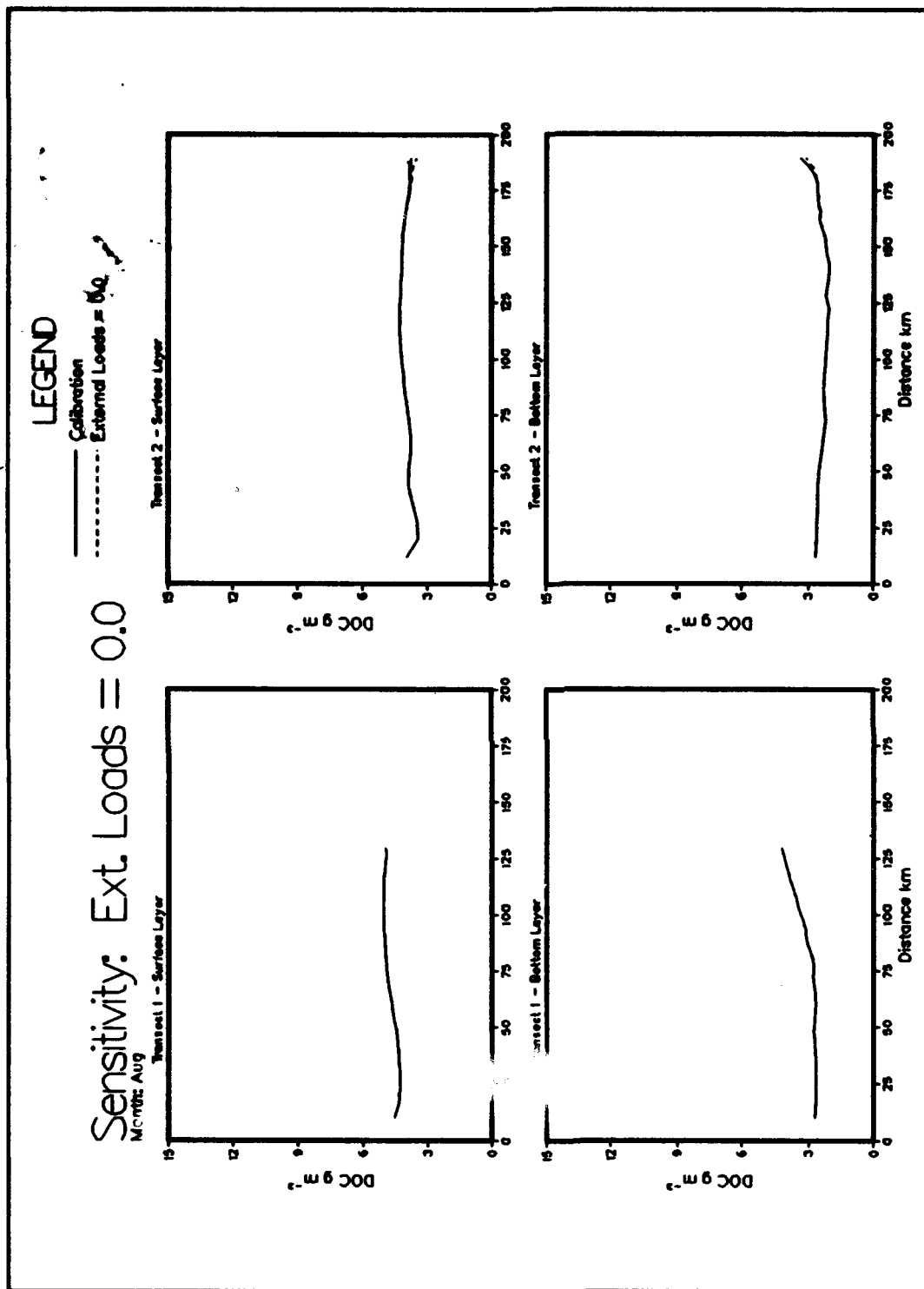
Plate D14. (Sheet 2 of 3)
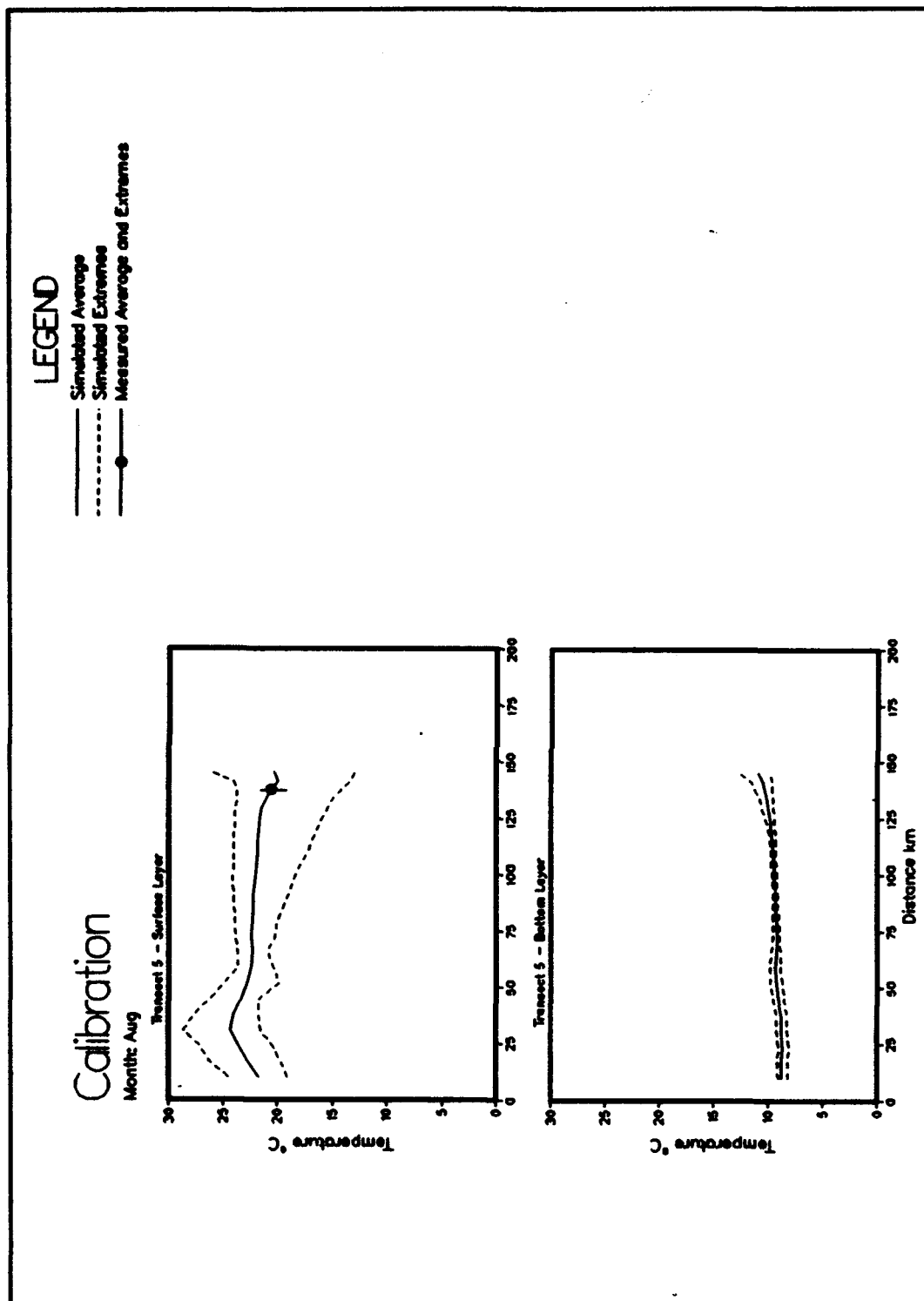
Plate D14.   (Sheet 3 of 3)

Calibration

Month: Aug
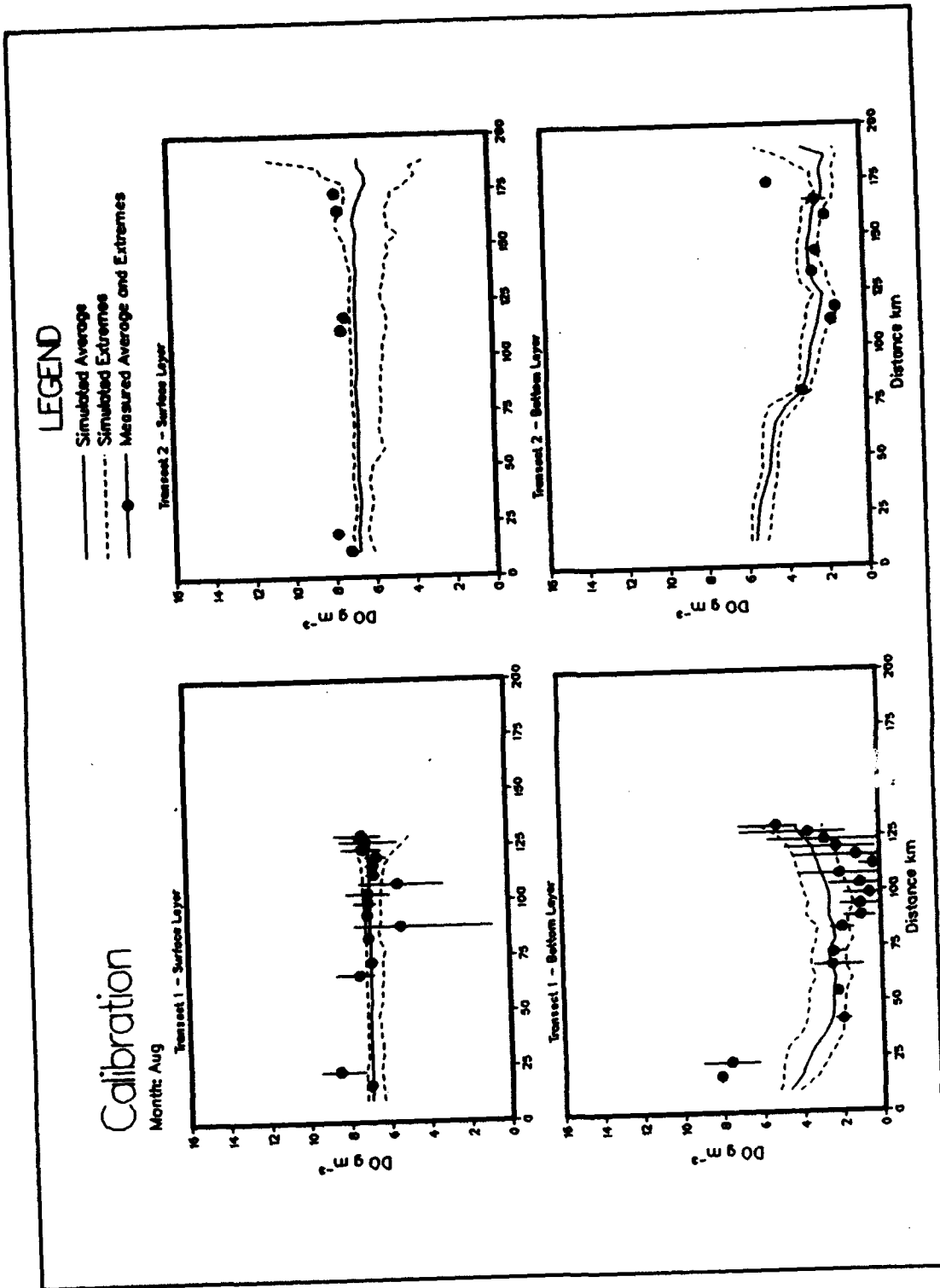
Plate D15. (Sheet 1 of 3)
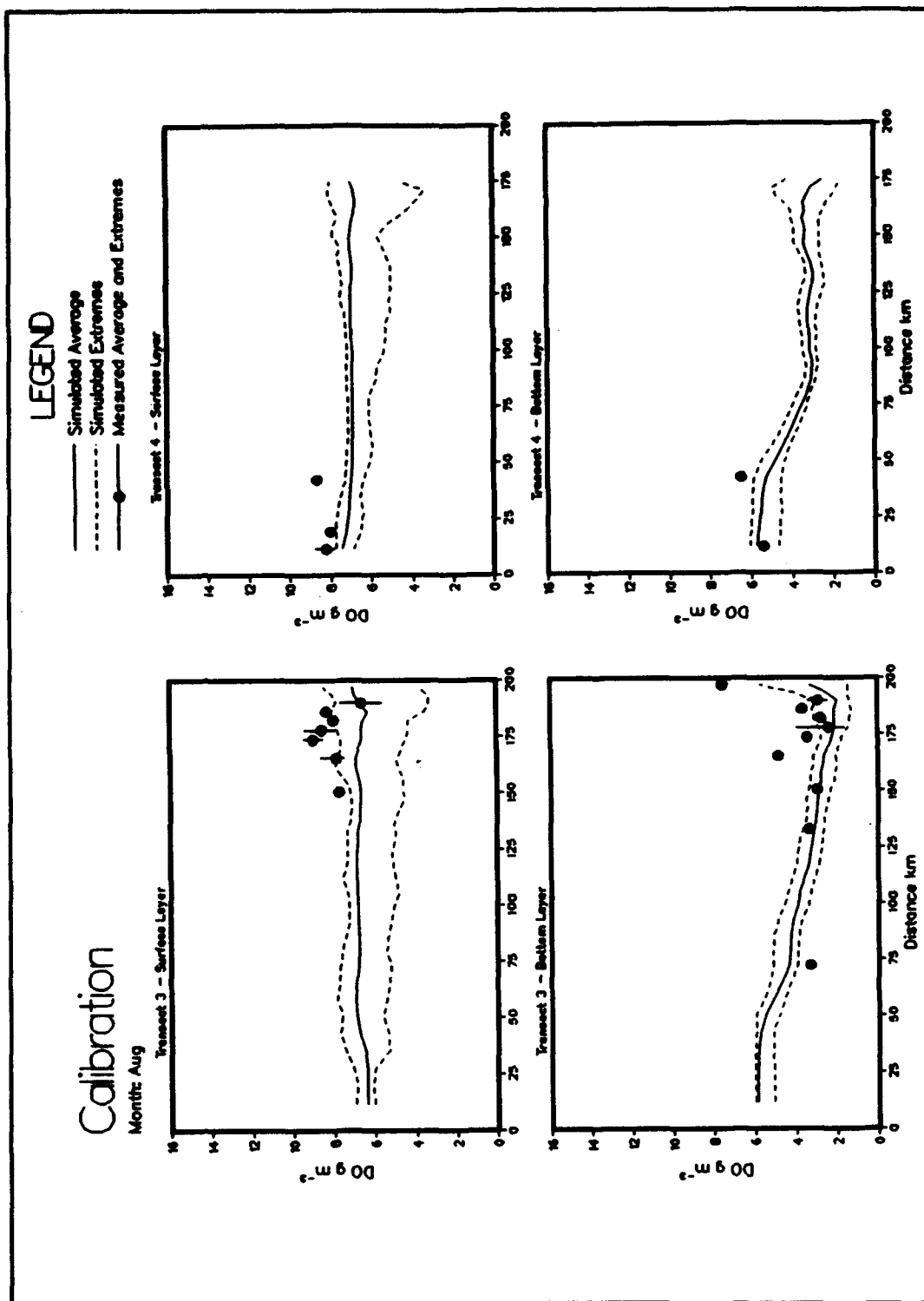
Plate D15. (Sheet 2 of 3)
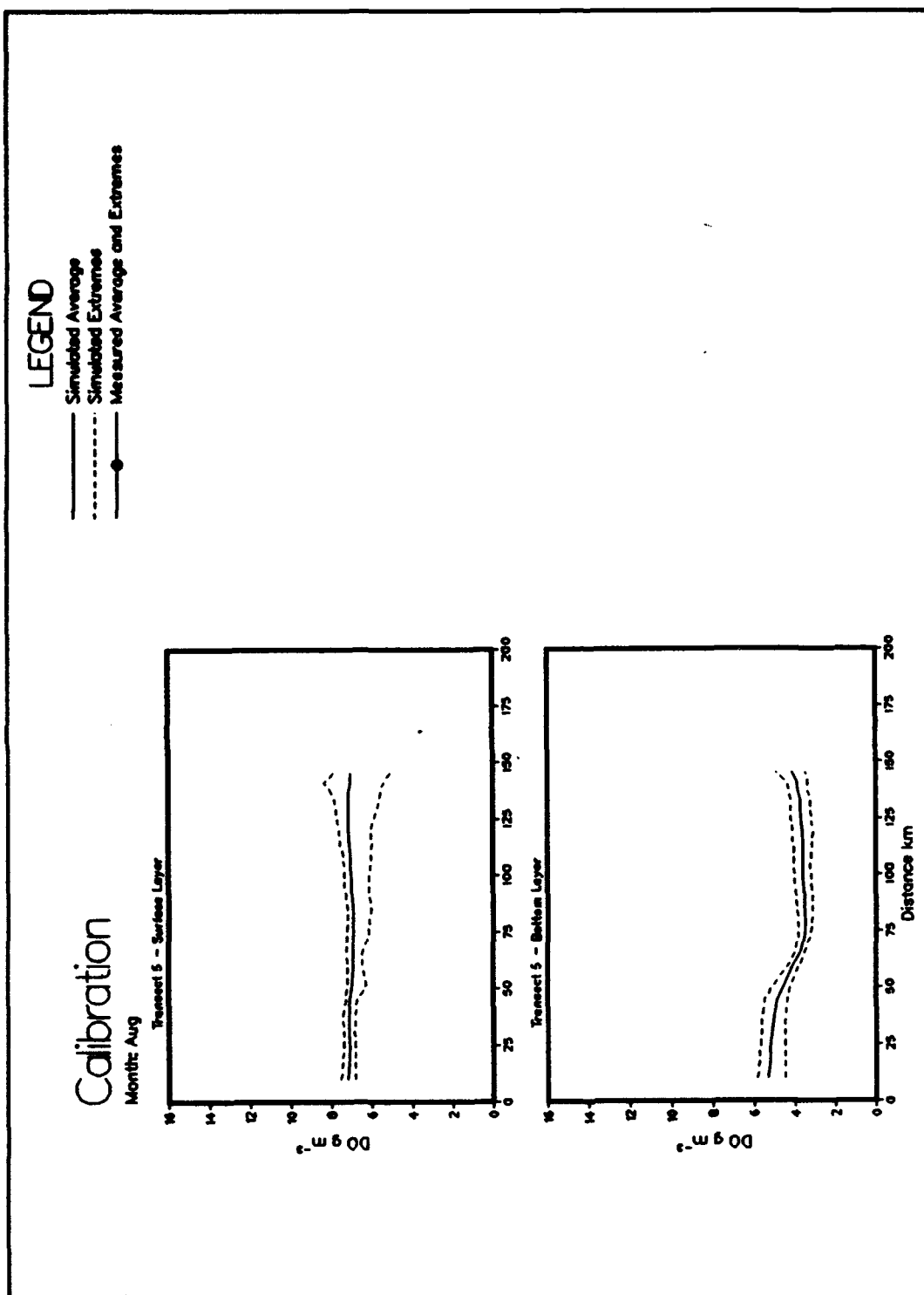
Plate D15. (Sheet 3 of 3)

Appendix E
Sensitivity Test Plots

NEW YORK BIGHT

Aggregated by Area, Layer, and Month - 1976

Sensitivity: SOD=0.0

Plate E1

E2

Plate E2. (Sheet 1 of 2)

Sensitivity: SOD = 0.0
Month: Jun

LEGEND
—— Calibration
------ SOD = 0.0

Plate E2. (Sheet 2 of 2)

Sensitivity: SOD = 0.0
Month: Aug
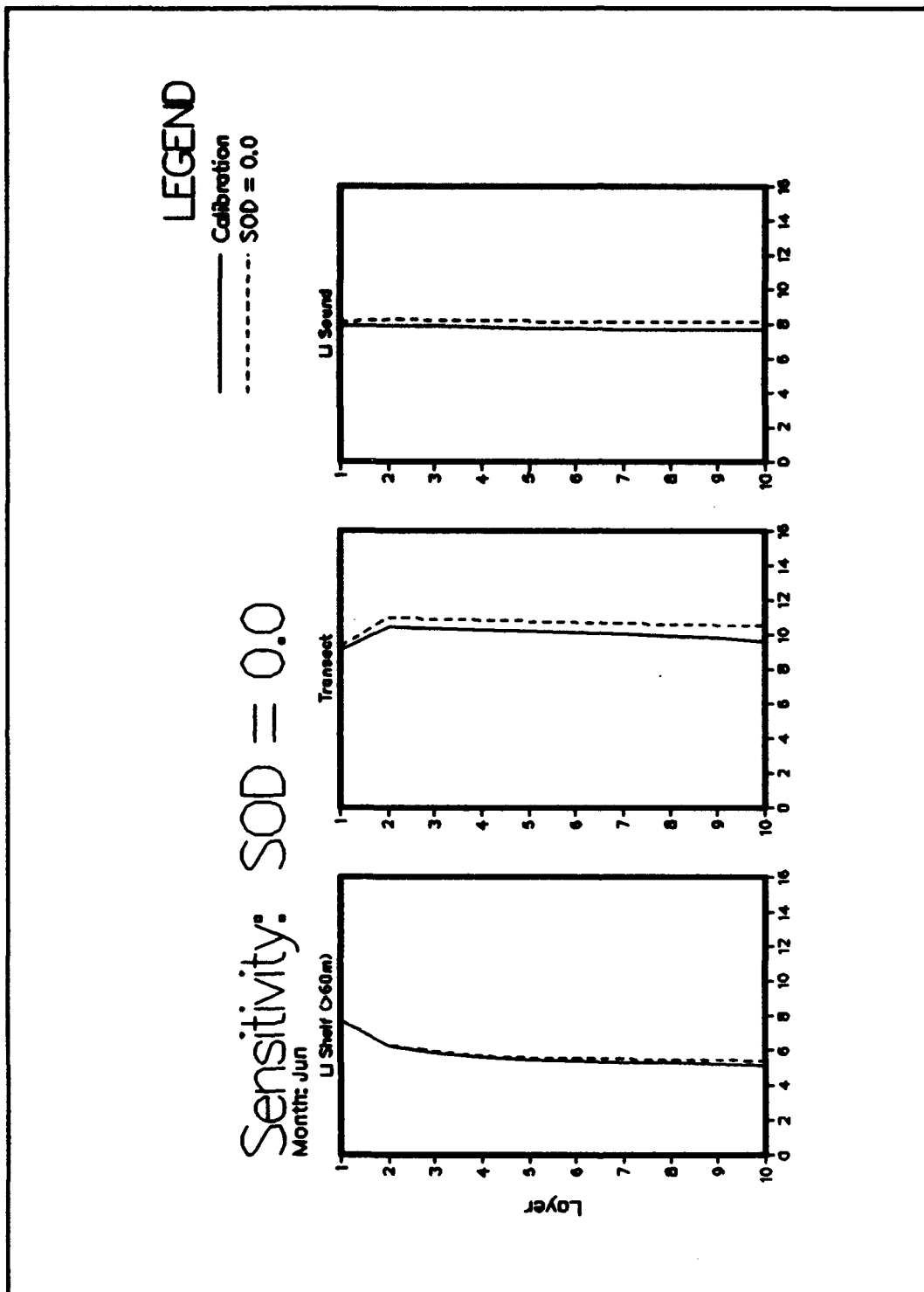
LEGEND
Calibration
SOD = 0.0
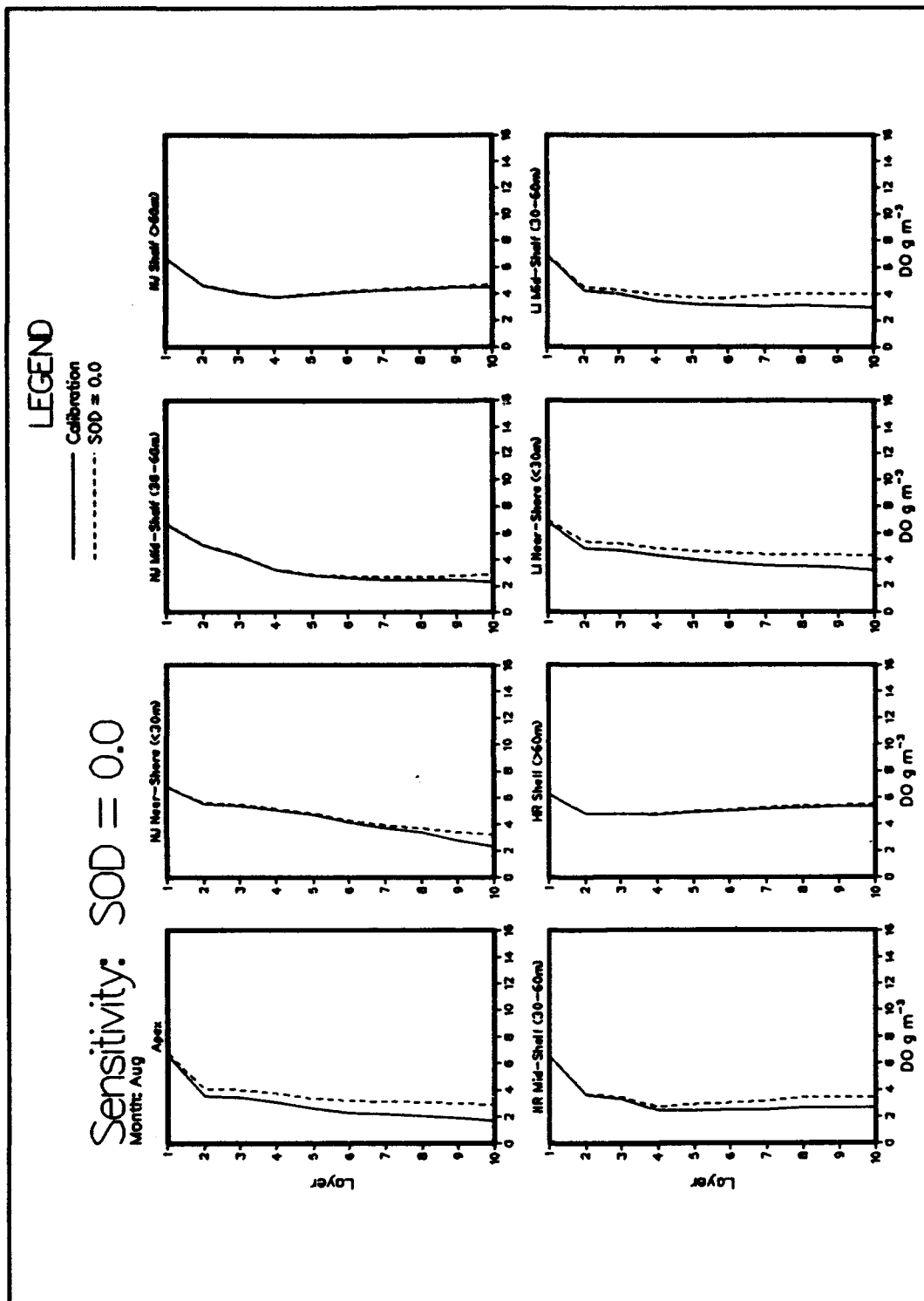
Plate E3. (Sheet 1 of 2)

Sensitivity: SOD = 0.0
Month: Aug

LEGEND
Calibration
SOD = 0.0
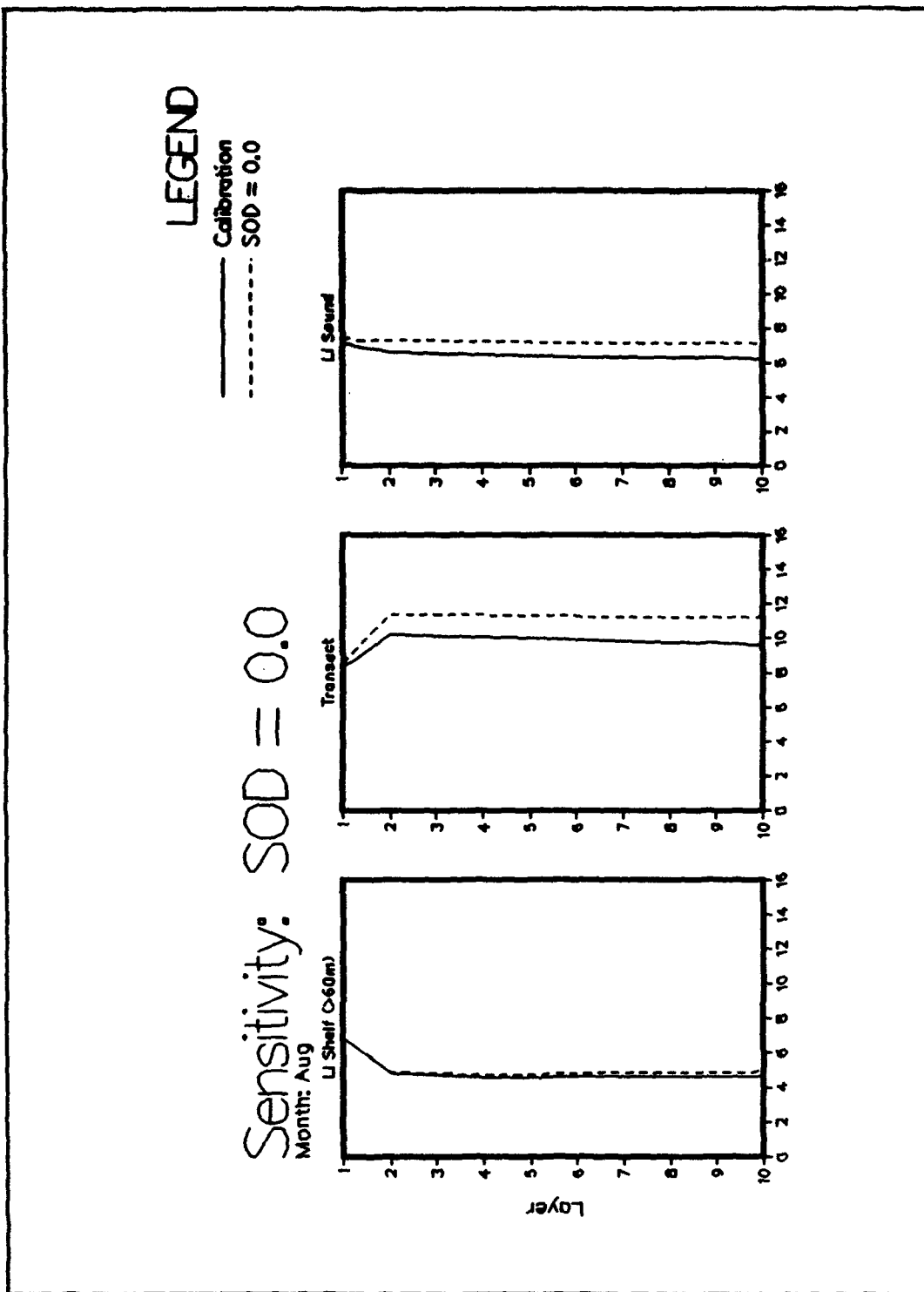
Plate E3. (Sheet 2 of 2)

NEW YORK BIGHT
Aggregated by Area, Layer, and Month - 1976

Sensitivity: SOD=−10.0

DO g m^{-3}

X-axis: Simulated
Y-axis: Observed
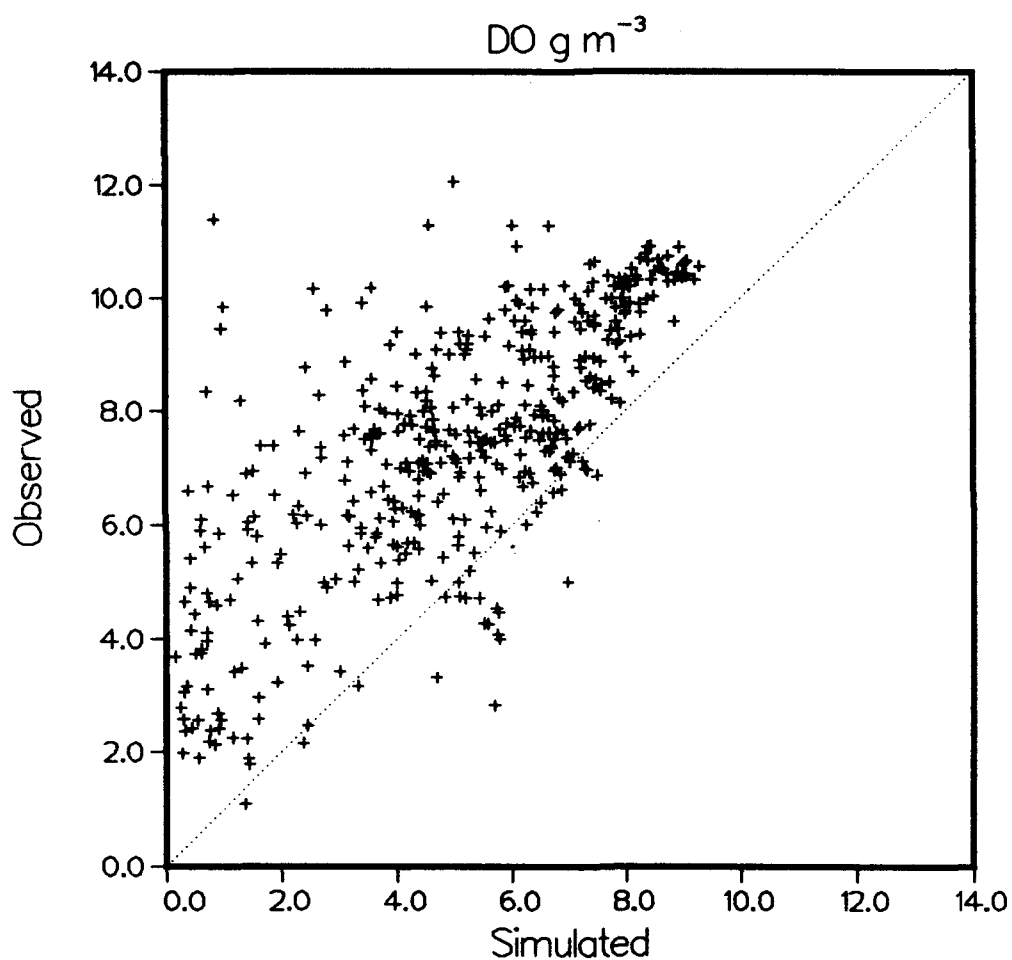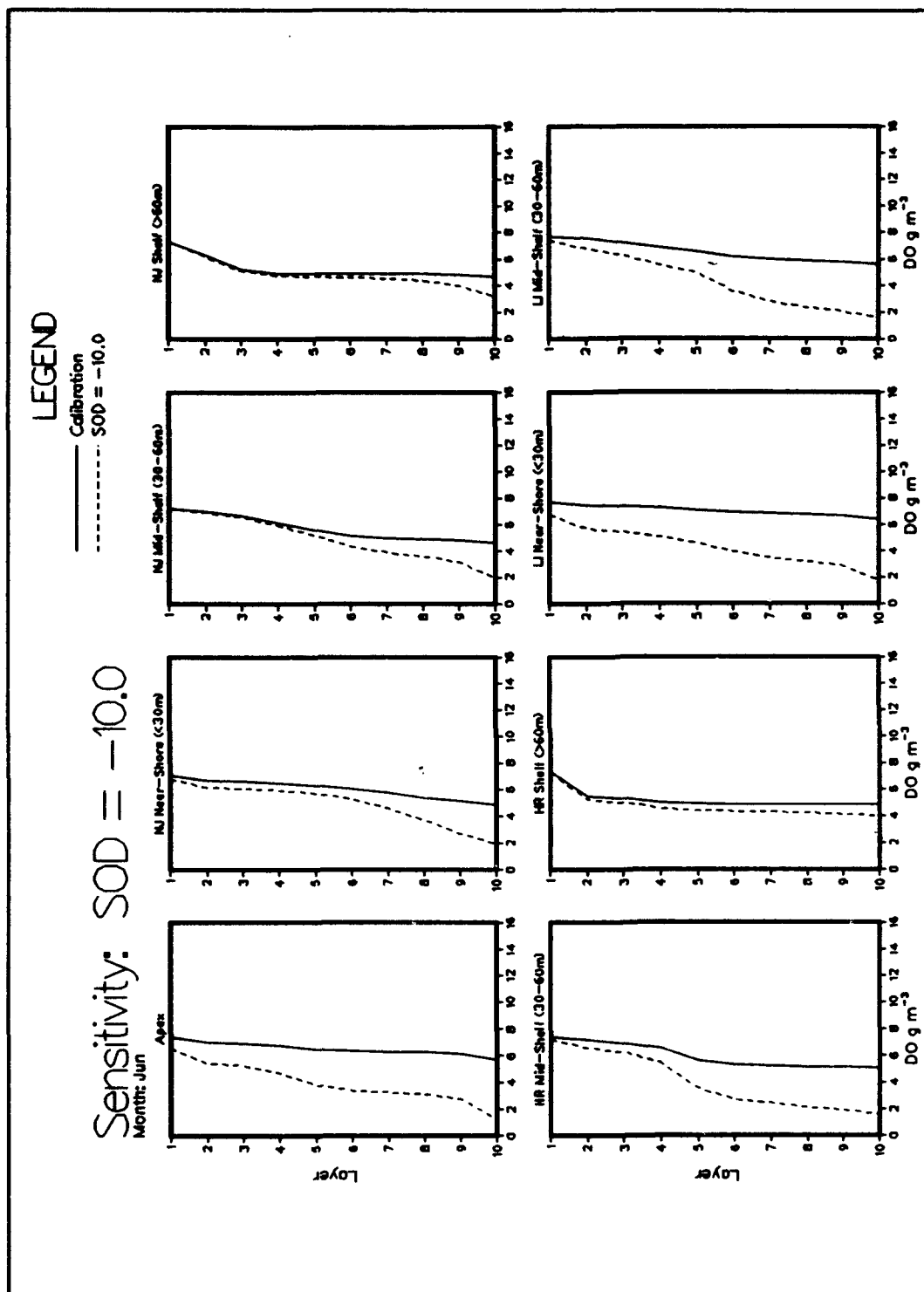
Plate E5. (Sheet 1 of 2)

Plate E5.   (Sheet 2 of 2)

Plate E6.   (Sheet 1 of 2)

Sensitivity: SOD = -10.0
Month: Aug
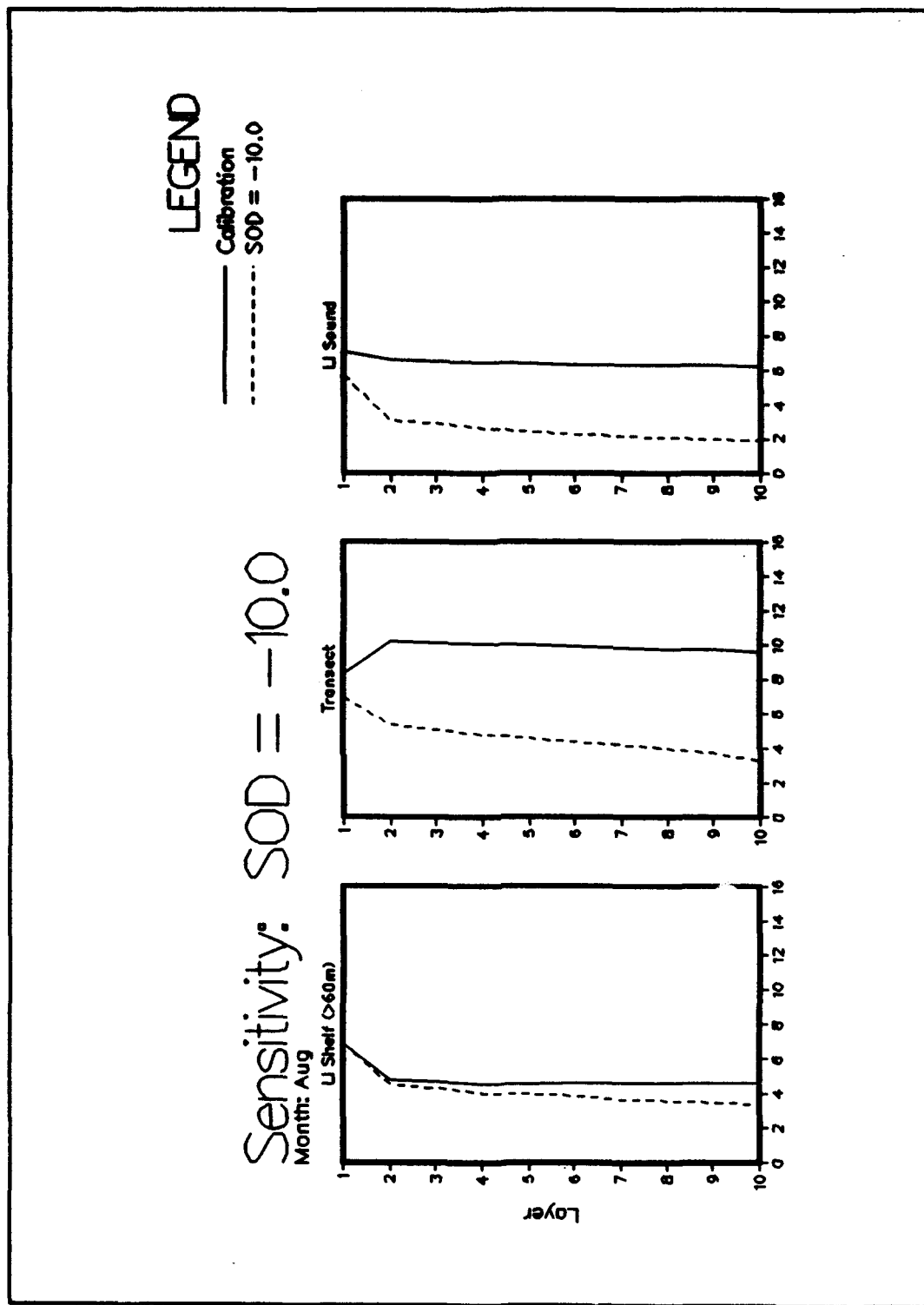
Plate E6. (Sheet 2 of 2)

NEW YORK BIGHT

Aggregated by Area, Layer, and Month - 1976

Sensitivity: N Boundary Conditions=0.0

NEW YORK BIGHT

Aggregated by Area, Layer, and Month – 1976

Sensitivity: N Boundary Conditions=0.0

Plate E7.   (Sheet 2 of 3)

NEW YORK BIGHT

Aggregated by Area, Layer, and Month - 1976

Sensitivity: N Boundary Conditions=0.0
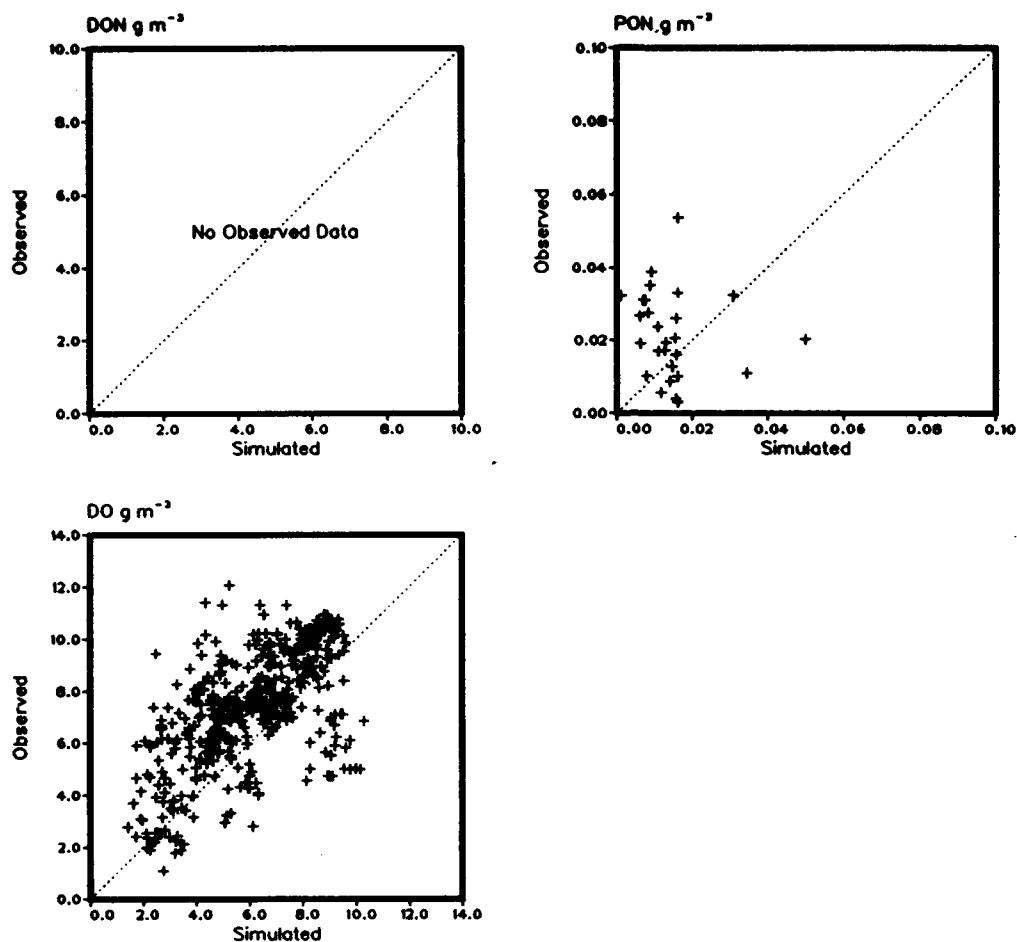
Plate E7.   (Sheet 3 of 3)
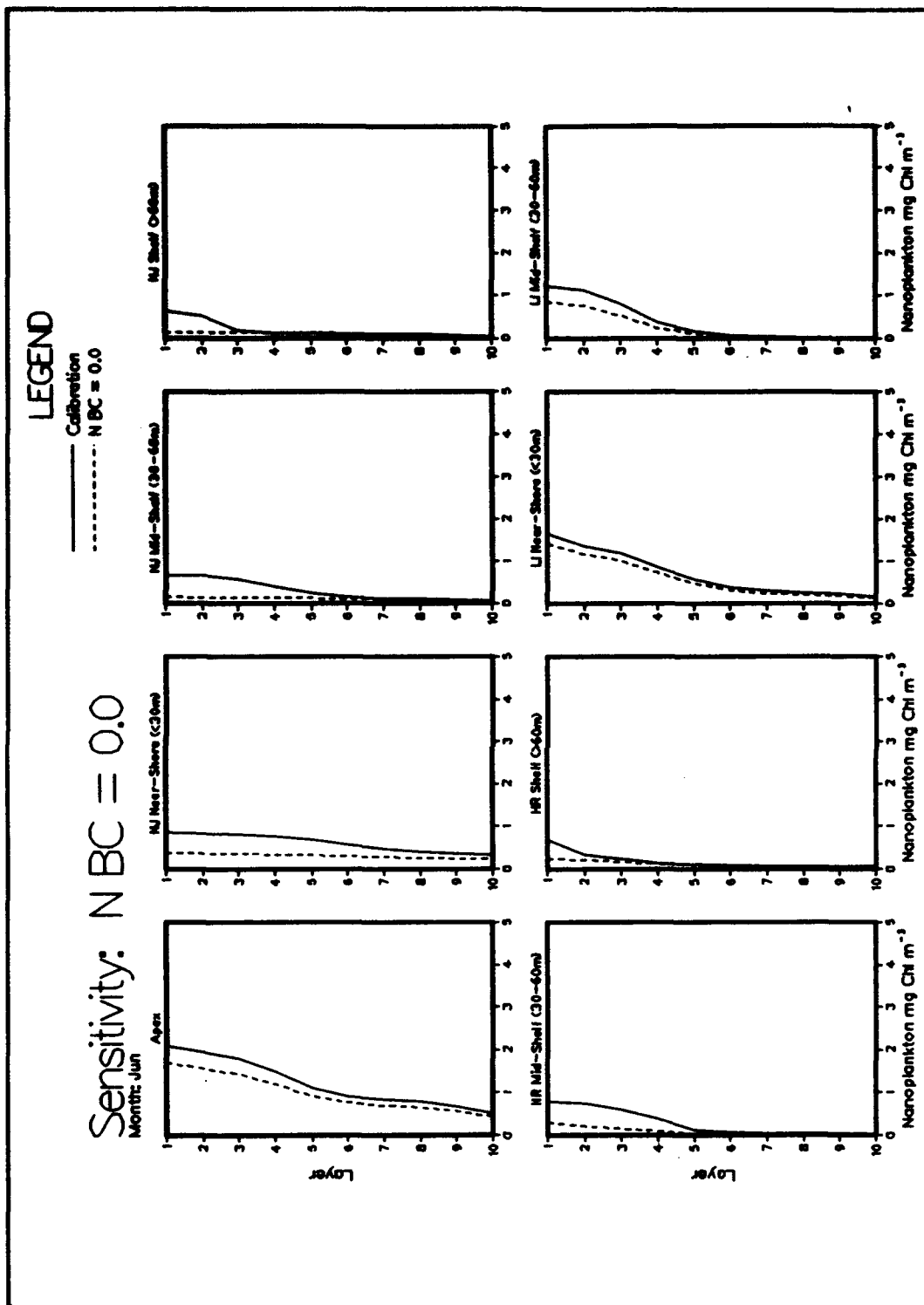
Plate E8. (Sheet 1 of 2)
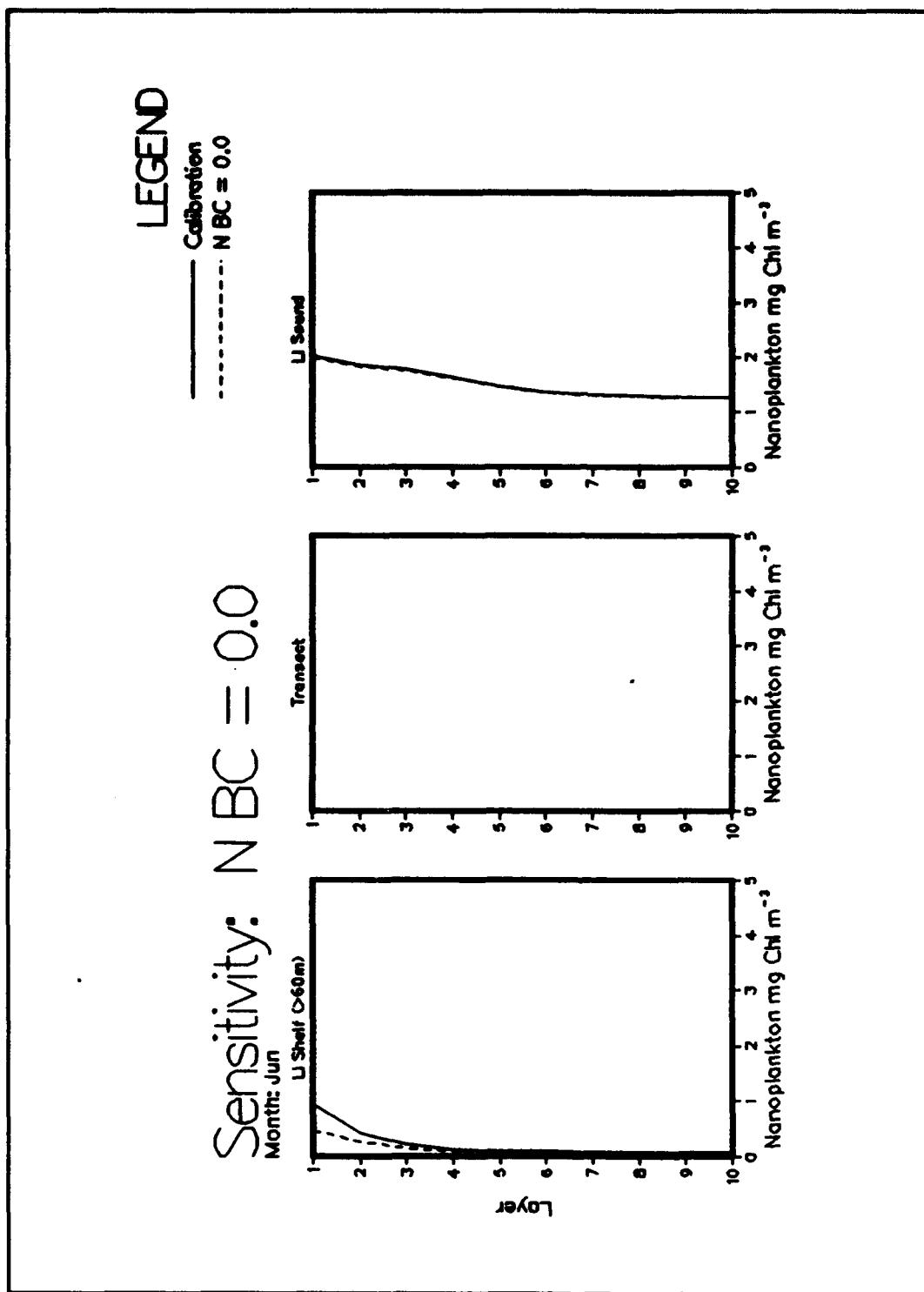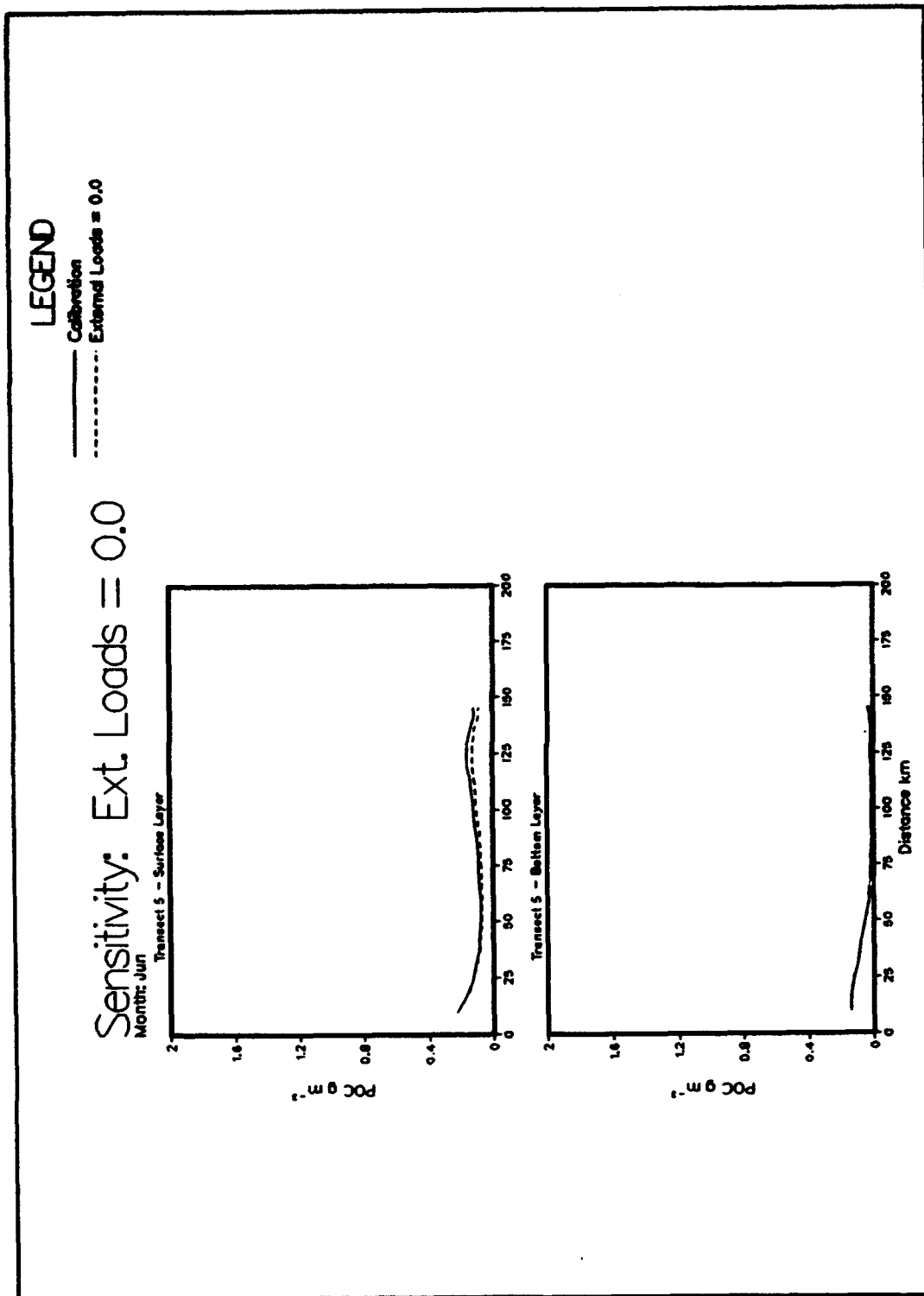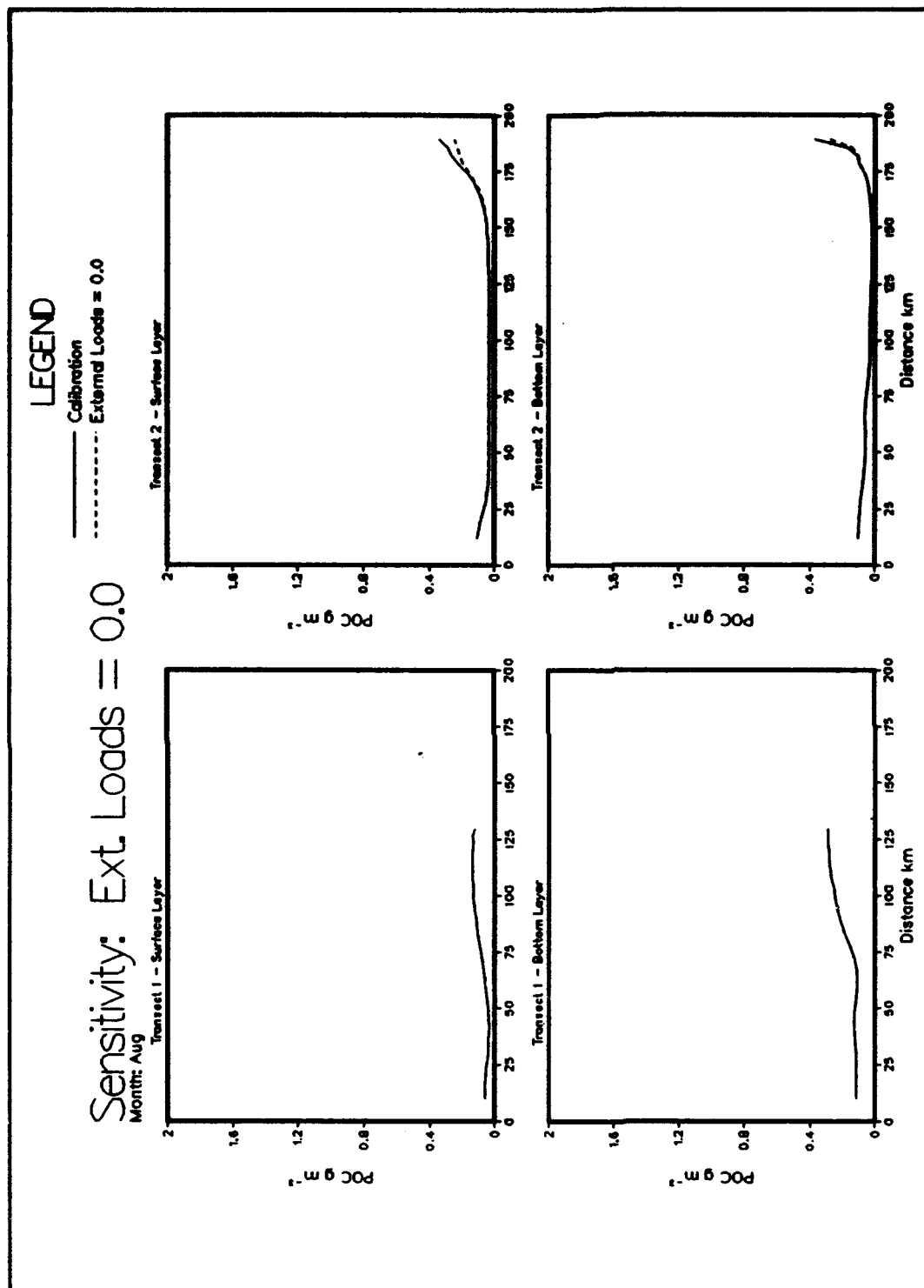
Plate E8. (Sheet 2 of 2)
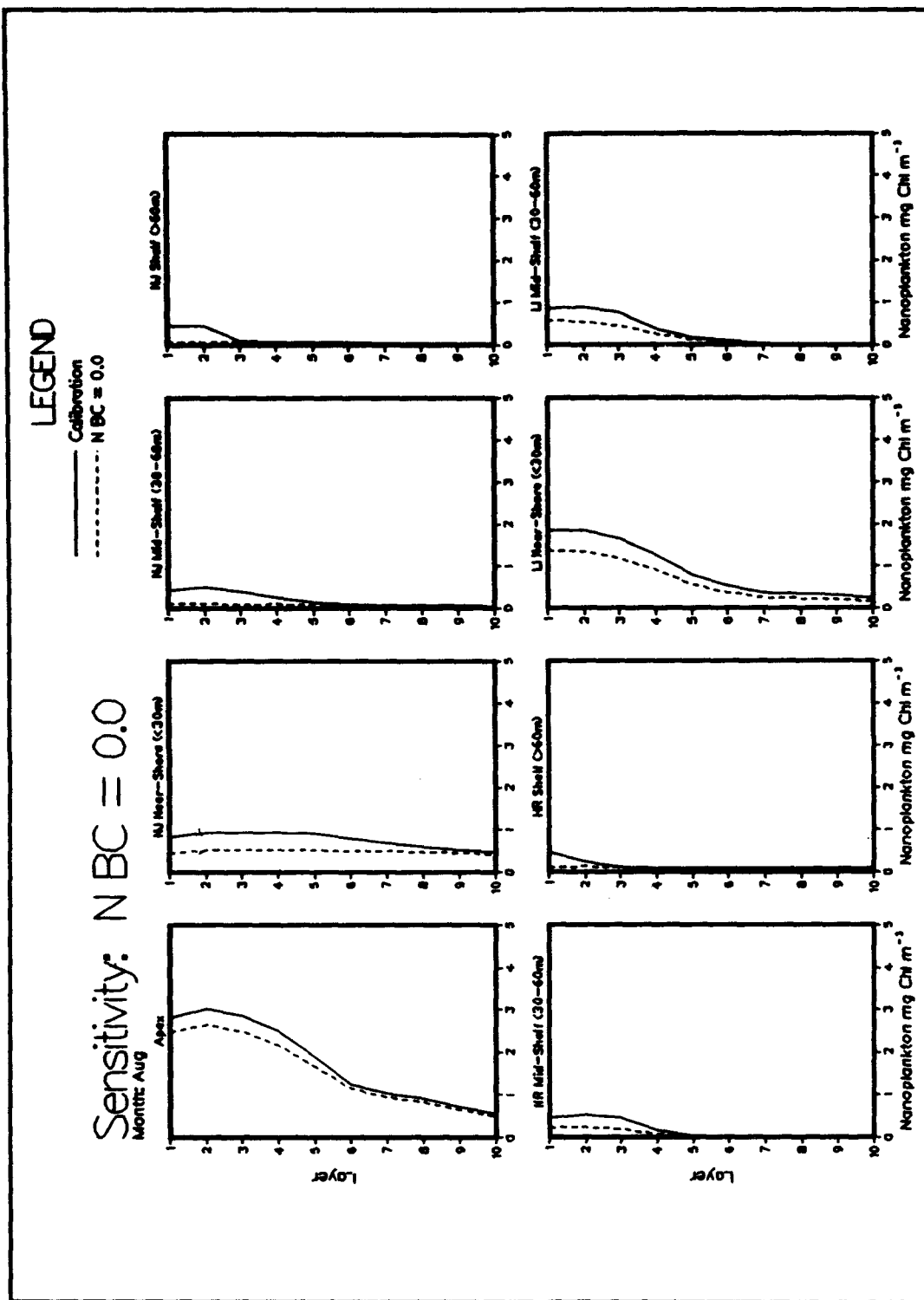
Plate E9. (Sheet 1 of 2)

Plate E9. (Sheet 2 of 2)

Sensitivity: N BC = 0.0
Month: Jun
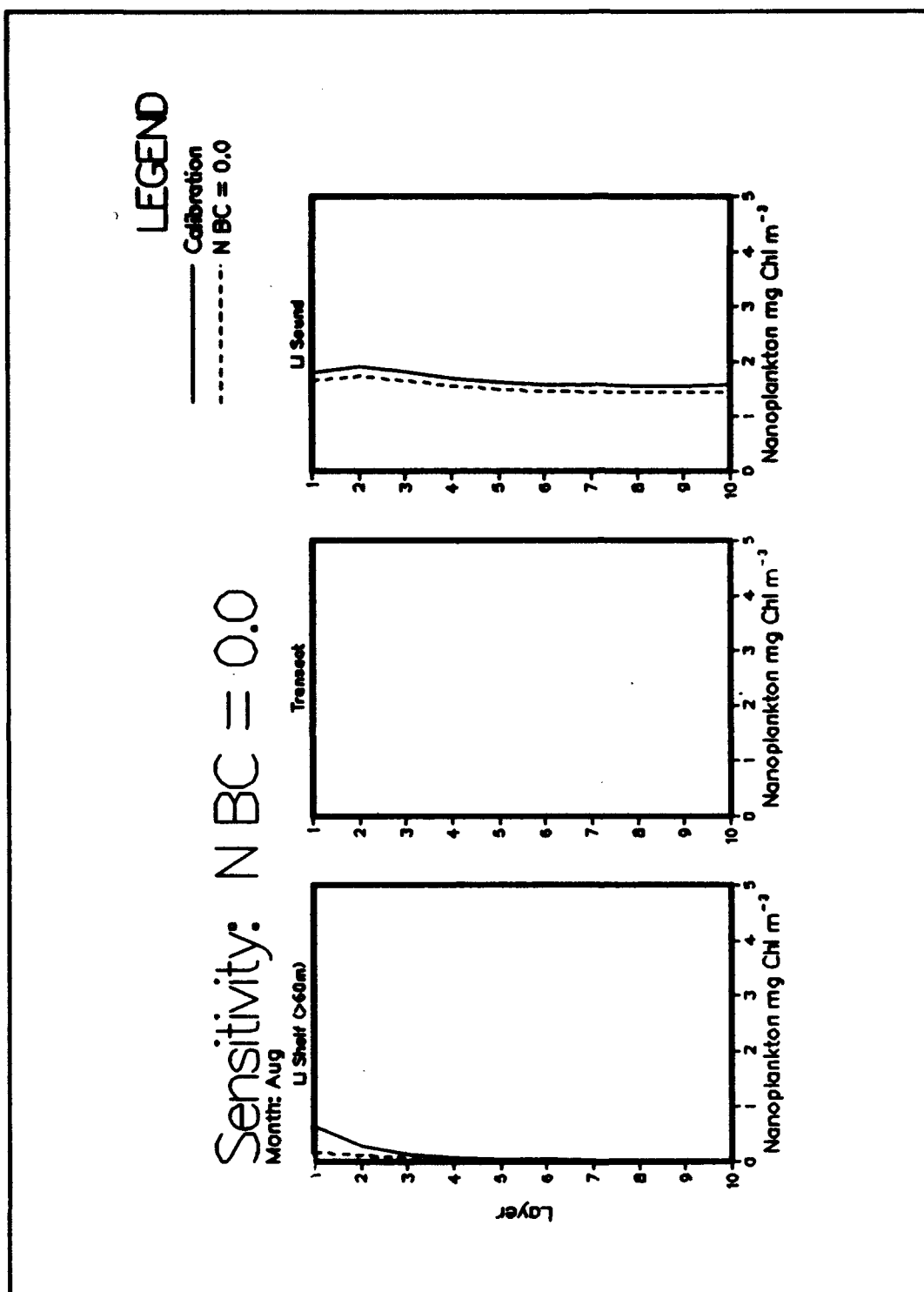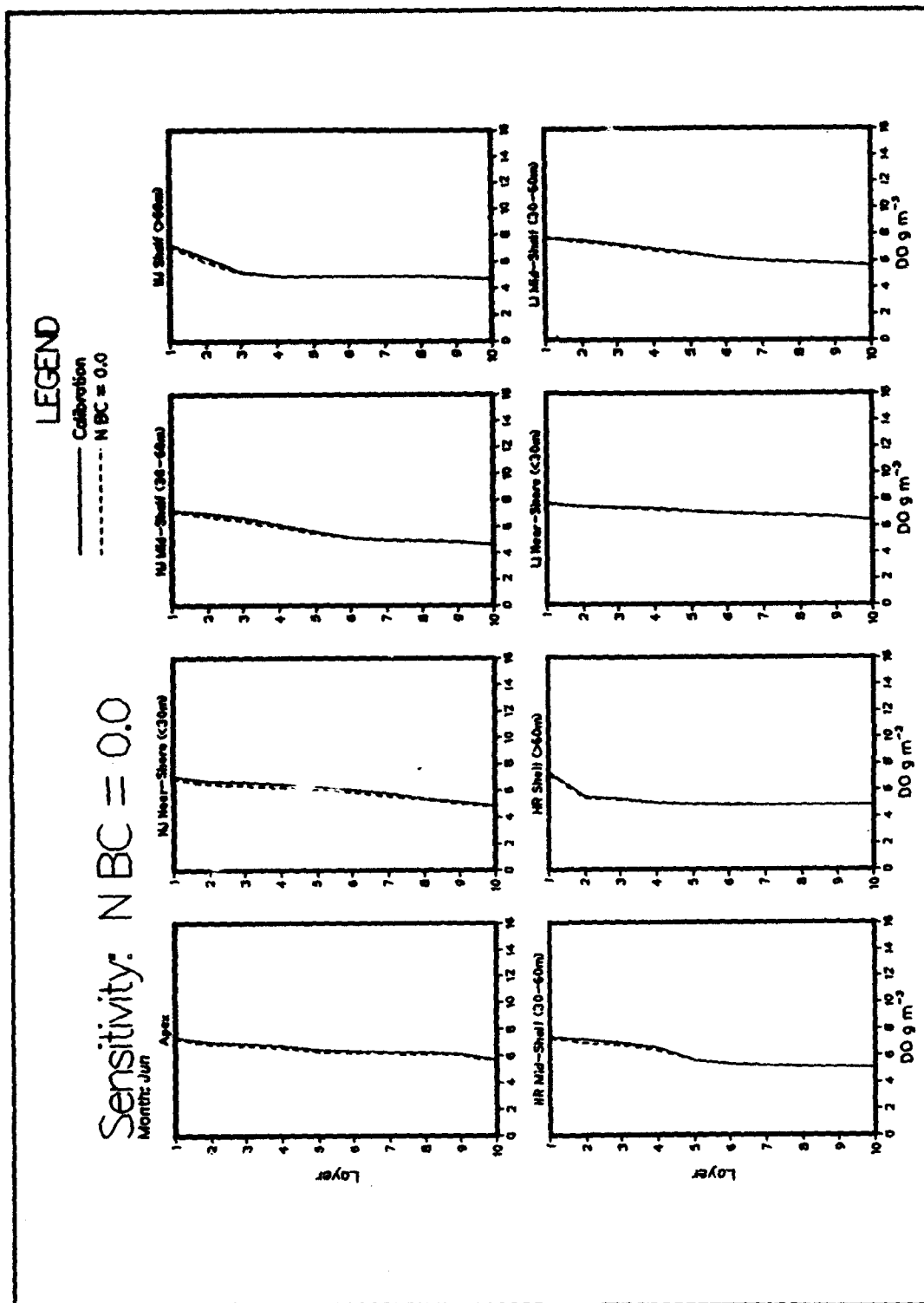
Plate E10. (Sheet 1 of 2)
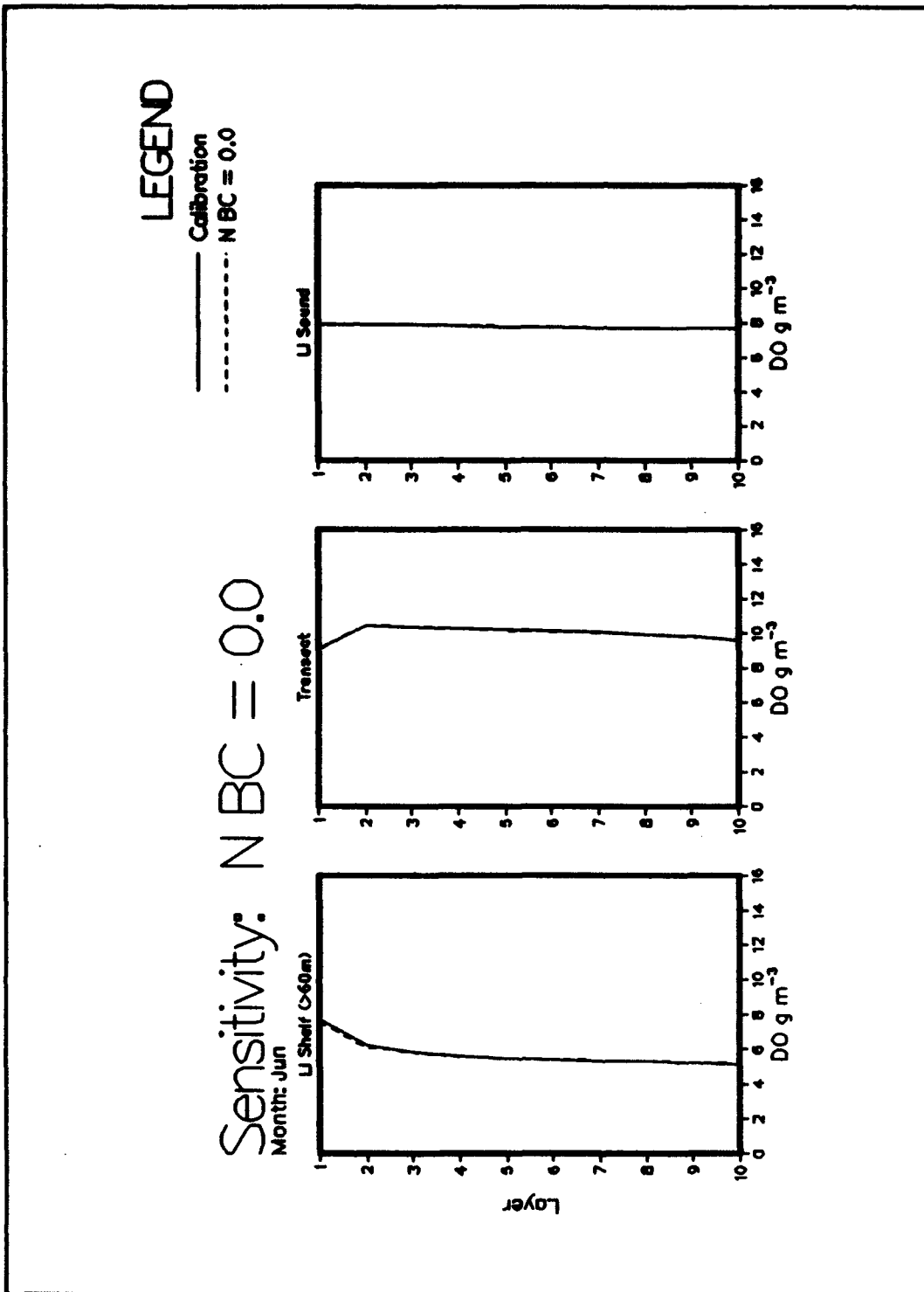
Plate E10. (Sheet 2 of 2)
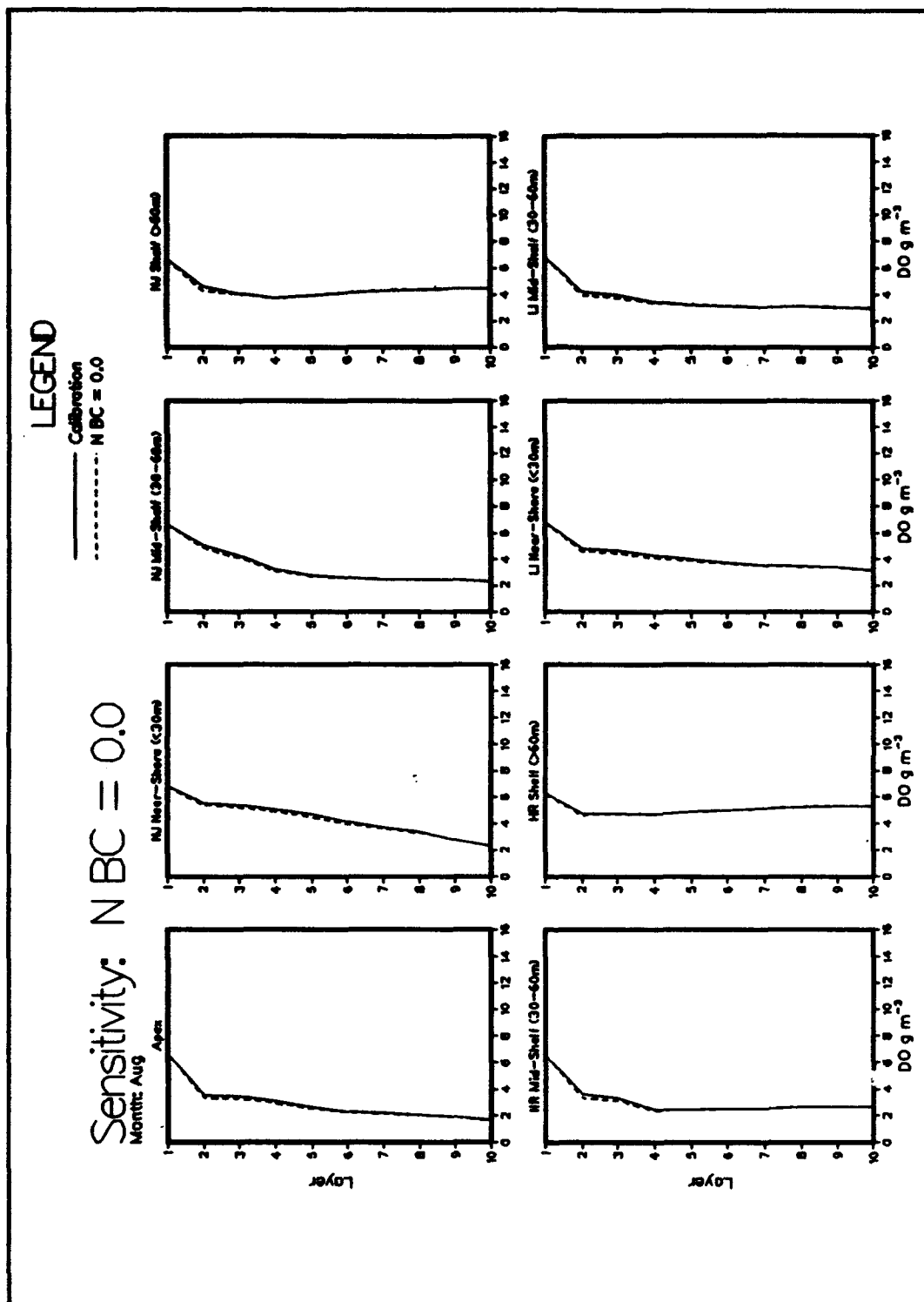
Plate E11.   (Sheet 1 of 2)

Sensitivity: N BC = 0.0
Month: Aug

LEGEND
Calibration
N BC = 0.0
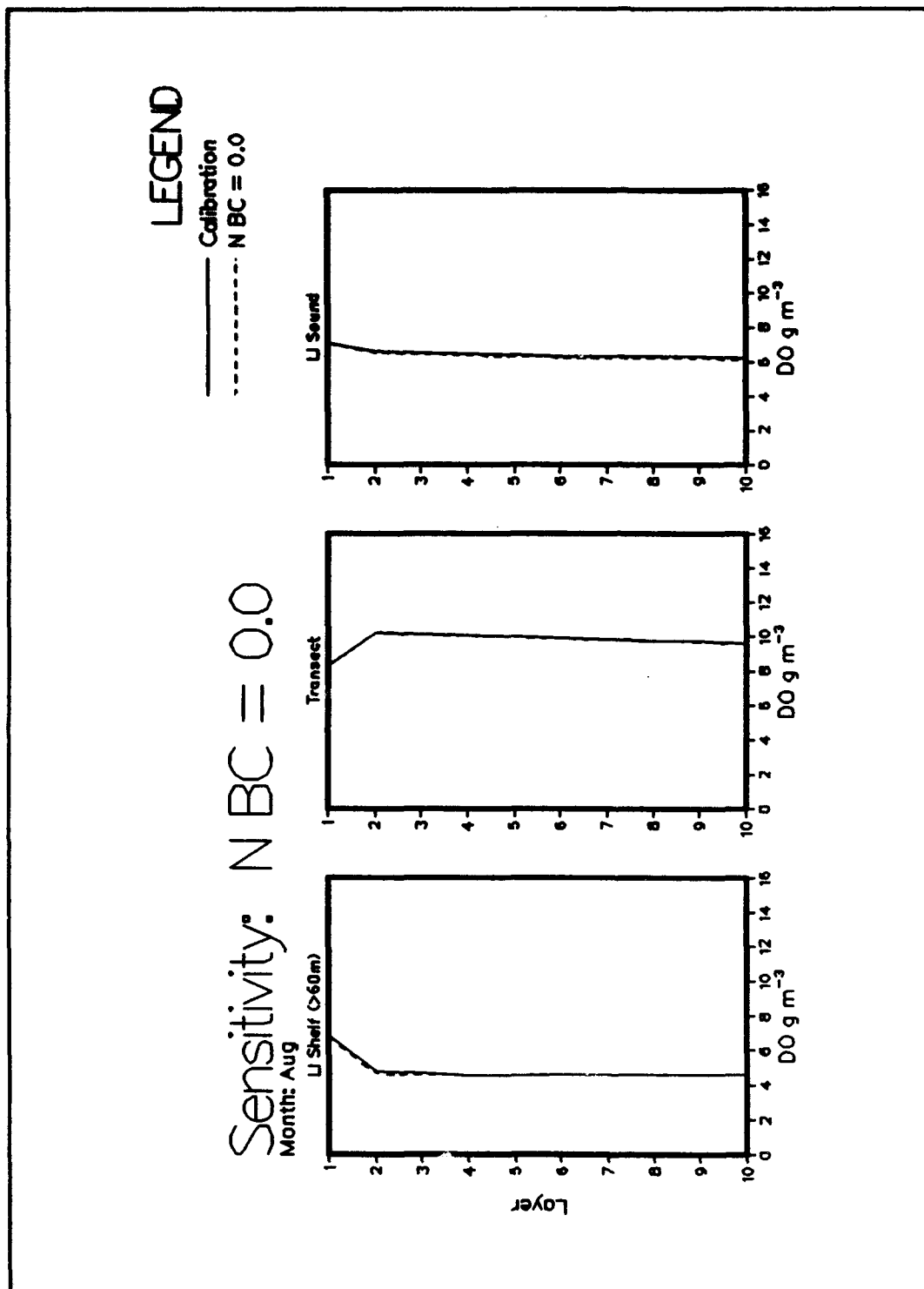
Plate E11. (Sheet 2 of 2)

E22

NEW YORK BIGHT

Aggregated by Area, Layer, and Month - 1976

Sensitivity: N Boundary Conditions=2*
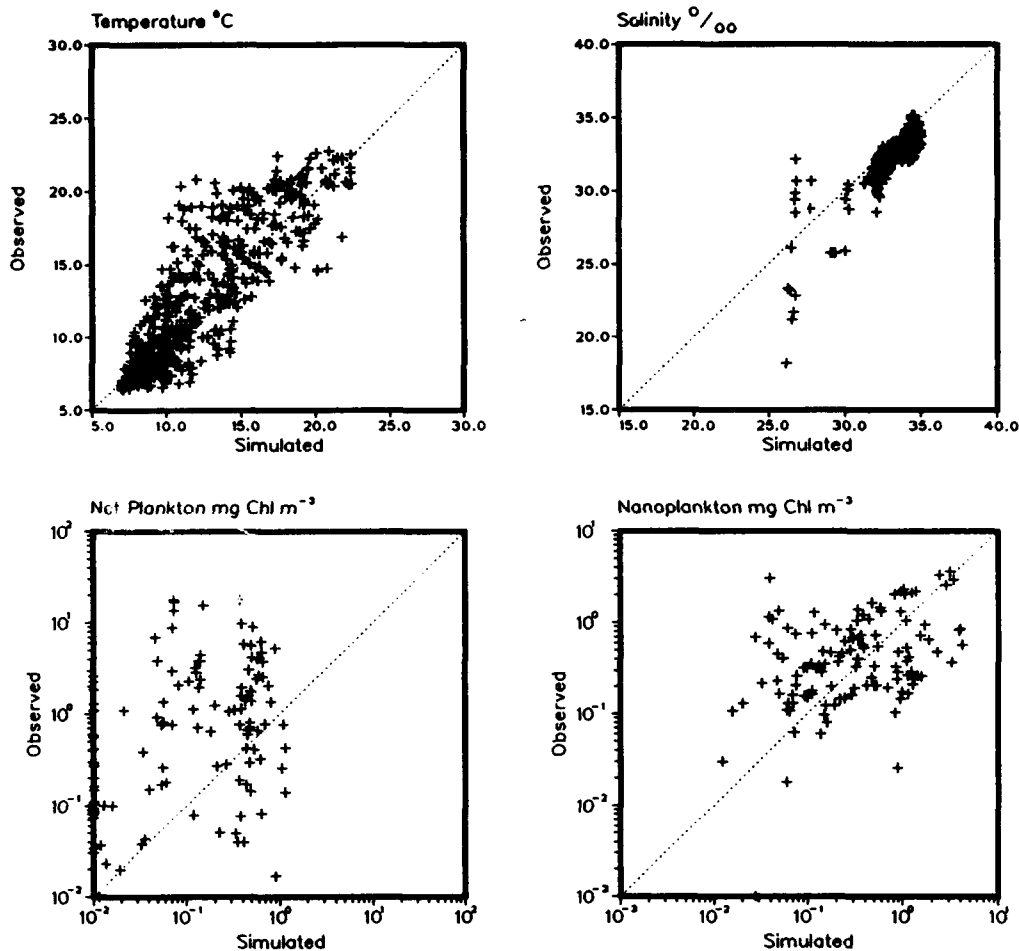
Plate E12.   (Sheet 1 of 3)

NEW YORK BIGHT

Aggregated by Area, Layer, and Month - 1976

Sensitivity: N Boundary Conditions=2*
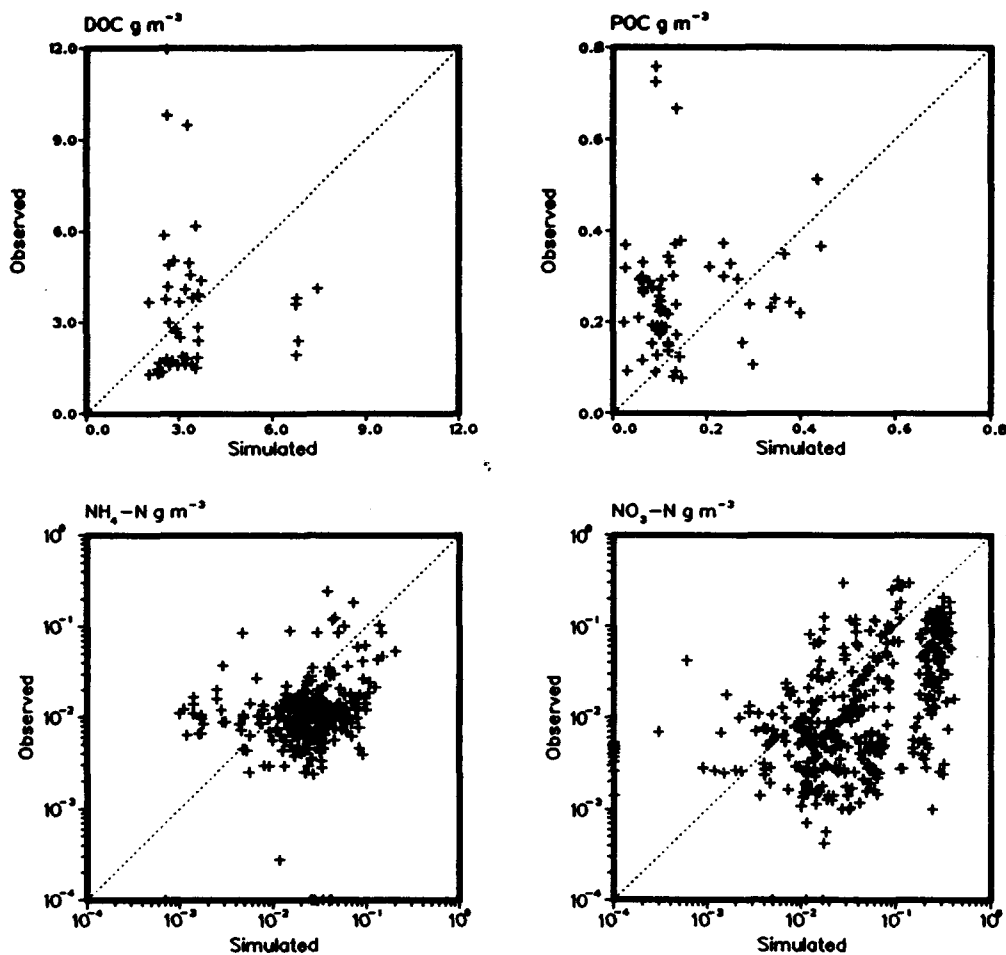
Plate E12. (Sheet 2 of 3)

NEW YORK BIGHT

Aggregated by Area, Layer, and Month - 1976

Sensitivity: N Boundary Conditions=2*

Plate E12. (Sheet 3 of 3)
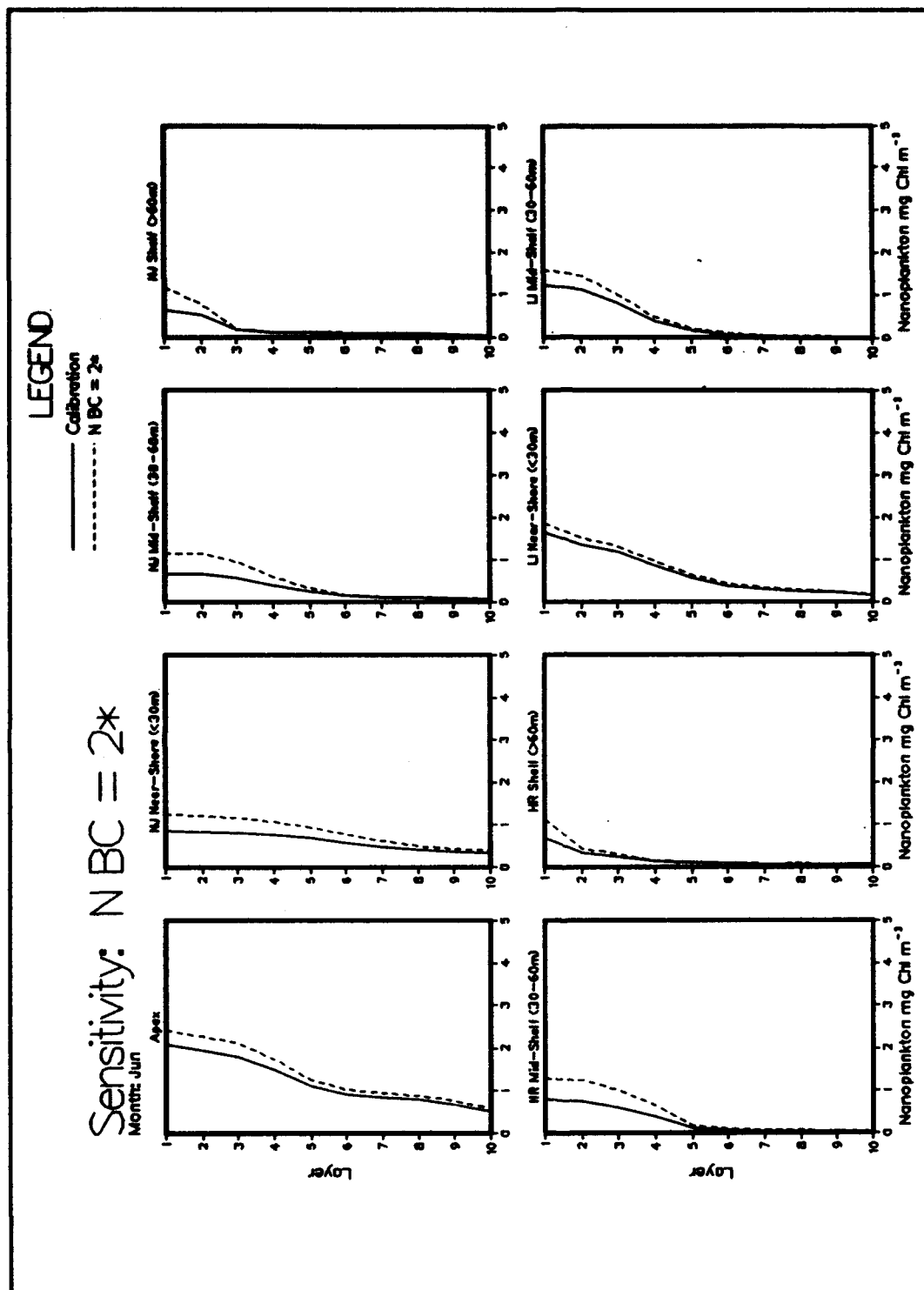
Plate E13. (Sheet 1 of 2)
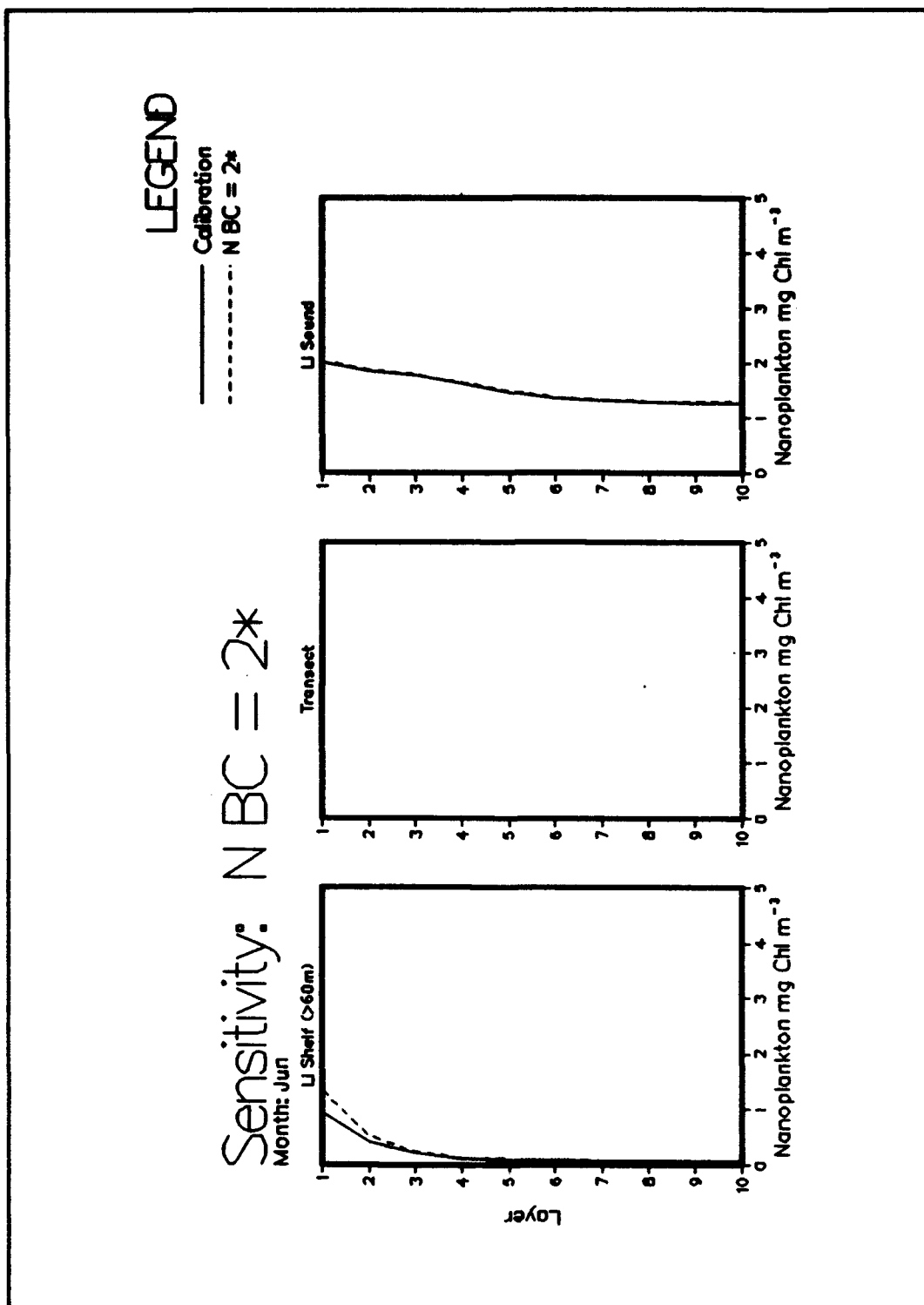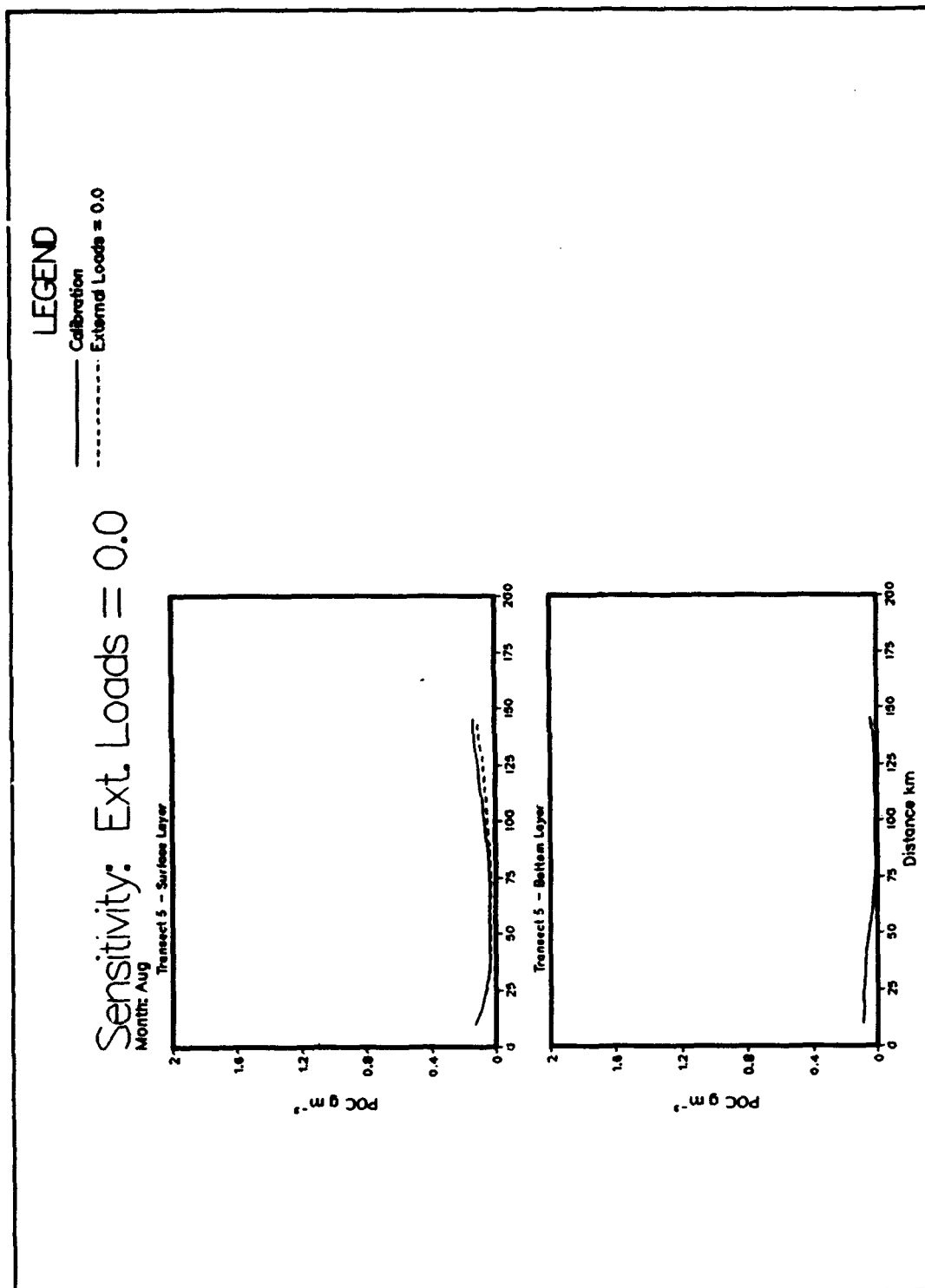
Plate E13.   (Sheet 2 of 2)
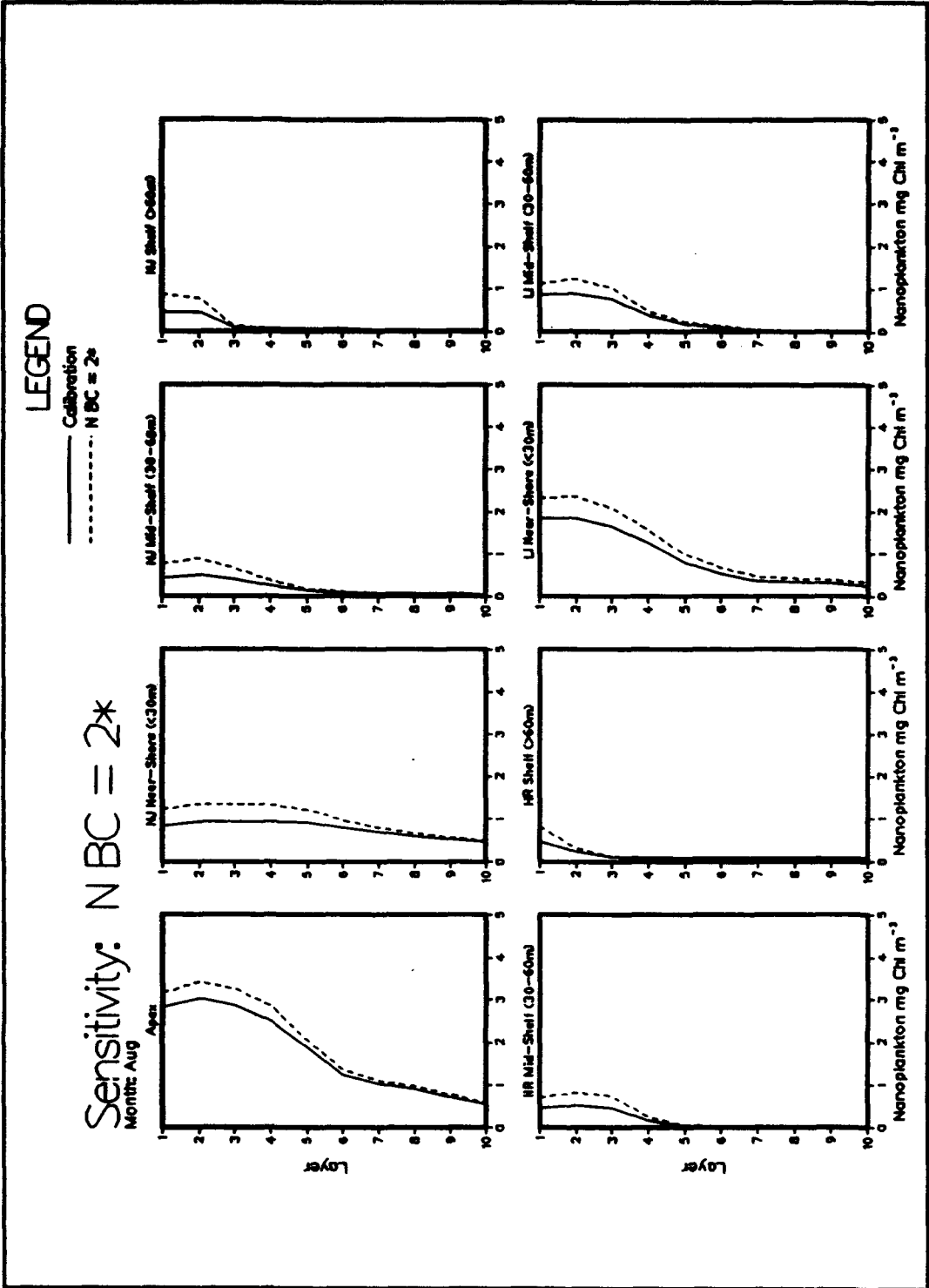
Plate E14. (Sheet 1 of 2)

Plate E14.   (Sheet 2 of 2)

Plate E15. (Sheet 1 of 2)
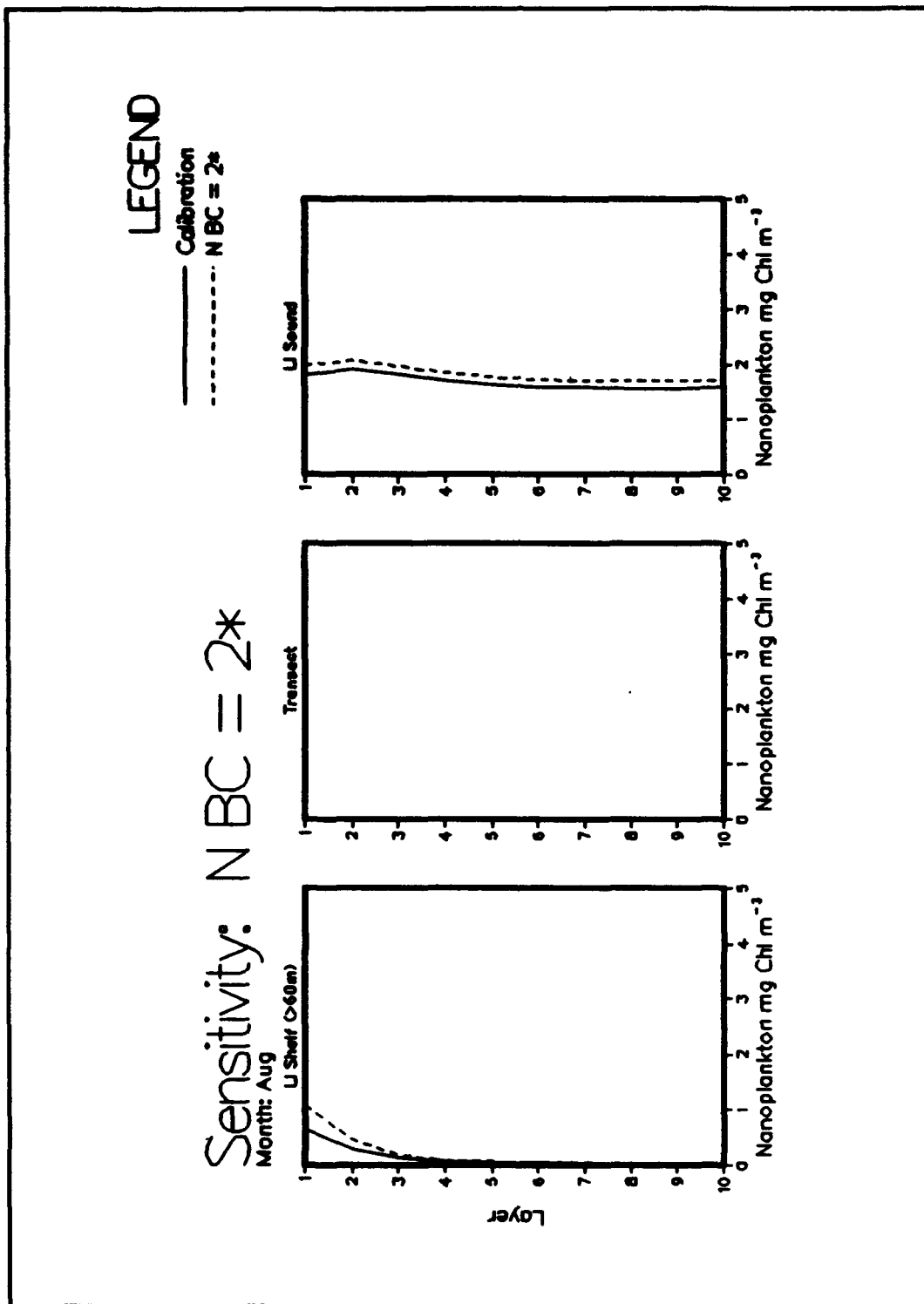
Plate E15.   (Sheet 2 of 2)

Sensitivity: N BC = 2*
Month: Aug
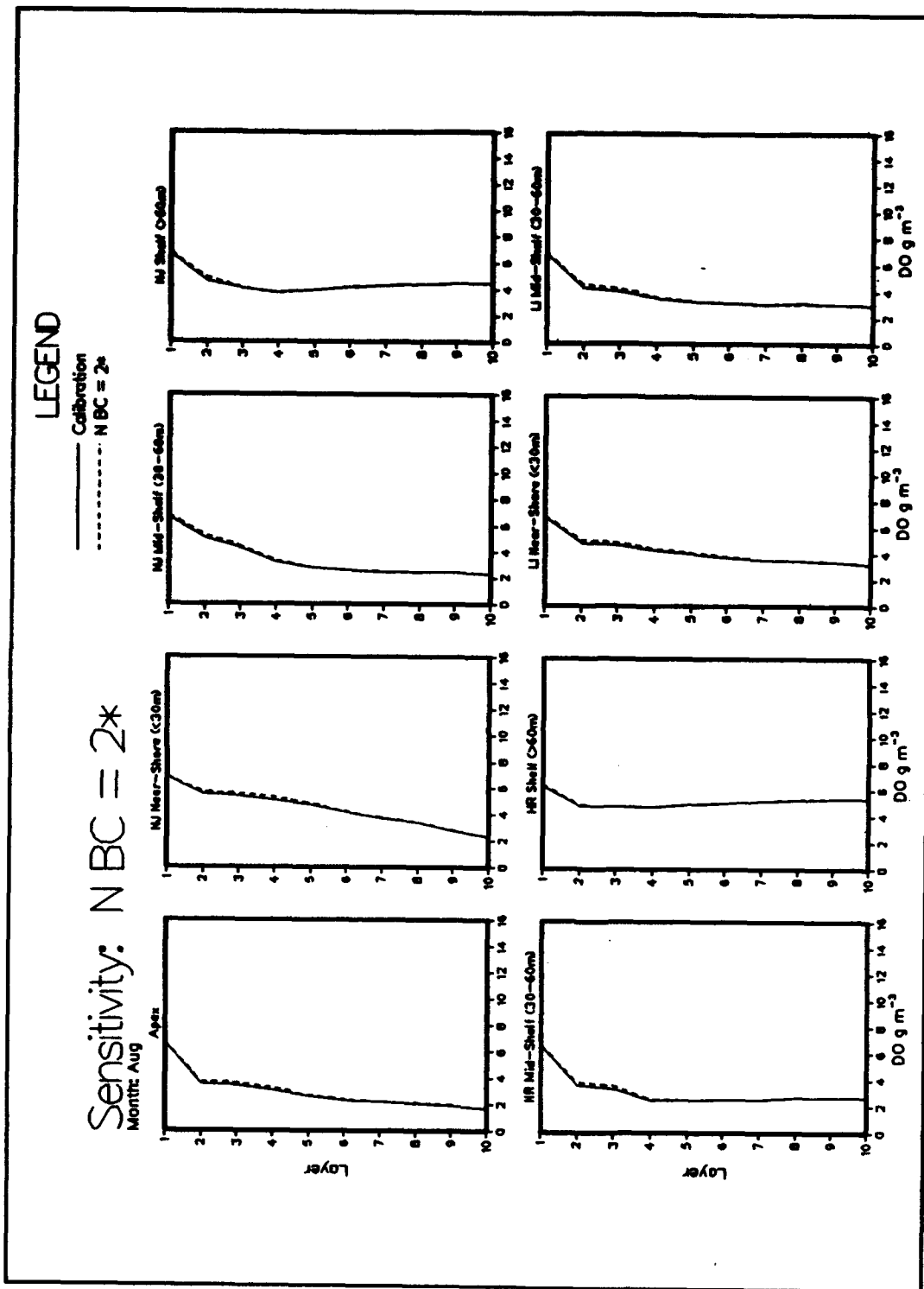
Plate E16. (Sheet 1 of 2)
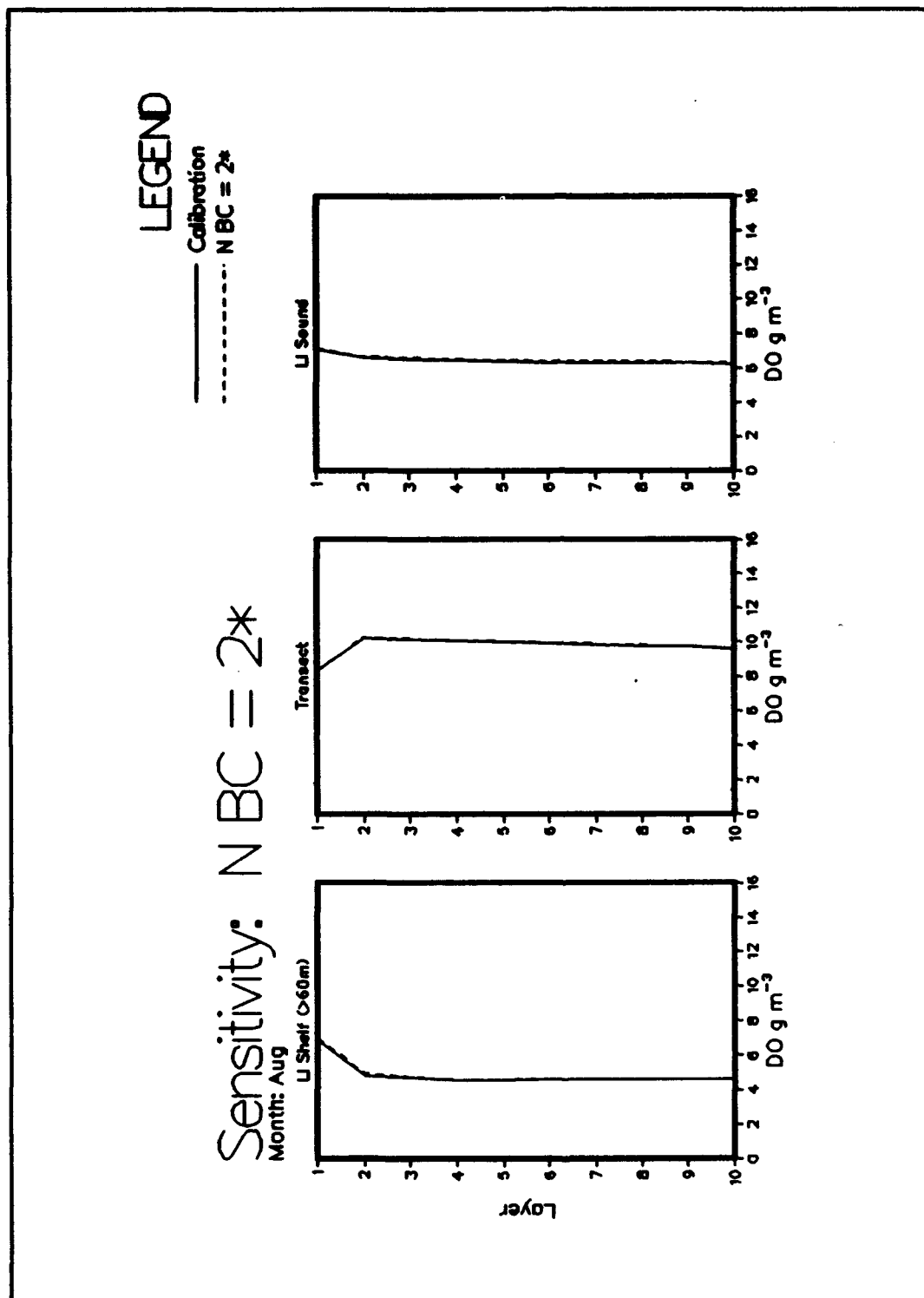
Plate E16.   (Sheet 2 of 2)

Appendix F
Demonstration Scenario Plots

NEW YORK BIGHT

Aggregated by Area, Layer, and Month - 1976
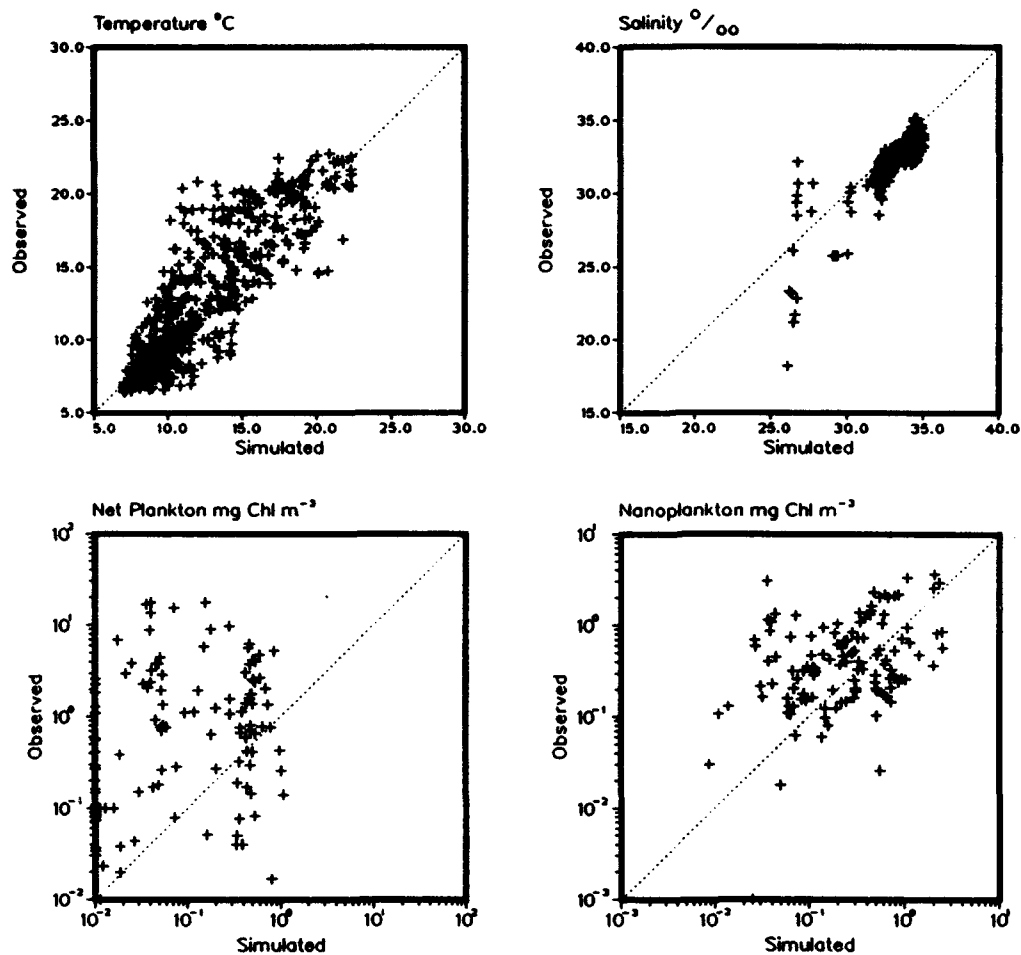
Sensitivity: External Loads=0.0

Plate F1.   (Sheet 1 of 3)

NEW YORK BIGHT
Aggregated by Area, Layer, and Month - 1976
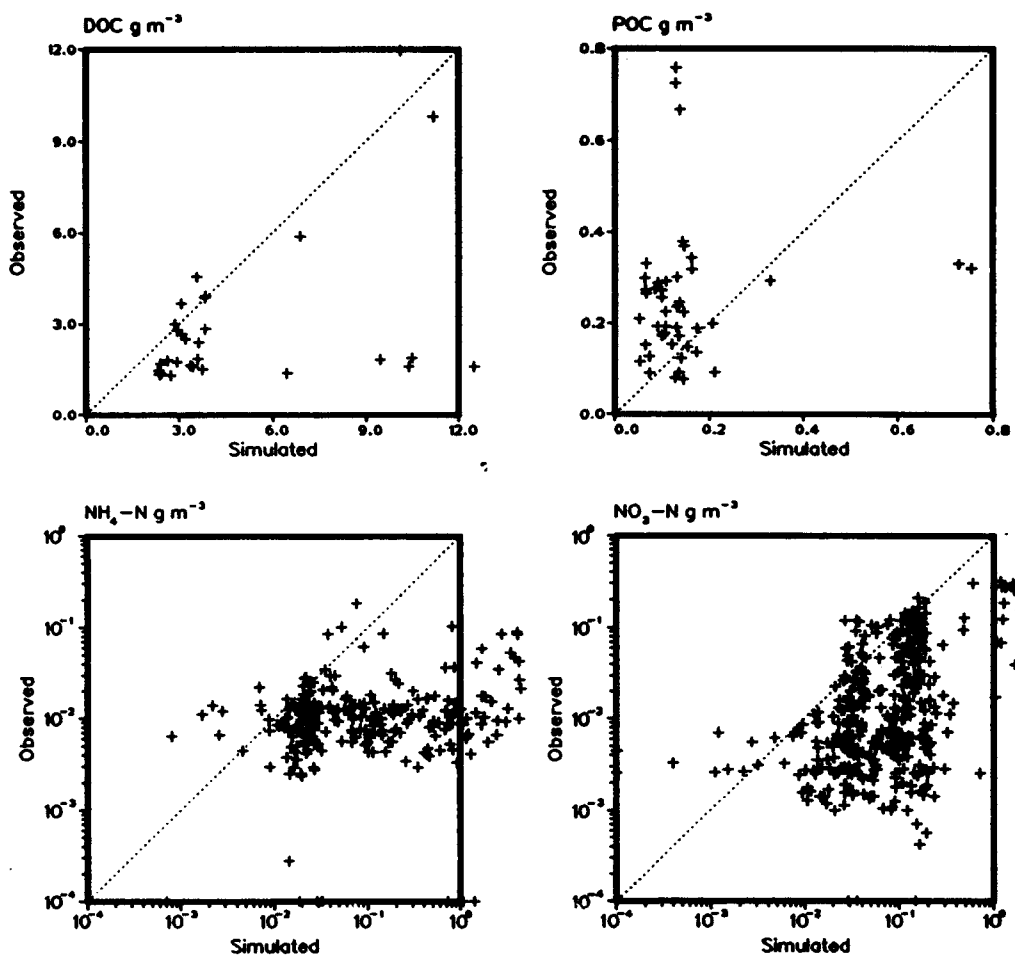
Sensitivity: External Loads=0.0
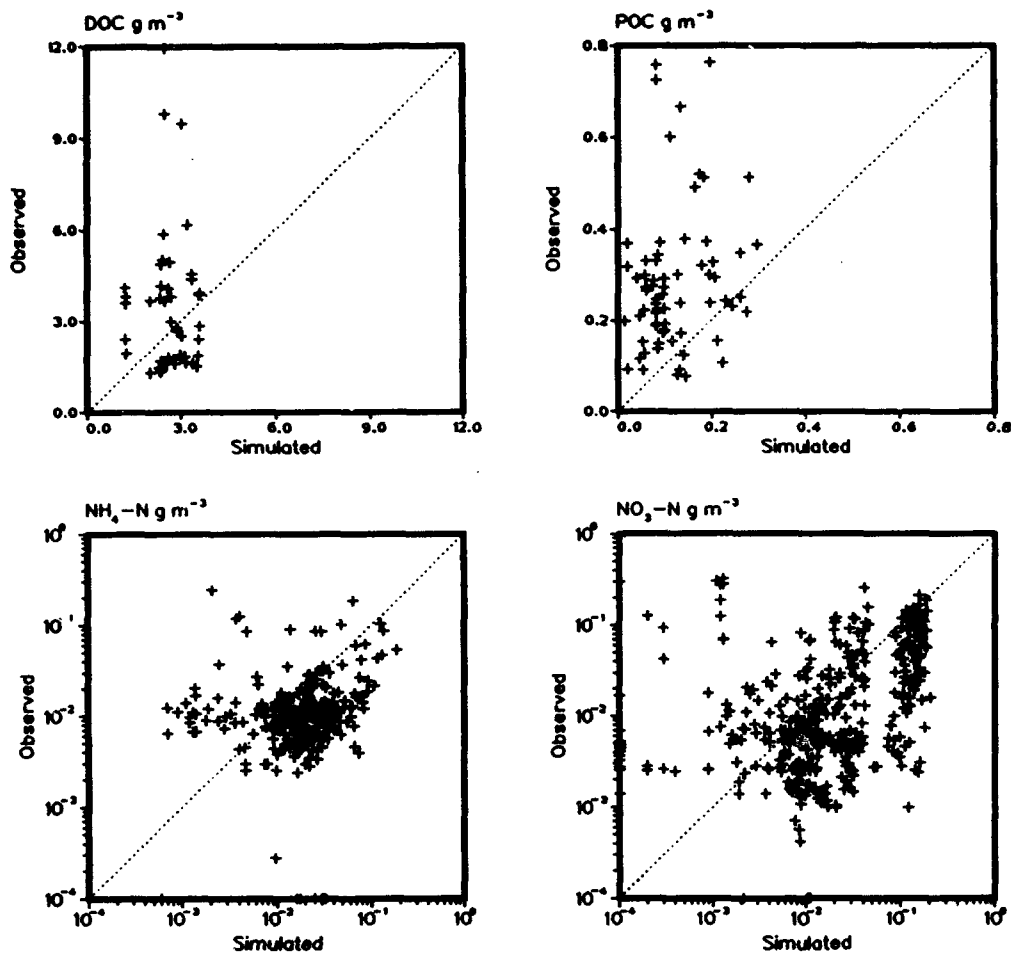
Plate F1.   (Sheet 2 of 3)

NEW YORK BIGHT
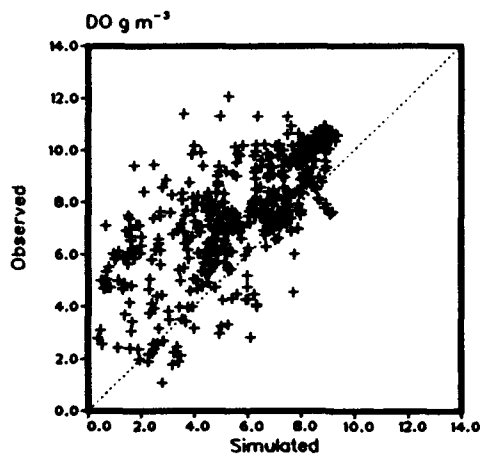### Aggregated by Area, Layer, and Month - 1976

Sensitivity: External Loads=0.0
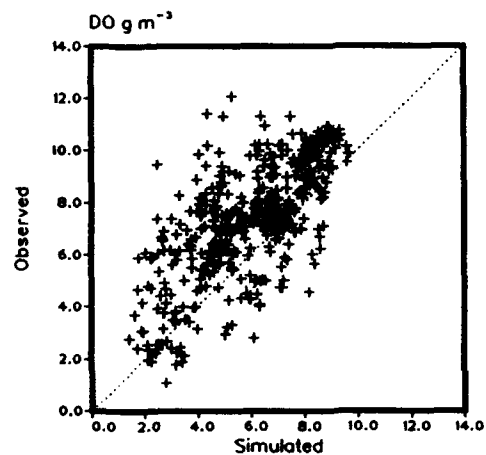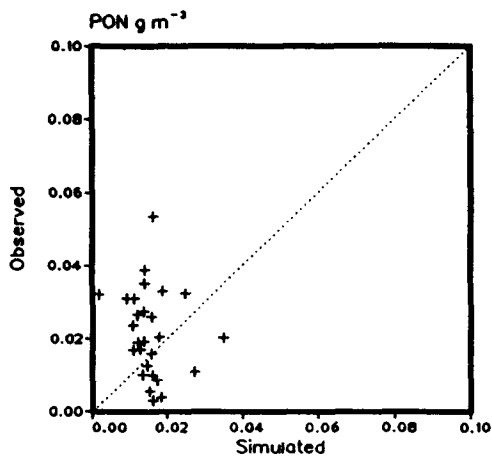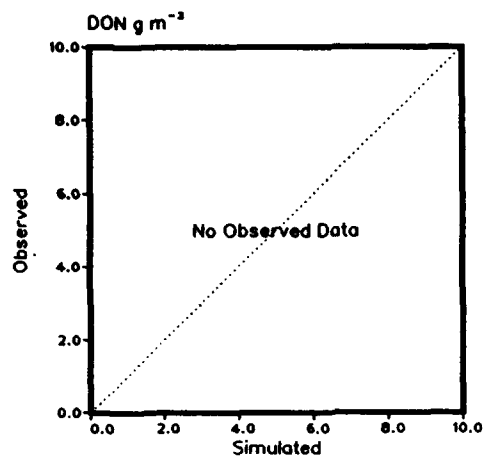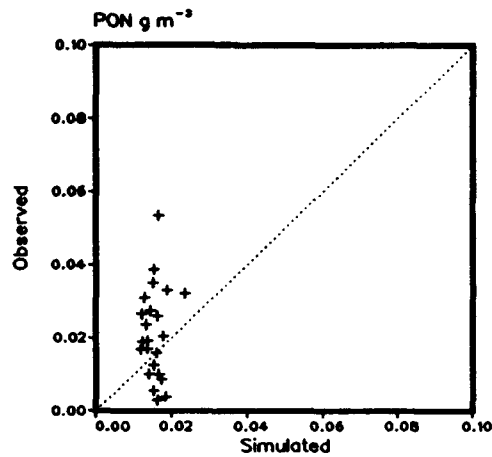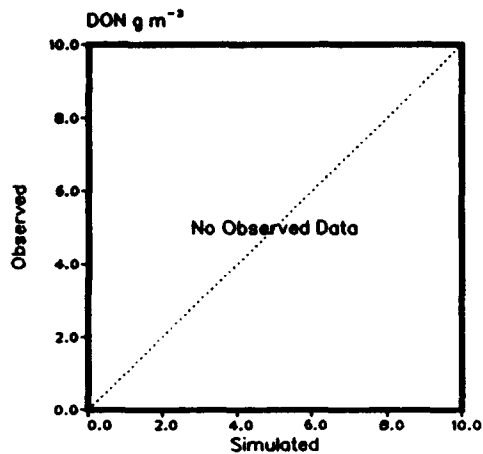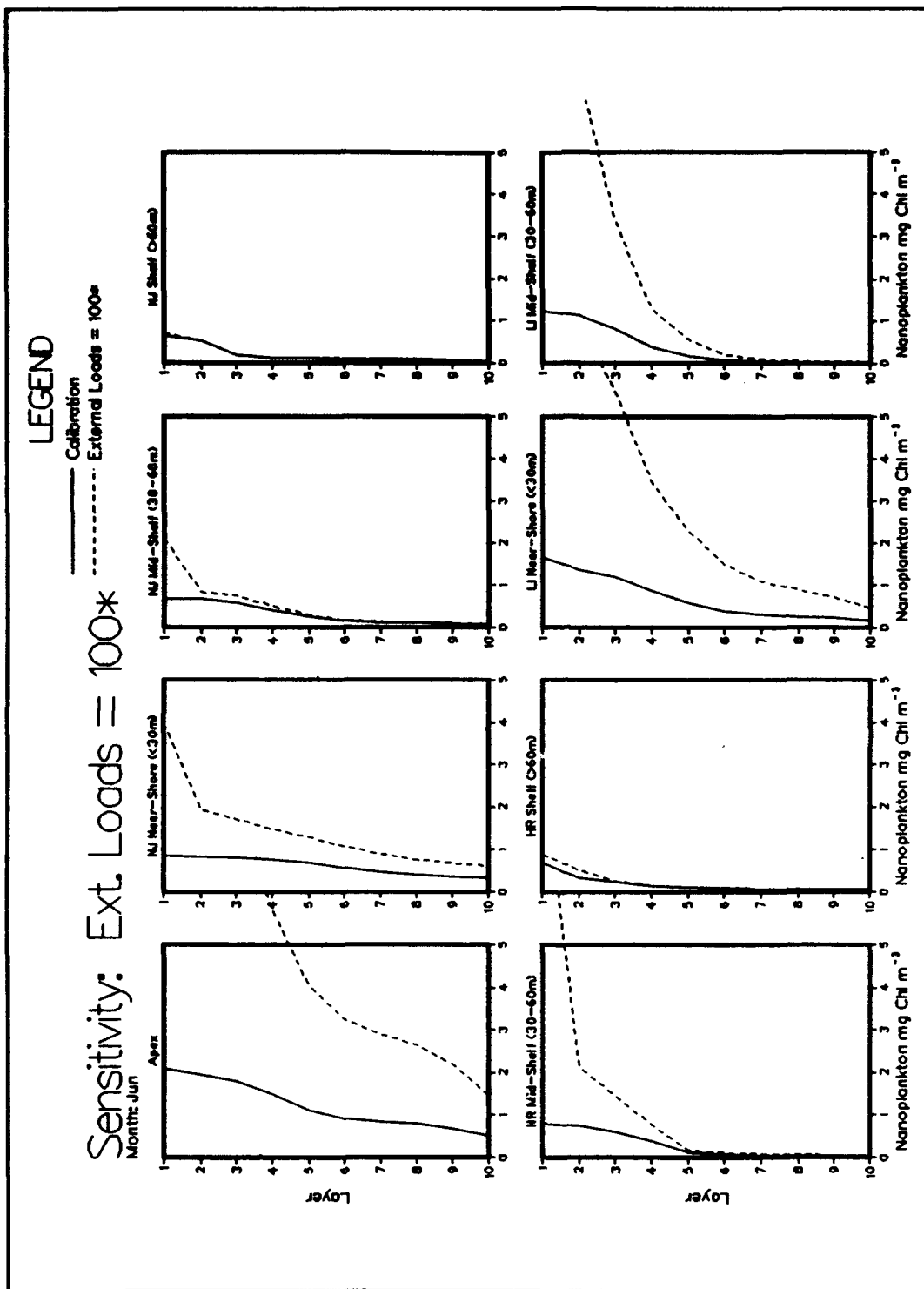
Plate F1.   (Sheet 3 of 3)
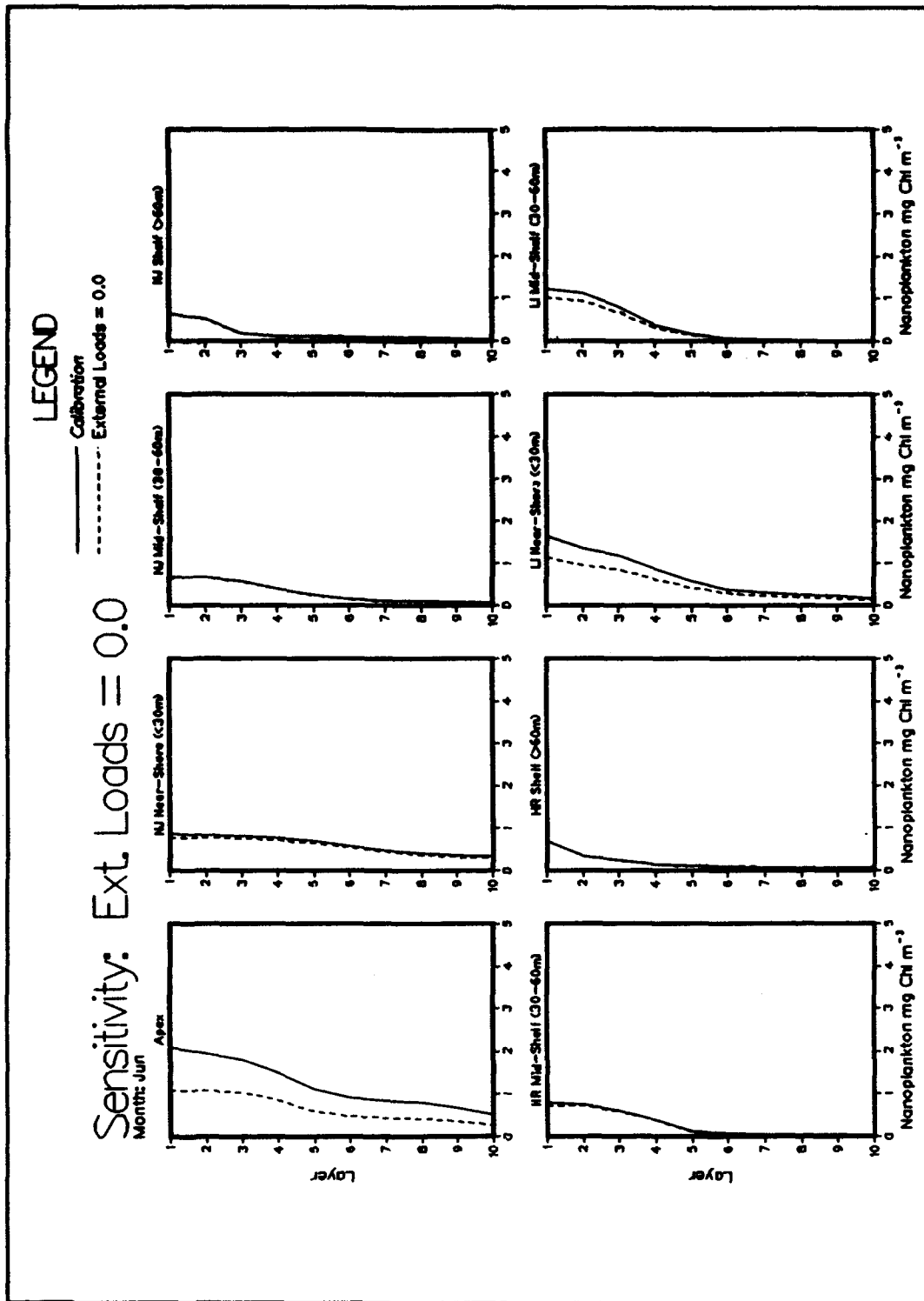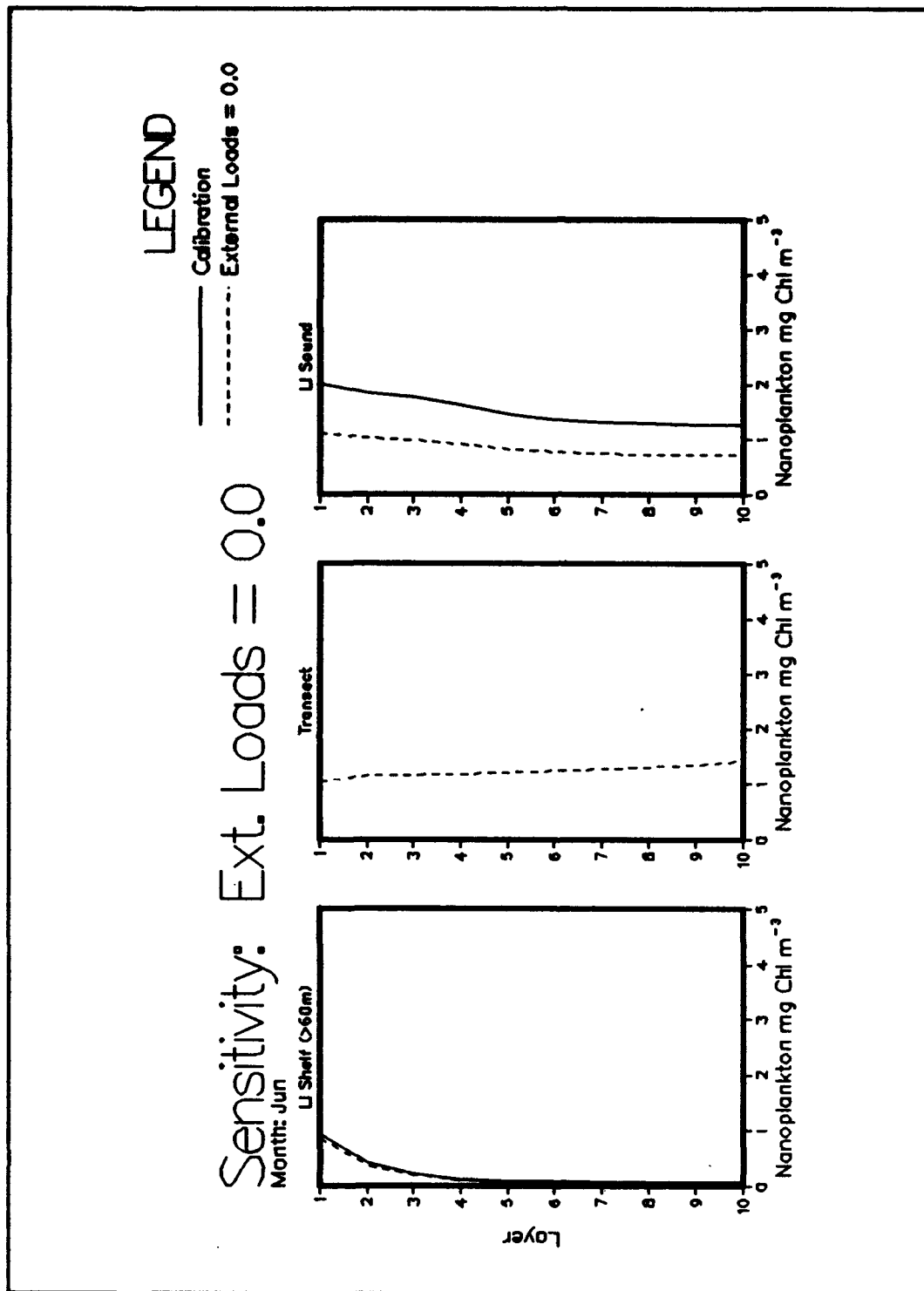
Plate F2. (Sheet 1 of 2)
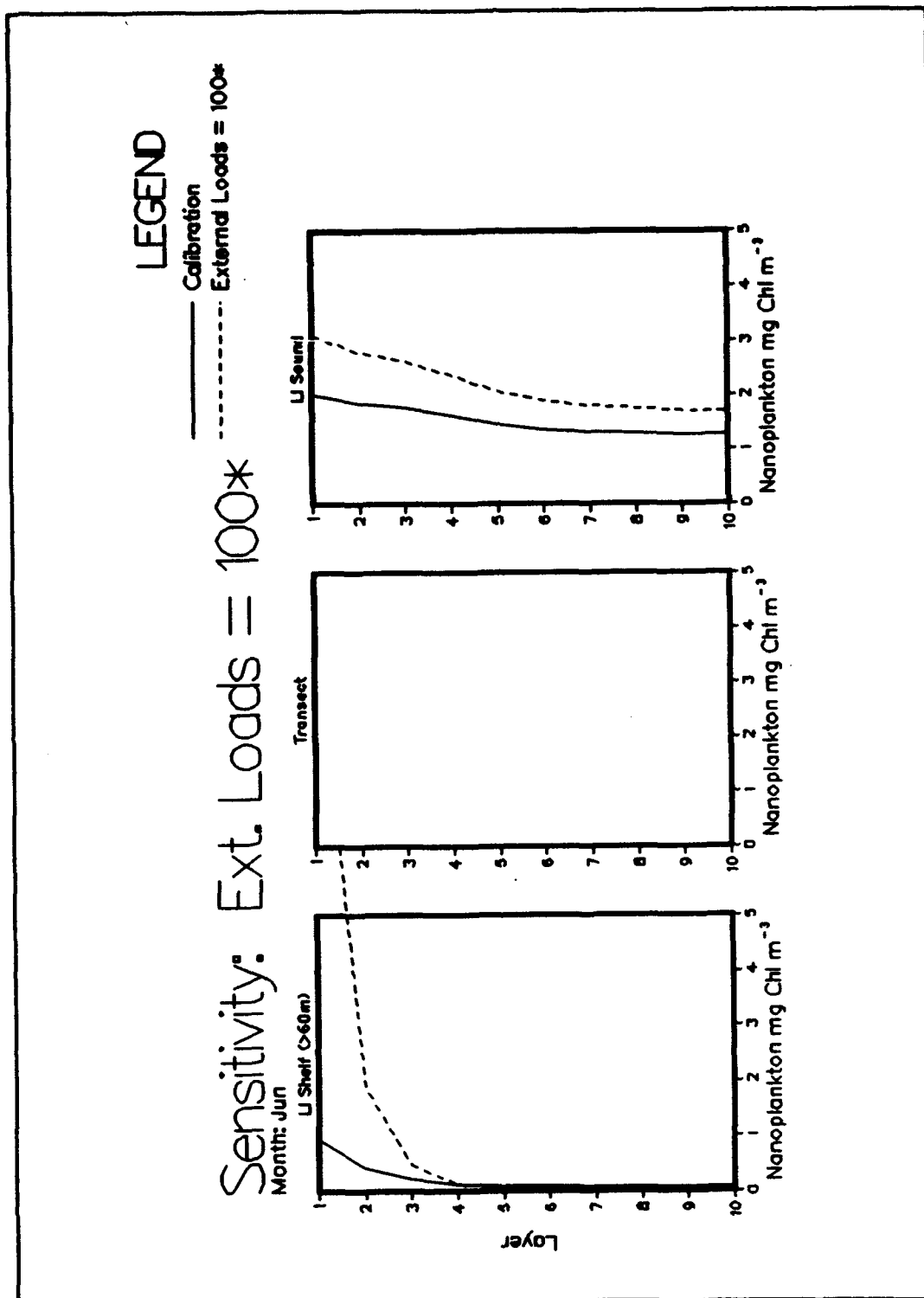
Plate F2.   (Sheet 2 of 2)
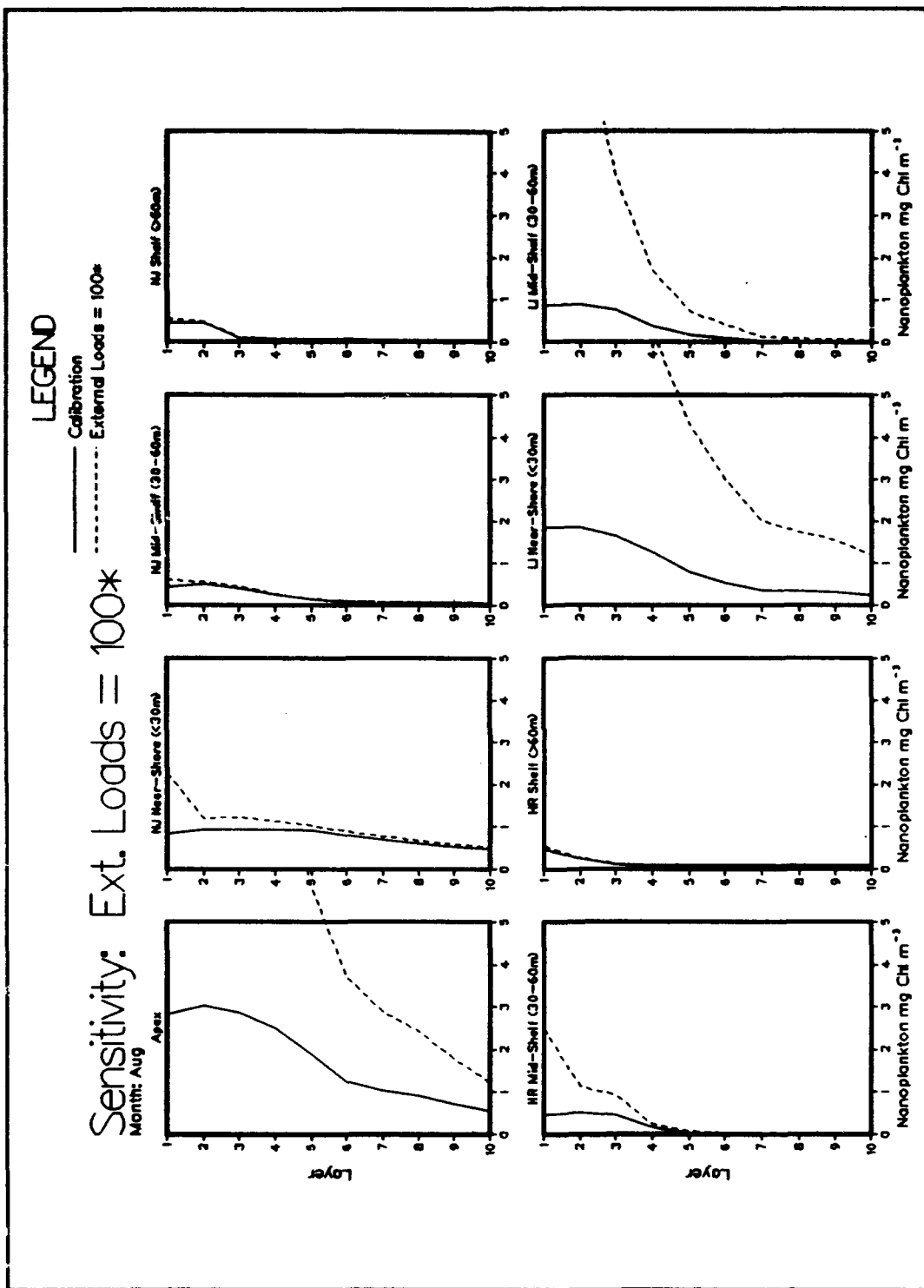
Plate F3.   (Sheet 1 of 2)
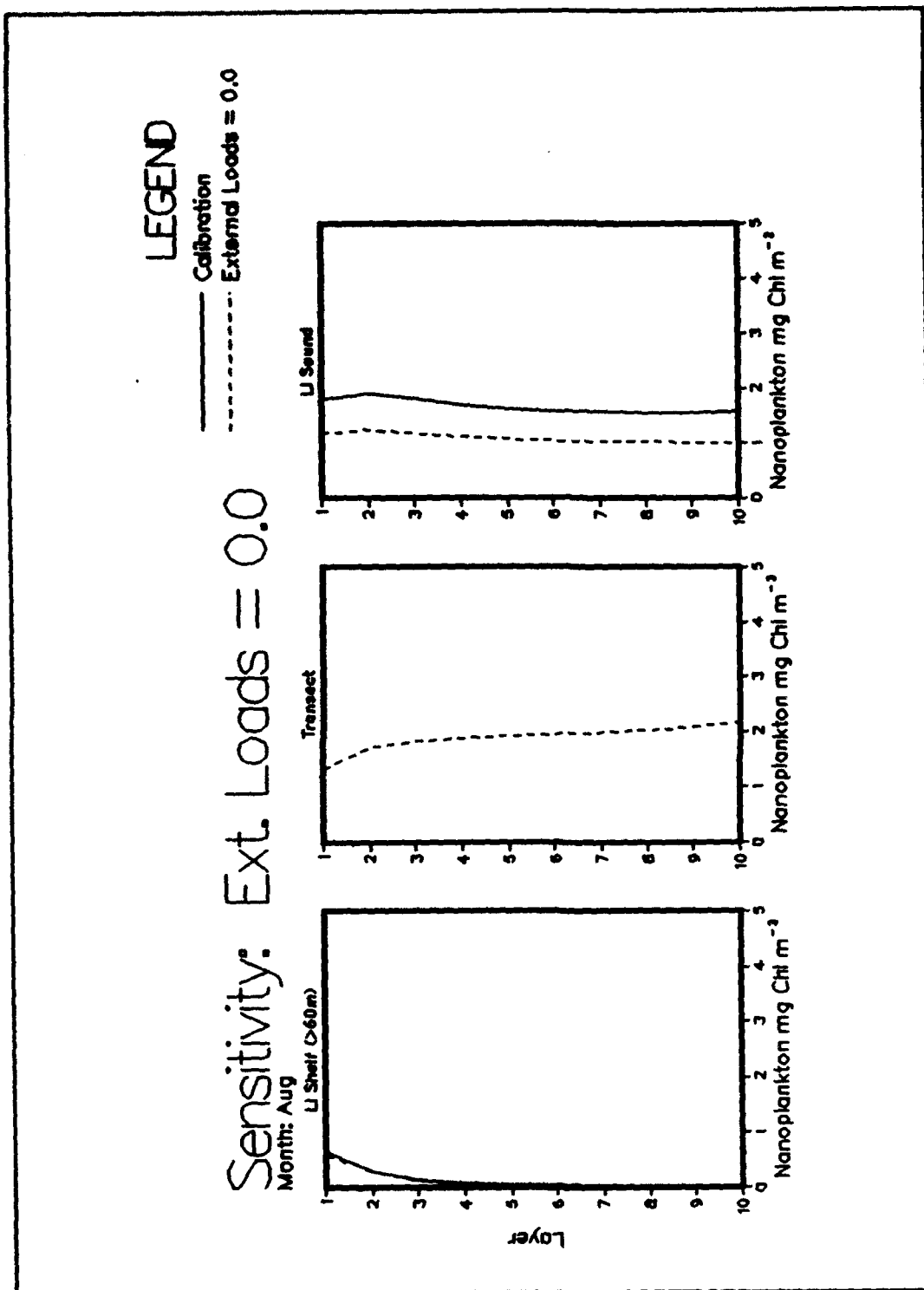
Plate F3. (Sheet 2 of 2)

Plate F4. (Sheet 1 of 2)

Plate F4. (Sheet 2 of 2)

Appendix F Demonstratin Scenario Plots

Plate F5.   (Sheet 1 of 2)

Appendix F   Demonstration Scenario Plots

Sensitivity: Ext. Loads = 0.0

LEGEND
— Calibration
---- Extend Loads = 0.0

Plate F5. (Sheet 2 of 2)

Sensitivity: Ext. Loads = 0.0

Plate F6. (Sheet 1 of 2)

Sensitivity: Ext. Loads = 0.0
Month: Jun

LEGEND
Calibration
External Loads = 0.0

Plate F6. (Sheet 2 of 2)

Appendix F   Demonstratin Scenario Plots

Plate F7.   (Sheet 1 of 2)

Sensitivity: Ext. Loads = 0.0
Month: Aug

LEGEND
Calibration
External Loads = 0.0

U Shelf (>60m)

Transect

U Sound

Layer

POC g m⁻³
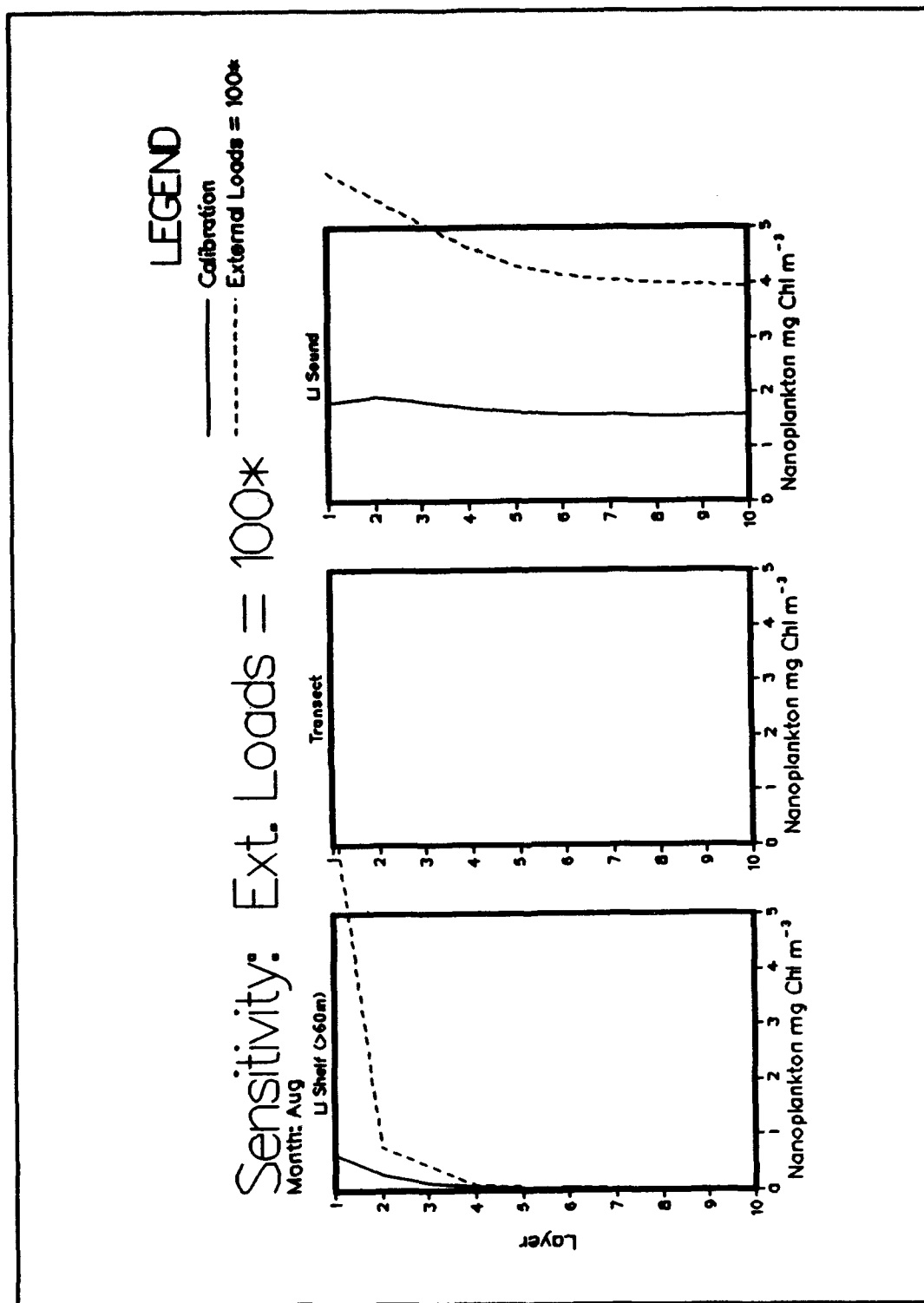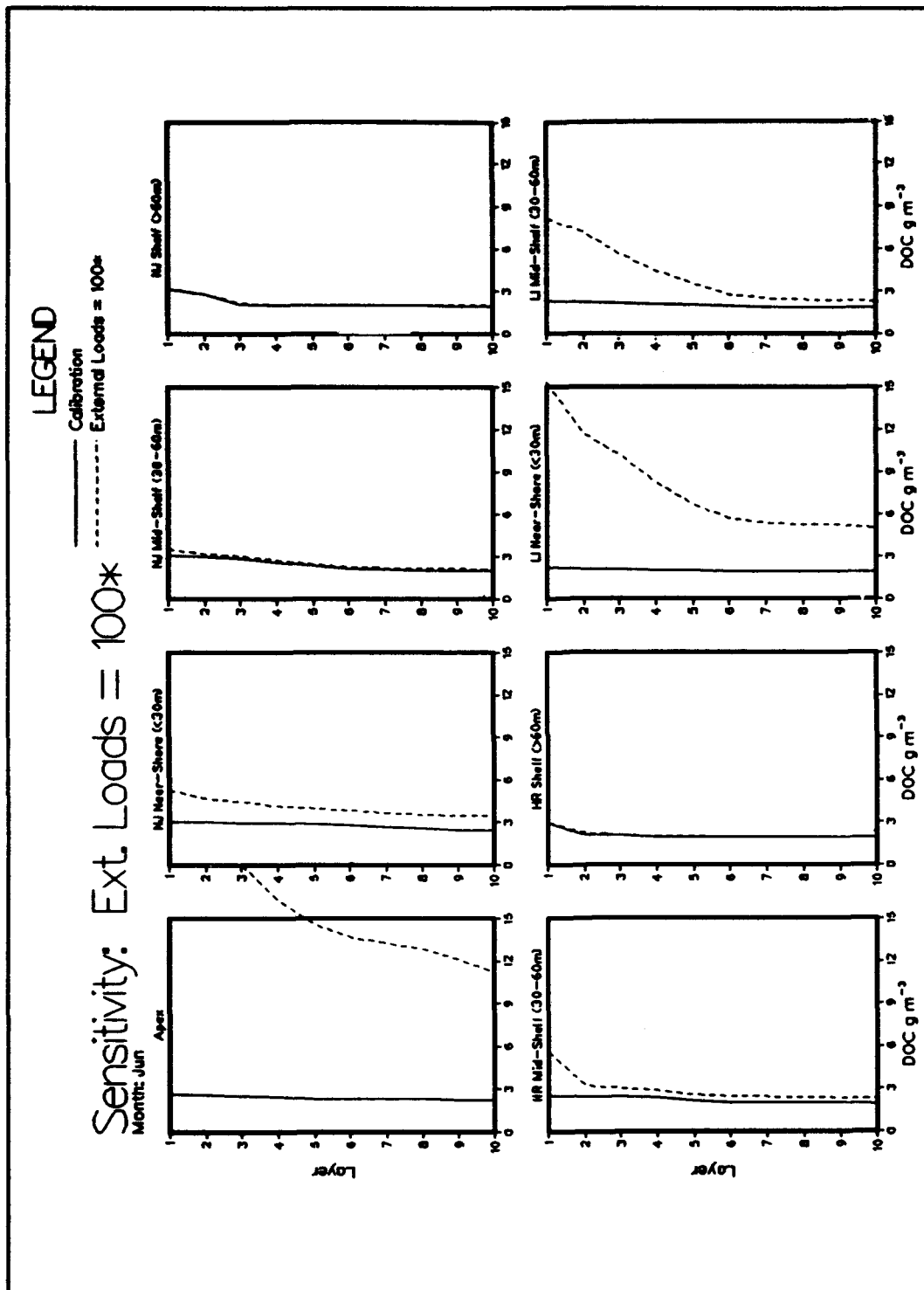
Plate F7. (Sheet 2 of 2)

Plate F8.   (Sheet 1 of 2)

Plate F8. (Sheet 2 of 2)

Sensitivity: Ext. Loads = 0.0
Month: Aug
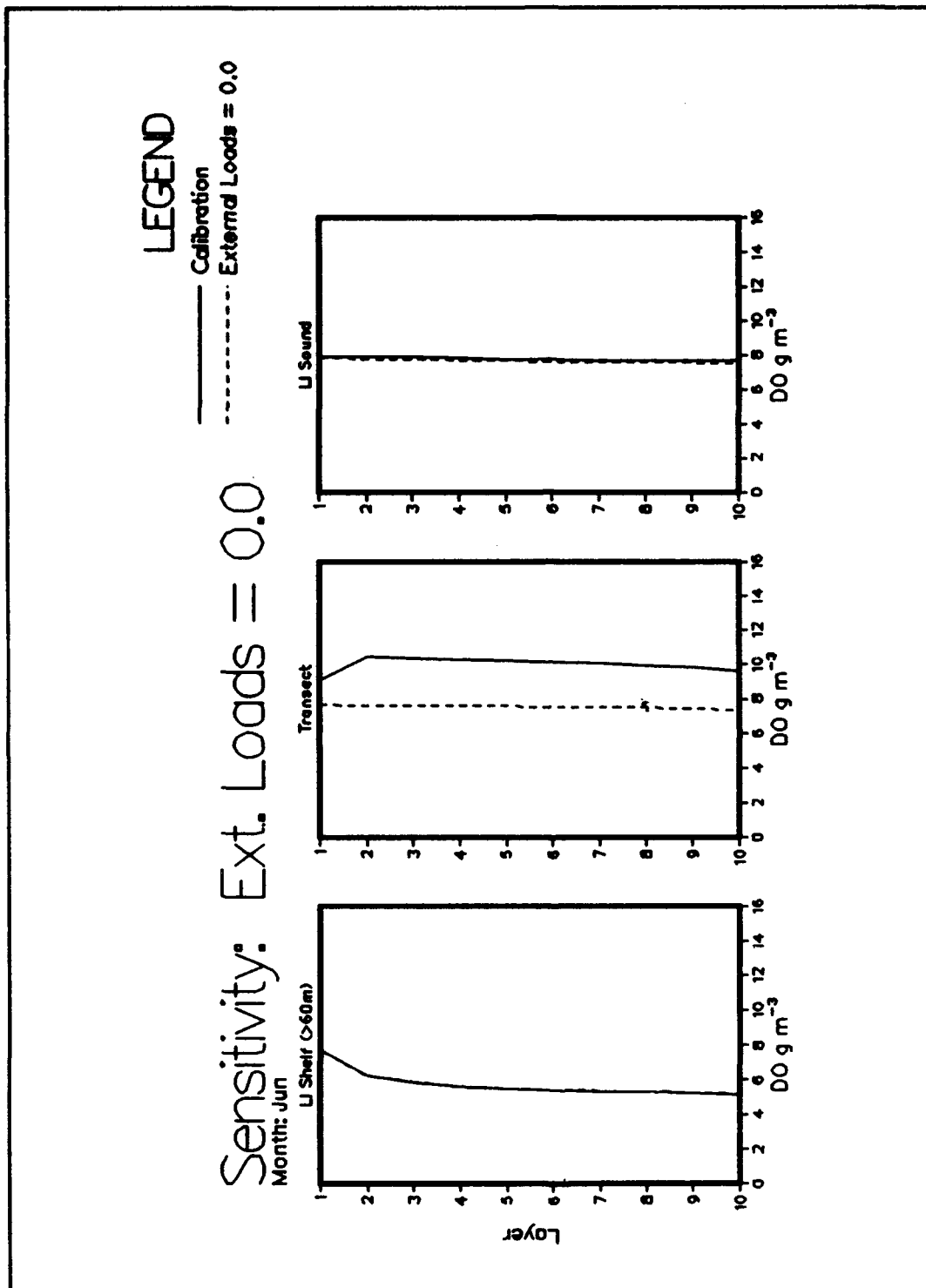
LEGEND
—— Calibration
-------- External Loads = 0.0
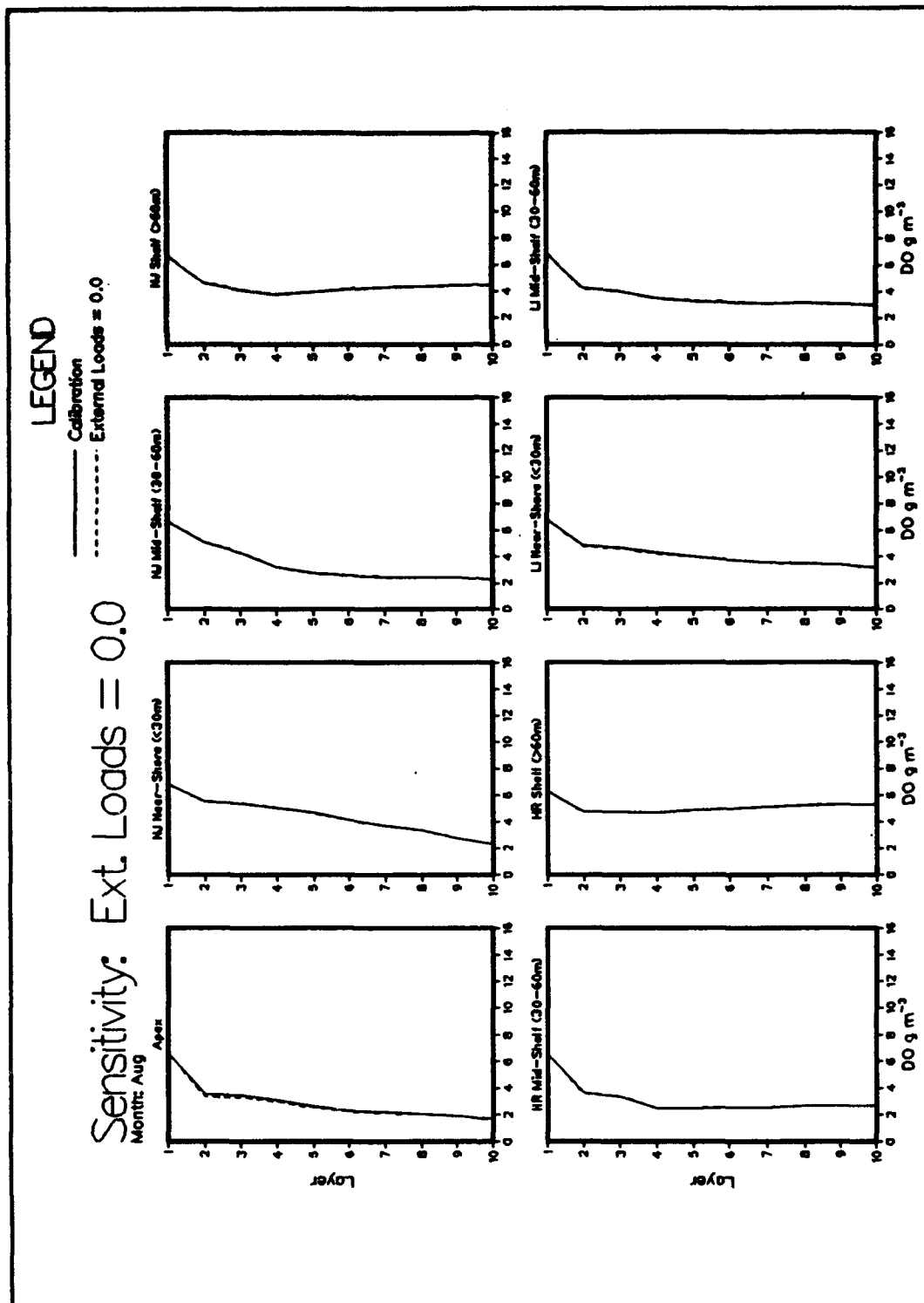
Plate F9.   (Sheet 1 of 2)

Sensitivity: Ext. Loads = 0.0

Plate F9. (Sheet 2 of 2)

Sensitivity: Ext. Loads = 0.0
Month: Jun

LEGEND
—— Calibration
------- External Loads = 0.0
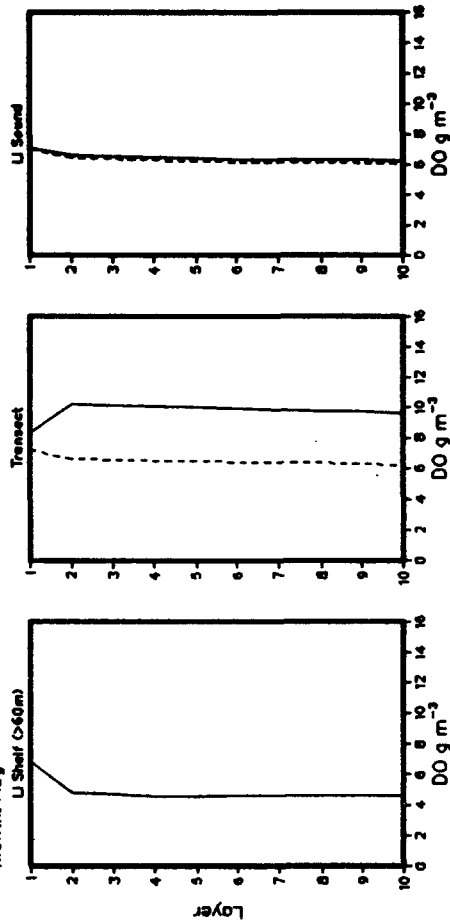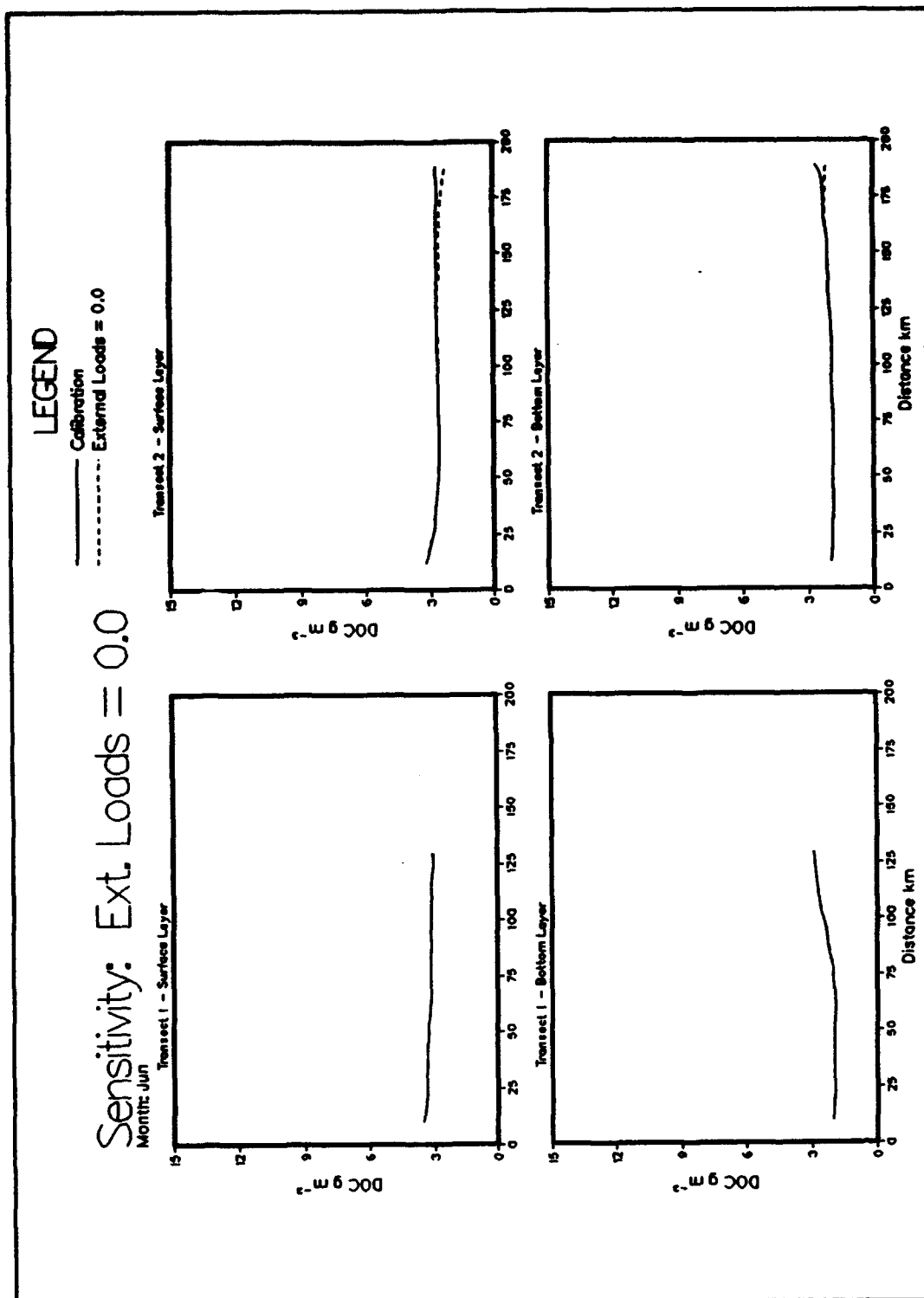
Plate F10.   (Sheet 1 of 3)

Plate F10.   (Sheet 2 of 3)

Sensitivity: Ext. Loads = 0.0

LEGEND

Calibration
Extended Loads = 0.0

Plate F10. (Sheet 3 of 3)

Plate F11.   (Sheet 1 of 3)

Plate F11. (Sheet 2 of 3)

LEGEND

—— Calibration
······· External Loads = 0.0

Sensitivity. Ext. Loads = 0.0
Month: Aug

Transect 5 – Surface Layer

Transect 5 – Bottom Layer

Distance km

DOC g m^{-3}

Plate F11.   (Sheet 3 of 3)

F26

Sensitivity: Ext. Loads = 0.0
Month: Jun

LEGEND
——— Calibration
········· External Loads = 0.0

Plate F12. (Sheet 1 of 3)

Sensitivity: Ext. Loads = 0.0
Month: Jun

LEGEND
Calibration
Extend Loads = 0.0

Transect 4 – Surface Layer
Transect 4 – Bottom Layer
Transect 3 – Surface Layer
Transect 3 – Bottom Layer

Plate F12. (Sheet 2 of 3)

Appendix F   Demonstratin Scenario Plots

Sensitivity: Ext. Loads = 0.0

LEGEND
Calibration
External Loads = 0.0

Plate F12.   (Sheet 3 of 3)

Sensitivity: Ext. Loads = 0.0

Plate F13. (Sheet 1 of 3)

Sensitivity: Ext. Loads = 0.0
Month: Aug

Plate F13. (Sheet 2 of 3)

Sensitivity: Ext. Loads = 0.0

Month: Aug

LEGEND
——— Calibration
----- External Loads = 0.0

Plate F13.   (Sheet 3 of 3)

Appendix F   Demonstratin Scenario Plots

NEW YORK BIGHT

Aggregated by Area, Layer, and Month - 1976

Sensitivity: External Loads=100*

Plate F14.   (Sheet 1 of 3)

NEW YORK BIGHT
Aggregated by Area, Layer, and Month - 1976

Sensitivity: External Loads=100*

Plate F14. (Sheet 2 of 3)

NEW YORK BIGHT
Aggregated by Area, Layer, and Month - 1976

Sensitivity: External Loads=100*

Plate F14.   (Sheet 3 of 3)

Sensitivity: Ext. Loads = 100*
Month: Jun

LEGEND
——— Calibration
--------- External Loads = 100*

Plate F15. (Sheet 1 of 2)

Sensitivity: Ext. Loads = 100*
Month: Jun

LEGEND
—— Calibration
----- Extend Loads = 100*

Plate F15. (Sheet 2 of 2)

Plate F16.   (Sheet 1 of 2)

Sensitivity: Ext. Loads = 100*

Month: Aug

Plate F16.   (Sheet 2 of 2)

Plate F17. (Sheet 1 of 2)
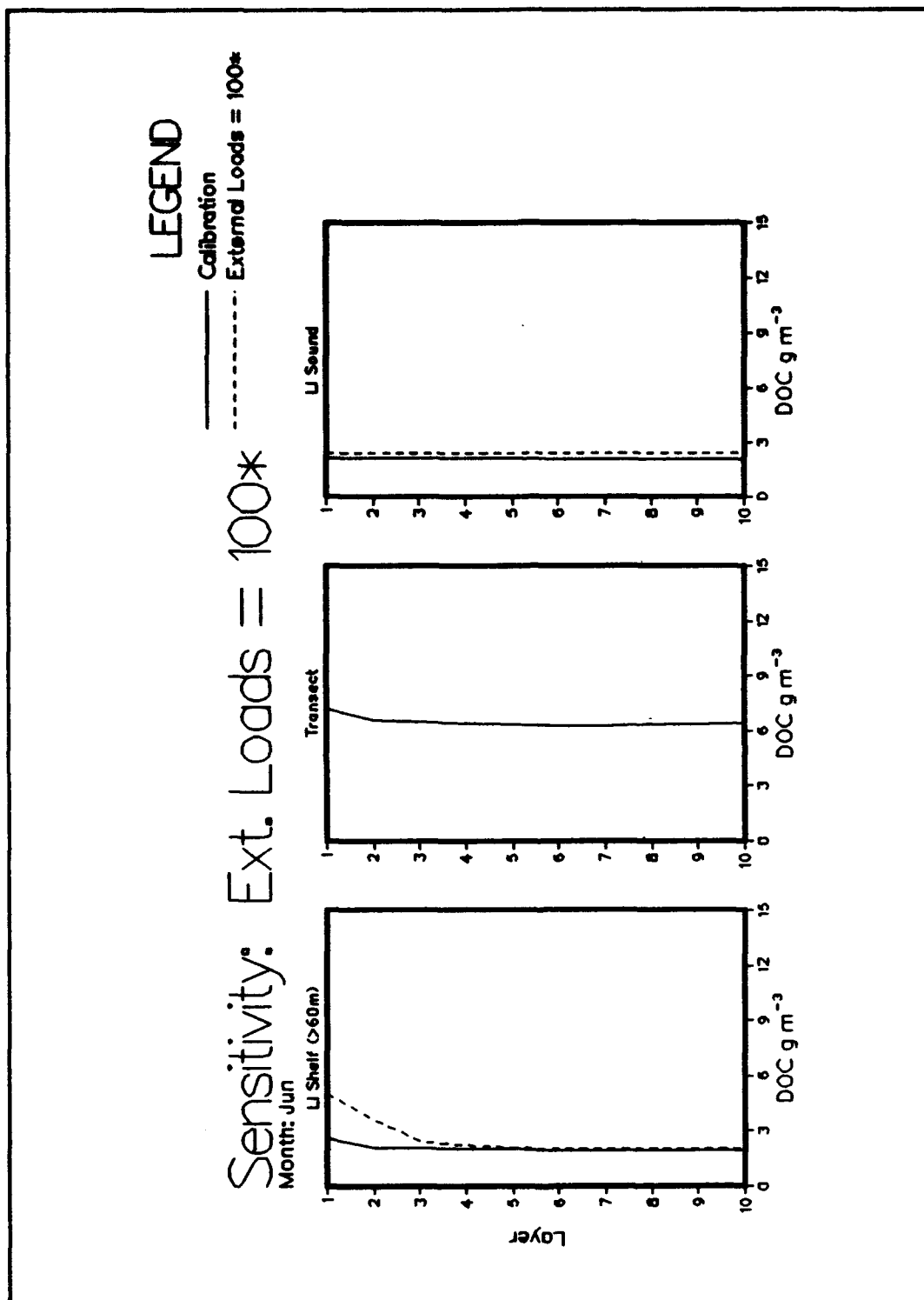
Plate F17. (Sheet 2 of 2)
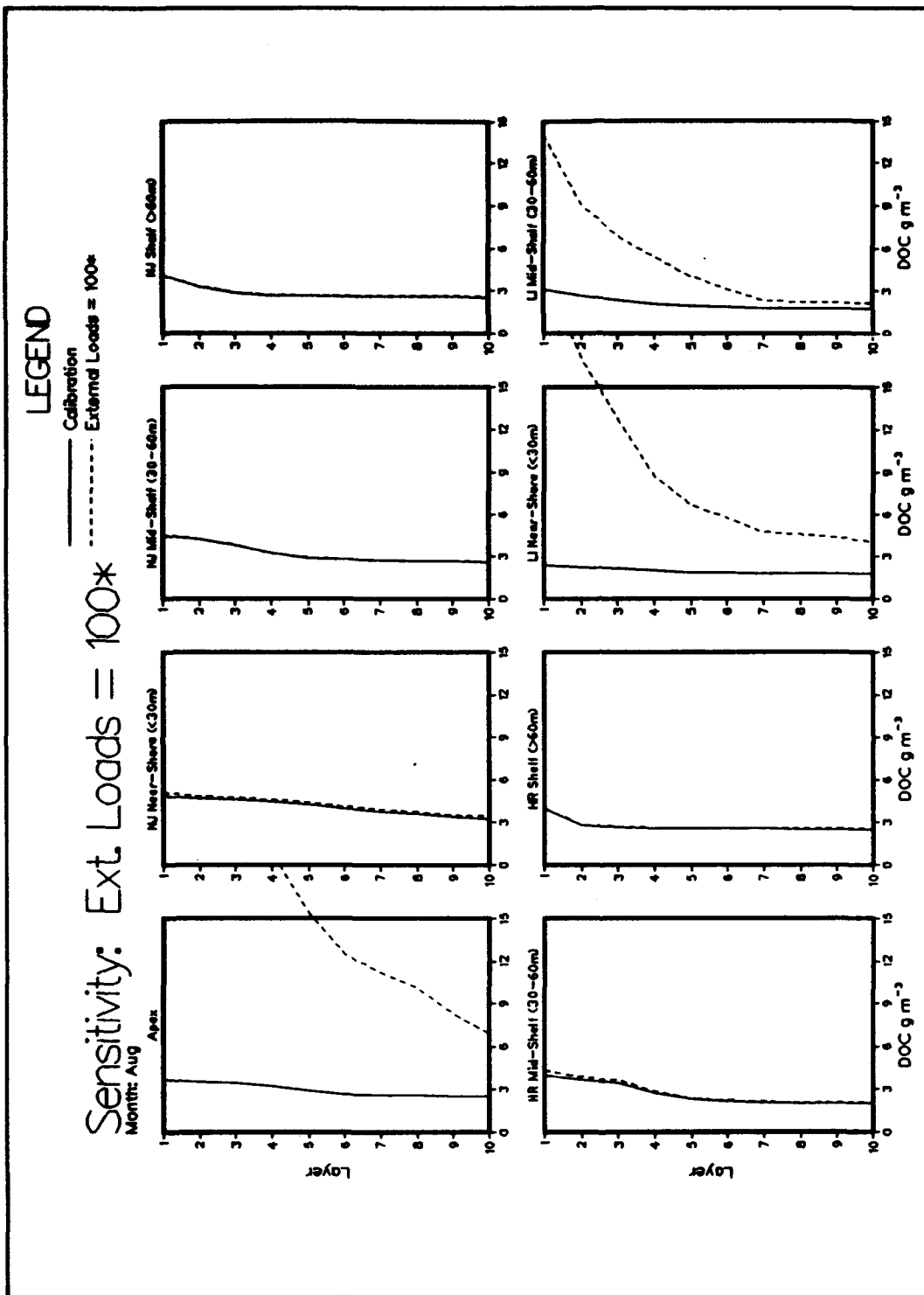
Sensitivity: Ext Loads = 100×

Plate F18. (Sheet 1 of 2)

Sensitivity: Ext. Loads = 100×

Plate F18. (Sheet 2 of 2)

Sensitivity: Ext. Loads = 100*

Plate F19. (Sheet 1 of 2)

F44

Sensitivity: Ext. Loads = 100*
Month: Jun

LEGEND
——— Calibration
-------- External Loads = 100*

Plate F19. (Sheet 2 of 2)

Sensitivity: Ext. Loads = 100*

Plate F20.   (Sheet 1 of 2)

Appendix F   Demonstratin Scenario Plots

Plate F20. (Sheet 2 of 2)

Sensitivity: Ext. Loads = 100*

Plate F21.   (Sheet 1 of 2)

Appendix F   Demonstratin Scenario Plots

Sensitivity: Ext. Loads = 100✕

Month: Jun
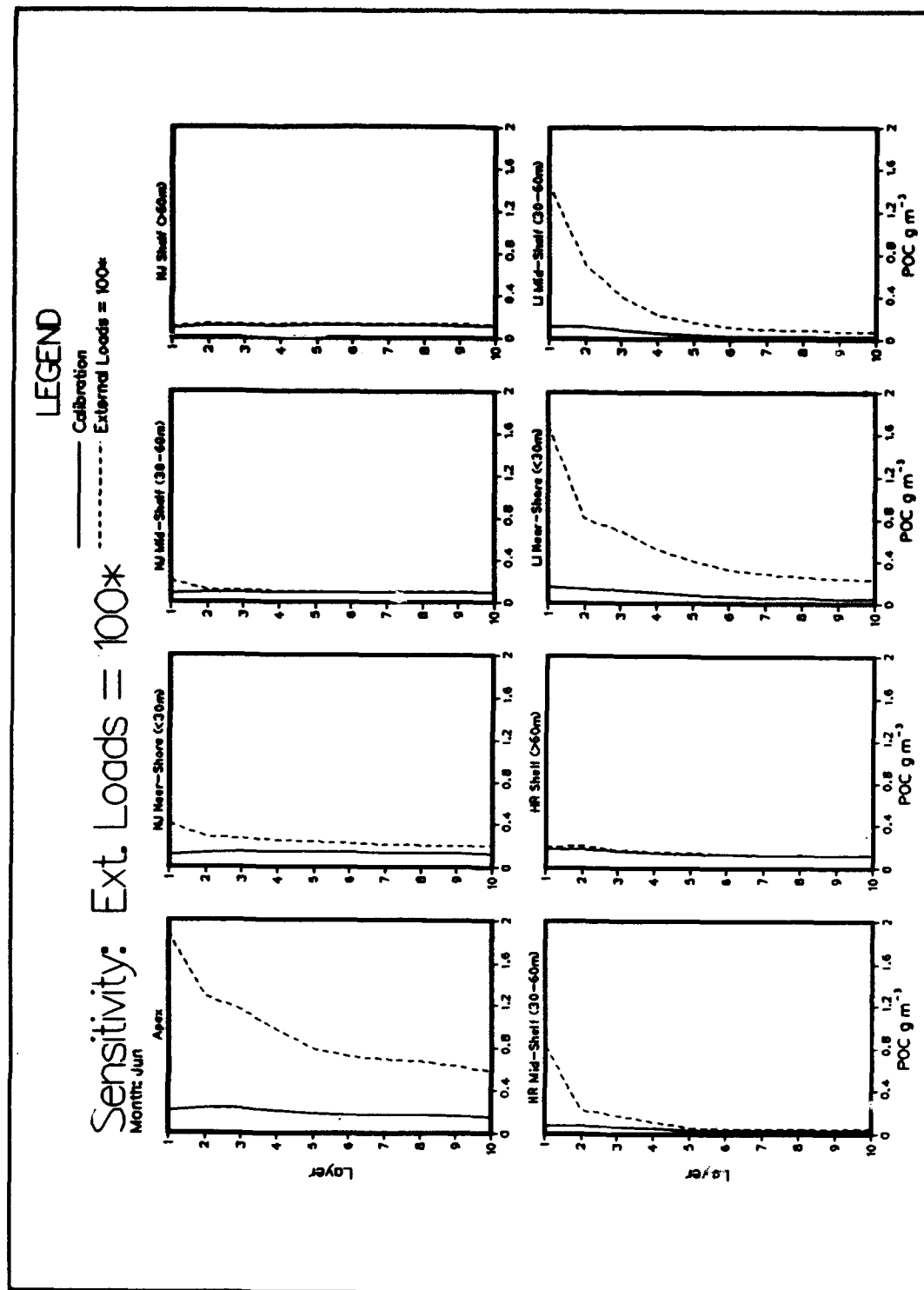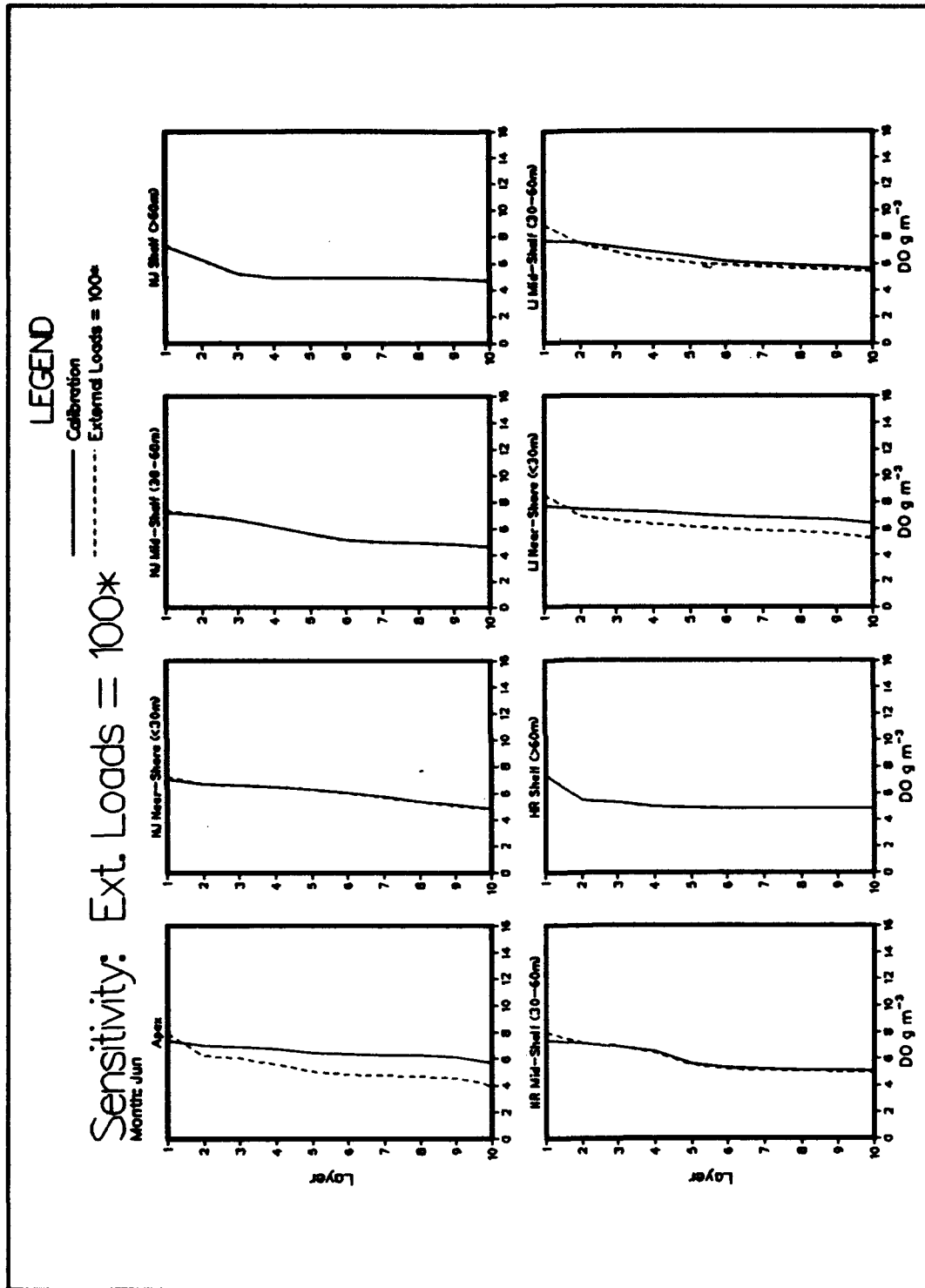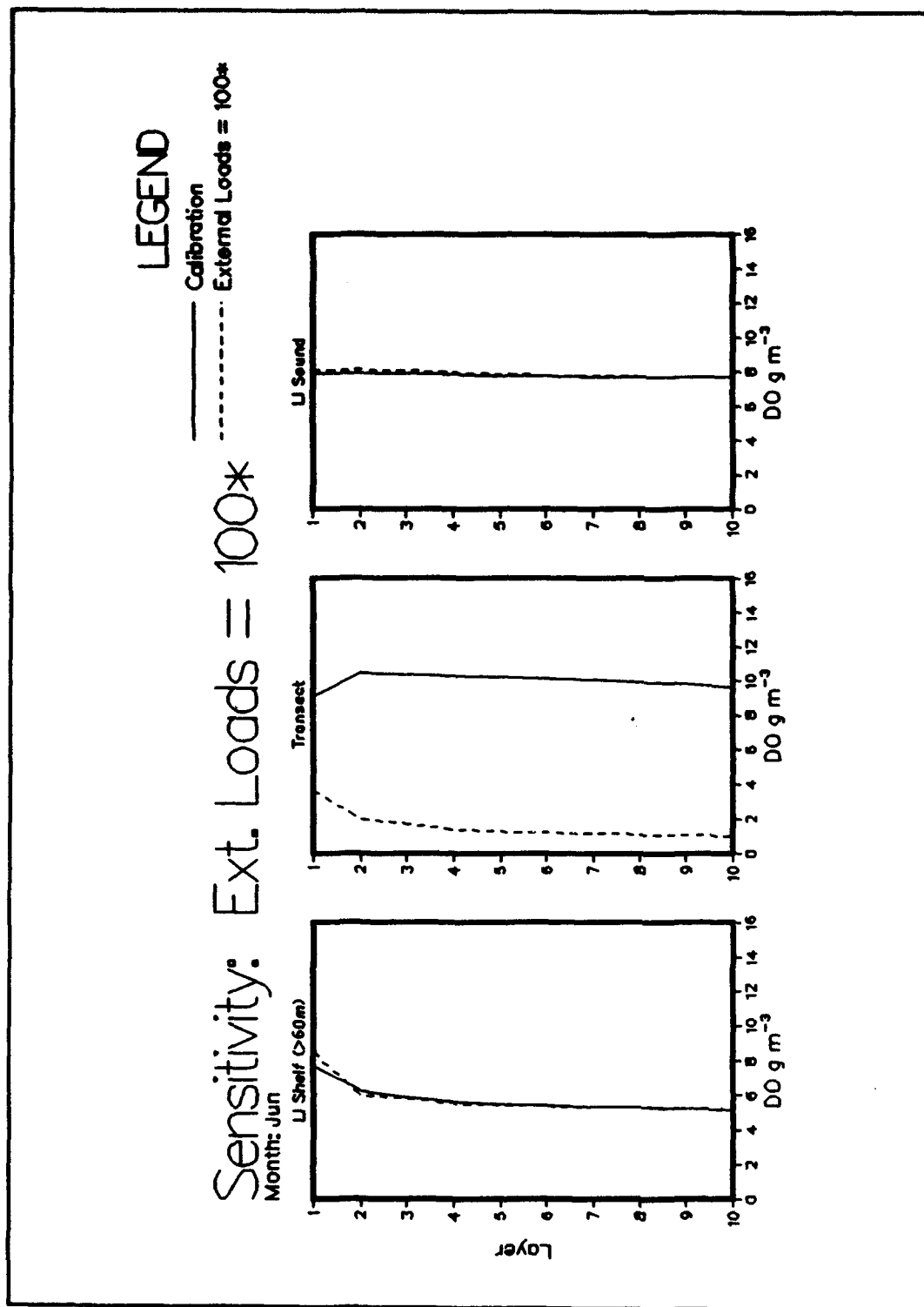
Plate F21.   (Sheet 2 of 2)

Plate F22. (Sheet 1 of 2)

Sensitivity: Ext. Loads = 100×

Plate F22.   (Sheet 2 of 2)

Sensitivity: Ext. Loads = 100*
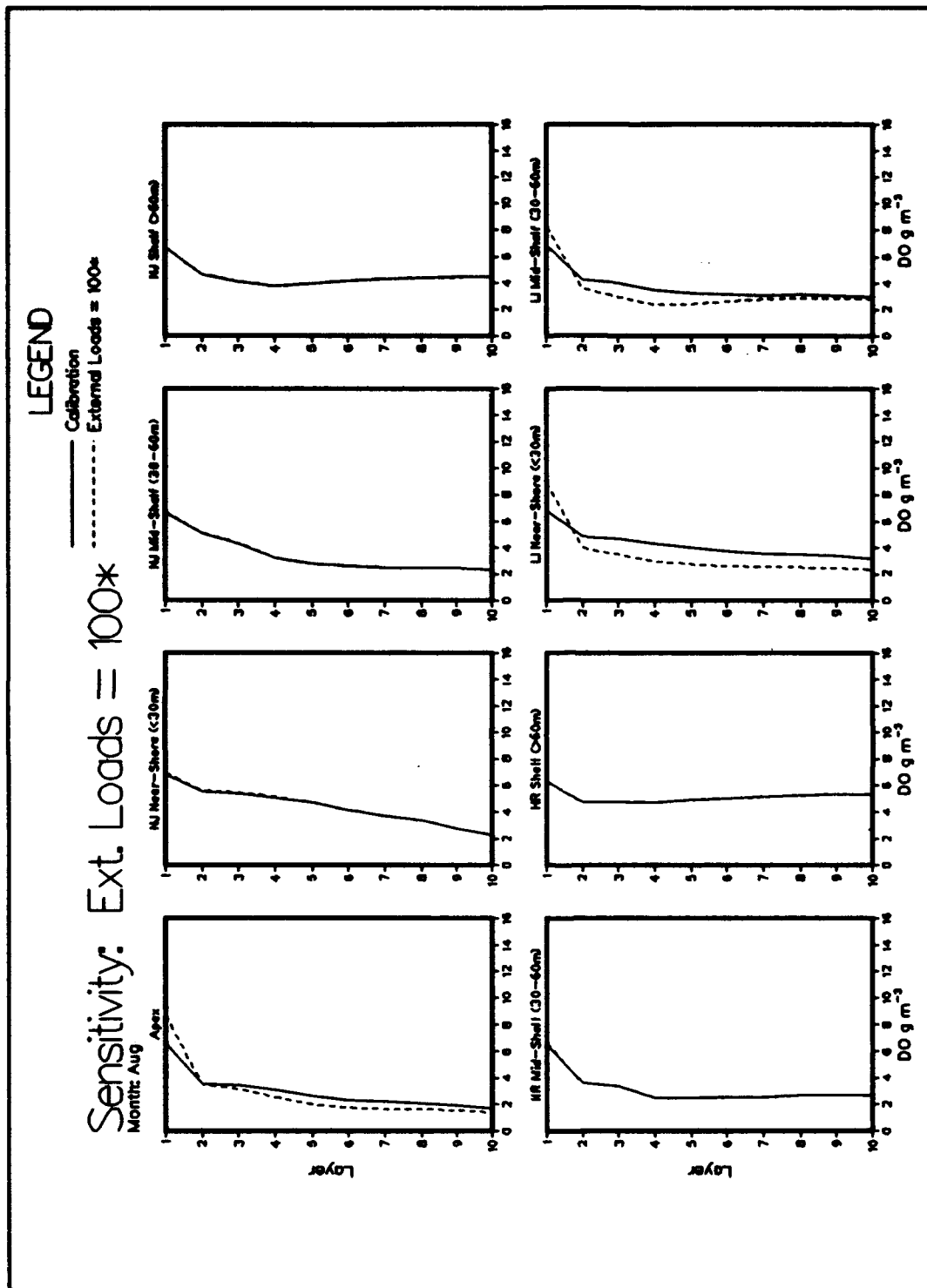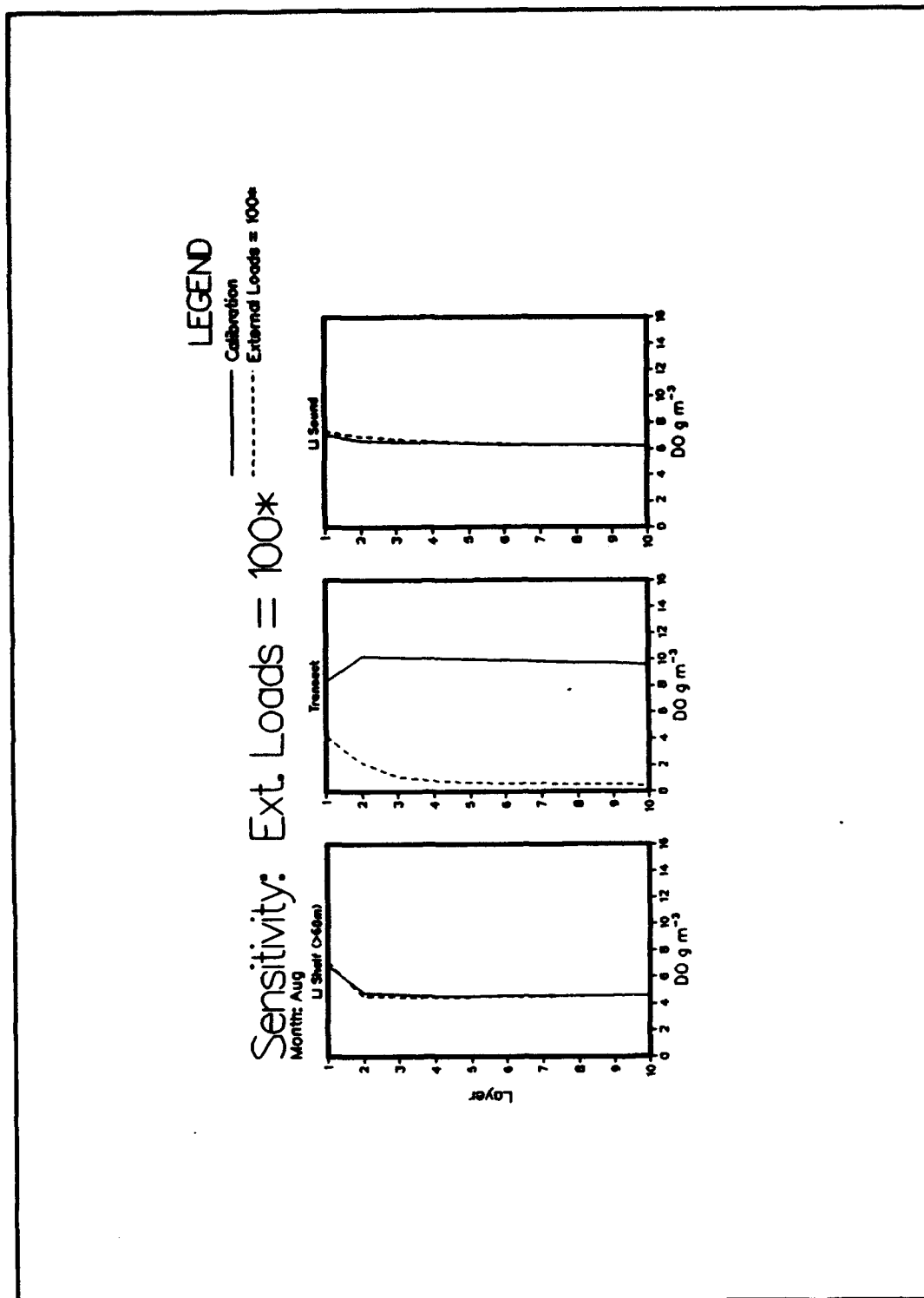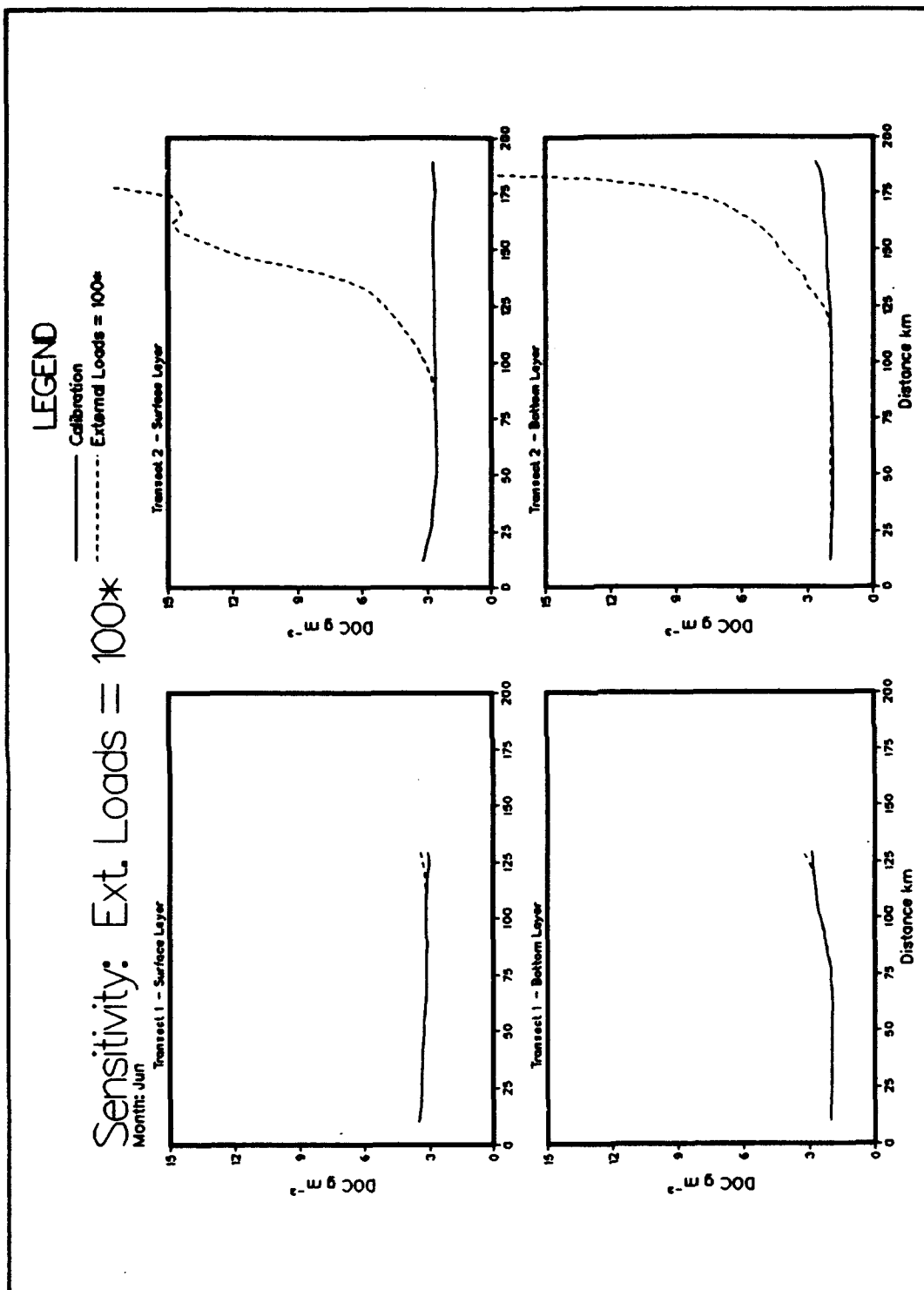
Plate F23. (Sheet 1 of 3)

Plate F23.   (Sheet 2 of 3)

Sensitivity: Ext. Loads = 100*
Month: Jun

LEGEND
——— Calibration
········· External Loads = 100×

Plate F23.   (Sheet 3 of 3)

F54

Plate F24. (Sheet 1 of 3)

Sensitivity: Ext. Loads = 100*
Month: Aug

LEGEND
—— Calibration
------ External Loads = 100*

Sensitivity: Ext. Loads = 100*

Month: Aug

LEGEND

Calibration
External Loads = 100*

Transect 5 - Surface Layer

Transect 5 - Bottom Layer

DOC g m⁻³

Distance km
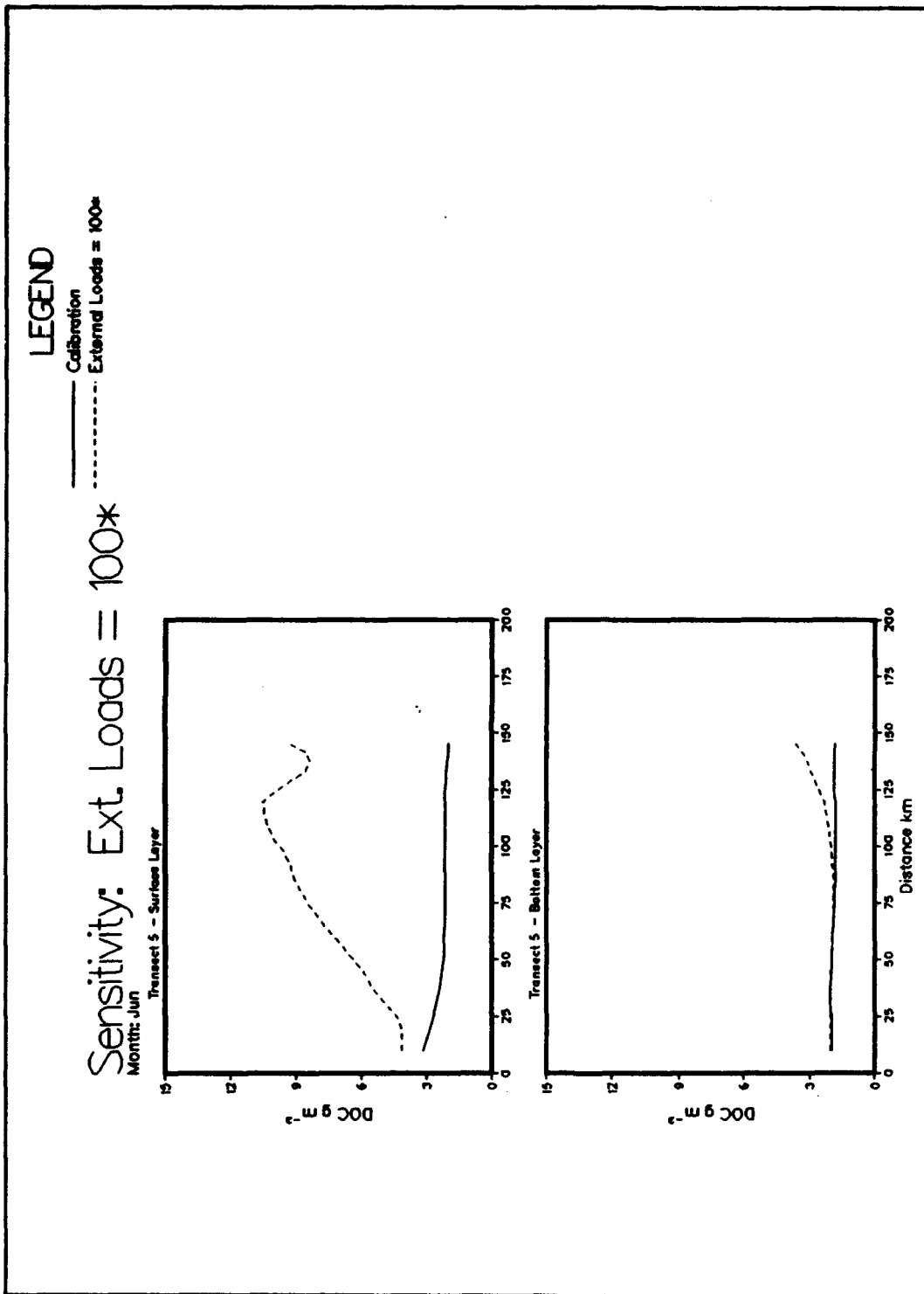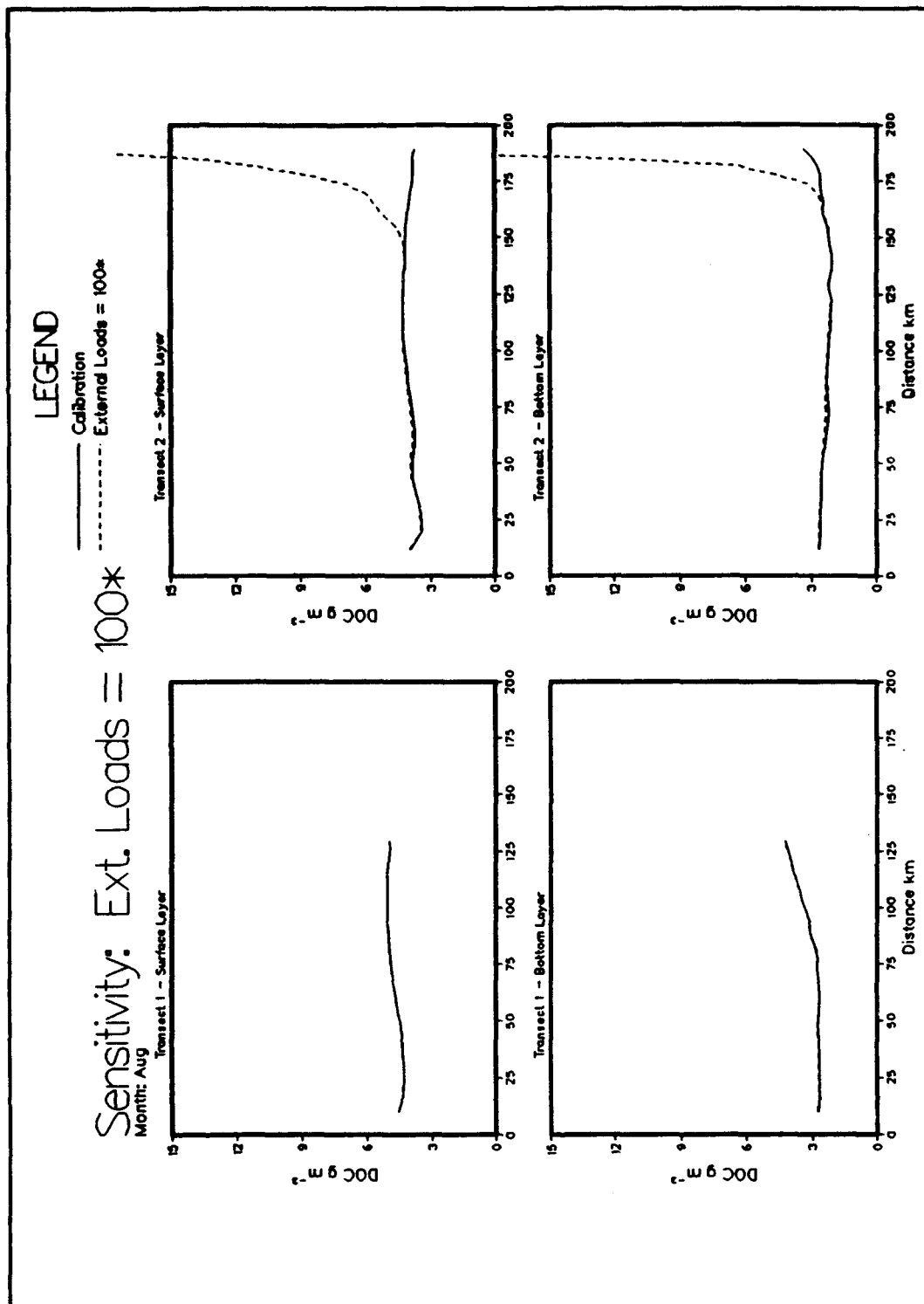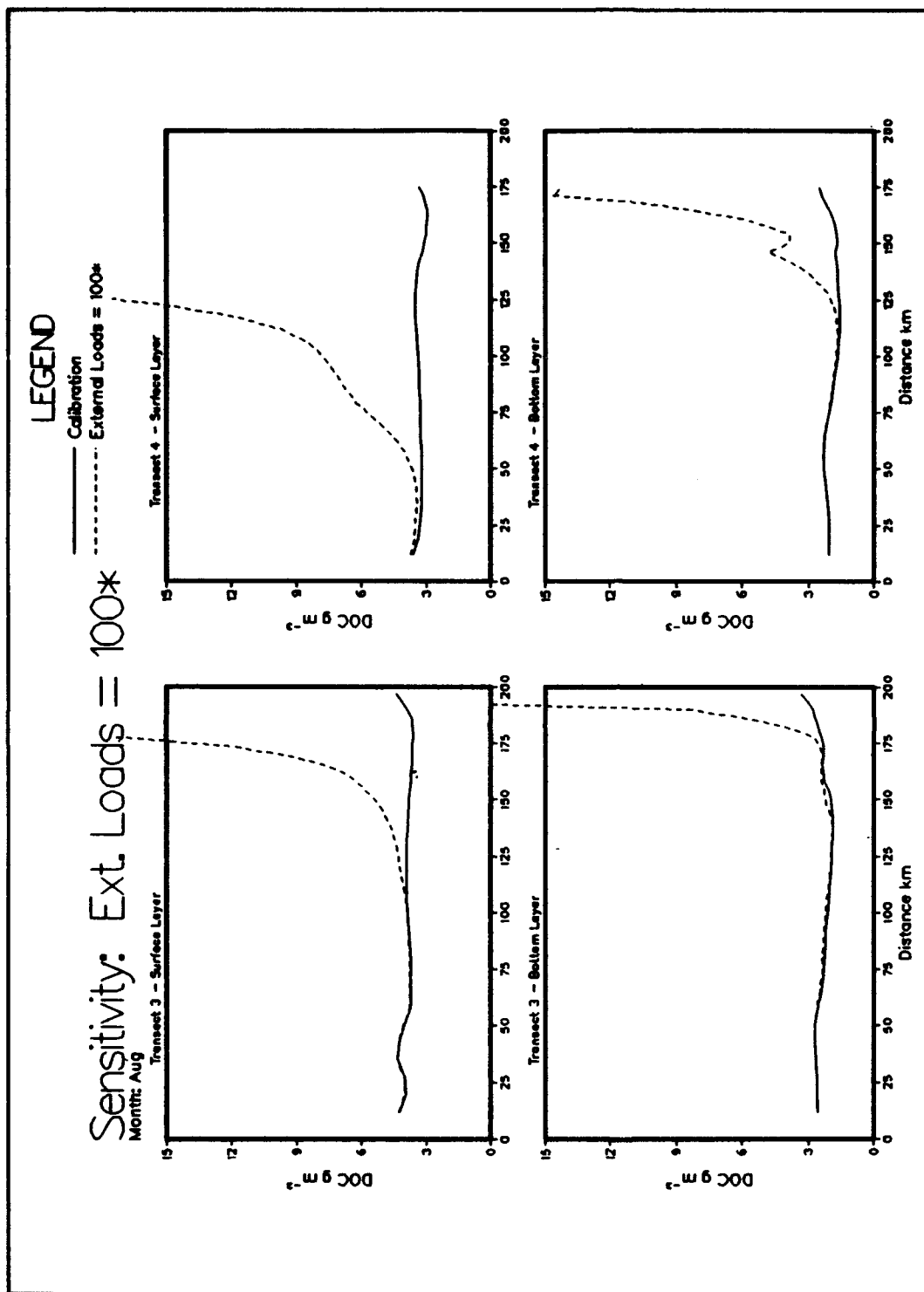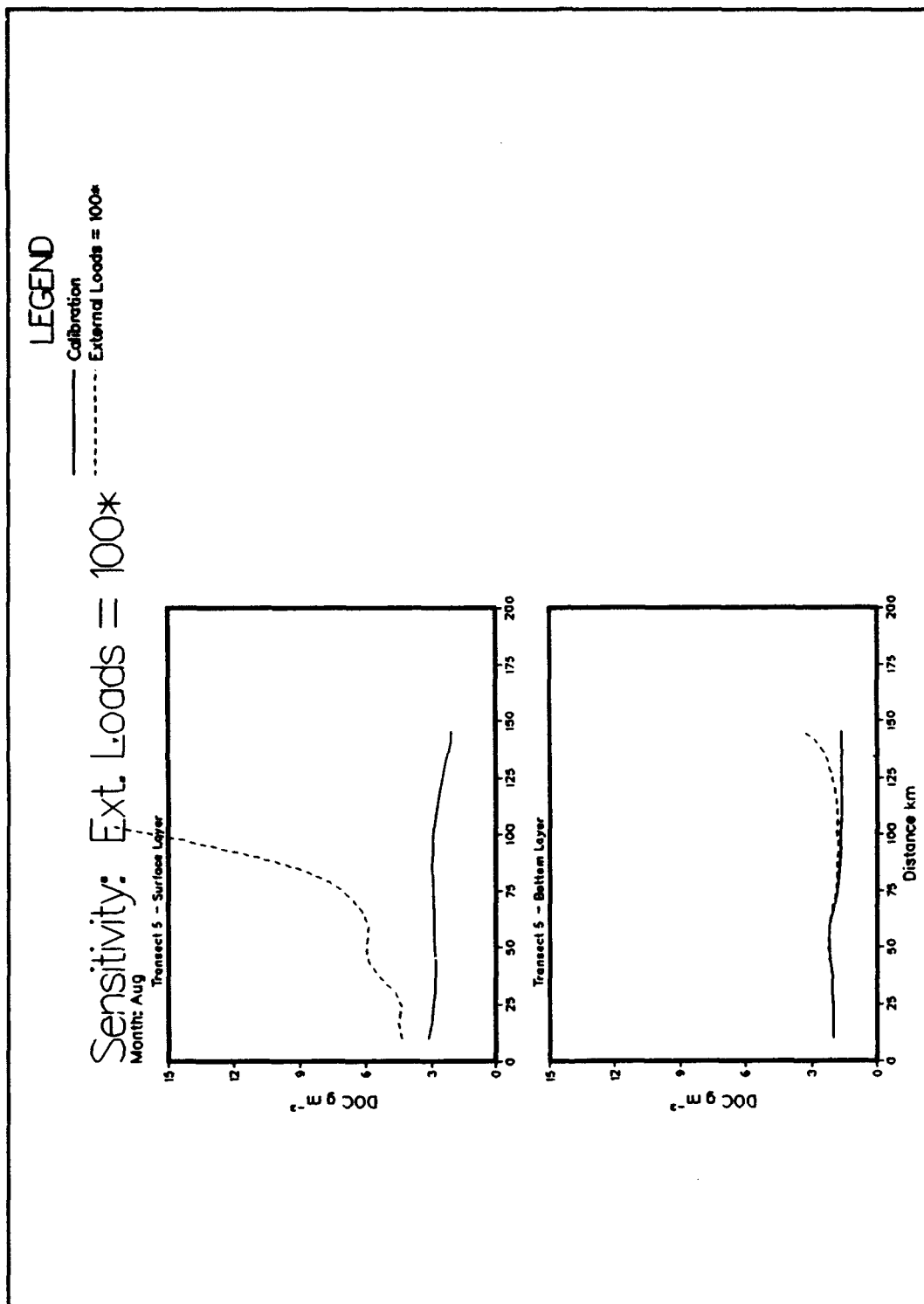
Plate F24.   (Sheet 3 of 3)

Plate F25. (Sheet 1 of 3)
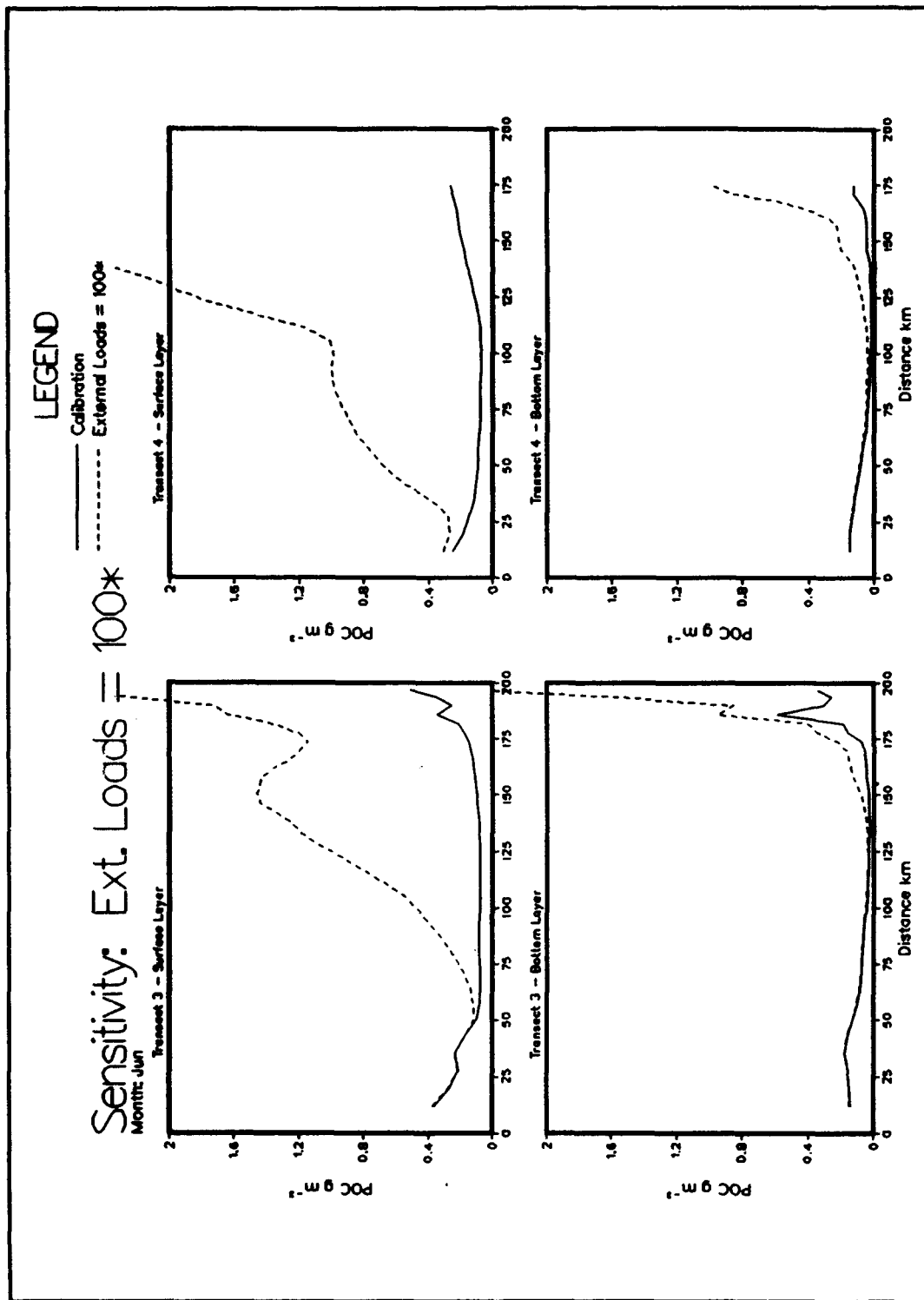
Sensitivity: Ext. Loads = 100×

Plate F25. (Sheet 2 of 3)

Sensitivity: Ext. Loads = 100*

LEGEND

Calibration
Extend Loads = 100*

Transect 5 - Surface Layer
Month: Jun

Transect 5 - Bottom Layer

Distance km

POC g m⁻³

Plate F25.   (Sheet 3 of 3)

Appendix F   Demonstratin Scenario Plots

Plate F26.   (Sheet 1 of 3)

Sensitivity: Ext. Loads = 100*
Month: Aug

LEGEND
——— Calibration
- - - - - External Loads = 100×

Sensitivity: Ext. Loads = 100*
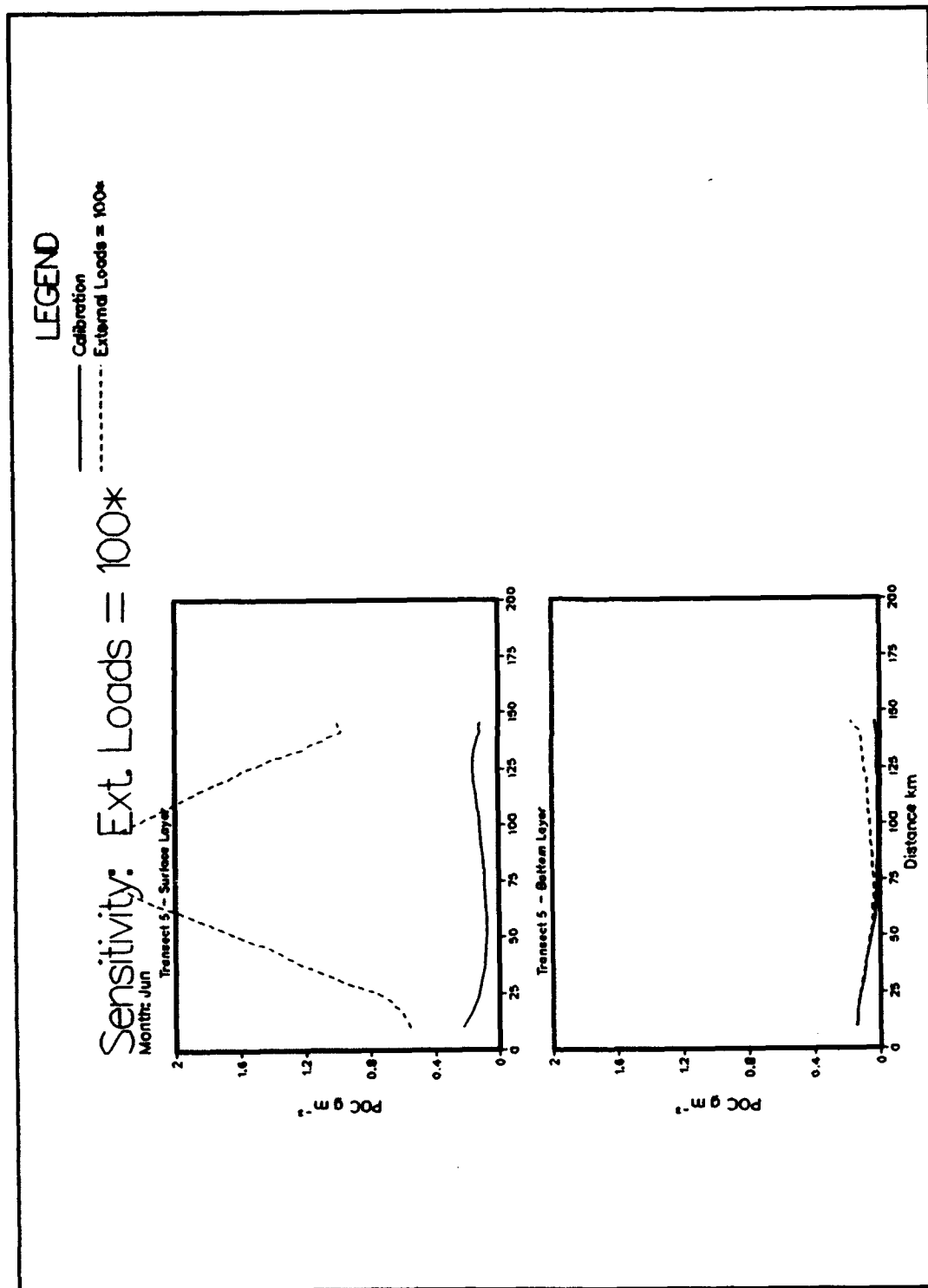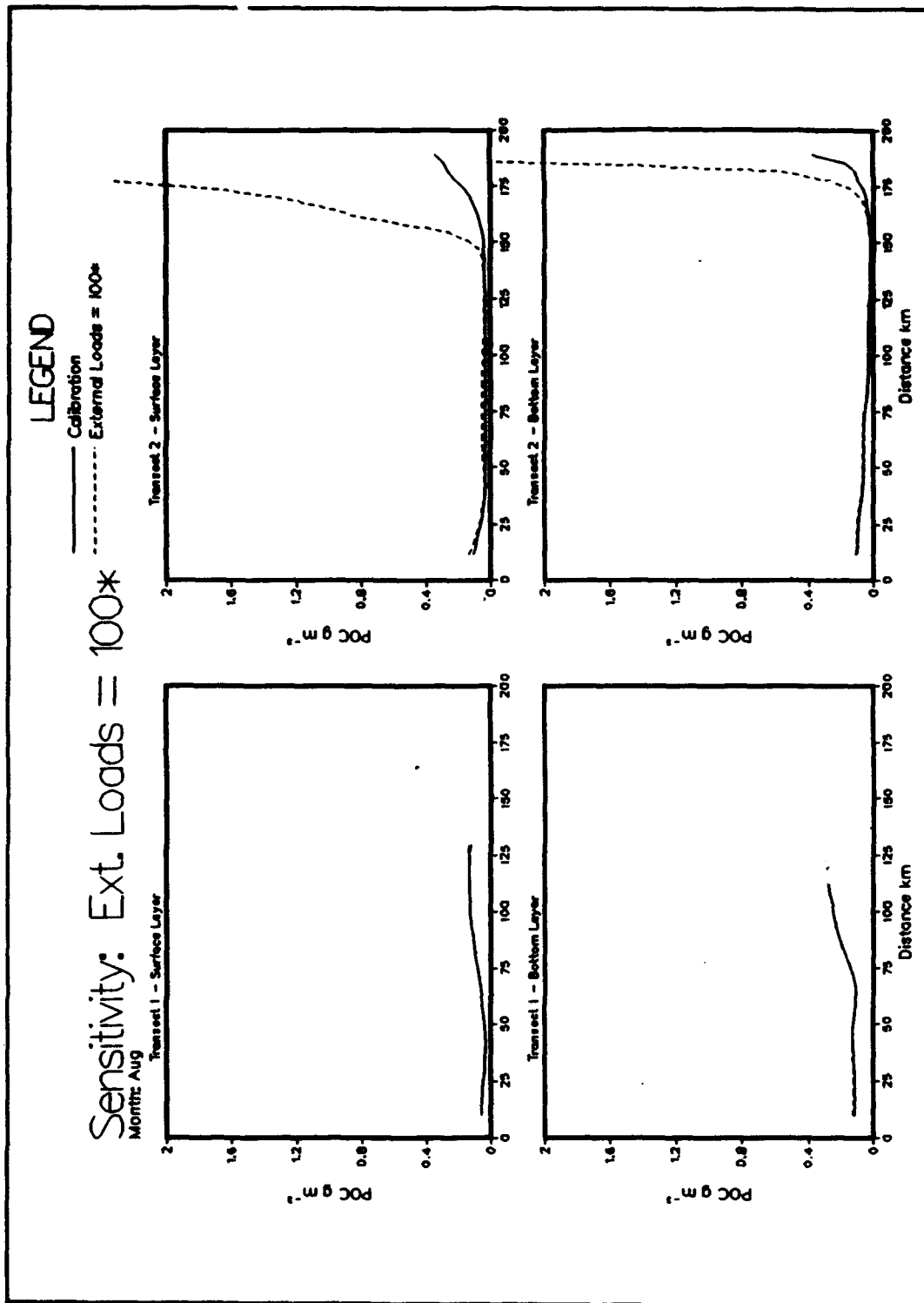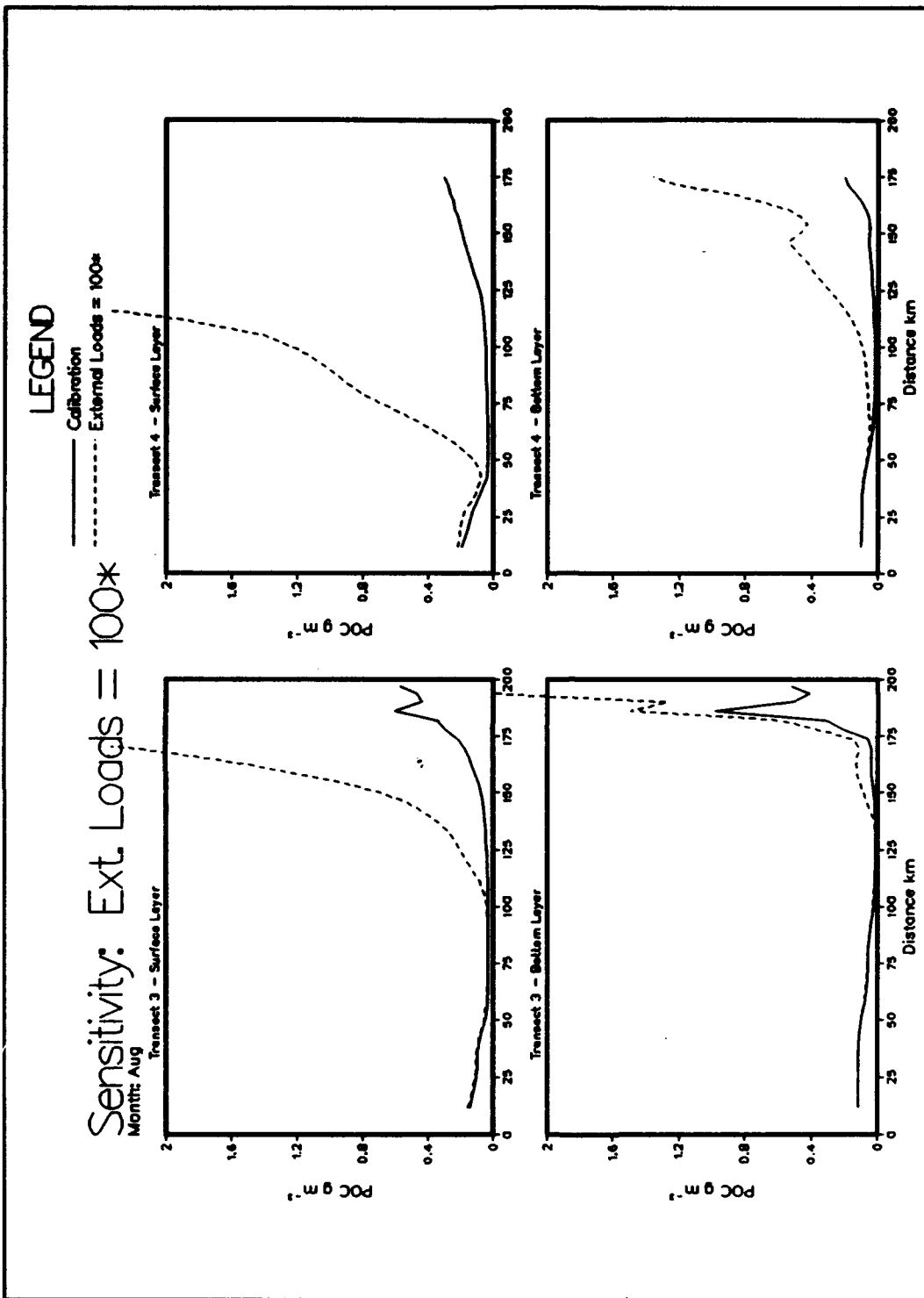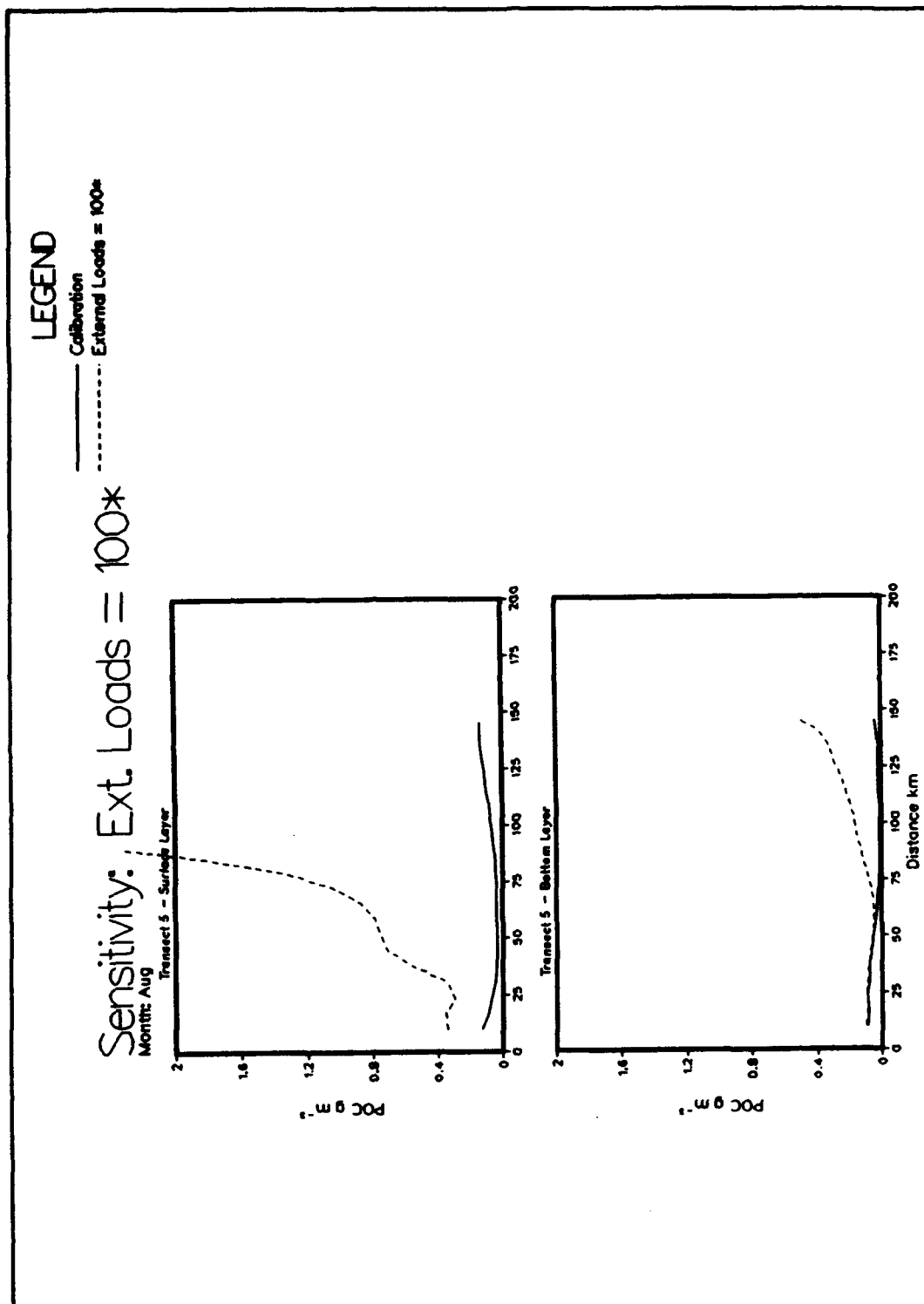
Plate F26. (Sheet 3 of 3)

REPORT DOCUMENTATION PAGE

1. AGENCY USE ONLY (Leave blank)	2. REPORT DATE April 1994	3. REPORT TYPE AND DATES COVERED Report 2 of a series

4. TITLE AND SUBTITLE

New York Bight Study; Report 2; Development and Application of a Eutrophication/General Water Quality Model

5. FUNDING NUMBERS

6. AUTHOR(S)

Ross W. Hall
Mark S. Dortch

7. PERFORMING ORGANIZATION NAME(S) AND ADDRESS(ES)

U.S. Army Engineer Waterways Experiment Station
3909 Halls Ferry Road
Vicksburg, MS 39180-6199

8. PERFORMING ORGANIZATION REPORT NUMBER

Technical Report
CERC-94-4

9. SPONSORING/MONITORING AGENCY NAME(S) AND ADDRESS(ES)

U.S. Army Engineer District, New York
New York, New York 10278-0090

10. SPONSORING/MONITORING AGENCY REPORT NUMBER

11. SUPPLEMENTARY NOTES

Available from National Technical Information Service, 5285 Port Royal Road, Springfield, VA 22161.

12a. DISTRIBUTION/AVAILABILITY STATEMENT

Approved for public release; distribution is unlimited.

12b. DISTRIBUTION CODE

13. ABSTRACT (Maximum 200 words)

The New York Bight (NYB) Water Quality Model Study was an investigation of the technical feasibility of applying a numerical three-dimensional (3-D) water quality model to assess the impacts of natural and human activities on the NYB. For this study, the NYB consisted of tidally influenced estuaries, harbors, and bays; Long Island Sound; the Apex region between the open waters of the Bight and the harbors/estuaries; and the Bight, which for this study extended from Cape May, New Jersey, northeasterly approximately 550 km along the coastline to Nantucket Island, Massachusetts, and approximately 160 km offshore to the continental shelf. The depth of the study site varied from 3 m to near 900 m seaward toward the continental shelf.

The modeling technology recently developed for the Chesapeake Bay was applied to the Bight. This technology consisted of 3-D, time-varying hydrodynamic and water quality models. The model employed a 76 × 45 curvilinear or boundary-fitted, planform grid and 10 stretched (sigma) coordinate layers for the vertical dimension.

The summer hypoxia event of 1976 was selected for the water quality model application, where simulations extended from 15 April through 30 September 1976. The model compared relatively well with observations in the Bight and successfully captured the summer hypoxia of 1976. Simulated net plankton, dissolved organic carbon

(Continued)

14. SUBJECT TERMS

Dissolved oxygen	Models	Nitrogen
Eutrophication	New York Bight	

15. NUMBER OF PAGES
302

16. PRICE CODE

17. SECURITY CLASSIFICATION OF REPORT UNCLASSIFIED	18. SECURITY CLASSIFICATION OF THIS PAGE UNCLASSIFIED	19. SECURITY CLASSIFICATION OF ABSTRACT	20. LIMITATION OF ABSTRACT

13. (Concluded).

(DOC), and particulate organic carbon (POC) were generally underestimated. Simulated and measured dissolved oxygen (DO) indicated relatively close agreement except in Raritan Bay, where a nanoplankton bloom greatly inflated the simulated DO concentrations.

Sensitivity tests were conducted to examine the importance of the benthic sediment oxygen demand (SOD) and ocean nitrogen boundary conditions. An SOD value of zero increased the DO 3 percent Bight-wide while an increase in SOD by a factor of 10 decreased the DO 15 percent. Importantly, the most detectable decrease in DO (38 percent) occurred in the more shallow bays and estuaries. Model DO was relatively insensitive to the nitrogen seaward boundary conditions.

Demonstration scenarios included external load increase and reduction as well as use of the model for investigating the cause of the New Jersey nearshore hypoxia. Constant external loads were varied for the Transect, New Jersey Coast, and Long Island Coast. Decreasing the external load to zero had the effect of decreasing algal, DOC, and POC concentrations. Although organic carbon decreased, the net effect of these changes resulted in a slight decrease in DO. The decrease in algae had greater impact on decreasing DO, compared with the effect that decreasing organic carbon had on increasing DO. Dramatic loading increases by a factor of 100 caused slight DO decrease Bight-wide and a substantial DO decrease in the Transect.

Model simulations revealed that low DO simulated off the coast of New Jersey was the result of three major interacting components: the prevailing southwest to northeast residual flows, DOC and DO boundary conditions along the southwest ocean boundary of the model grid, and SOD. Of these three processes, the advection of low DO had the greatest effect.